This thesis is about diel vertical migration, the most important synchronized animal movement in the ocean. The study focuses on migratory micronekton of the Canary Islands, a community that is mainly composed of small fish, shrimp and squid, which feed in shallow waters during the night and remain deep during the day. Through this process, the atmospheric carbon incorporated into shallow-living organisms is exported to deeper waters and thus affects the global carbon cycle. Here, the author deals with the extent and magnitude of migrations, their role in carbon sequestration, and their variability accross diverse oceanographic features. The results show both the importance and sensitivity of vertical migratory micronekton in a changing ocean, highlighting the need to incorporate this community into future ecosystem models.

Micronekton diel vertical migration and active flux in the subtropical Northeast Atlantic

ULPGC

UNIVERSIDAD DE LAS PALMAS DE GRAN CANARIA

DOCTORAL THESIS

Micronekton diel vertical migration and active flux in the subtropical Northeast Atlantic

Author
Alejandro
VICENTE ARIZA

Supervisor
Santiago
HERNÁNDEZ LEÓN

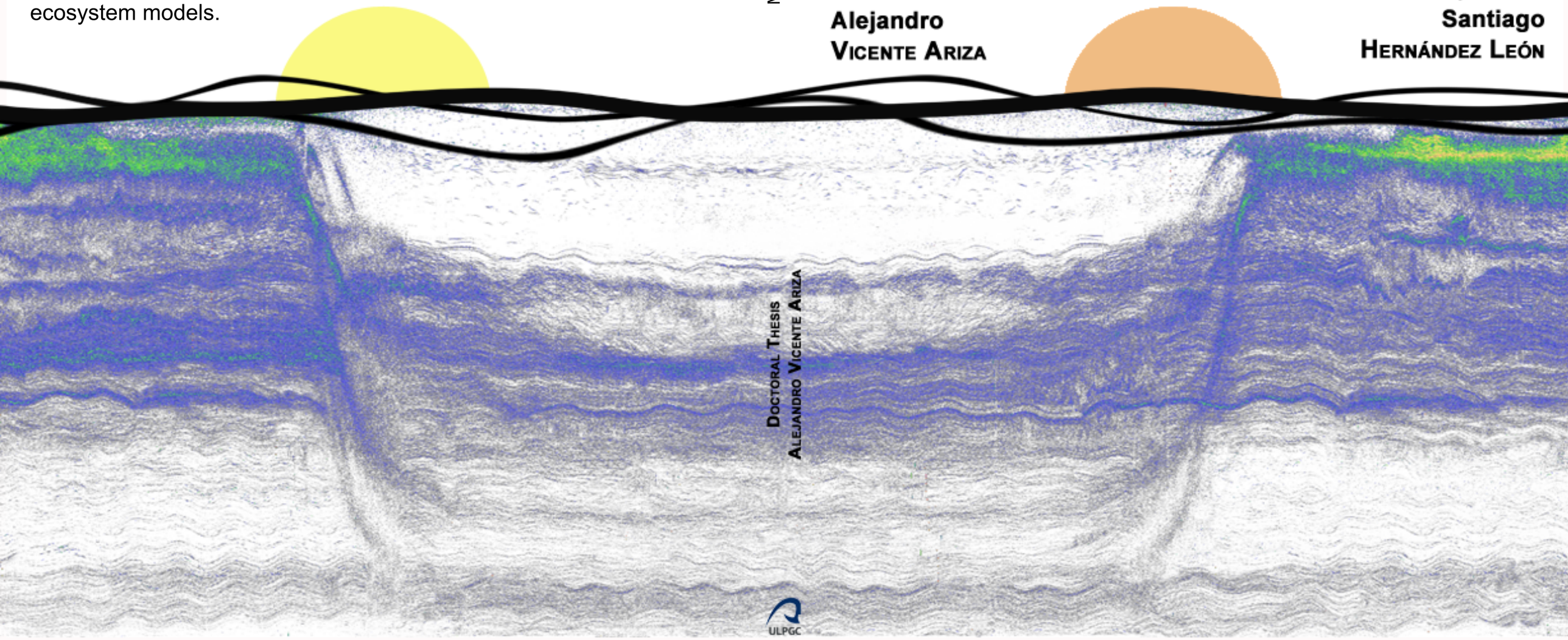

DOCTORAL THESIS
ALEJANDRO VICENTE ARIZA

ULPGC

D. José Manuel Vergara Martín, Secretario del Departamento de Biología de la Universidad de Las Palmas de Gran Canaria,

Certifica,

Que el Consejo de Doctores del Departamento en sesión permanente tomó el acuerdo de dar el consentimiento para su tramitación, a la tesis doctoral titulada *"Micronekton diel vertical migration and active flux in the subtropical Northeast Atlantic"* presentada por el doctorando D. Alejandro Vicente Ariza y dirigida por el Doctor Santiago Hernández León.

Y para que así conste, y a efectos de lo previsto en el Art° 6 del Reglamento para la elaboración, defensa, tribunal y evaluación de tesis doctorales de la Universidad de Las Palmas de Gran Canaria, firmo la presente en Las Palmas de Gran Canaria, a 19 de Noviembre de 2015.

Universidad de Las Palmas de Gran Canaria

Doctoral Thesis

Micronekton diel vertical migration and active flux in the subtropical Northeast Atlantic

Author:
Alejandro
Vicente Ariza

Supervisor:
Dr. Santiago
Hernández León

A thesis submitted in fulfilment of the requirements for the degree of Doctor of Philosophy

Programa de Doctorado en Oceanografía
Instituto de Oceanografía y Cambio Global

November 16, 2015

Declaration of Authorship

I, Alejandro Vicente Ariza, declare that this thesis titled, 'Micronekton diel vertical migration and active flux in the subtropical Northeast Atlantic' and the work presented in it are my own. I confirm that:

- This work was done wholly or mainly while in candidature for a research degree at this University.
- Where any part of this thesis has previously been submitted for a degree or any other qualification at other institution, or for publication in a scientific journal, this has been clearly stated.
- Where I have consulted the published work of others, this is always clearly attributed.
- Where I have quoted from the work of others, the source is always given. With the exception of such quotations, this thesis is entirely my own work.
- I have acknowledged all main sources of help.
- Where the thesis is based on work done by myself jointly with others, this has been clearly indicated.

Signed: _____

Date: _____

"The tow-net experiments carried out on board the Challenger during several years in all parts of the world led me to the conviction that these intermediate regions were inhabited"

John Murray (1895)

UNIVERSIDAD DE LAS PALMAS DE GRAN CANARIA

Abstract

Instituto de Oceanografía y Cambio Global

Doctor of Philosophy

Micronekton diel vertical migration and active flux in the subtropical Northeast Atlantic

by Alejandro Vicente Ariza

Diel Vertical Migration (DVM) is the most important synchronized animal movement in the ocean, and probably represents the largest migration on the planet in terms of biomass. The most extensive vertical displacements (hundreds of meters) are mainly undertaken by large zooplankton, as well as by small fish, shrimp and squid commonly known as micronekton. By feeding at the surface and then moving back to the deep, migrants play a key role in transferring energy and organic matter from productive shallow waters to the deep ocean. In this way, the atmospheric carbon incorporated into shallow-living organisms is exported to deeper waters and thus affecting the global carbon cycle. Despite their importance, the micronekton have been systematically neglected by those developing biogeochemical budgets for the ocean. In this thesis we study micronekton vertical migration and its contribution to carbon export at the Canary Islands (subtropical northeast Atlantic). Since vertical migration can be monitored acoustically using echosounders, we first described the main organisms causing sound scattering in the region. We have identified diverse animal layers and migrations extending down to at least 800 m depth according to acoustic records and net sampling. Migrant biomass estimates and respiration rates also demonstrate that micronekton are as efficient as zooplankton in storing carbon in intermediate waters (200-1000 m depth), with fish being the most important group. We also found that vertical distribution and migrant behavior changes drastically during light attenuation and pollution episodes associated with a submarine volcano eruption. The horizontal distribution of the micronekton was likewise affected by oceanic eddies, which introduced a high degree of patchiness in animals inhabiting down to 900 m depth. We further discuss the potential contribution of micronekton to sequestering of carbon beyond 1000 m depth, based on their extensive migrations and physiological features. Our results show both the importance and sensitivity of vertical migratory micronekton in a changing ocean, highlighting the need to incorporate this community into future ecosystem models.

Acknowledgements (Agradecimientos)

Esta tesis ha sido financiada por el programa FPI del Ministerio de Ciencia e Innovación del Gobierno de España (BES2009- 028908), en el marco del proyecto de investigación LUCIFER (CTM2008-03538) concedido a la Universidad de Las Palmas de Gran Canaria. Además, esta tesis se ha nutrido de los proyectos CETOBAPH (CGL2009-13112), MAFIA (CTM2012-39587) y PUMP (CTM2012-33355). También ha contado con la colaboración de otras instituciones, como la Universidad de La Laguna, el Instituto Canario de Ciencias Marinas, el Instituto Español de Oceanografía o la *King Abdullah University of Science and Technology*.

Qué decir en estos momentos... Confieso que llevo un rato con la mirada perdida tratando de recordar todo lo acontecido desde que llegué a Canarias. Menudo viaje...

Sois muchos, sois imposibles. Imposibles de olvidar.

Tal vez algunos se sorprendan, pero mis andaduras en la investigación no empezaron en la Universidad de Las Palmas. Mi versión investigadora nació en La Laguna. Fueron Zeque, Erika, Ale y Jaume los que me engancharon al mar canario. Éramos los ULL *Navy Seals*, gracias amigos, no os olvido. Fueron los profes laguneros los que me introdujeron en las ciencias marinas. A algunos los llamo maestros, gracias Nacho. Mis primeros compañeros de laboratorio fueron Adri, Kilian, Dominique, Laura, Sabri, Eli, Jose, ... Gracias por las primeras lecciones para conseguir y superar una tesis en España, que no es poco. Jose, qué lugar más especial ocupas... Eres un *jumper*, has estado en mis dos universos, el chicharrero y el canarión. Siempre cerca, siempre en las grandes decisiones. Gracias por ser mi amigo y mi mentor. Conocerte si que fue "entrar en primera división". Natacha, menuda jugarreta te hice. Me fichaste para los cetáceos, pero me quedé con lo que se comían los cetáceos. Tú y ellos me llevasteis al océano profundo. Aún sigo allí. Gracias por las primeras oportunidades. Fátima y Alba, fuisteis las tutoras no oficiales de mi tesina, y puede que de una tesis que aún no existía. Pero fuisteis más que eso, fuisteis el hogar tras el laboratorio, me disteis amigos y momentos inolvidables. Gracias Albita por no haberte ido nunca.

Cualquiera que lea esta tesis, comprobará que la colaboración de la Universidad de La Laguna fue imprescindible. Tenerife fue la primera etapa, pero estuvo presente durante todo el camino, siempre tendiendo la mano. Gracias a todos los chicharreros por hacer que siempre quisiera volver.

Esta tesis apuntó por primera vez a una dirección fija cuando puse el pie en la Universidad de Las Palmas de Gran Canaria. Hasta entonces todo era un poco inestable. No me falla la memoria, Santiago. Gracias por brindarme mi gran oportunidad y por mostrarme el mundo de la biogeoquímica y los migradores. No es fácil construir a un oceanógrafo a partir de un biólogo marino. Después de todo creo que el balance ha sido positivo, gracias por los buenos momentos. Siempre dije que el proyecto Lucifer era un proyecto del demonio, para que les voy a engañar. Pero fue el proyecto que me hizo oceanógrafo, dos años de endurecimiento en la mar. Es difícil olvidar a mis compañeras de mareas y mareos, Lidia, Gara, Laia, Loreto, Sabrina, Almudena, Claire, ... Muchos más nos acompañaron eventualmente, pero nosotras fuimos el núcleo duro del *Atlantic Explorer*, sí, nosotras. Gracias por la fortaleza, las risas, y por no terminar de perder la cabeza en aquella aventura.

El laboratorio B201 no fue más tranquilo, y es que aquel barco estaba gobernado por Mine. Eres la mami del laboratorio y me encantas, lo sabes. Aquí quiero aprovechar para destacar la labor de las técnicos del B201, Lidia, Mine, Ico y Cori, bendita paciencia hay que tener para explicarme cientos de veces dónde están las pipetas, los matraces, o la cinta americana. Sois especialistas en tender puentes entre grupos, agentes dobles y las mejores intermediarias. Gracias por hacerlo todo más fácil.

El laboratorio canarión también me dio algo que bien se merece estar a la altura de los *Navy Seals* laguneros. Tomó distintas formas, como nuestro equipo de carreras de montaña o el consejo de sabios con sede en Telde. Juanca, Yera, Zeben, Igor, Natalia, Iván, Nau, Jose (el *jumper*), gracias a todos por mantener hoy más vivo que nunca aquello que gritábamos en Cádiz: "No nos recordarán por nuestros *papers*". Algunos se reirán, pero nosotros sabemos bien por qué queremos que nos recuerden. Gracias amigos por ayudarme a dejar la tesis en segundo puesto mientras corríamos por volcanes. Gracias por los bocadillos de pata acompañados de toneladas de risas y conocimiento. Yera, sabes que ocupas un lugar especial, he llorado de la risa contigo más veces de las que puedo recordar. Eres mi hermano de Telde, has estado en los mejores y en los peores momentos, gracias *bro*. Juanca, qué puedo decirte a ti que no hayas oído ya. Compañero de las más épicas andadas, amigo. Todo contigo ha tenido sentido, la más alta decencia, y muchísimo aprendizaje, incluso perdiendo. Repetiría una y otra vez. Lo que te voy a decir es sencillo, gracias por hacerme mejor persona.

No quiero olvidarme de muchos otros que ayudaron en esta tesis y que amenizaron las largas horas en la universidad. Federico, te llevas el galardón al entretenimiento. Por mucho que te critiquen, yo te doy las gracias por tus chistes malos a las cuatro de la tarde. Eres un buen tipo, y me alegra haber compartido laboratorio contigo. Mar, me has ayudado en Las Palmas y también estando al otro lado del mundo. Tu entusiasmo

por la oceanografía y por una buena cerveza es lo que más recuerdo de ti. Gracias por transmitirme tanta pasión por tu nombre. Don Fernando Bordes, se me escapa una sonrisa cuando te recuerdo, vaya pareja hicimos... Aún guardo mi primer ecograma, a 120 kHz y firmado por ti. Hicimos un trato, ¿te acuerdas? Tú me dabas un poco de conocimiento en forma de decibelios y yo un poco de entusiasmo en forma de juventud. Hasta me diste un lugar donde trabajar decentemente. Te agradezco mucho lo que hiciste por ese jovencillo ingenuo. Espero, de verdad espero, haber cumplido con mi parte del trato. Si no, házmelo saber y vuelvo allí para volverte loco. David Sosa, sería un terrible agravio olvidarme de ti. Nadie ha dedicado tantas horas como tú a enseñar a un compañero sin esperar nada a cambio. Qué paciencia con Matlab, con el LADCP, y con este torpe biólogo, gracias colega. Javier, hemos compartido campañas, hemos colaborado en proyectos, y tu despacho ha estado siempre abierto para mi. Gracias por mostrarme el otro lado de la biogeoquímica y por echarme un cable cuando lo he necesitado. May y Ted, con vosotros siempre me he sentido como de la casa, muchas gracias. Tengo que agradecerte especialmente a ti, Ted, el entusiasmo y los valores científicos que nos has transmitido a mi y a todos mis compañeros durante estos años en la facultad.

I shall continue in English to thank my colleagues and friends outside Spain. To Rupert Wienerroither, for sharing your knowledge in mesopelagic fish taxonomy with me. Many thanks for collaborating with us, for coming back to the Canaries and getting involved in our research. It has been a pleasure to work with you. Stein Kaartvedt, thanks for accepting me in your research group. The skills that I acquired in acoustics and your involvement in my research have been essential to progress in this thesis. Anders Røstad, many thanks for your patience teaching me Matlab and for sharing those valuable codes. This opened a world of possibilities in my research. I enjoy coding every day. Hope to see you all in the future.

Parecería que el orden ha sido cronológico, pero no es cierto. He dejado el principio para el final, porque es importante.

Soy de Almería, todo comenzó aquí y termina aquí. Escribo estos agradecimientos en el Cabo de Gata, y es que cuando se trata de agradecer es mejor hacerlo en un lugar bonito. Mis padres no fueron a la universidad, ni proyecto de fin de carrera, ni nada. Su proyecto fuimos nosotros, cinco sobresalientes *cum laude*. Papá, Mamá, os doy las gracias por darme la oportunidad que vosotros nunca tuvisteis, pero sobre todo por educarme en valores y siempre cerca del mar. Jamás hubiera conseguido esto sin vosotros, y por eso os dedico esta tesis. A mis hermanos, Begoña, Francisco, Blanca y Sergio. Sois mis primeros amigos y siempre me habéis apoyado, incluso cuando esta tesis me ha vuelto loco. Con nuestras diferencias, aun sin entender lo que hacía, aun sin saber como hacerlo,

aun cuando me equivoco, ... Siempre me he sentido blindado. Soy el resultado directo de mi familia, gracias.

También guardo amigos muy especiales en mi tierra. Amigos que han tenido un papel especial durante, y sobretodo, al final de esta tesis. José Alberto, Edi, Alberto y Domin, os agradezco esas escapadas de vuestra cotidianidad para apoyar a un amigo que aún lleva ritmo universitario. Nada mejor que unas cervezas en nuestro viejo bar para descansar de la ciencia. Otros estáis un poquito lejos pero siempre cerca. Nuria, que siempre has tenido un interés tan especial por mi tesis que hasta me daba la risa, supongo que no estoy acostumbrado. Gracias por tu apoyo y por tu amistad a pesar de la distancia. Hugo, eres uno de los amigos más especiales que tengo. Se supone que yo tenía que enseñarte a ti pero fue al revés. Has estado siempre cerca aun estando tan lejos. Gracias por sacar el niño que llevo dentro en los momentos más difíciles y aburridos de la vida adulta. Pocas cosas sientan tan bien.

A todos y a todas, gracias por haberme acompañado en este viaje.

Alejandro.

Contents

List of Figures

I Introduction

II Results

List of Tables

II Results

IV Resumen en español (Spanish summary)

V Appendices

Abbreviations

AAI	**A**coustic **A**nomaly **I**ndex
CPUE	**C**apture **P**er **U**nit **E**ffort
CTD	**C**onductivity **T**emperature and **D**epth (profiler)
DCM	**D**eep **C**hlorophyll **M**aximum
DOC	**D**issolved **O**rganic **C**arbon
DSL	**D**eep **S**cattering **L**ayer
DVM	**D**iel **V**ertical **M**igration
DW	**D**ry **W**eight
ESR	**E**quivalent **S**pherical **R**adius (swimbladder)
ETS	**E**lectron **T**ransport **S**ystem
ITE	**I**ntra**T**hermocline **E**ddy
MSL	**M**igrant **S**cattering **L**ayer
MVBS	**M**ean **V**olume **B**ackscattering **S**trength
POC	**P**articulate **O**rganic **C**arbon
PP	**P**rimary **P**roduction
SSL	**S**hallow **S**cattering **L**ayer
SSR	**S**ea **S**urface **R**eflectance
WW	**W**et **W**eight

Symbols

S_A	Nautical Area Scattering Coefficient (NASC)	m^2 nmi^{-2}
Sv	Volume backscattering strength	dB re 1 m^{-1}
TS	Target Strength	dB re 1 m^2

A mis padres...

Part I

Introduction

Background

Diel vertical migration: History and the protagonists

Diel vertical migration (DVM) is the most important synchronized mass movement of animal populations in the ocean and probably represents the largest migration on the planet [Angel and Pugh, 2000, Hidaka et al., 2001, Hays, 2003]. The earliest documented evidence for DVM dates back to the late 19^{th} century when increased night-time catches were observed at the sea surface during the Challenger Expedition [Murray and Hjort, 1912]. However, it was not until the development of modern sonar by the middle of 20^{th} century that the vertical extent and timing of DVM was reported for the first time [Dietz, 1948, Eyring et al., 1948]. Acoustic recordings of marine biota, today called echograms, showed scattering layers occurring between 400-700 m depth during the day, and above 100 m depth at night. The layers were connected through a dusk ascent and a dawn descent (Fig. I1). This diel rhythm promptly suggested that the phenomenon was due to migrating organisms, a fact that was later corroborated by concurrent net trawling across the acoustic scattering layers [Tucker, 1951].

We know now that although the main cause of oceanic acoustic resonance is gas-bearing animals such as swimbladder fish or siphonophores [Hersey and Backus, 1954, Barham, 1966], a huge variety of planktonic and nektonic organisms are actually involved in DVM (Fig. I2). Copepods [Roe, 1984b], euphausiids [Roe et al., 1984b], decapods [Roe, 1984a], fish [Roe and Badcock, 1984] and cephalopods [Roper and Young, 1975] are the most common taxa that undertake interzonal migrations, that is, between the epipelagic ($\sim$0-200 m) and the mesopelagic zone ($\sim$200-1000 m). In fact, when taking into account the whole community regardless of their visibility on echograms, the entire mesopelagic zone is indeed inhabited by interzonal migrants, with each species covering different migratory ranges [Domanski, 1984].

However, although DVM is undertaken by a wide range of species and sizes, it is fair to say that the most abundant and extensive movements are performed by large zooplankton and micronekton, which mostly comprise crustaceans and fishes from 1 to 10 cm in length [Brodeur et al., 2005]. While krill (*Euphausiidae*) is probably the most important migrant group within the zooplankton, lanternfishes (*Myctophidae*) dominate within the micronekton, the latter accounting for almost 80% of total migrant biomass [Koslow et al., 1997, Hidaka et al., 2003]. Since myctophids are very numerous and their swimbladder properties make them highly resonant targets [Butler and Pearcy, 1972, Yasuma et al., 2010], they are indeed the main source of acoustic scattering layers, frequently masking the presence of other migrant groups in routine echograms [Godø et al., 2009, Kloser et al., 2009].

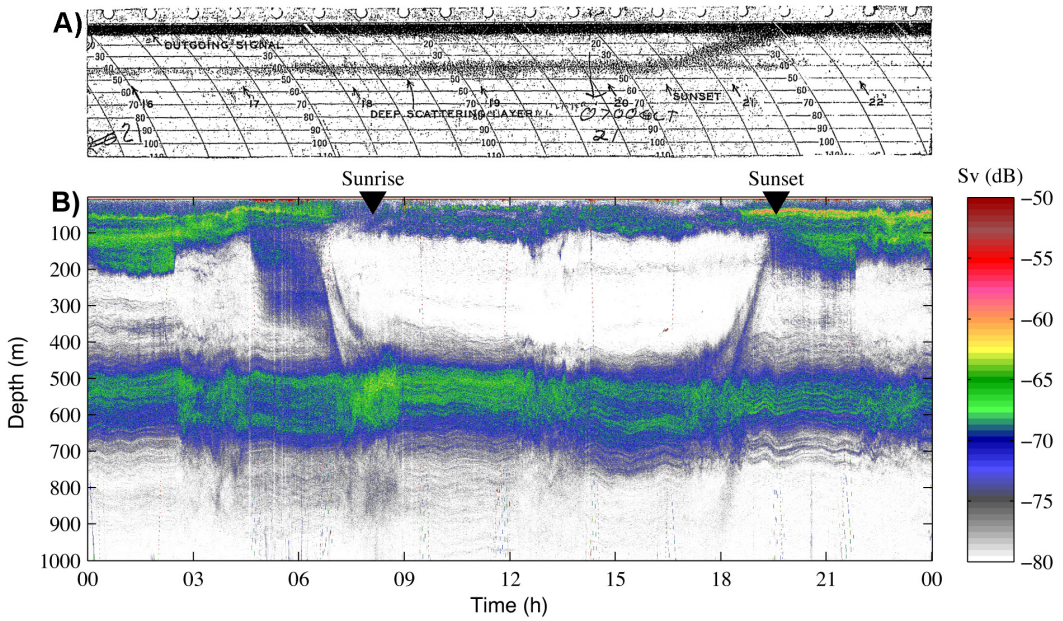

FIGURE I1: (A) First documented echogram showing diel vertical migration (nocturnal ascent) from the mesopelagic zone to shallow waters in the central equatorial Pacific [Dietz, 1948]. (B) Modern echogram showing a dawn descent and a dusk ascent in oceanic waters around the Canary Islands. *Sv* (volume backscattering strength) indicates the echo intensity.

Factors governing diel vertical migration

The unveiling of the nature of acoustic scattering layers lead to questions about the triggers and adaptive significance of DVM. Since the first descriptions of DVM, the coincidence of vertical movements associated with dusk and dawn pointed to light as the main factor governing this behavior [Johnson, 1948]. Earlier hypotheses had suggested that DVM resulted from vertical habitat selection based on highly specific isolumes [Kampa and Boden, 1954, Boden and Kampa, 1967, Blaxter, 1974]. However, later studies showed that migrant biota were actually found within broad light intensity zones [Roe, 1983, Frank and Widder, 2002, Staby and Aksnes, 2011]. The isolume concept was therefore abandoned and today it is widely accepted that different mesopelagic species settle within preferred ranges of light intensities [Badcock, 1970, Foxton, 1970b]. Alternatively, a reasonable question raised was whether DVM was controlled by internal clocks (circadian rhythms) adjusted to natural light variations rather than by light per se [Neilson and Perry, 1990]. However, this hypothesis seemed unlikely to be true since acoustic scattering layers were observed to respond under unpredictable light fluctuations, such as variable cloudiness or solar eclipses [Kampa, 1975, Baliño and Aksnes, 1993].

Hence, that light is the main factor governing DVM is today a widely accepted fact. There is, however, ongoing debate concerning the adaptive significance of this behavior.

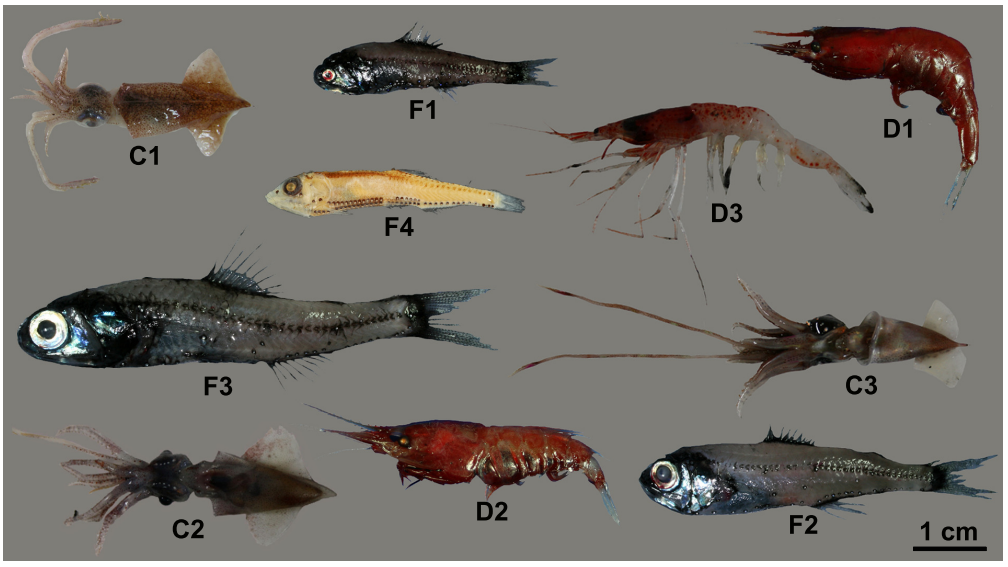

FIGURE I2: The main fishes, decapods and cephalopods that undertake DVM in the subtropical northeast Atlantic: (F1) *Lobianchia dofleini*, (F2) *Hygophum hygomii*, (F3) *Ceratoscopelus warmingii*, (F4) *Vinciguerria attenuata*, (D1) *Systellaspis debilis*, (D2) *Oplophorus spinosus*, (D3) *Deosergestes corniculum*, (C1) *Onychoteuthis banksii*, (C2) *Abraliopsis morisii*, and (C3) *Pyroteuthis margaritifera*.

The most accepted explanation is that since light is essential for visual foraging, but also increases the likelihood of being seen by predators, DVM would be a habitat selection game consisting of a trade-off between the availability of food and the necessity to avoid predators [Clark and Levy, 1988, Hays, 2003]. The extent to which a particular species is exposed to a certain light level will depend on its prey detection threshold and its capacity for camouflage [Warrant and Locket, 2004], factors that will determine the depth and timing of the migration [Aksnes and Giske, 1993, De Robertis, 2002, Busch and Mehner, 2011]. On the other hand, the bioenergetic efficiency hypothesis "hunt warm, rest cool" postulates that saving energy by staying in cold waters is the primary reason for the descent, rather than the avoiding of predators [Brett, 1971, Sims et al., 2006]. A reduced metabolism is a common feature in deep-sea animals. It is a consequence of low temperature and might be advantageous for saving energy [Childress, 1975, Torres et al., 1979, Childress and Seibel, 1998]. However, this does not necessarily imply that bioenergetics are the main reason for diel migration. A reasonable proposition is that none of the proposals can explain DVM in all cases, since there is a broad spectrum of species and circumstances. The ultimate causes for DVM probably encompass feeding opportunities, predator avoidance, and energy saving [Mehner, 2012].

In fact, as a consequence of changing prey distributions, light, and temperature regimes in marine ecosystems, varied migrant strategies have been observed in different oceanographic regions. The normal DVM pattern (NDVM) of "a dusk ascent and a dawn descent" is therefore currently a generalized and simplistic description rather than a

model explaining all variants of this phenomenon. For instance, recent studies have described migratory patterns where some individuals remain at depth, not performing migration [NoDVM, Dypvik et al., 2012], as well as others where the total population migrates [TDVM, Dypvik and Kaartvedt, 2013]. Even inverse migrations [IDVM, Dypvik et al., 2011], or midnight sinking between the ascent and descent have been documented [Prihartato et al., 2015]. All of these strategies must be related to changing resources and physical features over the water column, which are expected to change according to seasons and ecosystems.

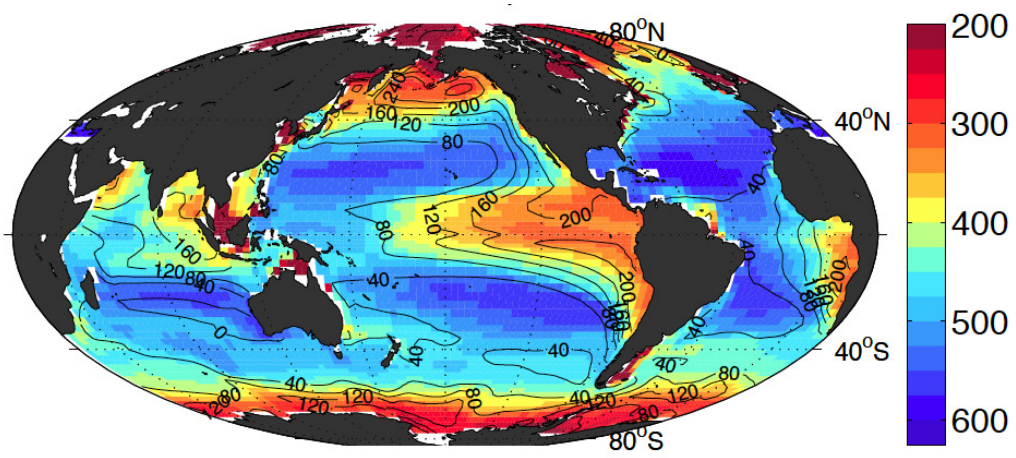

FIGURE I3: Daytime diel vertical migration depth (colours) modeled from oceanographic variables such as subsurface oxygen, epipelagic temperature gradient, surface chlorophyll or mixed-layer depth. Contours show the surface (0 - 25 m) to upper mesopelagic zone (150 - 500 m) oxygen difference (mmol m^{-3}). From Bianchi et al. [2013a].

On the other hand, light not only governs DVM on a temporal basis, but its influence is also evident over spatial scales. Changing turbidity at the sea surface modulates light irradiance, affecting in turn the vertical distribution of scattering layers at both small and large scales over the oceans [Kaartvedt et al., 1996, Dickson, 1972]. Aside of light, there are other oceanographic factors likely to affect the distribution of deep-sea animals, such as temperature, dissolved oxygen, or water masses [Fasham and Foxton, 1979, Bianchi et al., 2013a, Wang et al., 2014, Cade and Benoit-Bird, 2015]. Other studies have even reported variability in the deep scattering layers, apparently driven by mesoscale eddies [Godø et al., 2012, Béhagle et al., 2014]. Recently, Bianchi et al. [2013a] modeled the daytime depth of migrants at global scale based on several oceanographic predictors. Most variance in their model was explained by oxygen concentration, which limited the depth of the migrants (Fig. I3). However, they found a weak correlation with light. The main constraint of this model is that it refers to the migration depth of specific targets detected with acoustic doppler current profilers (ADCP). As previously stated, migrants also extend above and below the scattering layers. Many of them are well adapted to oxygen minimum zones [Childress and Seibel, 1998, Ekau et al., 2010],

and are highly influenced by light [e.g., Roe, 1983, Frank and Widder, 2002, Staby and Aksnes, 2011]. Therefore, the model of Bianchi et al. [2013a] should be regarded as a fairly good illustration of the migration depth of a specific scattering layer, but not representative of the whole migrant biota. The conjunction of all these factors (light, temperature, oxygen, water masses, and mesoscale activity) may lead to patchy distributions of the migrant biota.

In summary, DVM is not simply a vertical movement of resonant fish in the ocean. It is a much more complex mechanism involving a huge variety of species, covering different depth ranges, while occurring through diverse migratory modalities in the world ocean.

Importance of diel vertical migration for marine foodwebs

While zooplanktonic migrants mainly feed on phytoplankton and microzooplankton, alternating between the second and the third trophic level [Vinogradov, 1962, Wilson et al., 2010], most micronekton are zooplanktivorous occupying the third position in oceanic food webs [Kozlov, 1995, Burghart et al., 2010, Choy et al., 2012]. As such, interzonal migrants can be classified as first or second order consumers. This means that primary productivity in shallow waters is transformed into mesopelagic biomass at most through two intermediate steps, such that it is a short trophic pathway which implies an effective energy transfer from the surface to the deep ocean (Fig. I4). In fact, very recent midwater fish biomass estimates suggest that transfer efficiencies between primary producers and the mesopelagic fauna in oligotrophic regions are actually much higher than previously assumed [Davison et al., 2013, Irigoien et al., 2014].

However, not all the biological production derived from DVM ends below the euphotic zone. In addition to deep predators such as midwater fishes [Choy et al., 2013] or cephalopods [Passarella and Hopkins, 1991], interzonal migrants are also preyed upon by many shallow living animals that either dive down into the mesopelagic zone or wait within the epipelagic to hunt them during the nocturnal ascent. Amongst the deep diving predators are marine mammals [Santos et al., 2001] and tuna species [Matsumoto et al., 2013], while the most common nocturnal shallow predators are small pelagic fishes [Cabral and Murta, 2002], dolphins [Pusineri et al., 2007], swordfish and also tuna [Potier et al., 2007]. Indeed, a significant mortality risk is faced in shallower waters because migrants there are highly motile during feeding periods, and therefore, more easily tracked by predators.

Hence, interzonal migrants play an important role in pelagic ecosystems not only because they occupy a key trophic status, but also because their migratory behavior converts

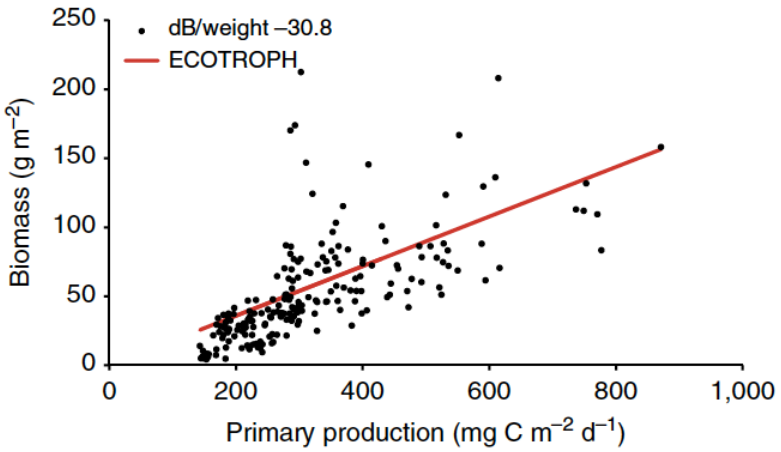

FIGURE I4: Mesopelagic fish biomass as a function of primary production. Black dots are *in-situ* acoustic biomass estimates. The red line is the modeled biomass assuming a transfer efficiency of 0.1 and considering that 90% of primary production enters the food web. From Irigoien et al. [2014].

them into an essential food supply in both the epipelagic and mesopelagic zones. Indeed, their trophic interactions suggest that they are also important for driving primary production into the deep ocean [Irigoien et al., 2014], as well as for sustaining global fisheries [Pauly and Christensen, 1995, Lam and Pauly, 2005].

Relation to the ocean carbon cycle and climate change

The ocean carbon pump refers to a conjunction of physiological, ecological and physical processes through which atmospheric carbon dioxide (CO_2) is sequestered into the deep sea (Fig. I5). The sequestration begins at the surface with the fixation of inorganic carbon by photosynthesis (see equation below) and its subsequent transformation by foodweb associated processes into different forms of organic carbon, either forming part of living organisms or as inert organic matter in the water column. Through this process, photosynthetic organisms displace the equilibrium of the carbonate system in seawater, in this way accelerating CO_2 diffusion from the atmosphere into the ocean [Millero, 1995]. After this point, the organic carbon may be remineralized back via respiration of epipelagic consumers and microbial activity [del Giorgio and Duarte, 2002], or it may be exported to the ocean interior through three main mechanism, namely: (1) ocean dynamics, (2) gravity, or (3) mediation by DVM.

$$CO_2 + H_2O \underset{photosynthesis}{\overset{respiration}{\leftrightarrows\leftrightarrows\leftrightarrows\leftrightarrows}} CH_2O + O_2$$

The first mechanism refers to dissolved organic or inorganic carbon (DOC and DIC) exported by physical processes, such as convective mixing [Arístegui et al., 2003], water-mass sinking [Sarmiento et al., 2004], or isopycnal diffusion [Arcos-Pulido et al., 2014]. The second, known as the "passive" or "gravitational flux", occurs with the formation of particulate aggregates of organic carbon (POC) with highly specific sinking rates [Fowler and Knauer, 1986]. In the last case, the so-called "active" or "migratory flux", the organic carbon is incorporated into the tissues and gut contents of interzonal migrants, and is later released in deeper waters through respiration [Longhurst et al., 1990], defecation [Steinberg et al., 2000], excretion [Turner, 2002] and mortality [Zhang and Dam, 1997]. When carbon export is exclusively driven by physical processes, we refer to it as the physical pump, whereas both the passive and active flux are known as the biological pump.

Understanding the processes involved in the air-sea CO_2 balance is not a trivial matter. The oceans contain about 50 times as much carbon as the atmosphere, which means that small changes in the ocean carbon cycle could have large atmospheric consequences. This is of paramount importance considering that CO_2 is the main gas responsible for the current global warming scenario, and its partial pressure levels in the atmosphere are expected to double by the end of this century [IPCC, 2014]. In this respect, the oceanic carbon pump not only plays a key role in global climate, but it is also expected to be altered in a future high CO_2 world, though the nature of the change is still controversial [Robinson et al., 2010, Doney et al., 2012].

Approximately two-thirds of the carbon vertical gradient in the ocean is attributed to the biological pump with the rest due to the physical pump [Passow and Carlson, 2012]. Consequently, international research programs about the oceanic role in climate change (JGOFS, GLOBEC, IMBER) have been focused on the biological processes involved in carbon sequestration [Steinberg et al., 2001, Weingartner et al., 2002]. However, while the passive flux has been the object of much attention, the role of DVM has scarcely been considered by the developers of oceanic carbon budgets.

Current estimates indicate that migrant zooplankton might be exporting roughly between 10 and 50% of the integrated passive flux down to the mesopelagic zone in subtropical waters [Steinberg et al., 2000, Hernández-León et al., 2001, Steinberg et al., 2008]. Therefore, in recent studies this export mechanism has been considered in biogeochemical conceptual models [Arístegui et al., 2009, Robinson et al., 2010, Passow and Carlson, 2012], yet its contribution is rarely considered in oceanic global budget calculations. However, even summing up carbon fluxes mediated by migrant zooplankton and sinking POC, the total carbon export continues to be lower than global estimates derived through ecosystem modeling [Schlitzer, 2002, Falkowski et al., 2003, Usbeck et al.,

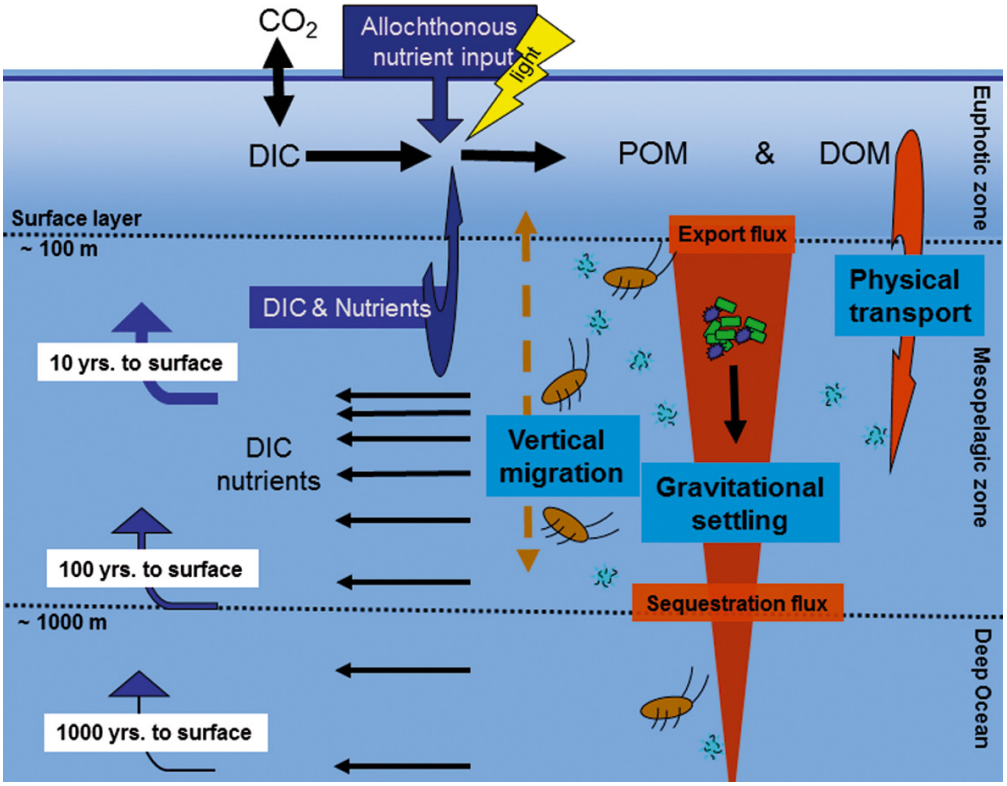

FIGURE I5: Schematic of the biological carbon pump. Note that active flux is not considered beyond 1000 m depth, while micronekton are not represented in the diel vertical migration, only zooplankton. From Passow and Carlson [2012].

2003]. Discrepancies are also evident below the mesopelagic zone, where both the carbon pool and microbial carbon demand cannot be sustained by the passive flux alone [Baltar et al., 2009]. All these imbalances have traditionally been ascribed to artifacts in the measurement of sinking POC [Buesseler et al., 2007], to unaccounted lateral inputs of POC [Alonso-González et al., 2009], and ultimately to biased carbon inputs mediated by migratory zooplankton [Steinberg et al., 2008]. However, the micronekton are rarely considered as an option (see Fig. I5).

Micronekton are known to be involved in DVM and, therefore, in the active flux since the first faunistic descriptions of migrant scattering layers in the ocean [Tucker, 1951, Hersey and Backus, 1954, Barham, 1966]. Hence, it was not ignorance that kept the micronekton out of the scope of biogeochemical oceanographers. In reality, difficulties associated with sample collection were most likely the reason why the micronekton have been systematically excluded from carbon budgets. This community exhibits faster swimming capacity than the zooplankton, therefore requiring larger, more expensive and time-consuming trawls for sampling [Koslow et al., 1997, Pakhomov et al., 2010, Kaartvedt et al., 2012b]. However, precisely due to their high mobility, the micronekton are able to undertake extensive migrations from surface to deep waters, even beyond 1000 m depth [Badcock and Merrett, 1976, Kinzer and Schulz, 1985, Burghart, 2006].

This potentially converts migratory micronekton into highly effective agents of carbon sequestration in the interior ocean.

To our knowledge, the only work that encompasses the active flux by zooplankton and micronekton was conducted by Hidaka et al. [2001] in the western equatorial Pacific, and their estimates doubled when including both migrating components. Hernández-León et al. [2010], based on zooplankton mortality rates caused by the micronekton, pointed to this community as an important missing component of the biological pump in the northeast Atlantic. Other studies have recently reported significant contributions to carbon export by both micronektonic fish [Davison et al., 2013] and decapods [Schukat et al., 2013] in the northeast Pacific and the Benguela upwelling system, respectively. However, the few existing measurements differ in orders of magnitude depending on the group analyzed, the oceanographic region, or the sampling gear used. The latter condition, probably introduces the major source of variability due to uncertainties concerning net capture efficiency [Pakhomov et al., 2010]. In this respect, zooplankton estimates are better known since more studies are available and they are based on more accurate standard procedures [UNESCO, 1968]. In addition, most active flux estimates refer to carbon export below the base of the euphotic zone (∼200 m depth), whereas little is known about the magnitude and extent of transport beyond this depth. This would be of special interest in the case of micronekton as they can cover wider migratory ranges in comparison with zooplankton, thereby increasing the efficiency of the biological pump.

Hence, assessment of ocean carbon exports requires further research into DVM, with particular focus on the micronekton contribution in the mesopelagic zone and beyond. The alternative is a considerable bias in a major component of the biological carbon pump.

Thesis objectives and outline

An efficient assessment of diel vertical migration and active carbon flux requires knowledge of the nature of specific acoustic scattering layers in a given region, their distribution within oceanographic structures, as well as the extent and magnitude of carbon inputs from each migrating component. However, little is known about migratory scattering biota in the subtropical northeast Atlantic, where most active flux research has been focused on zooplankton export below the euphotic zone.

The aim of this thesis is to investigate the role of the micronektonic community in diel vertical migration and in the active flux of the subtropical northeast Atlantic, focusing on its composition, the environmental drivers governing its distribution, as well as on the magnitude and extent of migration over the water column. The specific objectives of this work are now outlined in order to answer the following questions:

What is the faunal composition of the acoustic scattering layers observed in the subtropical northeast Atlantic and which migration patterns do they follow? **Chapter 1**

To answer this question we describe acoustic phenomena found in shallow and mesopelagic waters of the Canary Islands by combining acoustic records at 18 and 38 kHz frequencies and net sampling at different hours of day and night.

What are the contributions of zooplankton and micronekton to migrant biomass and to carbon export in the subtropical northeast Atlantic? **Chapter 2**

To answer this question we simultaneously measured passive and active fluxes over several surveys performed in oceanic waters north of Gran Canaria. Migrant biomass of large zooplankton and micronekton were estimated by towing a new frame trawl across the migrant scattering layer, while carbon export was derived from the respiratory rates of the dominant migratory species.

How do environmental perturbations affect diel vertical migration and the deep-sea communities? **Chapter 3**

This question was able to be addressed opportunistically. During the present thesis a submarine volcano eruption occurring in the Canary Islands caused changes in the water light regime, temperature, and oxygen concentrations that induced anomalies in the pelagic community. The responses of the migrant biota were monitored through both acoustic and net sampling.

What is the effect of mesoscale eddies on the deep-sea fauna? **Chapter 4**

This question was addressed by combining hydrographic and acoustic *in-situ* measurements with satellite remote sensing to investigate, for the first time, the biophysical interactions between eddies and micronekton in the Canary Islands. The three-dimensional structure of the scattering biota was analyzed by systematically sectioning an anticyclonic eddy from surface to 1000 m depth with a 38 kHz echosounder.

What is the role of the micronekton in carbon export in the mesopelagic zone and beyond 1000 m depth? **Overall discussion**

Based on findings during the present thesis, as well as a review of micronekton vertical distributions in the region, we discuss the relative contribution of micronekton to carbon export in the mesopelagic zone and beyond 1000 m depth.

Part II

Results

Chapter 1

Vertical distribution, composition and migratory patterns of acoustic scattering layers in the Canary Islands.

Alejandro Ariza, José María Landeira, Alejandro Escánez, Rupert Wienerroither, Natacha Aguilar, Anders Røstad, Stein Kaartvedt, and Santiago Hernández-León (2015).

Submitted to *Journal of Marine Systems*.

Abstract

Diel vertical migration (DVM) facilitates biogeochemical exchanges between shallow waters and the deep ocean. An effective way of monitoring the migrant biota is by acoustic observations although the interpretation of the scattering layers poses challenges. Here we combine results from acoustic observations at 18 and 38 kHz with net sampling in order to unveil the origin of acoustic phenomena around the Canary Islands, subtropical northeast Atlantic Ocean. Trawling data revealed a high diversity of fishes, decapods and cephalopods (152 species), although few dominant species likely were responsible for most of the sound scattering in the region. We identified four different acoustic scattering zones in the mesopelagic realm: (1) at 400-500 m depth, a swimbladder resonance phenomenon at 18 kHz produced by gas-bearing migrant fish such as *Vinciguerria* spp. and *Lobianchia dofleini*, (2) at 500-600 m depth, a dense 38 kHz layer resulting likely from resonance of the gas-bearing and non-migrant fish *Cyclothone braueri*, and to a

lesser extent, from fluid-like migrant fish and decapods, (3) between 600-800 m depth, a weak signal at both 18 and 38 kHz ascribed either to migrant fish or decapods, and (4) below 800 m depth, a weak non-migrant layer at 18 kHz which was not sampled. All the dielly migrating layers reached the epipelagic zone at night, with the shorter-range migrations moving at about 4 cm s^{-1} and the long-range ones at nearly 12 cm s^{-1}. This work reduces uncertainties interpreting standard frequencies in mesopelagic studies, while enhances the potential of acoustics for future research and monitoring of the deep pelagic fauna in the Canary Islands.

Introduction

Acoustic scattering from marine organisms are caused by body structures with densities notably different from water, such as gas bladders or lipid inclusions [Simmonds and MacLennan, 2005]. Thanks to this phenomenon, the vertical distribution of pelagic animals can be easily monitored using scientific echosounders [Kloser et al., 2002, Kaartvedt et al., 2009, Cade and Benoit-Bird, 2015]. Two reflecting regions are normally visible in the ocean, the shallow and the deep scattering layers (SSLs and DSLs) occurring respectively in the epipelagic and the mesopelagic domains (0-200 and 200-1000 m depth), with the latter often portioned into multiple layers. Part of the biota forming the DSLs feed between dusk and dawn in the epipelagic zone, producing a thicker and more intense SSLs during the night. This displacement is known as Diel Vertical Migration (DVM), occurring on a daily basis around the world's oceans and performed by a large variety of zooplankton and micronekton species [Tucker, 1951, Barham, 1966, Roe, 1974, Pearre, 2003].

DVM promotes trophic interactions and biogeochemical exchanges between the upper layers and the deep ocean [Ducklow et al., 2001, Robinson et al., 2010], and its study is therefore important for understanding pelagic ecosystems functioning. Micronekton, the migrating component studied here, is expected to account for a substantial export of carbon to the deep ocean as they comprise a significant fraction of the migrant biomass [Angel and Pugh, 2000] and cover more extensive depth ranges than zooplankton [Badcock and Merrett, 1976, Roe, 1984b, Domanski, 1984]. In fact, the importance of micronektonic fishes and decapods in mediating carbon export has been recently highlighted by several studies [Hidaka et al., 2001, Davison et al., 2013, Schukat et al., 2013, Hudson et al., 2014, Ariza et al., 2015]. Therefore, using acoustic observations for monitoring their distribution and migrations may be a powerful tool for the ocean carbon pump assessment.

The present study was conducted in waters nearby the Canary Islands, a region in the subtropical northeast Atlantic exhibiting open-ocean and olygotrophic gyre characteristics [Barton et al., 1998, Davenport et al., 2002, Neuer et al., 2007]. Due to its position between temperate a tropical waters, this faunal province presents a high diversity of mesopelagic species in comparison to other latitudes [Backus and Craddock, 1977, Badcock and Merrett, 1977, Landeira and Fransen, 2012]. In the Canary Islands, the vertical distribution of fishes [Badcock, 1970], decapods [Foxton, 1970a,b], cephalopods [Clarke, 1969] and euphausiids [Baker, 1970] were thoroughly studied during the SOND cruise in the mid-sixties [Foxton, 1969], providing valuable knowledge about DVM in the area. More recent studies have contributed to a more detailed catalogue of mesopelagic species illustrating community differences between neritic and oceanic realms around the Canary Islands [Bordes et al., 2009, Wienerroither et al., 2009]. However, the lack of an integrated study combining acoustic data and biological information from net sampling has prevented the identification of the specific organisms responsible for each scattering layer occurring in the archipelago.

This study describes acoustic scattering layers at 18 and 38 kHz occurring from the surface to 1000 m depth in the Canary Islands, as well as their diel migrant movements between the epipelagic and the mesopelagic zone. We also present the first attempt to identify organisms causing these layers by trawling. The assessment of species composition of the scattering biota was complemented with a swimbladder resonance model, and also contrasted with previous reports of the micronekton vertical distribution in the region.

Methods

Survey

The survey was conducted in two locations southwest of La Palma and Tenerife Islands (Canary Islands), between the 1000 and 2000 m isobaths (Figure 1.1). From the 9^{th} to the 18^{th} of April, hydrographic and acoustic data, as well as micronekton samples were collected on board the R/V *Cornide de Saavedra*.

Hydrography

Vertical profiles of conductivity and temperature were collected using a SeaBird 9/11-plus CTD equipped with dual conductivity and temperature sensors. CTD sensors were calibrated at the SeaBird laboratory before the cruise. A sensor for measurements of

dissolved oxygen (SeaBird SBE-43) and fluorometer for chlorophyll *a* estimations (Wet-Labs ECO-FL) were linked to the CTD unit. Seawater analyses of dissolved oxygen (Winkler titrations) and chlorophyll *a* extractions were performed to calibrate the voltage readings of both sensors. Analyses were carried out in accordance with the JGOFS recommendations [UNESCO, 1994]. Temperature, dissolved oxygen and chlorophyll *a* profiles were averaged from 3 CTD casts performed within each sampling area off La Palma and Tenerife Islands (Figure 1.2).

Acoustics

Hull-mounted SIMRAD EK60 echosounders operating at 18 and 38 kHz (11° and 7° beam width, respectively) were used for recording acoustic data. Configuration was set at 1024 μs pulse duration and one ping every 3 seconds. Due to the draft of the transducer and to prevent near-field effects [Simmonds and MacLennan, 2005], acoustic data for the first 10 meters depth were not available. In order to avoid the range-increasing noise [Korneliussen, 2000], maximum depth of data used was 1000 m, and minimum threshold was set to -80 dB. The echosounders were calibrated *in-situ* by standard techniques [Foote et al., 1987]. Since acoustic records covered several days while trawling in each location, we opted for showing a composite echogram per location, which were obtained by averaging the daily acoustic data every minute (Figure 1.3 and 1.4). Fragments with scattering layers visibly affected by steaming noise or interferences from other acoustic devices were removed before averaging. Echograms were shown at 18 kHz and 38 kHz, and also as the difference between both frequencies (18 kHz minus 38 kHz). In order to calculate approximate vertical migration velocities, we manually marked sets of points over different migratory traces observed at 18 and 38 kHz. The velocities were extracted by averaging the slopes along the curves fitted to these points. All acoustic data were processed using customized applications in Matlab software.

Biological sampling

Micronekton was captured using a pelagic trawl with 300 m^2 mouth area and 45 m length. The mesh size was 80 cm near the opening, decreasing to 1 cm in the cod end. Hauls were performed horizontally along narrow depth ranges within the different scattering layers according to information provided by the echosounders and the Scanmar depth sensor attached to the trawl headline. Depth and time of each haul are pointed out by boxes overlaying a 24 hours echogram shown in Figure 1.3. Since the trawl had no opening-closing system, deploying and lifting were conducted minimizing towing to reduce the by-catch from non-desired strata. The towing speed varied between 2 and

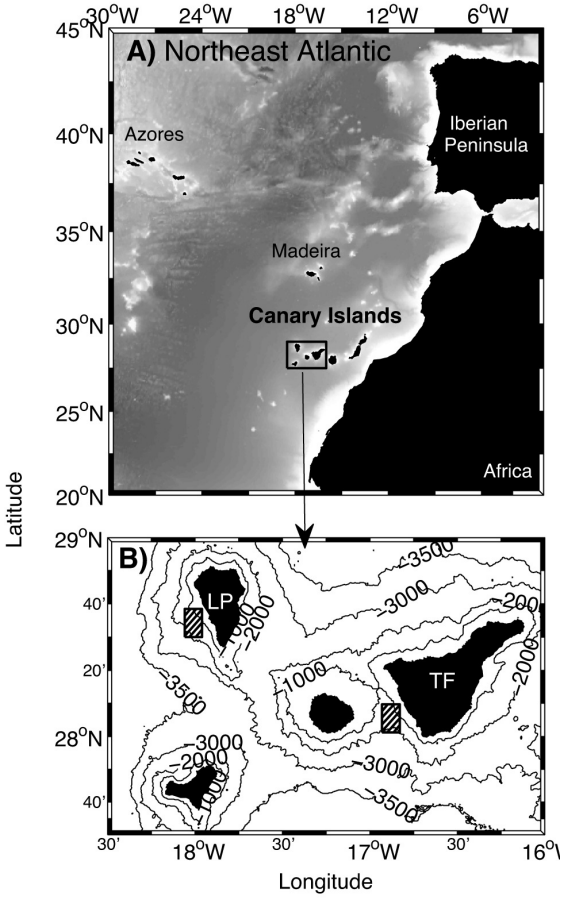

FIGURE 1.1: (A) Map showing the situation of the Canary Islands west off Africa. (B) Study areas southwest off La Palma and Tenerife Islands where acoustic recordings and net trawling were conducted (striped rectangles).

3 knots and the effective fishing time was one hour. Samples were frozen on board at -20°C. Once in the laboratory, they were fixed in 4% buffered formalin and later transferred to 70% ethanol for species identification, enumeration, weighing and length measurements. Catch results were not standardized by water volume filtered since the effective mouth size was uncertain due to the decreasing meshes along the trawl. Number of individuals were instead shown as "catch per unit effort" (CPUE), where effort was fishing time. Non-migrant species were excluded from abundances and biomass of the nocturnal epipelagic hauls (Table 1.1). For this, we checked the diel vertical distribution of micronekton species consulting the existing literature in the region [Clarke, 1969, Badcock, 1970, Foxton, 1970a,b, Badcock and Merrett, 1976, Roe and Badcock, 1984, Roe, 1984a]. We also excluded other non-migrant species that were detected in shallow waters during hauling tests performed at daytime.

The naming convention for hauls was, a first letter depicting whether the tow was conducted during the day (D) or during the night (N), followed by a 3-digit number indicating the averaged depth, and finally a letter indicating if the location was La

Palma (P) or Tenerife (T). For example, D450T would be a daytime haul conducted at an averaged depth of 450 m depth in Tenerife.

Community analyses

Community assemblage structure was analyzed through hierarchical agglomerative and unweighted arithmetic average (UPGMA) clustering based on the Bray-Curtis similarity matrix [Bray and Curtis, 1957]. Significant clusters were afterwards tested using the similarity profile procedure [SIMPROF, Clarke et al., 2008]. The high diversity of the sampled community posed difficulties for illustrating CPUE results for all the species identified in this study (152). Many of these species showed very low CPUE, presumably contributing poorly to acoustic scattering and migrations. For this reason, after clustering we focused the graphical results on dominant fishes, decapods and cephalopods involved in diel vertical migrations in the region, and also on the most abundant non-migrant species occupying the mesopelagic domain. Nevertheless, raw data of the entire community are also provided in supplementary material. Multivariate analyses were performed with Fathom toolbox for Matlab [Jones, 2014].

Source of scattering analysis

A target much smaller than its incident wavelength produces a weak echo that increases rapidly with higher frequencies. On the contrary, for large targets the frequency has little effect [Simmonds and MacLennan, 2005]. Besides, targets with densities very different from those of seawater resonate (high scattering) when their dimensions are shorter but near the wavelength of a given frequency. This is typically caused by "gas-bearing organisms", such as some swimbladdered fish found in this study. On the other hand, weaker scattering should be caused by "fluid-like organisms", which have a density similar to seawater [Stanton and Chu, 2000, Lavery et al., 2002, Korneliussen and Ona, 2003]. This is the case of crustaceans, squid or non gas-bearing fish also found in our samples. Accordingly, the frequency response at 18 and 38 kHz, together with the information from trawling, was used here to investigate the species most likely causing scattering. The condition and the equivalent spherical radius (ESR) of the swimbladder, if present, was noted for the dominant species inhabiting each scattering layer. Three different swimbladder conditions (gas-filled, contracted or fat-invested) were assigned according to the species and size consulting swimbladders studies of Marshall [1960], Kleckner and Gibbs [1972], and Badcock and Merrett [1977]. The ESRs were estimated on the basis of standard lengths using species-specific equations given by Saenger [1989]. If equations were not available from a given specie, the radius was obtained from swimbladder spherical

volumes of same size fishes given by Kleckner and Gibbs [1972] and using simple sphere calculations. Since swimbladder resonance also depends on the ambient pressure and the water density, a given swimbladdered fish may resonate or not depending on depth and frequency. Therefore, we also modeled the swimbladder scattering along depth at 18 and 38 kHz in order to investigate the cause of resonance on each strata. This was achieved following the model developed by Andreeva [1964], later adapted for prolate spheroids by Weston [1967], and applied as in Kloser et al. [2002].

$$\mathrm{TS} = 10\ \log_{10}(\sigma_{\mathrm{bs}}) \tag{1.1}$$

$$\sigma_{\mathrm{bs}} = a_{\mathrm{es}}^2 \left(\left(\left(\frac{f_{\mathrm{p}}}{f} \right)^2 - 1 \right)^2 + \frac{1}{Q^2} \right)^{-1} \tag{1.2}$$

$$f_{\mathrm{p}} = f_{\mathrm{o}} 2^{\frac{1}{2}} e^{-\frac{1}{3}} (1 - e^2)^{\frac{1}{4}} \left(\ln \left(\frac{1 + (1 - e^2)^{\frac{1}{2}}}{1 - (1 - e^2)^{\frac{1}{2}}} \right) \right)^{-\frac{1}{2}} \tag{1.3}$$

$$f_{\mathrm{o}} = \frac{1}{2\pi a_{\mathrm{es}}} \left(\frac{3\gamma P + 4\mu_1}{\rho} \right)^{\frac{1}{2}} \tag{1.4}$$

$$P = (1 + 0.103D)10^5 \tag{1.5}$$

TS is the target strength of the swimbladder. σ_{bs} is the acoustic backscattering cross-section at the incident acoustic frequency (f) of an equivalent spherical swimbladder volume of radius a_{es} with a prolate resonant frequency (f_{p}), and a resonance quality factor of Q. The prolate resonant frequency is a function of the prolate spheroid roundness (e) and the spherical resonant frequency (f_o) at a hydrostatic pressure (P) for fish depth (D) and fish tissue density (ρ), with a ratio of specific heats for the swimbladder gas (γ) and the real part of the complex shear modulus of the fish tissue defined by μ_1. The values assumed were: $\mu_1 = 105$ Pa, $\gamma = 1.4$, $\rho = 1.075$ kg m^{-3}, and $Q = 5$, following Kloser's et al. (2002) settings. We assumed e to be 0.3 according to swimbladder roundness values ranging from 0.2 to 0.4 for most mesopelagic fish species found in this study [Kleckner and Gibbs, 1972, Brooks, 1977]. Resonance was modeled for swimbladders of ESR from 0.3 to 1.8 mm, and from the surface to 1000 m depth.

Results

Hydrography

Both fishing areas were placed leeward of the islands presenting therefore similar hydrographical features (Figures 1.1 and 1.2). Sea surface temperature ranged between 19.5 and 19.8°C while seasonal thermoclines were not present in any location (mixing period). Subsurface chlorophyll maxima appeared between 50 and 100 m depth with values of 0.48 and 0.40 mg m^{-3} near La Palma and Tenerife Islands, respectively. Oxygen minima of about 3.3 mL L^{-1} were located between 700 and 800 m depth in both places. Values were well above hypoxia levels [<1.4 mL L^{-1}, Ekau et al., 2010].

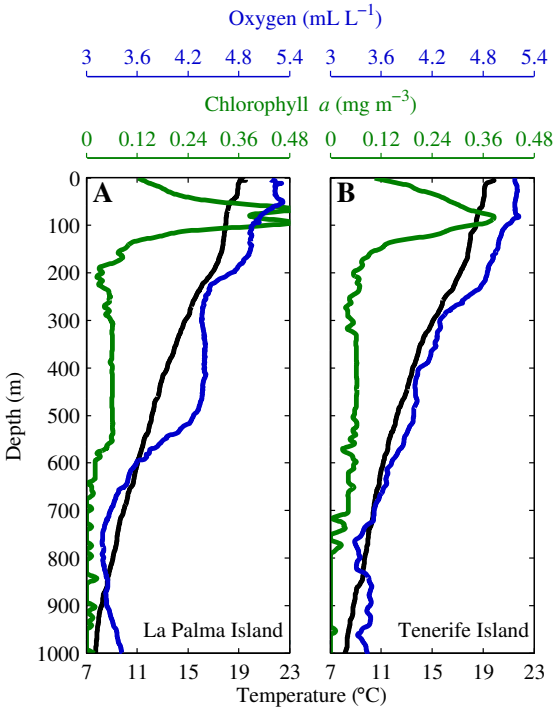

FIGURE 1.2: Averaged profiles of temperature, dissolved oxygen and chlorophyll *a* near (A) La Palma and (B) Tenerife Islands.

Distribution of acoustic scattering layers and migrations

According to the different responses shown at 18 and 38 kHz and the depth of occurrence, we distinguished one shallow scattering layer (SSL) in the epipelagic zone and four deep scattering layers (DSLs) in the mesopelagic zone. All of them occurring in waters around La Palma and Tenerife Islands (Figures 1.3 and 1.4). The SSL became denser and thicker at night as a consequence of the aggregation of migrant layers coming from deeper waters. This occurred roughly between the surface and 200 m depth coinciding with chlorophyll and oxygen maxima (Figure 1.2).

In the mesopelagic we identified (Figure 1.3): a zone characterized by a high backscattering at 18 kHz roughly between 400 and 500 m depth (DSL1), a zone mainly visible at 38 kHz between 500 and 600 m depth (DSL2), a weak backscattering zone at 18 and 38 kHz between 600 and 800 m depth (DSL3), and finally, a weak echo at 18 kHz approximately from 800 to 1000 m depth (DSL4). As exemplified in the echograms registered near La Palma, some scattering layers also exhibited diel vertical movements between the mesopelagic and the epipelagic zone. At sunset (Figures 1.4a and 1.4c), shallow upward migrations (U1) were registered from DSL1, moving at an averaged velocity of 4.5±2.6 cm s^{-1}. Simultaneously, deeper upward migrations (U2) moved from DSL3 to shallow waters at 11.4±4.4 cm s^{-1}. At sunrise (Figures 1.4b and 1.4d), shallow and deep migrations were observed following similar patterns but moving downwards (D1, D2). DSL1 at 18 kHz and DSL3 at 38 kHz practically disappeared during nighttime (signal close or below the minimum threshold, -80 dB). On the contrary, DSL2 at 38 kHz and DSL4 at 18 kHz apparently did not exhibit vertical movements. DSL2 was however slightly weaker during nighttime. These migratory patterns were visible at both frequencies everyday and everywhere regardless the location surveyed (La Palma or Tenerife Islands).

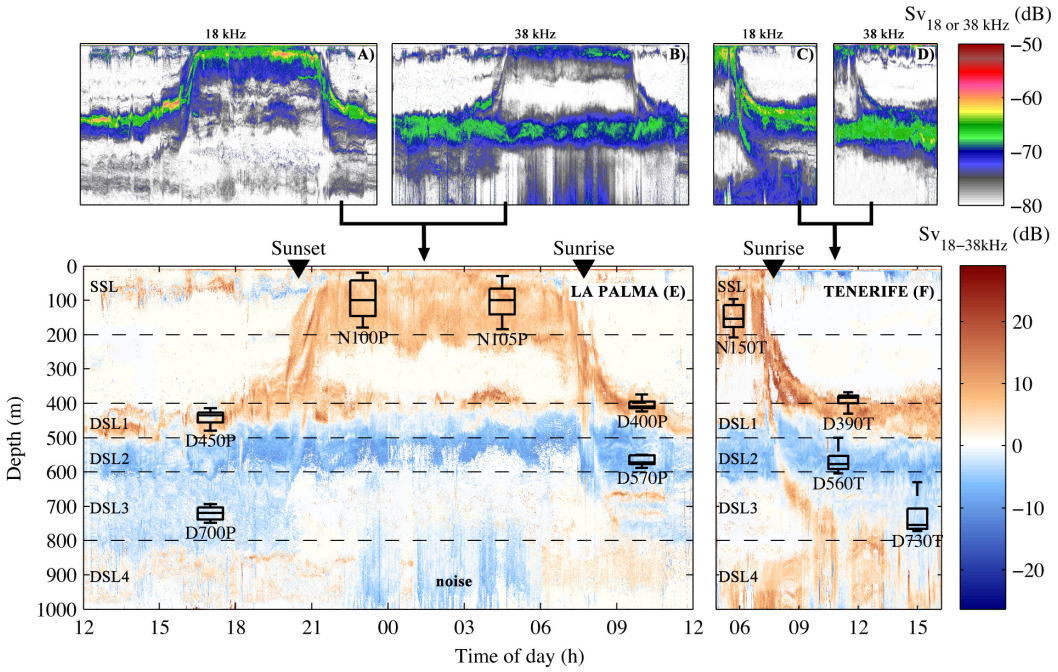

FIGURE 1.3: Echograms at 18 and 38 kHz in waters nearby La Palma (A and B) and Tenerife (C and D) Islands, and differential echograms (18 minus 38 kHz) from the same locations (E and F). Acoustic scattering layers are indicated according to frequency response and the depth of occurrence; one shallow scattering layer in the epipelagic (SSL), and four deep scattering layers in the mesopelagic (DSL1, DSL2, DSL3 and DSL4). Time and depth of fishing hauls are indicated with boxes, where the central lines are the trawling depth medians, the edges of the box are the 25th and 75th percentiles and the whiskers extend to the most extreme trawling depths not considered outliers.

Taxonomic composition of acoustic scattering layers

A total of 8199 individuals were classified, resulting in 104, 26 and 22 identified species of fishes, decapods and cephalopods, respectively. CPUE data per haul of all species captured during the survey is shown in supplementary material.

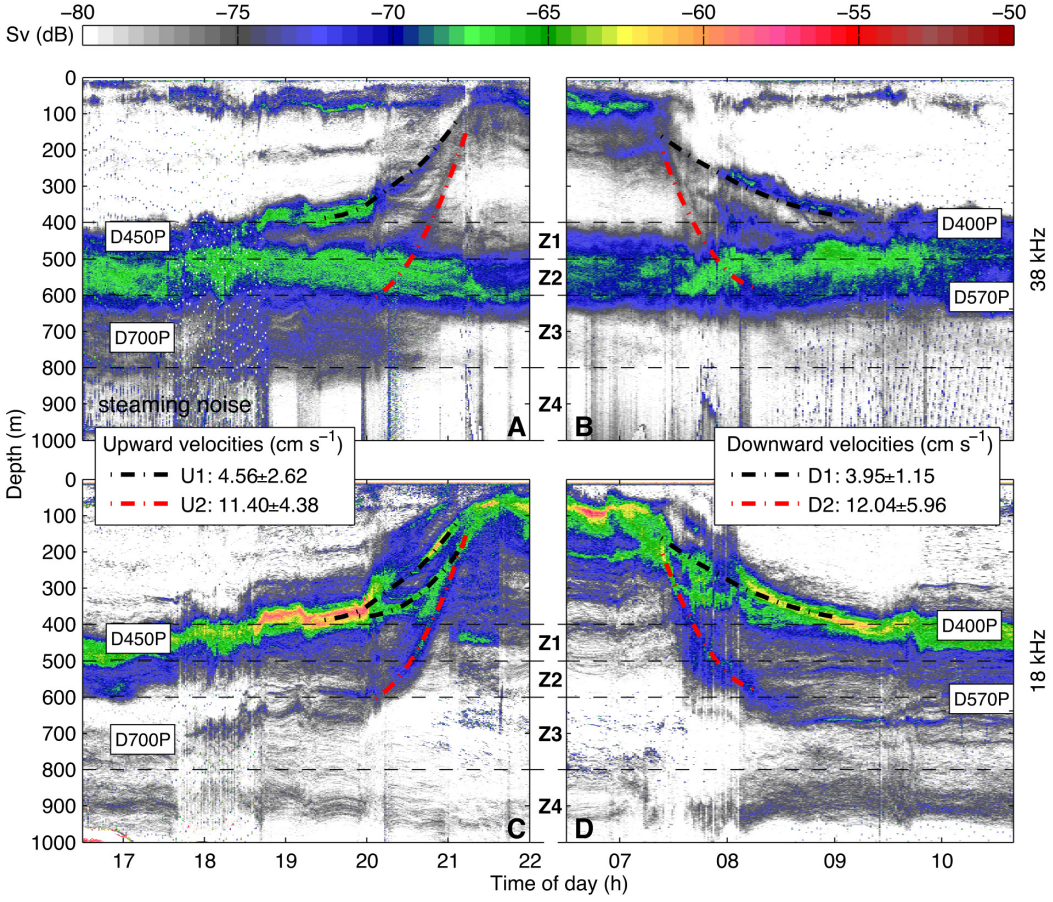

FIGURE 1.4: Same echograms at 38 (A and B) and 18 kHz (B and C) showing migratory pathways near La Palma Island. Different upward (U1, U2) and downward (D1, D2) tracks are indicated with dashed lines and their averaged migrant velocities are given in the legends. Distinct acoustic scattering layers (DSL1, DSL2, DSL3 and DSL4) are indicated according to divisions proposed in Figure 1.3. Text boxes over the echograms indicate depth and time of fishing hauls.

Fishes were the prevailing group captured within the nocturnal SSL (Table 1.1), contributing more than 70% in both abundance (%A) and biomass (%B). Myctophidae was the dominant fish family (54%A and 52%B), followed by Phosichthyidae (9%A and 4%B), Gonostomatidae (3%A and 5%B) and Sternoptychidae (1%A and 1%B). Among all fish species, only *Ceratoscopelus warmingii*, *Lobianchia dofleini*, *Hygophum hygomii* and *Vinciguerria attenuata* accounted for more than 30% of the migratory fish, both in abundance and biomass. Decapods were the second most important group in shallow waters at nigth (15%A and 9%B), dominated by the families Oplophoridae (9%A and 6%B) and Sergestidae (5%A and 1%B). The most abundant decapods were *Oplophorus*

spinosus, *Systellaspis debilis* and *Deosergestes corniculum*. Cephalopods were the least frequent taxon in terms of abundance but occupied the second place in biomass (13%A and 20%B). This group was dominated by the families Pyroteuthidae (9%A and 14%B) and Onychoteuthidae (2%A and 3%B), with *Pyroteuthis margaritifera*, *Pterygioteuthis giardi* and *Onychoteuthis banksii* as the prevalent migrating species.

Group	Family	CPUE (%)	Biomass (%)
Fis	**Myctophidae**	**53.56**	**51.65**
	Lepidophanes gaussi	10.64	6.54
	Lobianchia dofleini	8.73	4.66
	Ceratoscopelus warmingii	7.57	18.53
	Hygophum hygomii	7.26	3.95
	Lobianchia spp.	3.36	1.36
	Hygophum taaningi	2.49	0.94
	Hygophum reinhardtii	2.41	1.70
	Bolinichthys indicus	1.74	1.00
	Diaphus rafinesquii	1.47	0.83
	Lobianchia gemellarii	1.11	0.48
	Notoscopelus resplendens	0.88	3.70
	Phosichthyidae	**8.80**	**4.05**
	Vinciguerria attenuata	6.35	3.18
	Vinciguerria nimbaria	1.31	0.50
	Vinciguerria poweriae	1.14	0.37
	Gonostomatidae	**2.58**	**4.83**
	Gonostoma elongatum	1.85	4.09
	Gonostoma denudatum	0.54	0.64
	Sternoptychidae	**1.43**	**1.01**
	Argyropelecus aculeatus	1.43	1.01
Dec	**Oplophoridae**	**8.56**	**5.83**
	Oplophorus spinosus	7.08	4.58
	Systellaspis debilis	1.48	1.25
	Sergestidae	**5.04**	**1.22**
	Deosergestes corniculum	1.90	-
	Sergia splendens	0.55	-
	Sergestes spp.	0.51	-
Cep	**Pyroteuthidae**	**9.22**	**14.21**
	Pyroteuthis margaritifera	7.38	6.83
	Pterygioteuthis giardi	1.84	7.39
	Onychoteuthidae	**1.76**	**3.34**
	Onychoteuthis banksii	1.76	3.34

TABLE 1.1: **Relative abundance (%) and biomass (%) of species found in the nocturnal shallow scattering layer.** Values were averaged from hauls N100P, N105P and N150T (see Figure 1.3). Only organisms identified to the species level and with CPUEs above 0.5% are shown.

Cluster analyses of the faunistic composition revealed 4 significant groups (SIMPROF routine, $P<0.001$) at a similarity distance of 0.8. Further, the clusters grouped according to the towing depth and time, but regardless of the location surveyed (Figure 1.5). Nocturnal catches in shallow waters showed the highest CPUEs of vertical migrants, which assembled separately from the rest of hauls (red cluster). In the mesopelagic zone,

the hauls conducted within the DSL1 were almost exclusively composed by the myctophid *Lobianchia dofleini* and other small fishes from the genus *Vinciguerria* (green cluster). The DSL2 was characterized by the occurrence of the non-migrant fish *Cyclothone braueri* and also the presence of vertical migrants such as the lanternfish *Hygophum hygomii*, the dragonfish *Chauliodus danae* or the decapod *Oplophorus spinosus* (blue cluster). The deepest hauls conducted within the DSL3 also clustered together. Here, the most remarkable feature was the massive presence of the non-migrant fish *Cyclothone microdon*, but also the relative high CPUEs of lanternfishes such as *Lepidophanes gaussi* or *Hygophum reinhardtii*, and also several decapods species from the family Sergestidae.

		CPUE (%)	Length (mm)	Swimbladder	ESR (mm)
DSL1	*Lobianchia dofleini*	24 (6-43)	22	gas-filled[b]	0.6[d]
	Vinciguerria attenuata	18 (8-36)	35	gas-filled[a,b]	1.2[d]
	Vinciguerria poweriae	10 (7-16)	33	gas-filled[b]	1.1[d]
	Vinciguerria nimbaria	8 (4-14)	32	gas-filled[a]	n/a
	Diaphus rafinesquii	6 (1-8)	49	gas-filled[a,b]	2.2[d]
	Pyroteuthis margaritifera	5 (2-9)	22	none	-
DSL2	*Hygophum hygomii*	20 (15-25)	35	contracted[b]	0.9[d]
	Chauliodus danae	9 (9-10)	120	none	-
	Oplophorus spinosus	9 (4-13)	25	none	-
	Cyclothone braueri	8 (7-9)	23	gas[a,c]/fat[b]-invested	0.7[b]
	Gonostoma elongatum	7 (6-8)	133	fat-invested[a]	n/a
	Parasergestes armatus	5 (3-7)	51	none	-
DSL3	*Cyclothone microdon*	46 (38-54)	54	fat-invested[a,c]	n/a
	Lepidophanes gaussi	13 (11-14)	41	unknown	1.4[d]
	Cyclothone pseudopallida	10 (4-16)	43	fat-invested[a,c]	n/a
	Sergestes spp.	10 (7-12)	46	none	-
	Hygophum reinhardtii	8 (6-10)	34	unknown	n/a
	Deosergestes corniculum	6 (4-7)	75	none	-

[a]Marshall [1960]
[b]Kleckner and Gibbs [1972]
[c]Badcock and Merrett [1977]
[d]Saenger [1989]

TABLE 1.2: Dominant species forming each scattering layer with indications of relative abundances within catches (CPUE), modal lengths, and if present, the swimbladder condition according to the literature. ESR depicts the equivalent spherical radius of the swimbladder, as estimated from the standard length of fishes using species-specific equations given by Saenger [1989], or calculated from swimbladder spherical volumes given by Kleckner and Gibbs [1972]. CPUEs are given as means, but ranges are also noted between parentheses.

Dominant targets and their acoustic properties

Despite the high diversity, each scattering region was numerically dominated by a few species for which we collected information about their swimbladder, if present (Table

1.2). According to catch data, most of the organisms in the DSL1 were fishes from 22 to 35 mm in length, bearing gas-filled swimbladders with ESR from 0.6 to 1.2 mm. In the DSL2, the catches were dominated either by fishes or decapods with sizes ranging from 22 to 133 mm, and with *Cyclothone braueri* being the only specie susceptible to bear gas in the swimbladder. In the case of the DSL3, *Cyclothone microdon* accounted for most of the catches, a fish with a modal length of 54 mm and bearing a fat-invested swimbladder. Myctophids and sergestids were also well represented in the DSL3.

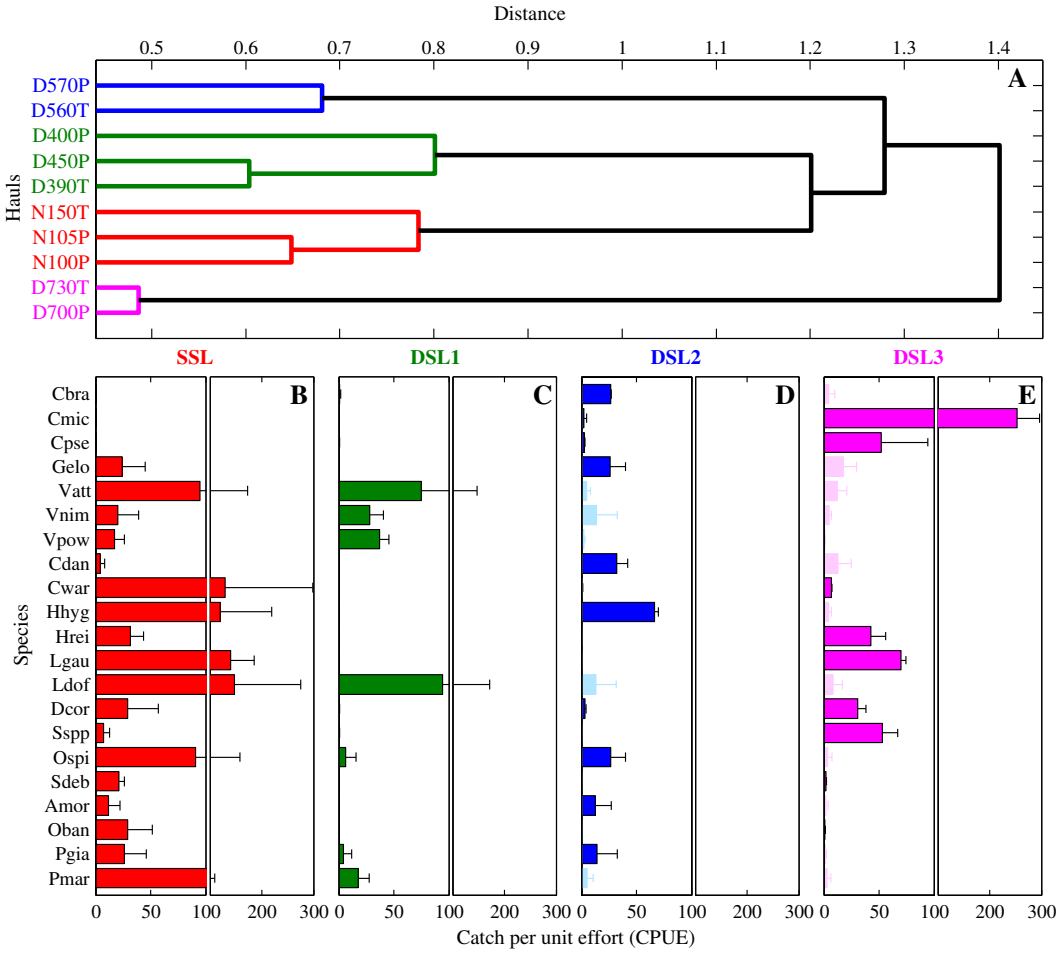

FIGURE 1.5: (A) Dendrogram showing classification of fishing hauls according to Bray-Curtis dissimilarity distances. Time and depth of each haul can be checked in Figure 1.3. (B-E) CPUEs of dominant species contributing to differences among clusters. Light-colored bars indicate possible contamination from upper strata (see discussion). Species abbreviations: Cbra= *Cyclothone braueri*; Cmic= *Cyclothone microdon*; Cpse= *Cyclothone pseudopallida*; Gelo= *Gonostoma elongatum*; Vatt= *Vinciguerria attenuata*; Vnim= *Vinciguerria nimbaria*; Vpow= *Vinciguerria poweriae*; Cdan= *Chauliodus danae*; Cwar= *Ceratoscopelus warmingii*; Hhyg= *Hygophum hygomii*; Hrei= *Hygophum reinhardtii*; Lgau= *Lepidophanes gaussi*; Ldof= *Lobianchia dofleini*; Dcor= *Deosergestes corniculum*; Sspp= *Sergestes* spp.; Ospi= *Oplophorus spinosus*; Sdeb= *Systellaspis debilis*; Amor= *Abraliopsis moriisi*; Oban= *Onychoteuthis banksii*; Pgia=*Pterygioteuthis giardi*; Pmar = *Pyroteuthis margaritifera*.

Discussion

Scientific echosounders are a powerful tool to study the distribution and behavior of the pelagic biota [Kloser et al., 2002, Kaartvedt et al., 2009, Cade and Benoit-Bird, 2015]. The potential to extract information of biological significance is enhanced when acoustic data are validated with net sampling, as in this study. However, trawling data should be interpreted with caution in order to accurately identify the animals most likely causing sound scattering in the region. First, as expected, a high diversity of mesopelagic species was found here in the subtropical Atlantic (152 species identified in this survey). This introduces a broad list of likely targets, each one with different acoustic properties. Secondly, it is possible that some species found in deep hauls came from contamination of upper layers due to the lack of an opening-closing system in our trawl. This contamination should be reduced according to the velocity of deploying and lifting maneuvers, where the trawl crossed other scattering layers within less than 5 minutes and not in an adequate fishing position. This represented less than 10% of the effective fishing time. With analogous trawling settings, Watanabe et al. [1999] calculated a contamination of less than 2% in the northwestern Pacific. In spite of this, we adopted the precautionary principle of considering susceptible of contamination all the species with CPUEs lower than 50, as long as these species also occurred at higher abundances in upper strata (see light-colored bars in Figures 1.5d and 1.5e). This did not apply therefore to hauls conducted in shallow waters, or those in the DSL1 at daytime. Contaminated or not, this approach only excludes non-dominant species, which on the other hand, are expected to poorly contribute to sound scattering due to their low abundances.

Therefore, in order to find the main cause of reverberation, here we focused on the acoustic properties of the dominant species captured within each scattering layer. It should be noted, however, that these scattering zones must also be inhabited by many species not visible in our echograms, either because their weak signal is easily masked by dominant sound reflectors, or because they do not respond at all under the insonifying frequency.

The distribution of scattering layers as well as their species composition was quite similar regardless the location surveyed, which in fact, also presented similar hydrographic conditions (Figure 1.2). We systematically observed two strong layers between 400 and 600 m depth (Figure 1.3), the upper one responding higher at 18 kHz (DSL1), and the lower one at 38 kHz (DSL2). This layout has been previously documented at other latitudes, where the upper layer at 18 kHz has been ascribed to the resonance of small swimbladdered fishes such as the pearlside *Maurolicus muelleri* [Kaartvedt et al., 2008, Godø et al., 2009] or different species of myctophids [Olivar et al., 2012, Peña et al.,

2014]. According to the model developed by Kloser et al. [2002], animals bearing gas bladders of ESR about 1.2-1.4 mm are susceptible to resonate at 18 kHz when inhabiting waters between 400-500 m depth (see Figure 1.6a). In our study the DSL1 was mainly inhabited by gas-filled swimbladdered animals, being the lightfishes *Vinciguerria* spp. the targets most likely producing resonance at 18 kHz (ESR= 1.2 mm, Table 1.2). According to the same model, *L. dofleini* might be causing swimbladder resonance at similar depths but at 38 kHz (ESR=0.6 mm, Table 1.2 and Figure 1.6b). Another clue supporting that these layers are mainly caused by swimbladder resonance is the changing backscattering during vertical migration (averaged Sv from -65 dB to -59 dB, see Figures 1.4c and 1.4d). This is because the effective scattering cross section of fishes varies substantially when changing depth due to little variations of the swimbladder dimensions, typically showing maximum values between 150 and 400 m depth [Andreeva, 1964, Godø et al., 2009].

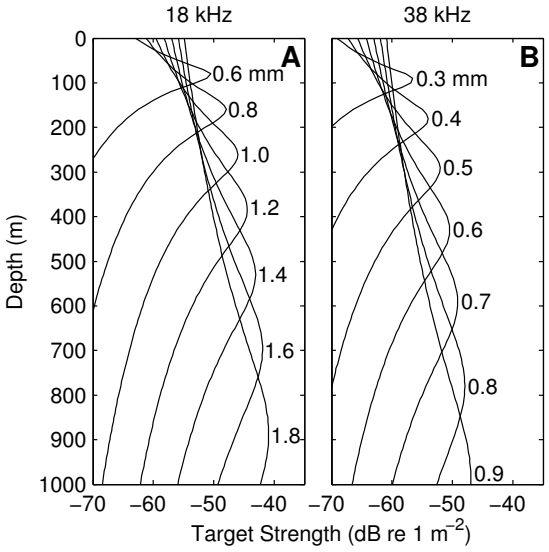

FIGURE 1.6: Modeled swimbladder resonance at (A) 18 and (B) 38 kHz along depth according to Kloser et al. [2002]. Each line represents expected target strengths for swimbladders of different equivalent spherical radius (ESR, mm).

Among the dominant animals inhabiting the DSL2, only the swimbladdered fish *Cyclothone braueri* was susceptible to bear gas, the rest should be considered as fluid-like targets according to the literature (see Table 1.2). *C. braueri* might be the main reflector, even though its presence was not especially prominent in our catches (Figures 1.5d and 1.5e). According to previous studies, *C. braueri* is extremely abundant at the DSL2 when using sampling gears with smaller meshes [Badcock, 1970, Badcock and Merrett, 1976, Roe and Badcock, 1984]. We think therefore that this species was widely underestimated due to the large meshes of the trawl used here. Although in low numbers, the prevalence of *C. braueri* between 500 and 600 m depth, and its scarcity at other strata, also suggests that this species was mainly constrained within the DSL2 in our

study. Another clue is that the DSL2 does not exhibit vertical movements, while *C. braueri* does not conduct diel vertical migrations either [Goodyear et al., 1972, Badcock and Merrett, 1976]. It is difficult to predict the size range over which fat-investment occurs in *C. braueri* since there is a considerable variability between individuals [Marshall, 1960, Kleckner and Gibbs, 1972, Badcock and Merrett, 1977]. Here, the swimbladder condition was assigned for individuals of 23 mm (modal length), not being clear whether gas was displaced by fat at this stage or later (see Table 1.2). However, it should be taken into account that we probably biased abundances of *C. braueri* towards large specimens. Proof of this can be seen in previous studies with smaller sampling gears, where specimens captured ranged approximately from 10 to 30 mm at similar depths [Badcock, 1970, Badcock and Merrett, 1976, Roe and Badcock, 1984]. Thus, it is probably that both gas-filled and fat-invested swimbladders occur in the population of *C. braueri* inhabiting near the DSL2. The former group, with swimbladders of ESR about 0.7 mm, could be responsible of the acoustic resonance at 38 kHz (see Table 1.2 and Figure 1.6b). Notwithstanding the foregoing, the slight weakening of this layer at night also suggests that part of the backscattering might be caused as well by dielly migrating animals (Figures 1.4a and 1.4b). This is supported by the presence of dominant migrants in the DSL2, such as the lanternfish *Hygophum hygomii* or the decapod *Oplophorus spinosus* (Figure 1.5d). Both would be fluid-like targets according to Table 1.2. Since the size of these species and many others would produce an optimum signal at 38 kHz according to acoustic principles [Simmonds and MacLennan, 2005], it is plausible therefore that the DSL2 was mainly caused by swimbladder resonance, but also by high densities of fluid-like organisms. Based on the above, *C. braueri* would likely be the most abundant and best reflector target.

Acoustic scattering was notably lower below 600 m depth, where differences in the frequency response suggested the existence of different community strata. From 600 to 800 m depth (DSL3) sound reflection was mainly caused by migrant biota as evidenced by the diel vertical movements of both the 18 and 38 kHz scattering layers (Figure 1.4). Here the captures were clearly dominated by *Cyclothone microdon* (Figure 1.5f), a fish which could in principle be a likely target causing scattering if it were not for the fact that this species does not conduct migrations [Goodyear et al., 1972, Badcock and Merrett, 1976]. Besides, *C. microdon* and other species of the genus inhabiting below 600 m depth, are no longer potential sound reflectors due to the fat investment of their swimbladders at earlier stages in shallower waters [Badcock and Merrett, 1976, 1977]. Therefore, dominant migrants in the DSL3 must be the most likely acoustic targets. Among others, the myctophids *Lepidophanes gaussi*, *Hygophum reinhardtii*, and many species of sergestids were especially abundant at these depths. According to the literature, *L. gaussi* and *H. reinhardtii* bear swimbladders which in case of being

functional (gas-filled) could cause resonance at 18 kHz (Figure 1.6a). Although we lack such information (Table 1.2), the scattering levels below 600 m depth are not indicative of swimbladder resonance. This is consistent with the fact that swimbladders are usually contracted (atrophied) in myctophids reaching these depths (see discussion below). Therefore, it is probably that both fishes and decapods inhabiting this strata behave as fluid-like targets, but uncertain which one causes more reflection.

Contracted swimbladders are a common feature in large myctophids, which is the same as saying that the functionality of the swimbladder decreases with migration depth [Marshall, 1960, Butler and Pearcy, 1972, Davison, 2011a]. This is especially true in our study area, where the smallest myctophid *Lobianchia dofleini* exhibits the shallower migration depth while largest species such as *Ceratoscopelus warmingii* or *Notoscopelus resplendens* reach bathypelagic waters [Badcock and Merrett, 1976]. Since a "cottony tissue" (expanded fibrous submucosa) fills most of the lumen in contracted swimbladders, the external size of the organ is probably not an accurate indication of the gas volume contained [Capen, 1967, Kleckner and Gibbs, 1972]. According to swimbladder catalogues, gas-bearing fishes occurred in our study only above 600 m depth, while swimbladders regressions in both *Cyclothone* species and myctophids are a common feature at deeper waters (see Table 1.2). In acoustic terms, this means that the deep mesopelagic zone must be dominated by fluid-like targets, where resonance models are hardly applicable. It would also explain why the relative high abundances from net sampling does not result in high backscattering at these depths.

The DSL4 (800-1000 m depth) was out of reach of our trawl and this impeded the assessment of the species producing reflection. Although the deeper migrations observed in this study are somewhat associated with the DSL3 and DSL4, the latter was clearly visible both during day and night. This suggests that the DSL4 would mainly be caused by non-migrating organisms. In this respect, literature may provide clues about the likely targets. Below 800 m depth, non-migrant fishes such as *Cyclothone pallida* and *Sternoptyx diaphana* are abundant, but also large migrant fishes which not conduct migrations every day, such as *Ceratoscopelus warmingii* or *Notoscopelus resplendens* [Badcock, 1970]. *C. warmingii* individuals dominated at night in the SSL but were scarce in our daytime mesopelagic hauls, suggesting that they must inhabit somewhere below 800 m depth. Besides, the DSL4 is the most frequented daytime foraging zone by short-finned pilot-whales in the Canary Islands (*Globicephala macrorhynchus*), whose diet is known to be mainly composed by squid but also large fishes [Aguilar Soto et al., 2008]. Hence, both fishes or squid might be responsible of the DSL4 but also many other targets. Deeper hauls with concurrent acoustic records are therefore required to unveil the specific origin of this reflection.

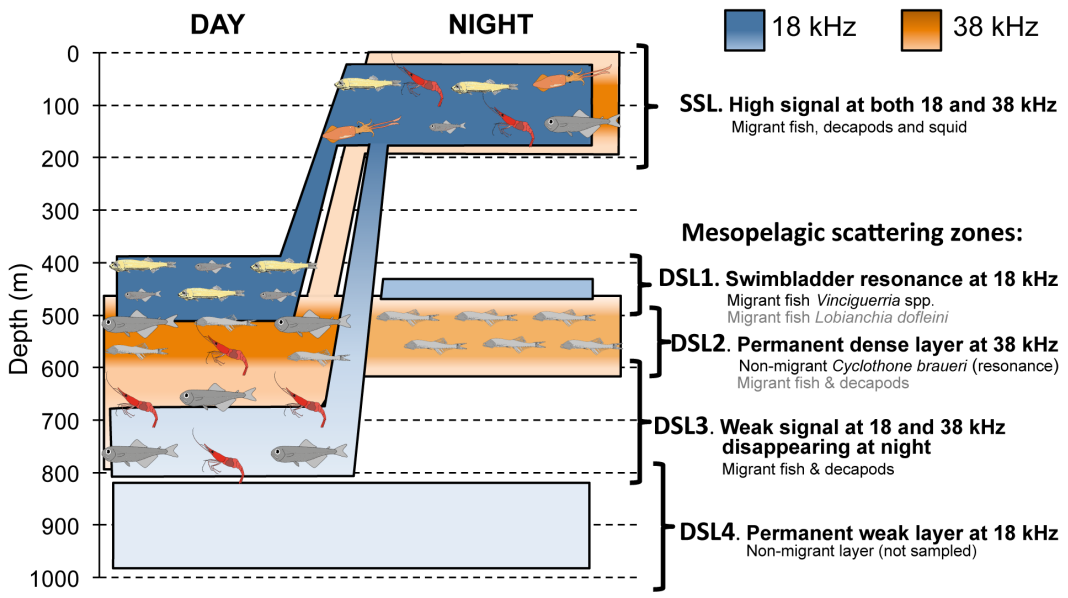

FIGURE 1.7: Distribution of shallow and deep scattering layers (SSL and DSLs) based on observations at 18 and 38 kHz in waters around the Canary Islands (threshold -80 to -50 dB). Only dominant animals likely to contribute more to backscattering are indicated (main scatterers in black, and secondary ones in gray). Blue and orange depict 18 and 38 kHz frequencies respectively, with dark colors indicating high backscattering and light colors representing weak backscattering. See discussion for further details.

Overall, the association of scattering layers and animals proposed here (Figure 1.7) is consistent with the vertical distribution previously observed during the SOND expedition in the Canary Islands and other surveys in nearby oceanic waters [Foxton, 1969, Badcock and Merrett, 1976, Roe et al., 1984a]. Specifically, Badcock [1970] and Badcock and Merrett [1976] noted that most myctophid species inhabited between 400 and 600 m depth, while less species of larger sizes appeared deeper than 700 m depth. Their abundance tables also evidenced the shallower distribution for *Lobianchia dofleini* and *Vinciguerria* spp., and showed a prominent peak of *Cyclothone braueri* between 500 and 600 m depth. This matches with our description of the DSL1 and the DSL2. On the other hand, Foxton [1970a] and Foxton [1970b] reported maximum densities of decapods below 650 m depth. In this respect, both Badcock's and Foxton's studies proposed a distinction between "shallow and deep mesopelagic fauna", which they ascribed to adaptations for different light conditions. Based on the above, the interphase of high and weak scattering seen here around 600 m depth might be outlying this "biocline" [Lezama-ochoa et al., 2014], with small and gas-bearing animals above, and larger and fluid-like organisms below. In fact, the increased migrant velocity of the deeper scattering biota (about 11-12 cm s^{-1}) also supports the idea of larger and non gas-bearing animals. They can move faster not only because of their increased size, but also for not requiring gas volume adjustments during vertical migrations [Marshall, 1960, Butler and Pearcy, 1972, Kleckner and Gibbs, 1972].

In conclusion, this study has revealed a high diversity within the micronekton mesopelagic community (152 species identified), yet with few dominant species likely being responsible for most of the acoustic phenomena in the region. We suggest that the DSL1 (400-500 m depth) is largely formed by swimbladder resonance, produced by the migrant fishes *Vinciguerria* spp. and *Lobianchia dofleini*. We ascribe the DSL2 (500-600 m depth) to resonance of the gas-bearing fish *Cyclothone braueri*, but also to high densities of fluid-like migrant fish and decapods. The DSL3 (600-800 m depth) was caused either by migrant fish or decapods, but as for other layers occurring deeper, the specific target identities remain unknown. All layers exhibiting diel vertical movements reached the epipelagic zone at night, with the shorter migrations moving at about 4 cm s^{-1} and the larges ones at nearly 12 cm s^{-1}. This work reduces uncertainties interpreting sound scattering, although more accurate results will be obtained with deeper and higher vertical resolution trawling, using multifrequency lowering echosounders, as well as improving scattering models for pelagic animals in the region.

Acknowledgements: We are grateful to the officers and the crew of the R/V *Cornide de Saavedra* for their work and support at sea. Thanks are also due to Verónica Benítez-Barrios, José Escánez, Laia Armengol and Erika González for hydrographic data collection and water samples analyses. We are as well indebted to Ángel Guerra, Ángel González, M^a del Carmen Mingorance and Vailett Müller for their valuable work on board identifying species. This work was funded by the Spanish Government projects CETOBAPH (CGL2009-13112) and MAFIA (CTM2012-39587). Alejandro Ariza was supported by a postgraduate grant from the Spanish Ministry of Science and Innovation (BES2009-028908).

Chapter 2

Migrant biomass and respiratory carbon flux by zooplankton and micronekton in the subtropical northeast Atlantic Ocean (Canary Islands).

Alejandro Ariza, Juan Carlos Garijo, José María Landeira, Fernando Bordes, and Santiago Hernández-León (2015).

Published in *Progress in Oceanography* 134:330-342.

Abstract

Diel Vertical Migration (DVM) in marine ecosystems is performed by zooplankton and micronekton, promoting a poorly accounted export of carbon to the deep ocean. Major efforts have been made to estimate carbon export due to gravitational flux and to a lesser extent, to migrant zooplankton. However, migratory flux by micronekton has been largely neglected in this context, due to its time-consuming and difficult sampling. In this paper, we evaluated gravitational and migratory flux due to the respiration of zooplankton and micronekton in the northeast subtropical Atlantic Ocean (Canary Islands). Migratory flux was addressed by calculating the biomass of migrating components and measuring the electron transfer system (ETS) activity in zooplankton and dominant species representing micronekton (*Euphausia gibboides*, *Sergia splendens* and

Lobianchia dofleini). Our results showed similar biomass in both components. The main taxa contributing to DVM within zooplankton were juvenile euphausiids, whereas micronekton were mainly dominated by fish, followed by adult euphausiids and decapods. The contribution to respiratory flux of zooplankton (3.4±1.9 mg C m^{-2} d^{-1}) was similar to that of micronekton (2.9±1.0 mg C m^{-2} d^{-1}). In summary, respiratory flux accounted for 53% (range 23 to 71) of the gravitational flux measured at 150 m depth (11.9±5.8 mg C m^{-2} d^{-1}). However, based on larger migratory ranges and gut clearance rates, micronekton are expected to be the dominant component that contributes to carbon export in deeper waters. Micronekton estimates in this paper as well as those in existing literature, although variable due to regional differences and difficulties in calculating their biomass, suggest that carbon fluxes driven by this community are important for future models of the biological carbon pump.

Introduction

The oceans play a key role in the global carbon cycle, sequestering roughly 30% to 50% of the total anthropogenic CO_2 since the beginning of the industrial revolution [Sarmiento, 1993, Sabine et al., 2004, Denman et al., 2007]. The biological pump is one of the most important pathways through which carbon is transported vertically into the ocean [Ducklow et al., 2001, Fasham, 2003]. Therefore, understanding how it functions is of paramount importance in developing accurate global carbon models [Usbeck et al., 2003]. Its process consists of the fixation of inorganic carbon into organic carbon by photosynthesis and its transport downwards by both passive and active mechanisms [Ducklow et al., 2001]. Much effort has been dedicated to the former mechanism, the so-called gravitational flux, which refers to the sedimentation of organic matter through the water column [Fowler and Knauer, 1986, Buesseler et al., 2007]. In contrast, the active flux has been largely neglected by those who have analyzed carbon budgets in oceanic ecosystems. This flux is also known as migratory flux and refers to organic material that is actively transported by animals. The photoassimilated carbon is ingested on the surface by herbivores and subsequently by carnivores that swim to deeper waters, where they release carbon by respiration [Longhurst et al., 1990], excretion [Steinberg et al., 2000], defecation [Turner, 2002] and mortality [Zhang and Dam, 1997].

The behavior involving this transport is known as diel vertical migration (DVM). This proccess occurs on a daily basis in all oceans and is performed by a large variety of species of zooplankton and micronekton [Tucker, 1951, Barham, 1966, Roe, 1974, Pearre, 2003]. Most research involving migratory flux has focused on zooplankton [Longhurst et al., 1990, Zhang and Dam, 1997, Hernández-León et al., 2001, Steinberg et al., 2008], as its

sampling is relatively simple compared to that of larger organisms. Micronekton, mainly composed of fish, crustaceans and cephalopods ranging from 2 cm to 10 cm [Brodeur et al., 2005], exhibit a faster swimming capacity, and require larger, more expensive and time-consuming trawls for sampling [Koslow et al., 1997, Pakhomov et al., 2010, Kaartvedt et al., 2012b]. Nevertheless, because of their high mobility, micronekton might export carbon to deeper waters than zooplankton does. In addition, most of the ingested carbon at the surface is exported to their maximum inhabiting depth, since their guts take from hours to days to be evacuated [Baird et al., 1975, Clarke, 1982], whereas gut clearances in zooplankton only take a few minutes [Dam and Peterson, 1988].

In view of the above, migrant micronekton, together with zooplankton, are expected to considerably increase current estimates of migratory flux. A few notable studies have recently reinforced this hypothesis. The work by Hidaka et al. [2001] in the western equatorial Pacific is to our knowledge unique, as it simultaneously evaluates gravitational and migratory fluxes by both zooplankton and micronekton. They reported respiratory flux due to total micronekton of 28% to 55% of the gravitational flux at 160 m depth, while summing up zooplankton, this value accounted for 46% to 89%. In the northeast Pacific, Davison et al. [2013] recently estimated a "fish-mediated export" of about 18% to 19% of the gravitational flux at a similar depth. Whereas in the Benguela upwelling system, Schukat et al. [2013] estimated a respiratory flux by decapods of 79% of the gravitational flux. The most recent attempt to estimate carbon transport by fish was conducted by Hudson et al. [2014] along the Mid-Atlantic Ridge and determined an export flux mediated by myctophids of up to 8% of the gravitational flux in the vicinity of the Azores Islands. Although these estimates are somewhat variable, they confirm that micronekton account for a significant fraction of the total carbon export in oceanic ecosystems.

To contribute to these emerging studies, we present in this paper the first simultaneous evaluation of the gravitational and migratory carbon flux north of the Canary Islands by including both zooplankton and micronekton. This region of the northeast subtropical Atlantic is located in the upstream Canary Current, 400 km west of the African coastal upwelling system and therefore exhibits open-ocean and oligotrophic gyre characteristics [Barton et al., 1998, Davenport et al., 2002, Neuer et al., 2007]. The composition of both communities is described and their migrant biomass estimated. We also measured the electron transfer system (ETS) activity in zooplankton and the dominant species representing micronekton (*Euphausia gibboides*, *Sergia splendens* and *Lobianchia dofleini*) in order to assess the respiratory carbon flux by both migrating components.

Methods

Surveys and hydrography

From 24 March to 2 June 2011, nine surveys were carried out on a weekly basis in the Canary Current waters, in an oceanographic station (28° 31' N, 15° 22' W) 30 nautical miles north of Gran Canaria island (see Fig. 2.1). During this period, hydrographic, acoustic and biological samplings were performed on board the R/V *Atlantic Explorer*. Water samples were obtained using a rosette of six 4-L Niskin bottles. Vertical profiles of conductivity, temperature and fluorescence were collected to a 200 m depth using a SeaBird SBE 25plus CTD and a Turner SCUFA fluorometer attached to the rosette. Seawater analyses of chlorophyll *a* were performed in accordance with JGOFS recommendations [UNESCO, 1994] in order to calibrate the voltage readings of the fluorometer.

Acoustics

Acoustic data were recorded using a SIMRAD EK60 echosounder (7° beam width) operating at 120 kHz. The configuration was set at a 1024 μs pulse duration and 1 s^{-1} ping rate. Prior to sunset and net trawling, the transducer was deployed into the water at roughly a 4 m depth, hanging from the starboard side while the vessel remained stationary. Data above a 10 m depth were excluded to prevent vessel-caused bubbles and near-field effects [MacLennan and Simmonds, 1992]; the maximum recorded depth was set at 200 m to avoid range-increasing noise [Korneliussen, 2000]. Once the DVM (nocturnal ascent) was completed and the migrant scattering layer appeared above a 200 m depth, the echosounder continued recording for 30 min. The Volume Backscattering Strength (S_v, units: dB re 1 m^{-1}) was used as a proxy for the relative density of the migrant fauna during the sampling period. The minimum detection threshold was set at -80 dB.

Gravitational flux

Sinking particles were collected at 150 m depth using a free-drifting sediment trap (Technicap) with a collecting area of 1.25 m^2. The trap was equipped with a 24-bottle carousel programmed to sample at 12 h intervals during day (08:00 to 20:00 h) and night (20:00 to 08:00 h). Each bottle was filled with a preserving solution consisting of 3.5% buffered formalin in filtered seawater with 5 g/kg NaCl. Upon trap recovery, samples were filtered through pre-combusted 0.7 μm Whatman GF/F filters and swimming organisms >1 mm

were manually removed under a microscope. Filters were wrapped in pre-combusted aluminum foil and frozen at -20°C until POC analyses, which were subsequently performed using a CHN analyzer (Carlo Erba EA 1108 Elemental) and according to procedures described by Alonso-González et al. [2010].

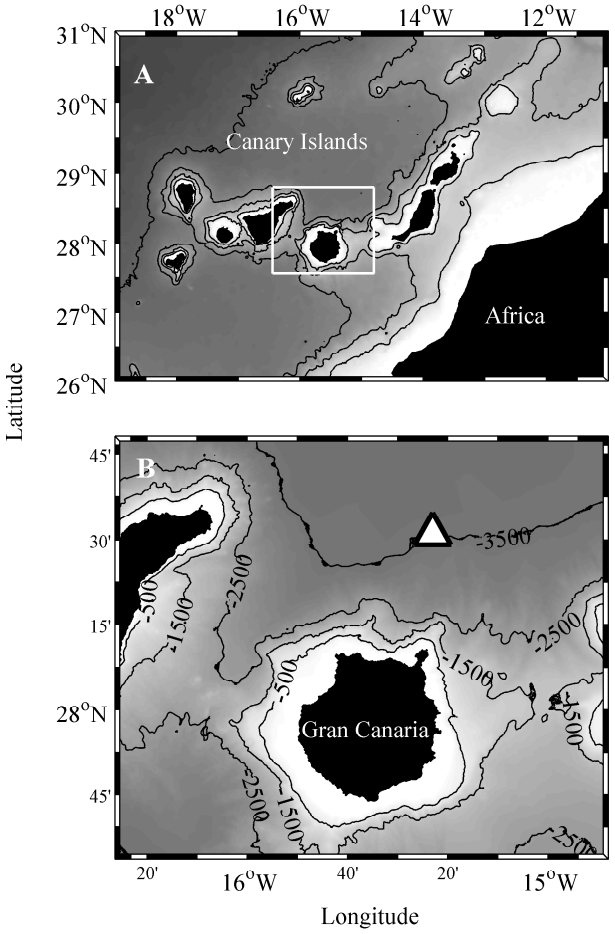

FIGURE 2.1: (A) Map showing the location of the Canary Islands west off Africa and Gran Canaria island inside the white box. (B) The time-series station (white triangle) in oceanic waters north of Gran Canaria.

Net sampling

Zooplankton was sampled during day and night from 200 m depth to the surface using a double WP-2 with 0.25 m^2 mouth areas and equipped with 100-μm mesh nets [UNESCO, 1968]. The volume of water filtered was determined using a calibrated TSK flowmeter. One of the samples was used for abundance and biomass measurements and the other for ETS assays (see section below). The first sample was preserved in 4% buffered formalin and divided into two subsamples on board. In the laboratory, one subsample was sieved and 0.1 to 0.2, 0.2 to 0.5, 0.5 to 1.0 and >1 mm size-fractions were obtained. Each fraction was subsequently dry weighed by standard procedures [after 24 h at 60°C,

Lovegrove, 1966]. The other subsample was digitized using a scanner at a resolution of 1200 dpi and the organisms were automatically counted, measured and classified using ZooImage software, according to the procedures described by Grosjean and Denis [2007]. Taxonomic groups were established by a manually performed training set, achieving a global error in the classification below 5%. The area of each organism was converted into dry weight using the equations provided by Hernández-León and Montero [2006], subsequently improved by Lehette and Hernández-León [2009]. The length distributions of faunistic groups were also obtained from image analysis. For this purpose, the long side of the rectangles enclosing the entire area of the organisms was used as a proxy of total length. The biomass of migrant zooplankton was estimated by averaging the biomass difference between day and night for each sampling day. For this calculation, we only considered the size fraction >1 mm, since it was the only one that systematically showed a greater biomass during nighttime (no significant differences for smaller fractions) and was also where we found large migrating organisms such as euphausiids (see Table 2.1). Total migrant biomass was calculated using the standard dry-weighing procedure, whereas dry weight derived from image analyses was used only for comparing the relative biomass of different taxonomic groups.

Micronekton were collected using a 5 m^2 Matsuda Oozeki Hu trawl [MOHT, Oozeki et al., 2004] with a 4-mm mesh size. According to the information provided by the echosounder, trawls were always performed 1 h after the nocturnal ascent and were towed obliquely across the acoustic scattering layer, distributed approximately from surface to 150 m depth. Towing speed was kept between three and four knots and the incoming water volume was measured using a calibrated General Oceanics flowmeter, mounted at the mouth of the trawl. The catch was sorted onboard into family taxa levels and once in the laboratory, wet-weight was immediately measured. Subsequently, samples were fixed in 4% buffered formalin and after two weeks were transferred into 70% ethanol for species identification, enumeration and length measurements. Due to the underestimation caused by extrusion through meshes and net avoidance [Pakhomov et al., 2010, Kaartvedt et al., 2012b], the catch biomass was corrected according to the MOHT capture efficiencies provided by Davison [2011b]: 14% for gas-bearing animals and 38% and 80% for large and small no gas-bearing animals. These efficiencies were applied in this instance to fish, decapods and euphausiids, respectively (see discussion for further details). Only vertically migrating micronekton were included in calculations (e.g., epipelagic fish and gelatinous organisms were removed). For this task, we checked the diel vertical distribution of micronekton species in the region according to the following literature: Badcock [1970], Foxton [1970a,b], Badcock and Merrett [1976], Baker [1970], Clarke [1969], Roe [1984a], Roe and Badcock [1984], Roe et al. [1984b]

Mass unit conversions between dry weight (DW), wet weight (WW) and carbon (C) were performed using averaged conversion factors obtained for fish and decapods by Childress and Nygaard [1973, 1974], whereas for euphausiids and mixed zooplankton, we used those provided by Kiørboe [2013]. Calculations and averaged conversion factors are provided in supplementary material.

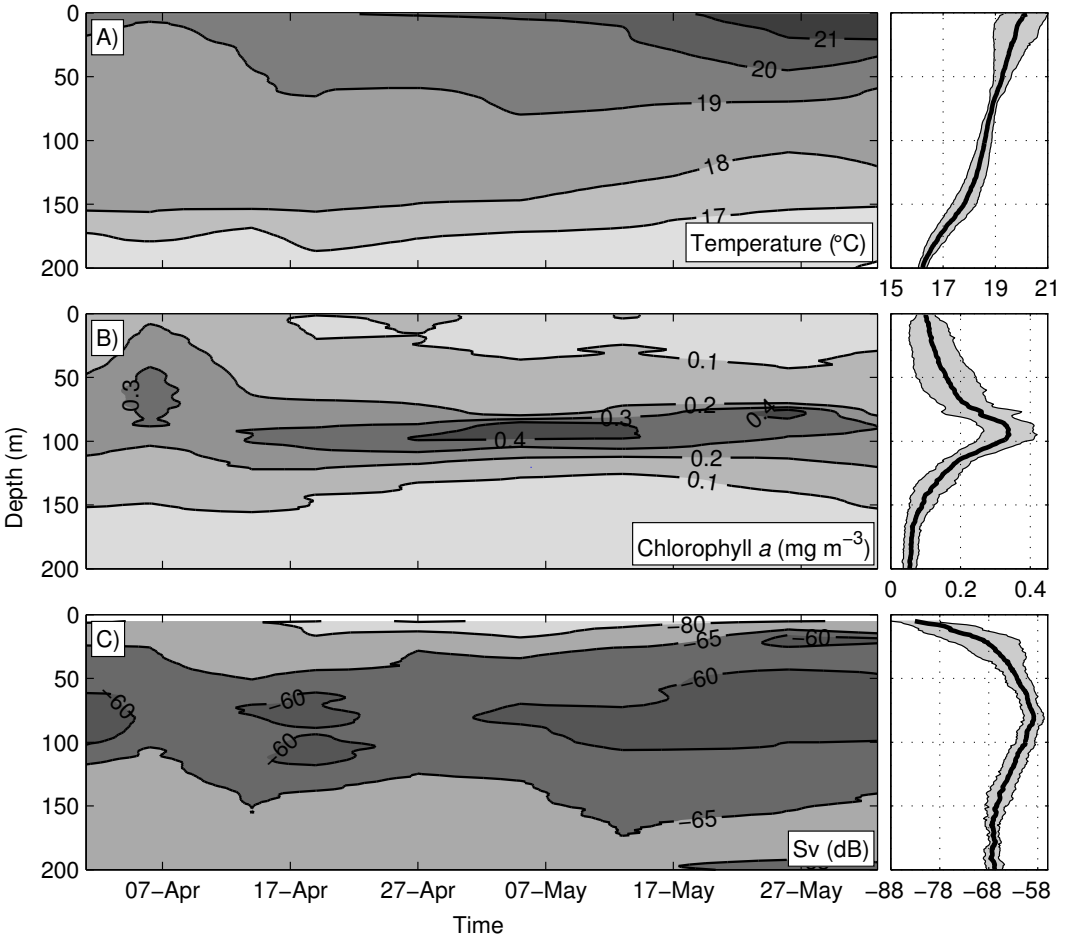

FIGURE 2.2: On the left: time-series vertical sections of (A) temperature, (B) chlorophyll *a* and (C) Mean Volume Backscattering Strength at 120 kHz (Sv). On the right: Mean profiles for the same parameters. Thick lines depict mean values and thin lines represent standard deviations.

Electron transfer system (ETS) activity

Zooplankton samples used for ETS assays were size-fractionated (see section above) and stored in liquid nitrogen (−196°C) immediately after collection. For micronekton, specimens of three species representing three dominant families were also frozen: *Lobianchia dofleini* (Myctophidae), *Sergia splendens* (Sergestidae) and *Euphausia gibboides* (Euphausiidae). Once in the laboratory, zooplankton size fractions and micronekton specimens were homogenized with a phosphate buffer (0.05 M PO_4) and ETS assays were

performed following the method of Packard [1971], subsequently modified by Gómez et al. [1996]. Although the primary results of ETS were shown at *in situ* temperatures (ranging from 18°C to 20°C), we also calculated the ETS at the standard temperature of 20°C for comparison purposes, as well as at 12°C to estimate the respiratory flux (see section below). Temperature corrections were performed using the Arrhenius equation and activation energy of 15 kcal mol^{-1} [Packard et al., 1975]. To show mass-specific ETS activities, the biomass of samples was also calculated. For zooplankton, protein content was measured following homogenization according to the method of Lowry et al. [1951] and dry weight was derived from protein using equation (2.1), provided by Hernández-León et al. [2001] for the Canary Island waters. For micronekton, specimens were wet weighed immediately prior to homogenization.

$$\mathrm{DW} = 1.445 + 4.283 \text{ protein } (\mathrm{r} = 0.900;\ \mathrm{n} = 306) \tag{2.1}$$

Respiratory flux

The respiratory flux below the euphotic zone (>150 m depth) was derived from ETS activities at mesopelagic temperatures. We assumed a mesopelagic residence time and depth by migrants of 12 h and 400 m to 500 m, according to the diel vertical distribution of the shallower migrant scattering layer observed in the region [Bordes et al., 2009, Ariza et al., unpub.]. We therefore used ETS activities corrected at 12°C (see section above), the approximate temperature at these depths. The respiratory flux of zooplankton was calculated using only the activity of the large size-fraction ($\mathrm{ETS}_{>1\mathrm{mm}}$) since as stated above in section "Net sampling", vertical migration was found to be significant among these animals. However, $\mathrm{ETS}_{>1\mathrm{mm}}$ activity was expected to be caused by both migrant and non-migrant biota, because this fraction also contained epipelagic organisms. We therefore developed an equation to roughly estimate the ETS activity that was due only to migrant zooplankton, based on the assumption that the ratio between migrant and non-migrant biomass in a sample determined the proportion of ETS activity corresponding to each. During the sampling period, the day/night biomass ratio of the size fraction >1 mm was 0.63±0.19, suggesting a night-time percentage of non-migrant and migrant biomass of about 60% and 40%, respectively. According to this assumption, we developed the following equations:

$$\mathrm{ETS}_N = 0.4\mathrm{ETS}_m + 0.6\mathrm{ETS}_{nm} \tag{2.2}$$

$$\mathrm{ETS}_m = \frac{\mathrm{ETS}_N - 0.6\mathrm{ETS}_{nm}}{0.4} \tag{2.3}$$

where ETS_N is the ETS activity measured during nighttime and ETS_m and ETS_{nm} are the activities of migrant and non-migrant organisms, respectively. Assuming that ETS_{nm} should equal the activity measured during daytime (ETS_D), we obtained the following equation to infer ETS_m from ETS_D and ETS_N:

$$\mathrm{ETS}_m = \frac{\mathrm{ETS}_N - 0.6\mathrm{ETS}_D}{0.4} \tag{2.4}$$

Respiration (R) was derived from ETS activities by applying a conservative R/ETS ratio of 0.50, according to values ranging from 0.46 to 0.65 for zooplankton >1 mm [Hernández-León and Gómez, 1996], euphausiids (Hernández-León et al., unpub.) and fish [Ikeda, 1989]. To express respiration in terms of carbon, oxygen consumption was converted to carbon units by a simple stoichiometry calculation (22.4 L O_2 = 12.0 g C) and a respiratory quotient (RQ) was subsequently applied. Since the RQ ranged between 0.90 for fishes [Brett and Groves, 1979] and 0.97 for diverse crustaceans [Omori and Ikeda, 1984, Pakhomov et al., 1999], we chose a conservative RQ of 0.90 for all calculations.

Finally, respiration rates were multiplied by the respective biomass to obtain the respiratory flux for each migrating component. For micronekton, we used the respiration rate of *L. dofleini*, *S. splendens* and *E. gibboides* to respectively calculate the respiratory fluxes of fish, decapods and euphausiids.

Data from other studies

Migrant biomass, respiration rates and carbon fluxes from other studies were also shown for comparison purposes. When necessary, values from the literature were recalculated in order to standardize units, using the averaged mass conversion factors given in supplementary material or the protein to dry weight formula given above (equation 2.1). When data were not available in the text or in tables, we obtained the values from the data points of figures using GraphClick software v3.0. In the case of Fig. 2.7, respiration rates were normalized at 20°C when necessary using a Q_{10} of 3.9 for myctophids and 2.2 for crustaceans [Donnelly and Torres, 1988]. The ETS measurements of Herrera et al. [2014] were converted to respiration by also applying a R/ETS of 0.5. As the respiration rates given by Donnelly and Torres [1988] were measured at several temperatures, we always used those nearest to 20°C.

Results

Vertical distribution of the scattering migrant biota

Water stratification increased during the period of study in spring as expected (Fig. 2.2a). During the entire period, deep chlorophyll maxima followed the 18°C to 19°C isotherms, which roughly ranged between 50 m and 100 m in depth (Fig. 2.2b). Once the DVM finished (nocturnal ascent), the migrant scattering biota established above 150 m depth, while higher acoustic densities were observed between 50 m and 100 m depths, apparently following subsurface chlorophyll maxima (Fig. 2.2c).

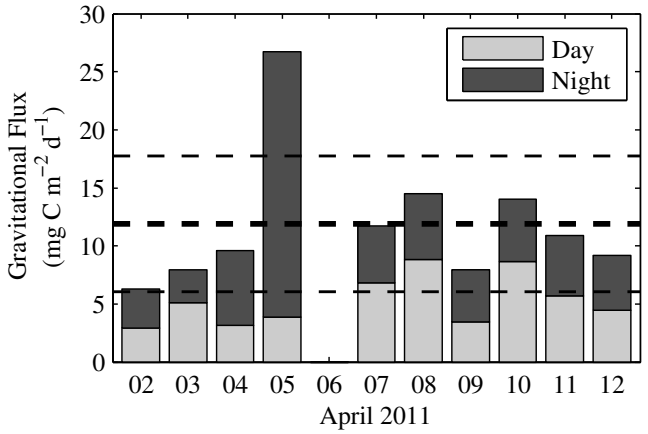

FIGURE 2.3: Daily gravitational flux measured at 150 m depth over eight days. Light and dark colors represent day and night fluxes, respectively, whereas whole bars represent flux over 24 h. Thick and thin dashed lines indicate the mean gravitational flux and the standard deviation, respectively.

POC flux

The mean POC fluxes at 150 m depth (Fig. 2.3) did not show significant differences (Student's t-test, $p = 0.62$) when comparing measurements by day (5.6±2.4 mg C m^{-2} d^{-1}) and by night (6.6±5.8 mg C m^{-2} d^{-1}), although nocturnal values showed a higher variability than those measured during daytime. Considering the entire day, the mean POC flux during the sampling period was 11.9±5.8 mg C m^{-2} d^{-1}.

Species abundance, biomass and size structure

Nocturnal zooplankton organisms from 0.1 mm to 0.5 mm were the most abundant within the WP-2 catches during the entire sampling period, whereas larger animals, especially those over 1 mm (Fig. 2.4a and 2.4b) accounted for the major proportion of

biomass. According to image analyses (Table 2.1), roughly 100% of the abundance and biomass of organisms below 1 mm corresponded to copepods, although this might also have resulted from the image-processing limitations for recognizing other groups below 0.5 mm. In the >1 mm fraction, we found a significant contribution of other taxa such as chaetognaths and euphausiids. The day/night ratios showed that euphausiids were the main group that increased during the night (Table 2.1).

		Per size fraction		Per taxonomic groups			
Size fraction	Taxa	Bio (D/N)	ETS (D/N)	Abd (%)	Bio (%)	Abd (D/N)	Bio (D/N)
1.0-2.0 mm	*Cop*	1.09±49	1.23±0.82	100±0.0	100±0.0	0.9±0.3	1.0±0.4
2.0-5.0 mm	*Cop*	1.06±0.36	0.83±0.40	100±0.0	100±0.0	1.1±0.4	1.1±0.3
5.0-1.0 mm	*Cop*	0.94±0.38	0.97±0.37	93.7±2.8	92.7±3.1	1.0±0.3	1.0±0.3
	Cha			4.5±2.5	4.7±2.7	0.9±0.4	0.9±0.5
>1.0 mm	*Cop*	0.63±0.19	0.66±0.39	59.3±9.3	33.0±14.4	1.0±0.5	0.9±0.4
	Cha			20.4±5.2	12.8±10.7	1.0±0.6	1.0±0.7
	Eup			8.2±3.6	47.0±21.8	0.3±0.2	0.1±0.2

TABLE 2.1: Zooplankton abundance (Abd), biomass (Bio) and electron transfer system activities (ETS). Percentages refer to nighttime, while D/N refers to day-night ratios. Results are given for each size fraction, and also differentiating between taxonomic groups. *Cop*, *Cha* and *Eup* represent copepods, chaetognatha and euphausiids, respectively.

Concerning micronekton, the abundance and biomass of the nocturnal shallow scattering layer remained substantially stable throughout the sampling period. The three most abundant families were Euphausiidae, Myctophidae and Sergestidae. In terms of biomass, myctophids accounted for the major contribution, followed by euphausiids and sergestids (Fig. 2.5a and 2.5b). At the species level (Table 2.2), *Euphausia gibboides* was the unique species identified among the Euphausiidae. Most of the specimens in this family were most likely *E. gibboides*, although this was impossible to verify due to bad preservation conditions. Myctophids comprised 16 identified species, the most abundant and recurrent being *Lampanyctus alatus*, *Ceratoscopelus warmingii* and *Lobianchia dofleini*. Among the nine identified species of the family Sergestidae, *Sergia splendens* was the dominant and most recurrent. The presence of the fish *Vinciguerria nimbaria* of the family Phosichthyidae and the decapod *Systellaspis debilis* belonging to family Oplophoridae were also noteworthy.

Regarding size structure, the WP-2-captured organisms were smaller than 7 mm (Fig. 2.6). Copepods were mainly below 1 mm in size, whereas chaetognaths and juvenile euphausiids roughly ranged between 1 mm and 7 mm. In the MOHT catches, we again found euphausiids but the adult fraction, ranging from 14 mm to 24 mm in length. Sergestids ranged from 26 mm to 40 mm and myctophids from 12 mm to 48 mm. Approximately 50% of these myctophids were less than 20 mm and mainly corresponded to juvenile specimens.

ETS activities

In zooplankton, the ETS activities of each size fraction remained relatively stable throughout the sampling period (Fig. 2.4c). Mean values were 1.4±0.6, 3.5±1.0, 2.8±0.8 and 2.5±1.6 μL O_2 mg DW^{-1} h^{-1} for the 0.1 to 0.2, 0.2 to 0.5, 0.5 to 1.0 and >1.0 mm size fractions, respectively (Fig. 2.4f).

	Family	Abundance (%)	Biomass (%)
Fis	**Myctophidae**	**27.8±8.2**	**40.8±13.8**
	Lampanyctus alatus	4.0±2.2	7.0±3.2
	Ceratoscopelus warmingii	3.6±2.4	11.0±6.7
	Lobianchia dofleini	3.0±1.9	3.1±1.9
	Benthosema suborbitale	3.0±1.8	2.2±1.2
	Bolinichthys indicus	2.6±1.5	4.4±2.4
	Lepidophanes gaussi	1.5±0.5	1.8±1.3
	Diaphus mollis	1.4±1.2	4.6±3.0
	Hygophum taaningi	1.4±1.3	7.3±6.3
	Hygophum reindhardtii	1.0±0.2	3.5±2.2
	Hygophum hygomii	0.5±0.3	0.4±0.3
	Phosichthyidae	**4.9±4.1**	**5.3±3.7**
	Vinciguerria nimbaria	4.4±4.0	5.2±3.5
	Vinciguerria attenuata	0.5±0.3	0.4±0.2
Dec	**Sergestidae**	**9.9±3.6**	**13.6±7.2**
	Sergia splendens	2.8±2.4	11.8±7.6
	Parasergestes vigilax	1.0±0.7	1.5±0.9
	Deosergestes henseni	0.9±0.4	2.0±0.9
	Sergestes atlanticus	0.5±0.4	0.9±0.2
	Oplophoridae	**2.8±1.5**	**6.5±3.6**
	Systellaspis debilis	1.9±1.2	4.4±1.5
	Oplophorus spinosus	0.9±0.4	1.3±0.5
Eup	**Euphausiidae**	**45.21±9.9**	**21.6±7.1**
	Euphausia gibboides	9.5±5.0	6.4±3.2

TABLE 2.2: Percentages of abundance and biomass of micronekton species. Only organisms identified to the species level and with abundances above 0.5% are shown. Families are indicated in bold.

The ETS measurements of the three micronekton species also showed little variability throughout the study period (Fig. 2.5c). *Lobianchia dofleini* specimens with an average body weight of 31±7 mg DW showed mean ETS activity of 4.8±1.3 μL O_2 mg DW^{-1} h^{-1}, while values for *S. splendens* (36±24 mg DW) and *E. gibboides* (12±3 mg DW) were 1.8±0.9 and 2.8±1.2 μL O_2 mg DW^{-1} h^{-1}, respectively (Fig. 2.5f). Respiration rates derived from ETS activities (R/ETS=0.5) were considerably close to other estimates in the literature (Fig. 2.7)

Migrant biomass and respiratory carbon flux

The mean total migrant biomass was 467±187 mg C m^{-2}, of which 266±127 mg C m^{-2} corresponded to zooplankton and 201±61 mg C m^{-2} to micronekton (Fig. 2.8a).

After correcting the MOHT sampling bias, we found that the largest contribution to the micronekton migrant biomass corresponded to fish, followed by small contributions by shrimps and krill (Fig. 2.8b).

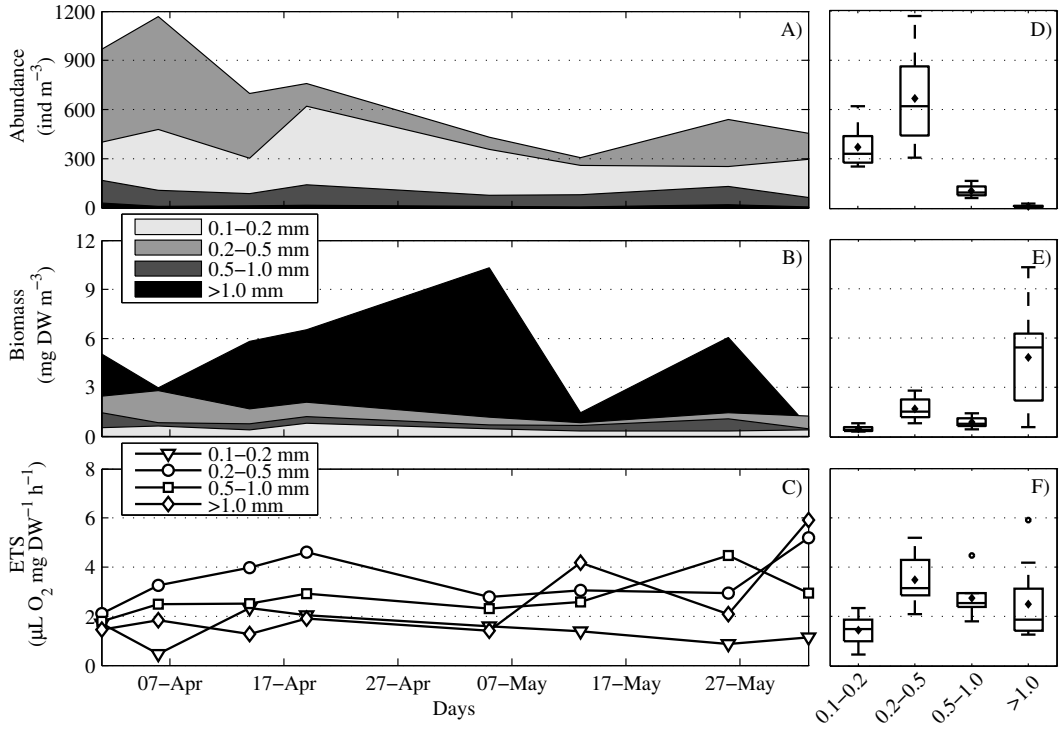

FIGURE 2.4: On the left: weekly time-series showing: (A) abundance, (B) biomass and (C) electron transfer system activity of different zooplankton size fractions captured during nighttime (at *in situ* temperatures ranging from 18°C to 20°C). On the right: (D, E, F), the same parameters averaged in a boxplot. In each box, the central diamonds represent the mean, the central lines the medians, the edges of the box are the 25th and 75th percentiles, the whiskers extend to the most extreme data points not considered outliers and outliers are plotted individually (circles).

Considering all the migrant biota, the mean respiratory carbon flux out of the euphotic zone was 6.4±2.9 mg C m^{-2} d^{-1}, which represents 53% (range 23 to 71) of the mean gravitational flux in the area. About 29% and 25% of this flux corresponded to zooplankton and micronekton, respectively (Fig. 2.8c). Within the micronektonic component, fish were by far the major contributors to the respiratory carbon flux, accounting for 23% of the gravitational flux (Fig. 2.8d).

Discussion

Methodological approaches and constraints

The WP-2 efficiently sampled migrant zooplankton such as juvenile euphausiids, but exhibited low performance for adult euphausiids, as they can easily avoid most of plankton

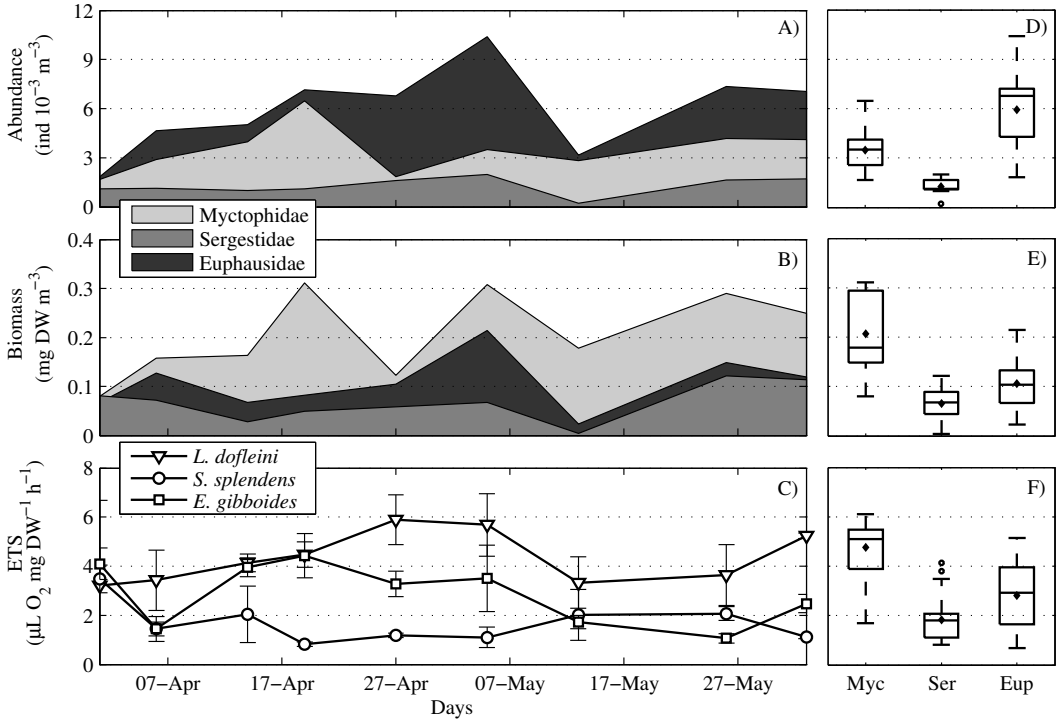

FIGURE 2.5: On the left: weekly time-series showing: (A) abundance, (B) biomass and (C) electron transfer system activity of three dominant taxa of migrant micronekton (at *in situ* temperatures ranging from 18°C to 20°C). On the right: (D, E, F), the same parameters are averaged in a boxplot. Capture-efficiency corrections are not applied in this figure. In each box, the central diamonds represent the mean, the central lines the medians, the edges of the box are the 25th and 75th percentiles, the whiskers extend to the most extreme data points not considered outliers and outliers are plotted individually (circles).

nets [Brinton, 1967, Mathew, 1988]. This fraction and other large migrant species were collected using the MOHT, a sampling device that has proved to be highly effective at capturing krill and juvenile fish [Oozeki et al., 2004, Yamamura et al., 2010]. In fact, our results showed that these small organisms are an important component of migrant micronekton, which has been systematically biased in previous studies using large commercial trawls [see Bordes et al., 2009, Wienerroither et al., 2009, Landeira and Fransen, 2012, Ariza et al., 2014]. However, these studies also revealed that the MOHT sampled the adult fraction of several myctophid species and other large migrating fish poorly (e.g., *Gonostoma* or *Chauliodus*). Squid were also notably undersampled. In summary, the combination of both nets properly sampled migrant specimens from 1 to 50 mm. However, it left a gap in euphausiids from 6 to 12 mm and showed less efficiency for micronekton larger than 50 mm (Fig. 2.6).

Micronekton net-sampling always involves biomass losses, either via the escapement of small animals through meshes or because of the evasion of large fast-swimmers [Koslow

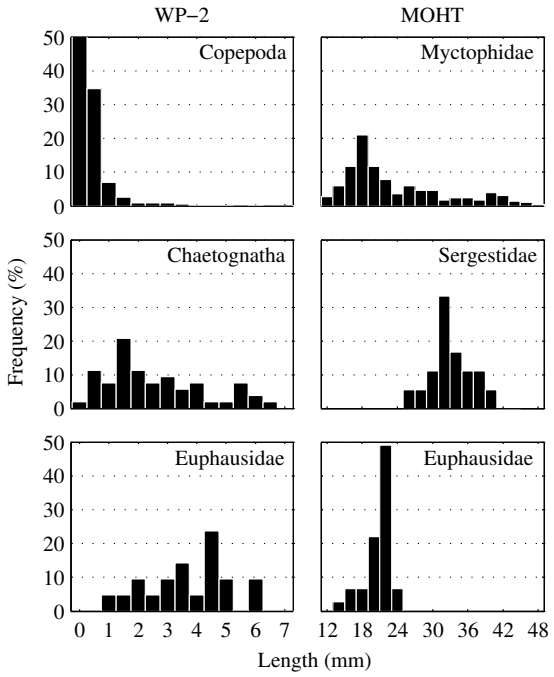

FIGURE 2.6: Length distribution (mm) of dominant taxa collected with the WP-2 (zooplankton) and MOHT (micronekton) nets. Measurements refer to total length, except for myctophids, which refer to the standard length.

et al., 1997, Kloser et al., 2009, Pakhomov et al., 2010, Kaartvedt et al., 2012b]. Capture-efficiency correction factors must therefore be applied in order to obtain more reliable results. For the present paper, we adopted those provided by Davison [2011b], who compared the MOHT catch with acoustic-based biomass estimations. Davison reported capture efficiencies of 14%, 38% and 80% for the following respective acoustic groups: (I) gas-bearing targets; (II) non-gas-bearing large targets; (III) non-gas-bearing small targets. According to our trawl data, group I corresponded to fish with inflated swimbladders and group III to euphausiids. We also extended the group I capture efficiency to the rest of fish, regardless of the absence of inflated swimbladders, as it is reasonable to assume that all of these would have similar avoidance capabilities. Major uncertainties are included in group II, which most likely includes non-gas-bearing fish, large crustaceans and cephalopods. Therefore, the estimated capture efficiency will likely result from the avoidance capabilities of these faunal groups together. Despite this problem, we adopted group II capture efficiency for decapods in the absence of more accurate correction factors. Squid were not corrected, as their occurrence was anecdotal and meaningless within the context of the surveys. Even though the uncertainty concerning decapods and squid biomass, the correction factors applied here for fish and euphausiids, the groups apparently more contributing to migrant biomass, are well supported by other studies. Similar to Davison [2011b], other acoustic surveys report fish biomass one order of magnitude higher than net-based estimates [Koslow et al., 1997, Kloser et al.,

2009, Yasuma and Yamamura, 2010, Kaartvedt et al., 2012b]. Concerning euphausiids, Yamamura et al. [2010] also reported capture-efficiencies close to 100% using the MOHT in the Bering Sea. Nevertheless, we consider our estimates to be somewhat conservative, since Davison [2011b] used a 1.7-mm mesh size and we used 4.0 mm; thus, our real capture-efficiencies will have been even lower due to higher escapement through meshes. In fact, Gartner et al. [1989] showed that the catch of myctophids smaller than 30 mm (standard length) increased by a factor of 2.7 if the mesh size of the trawl was reduced from 4.0 mm to 1.6 mm. The true *in situ* fish biomass will therefore be substantially higher considering that most myctophids caught for the current study were below this size (Fig. 2.6).

Aside from the biomass underestimation, the size-bias also involved other limitations for the assessment of the active flux. On the one hand, smaller migrants might have a higher metabolism [Ikeda, 1989], thereby increasing the respiratory flux, while the missing large fraction is expected to cover longer migratory ranges, sequestering carbon to deeper waters. Respiratory rates along the different sizes of myctophids roughly ranged from 1 to 3 μL O_2 mg DW^{-1} h^{-1}, according to data collected from the literature (Fig. 2.7a), while the respiration predicted for the average weight of myctophids studied here (31$\pm$7 mg DW) was 1.98 μL O_2 mg DW^{-1} h^{-1}, as derived from the regression equation of these data. It might therefore be expected that our estimates of fish-mediated export fluctuated by roughly 50% depending on the fish sizes analyzed. However, respiration in crustaceans seemed to not change within the size range showed in Figure 2.7b. Concerning the depth of the carbon inputs, we assumed a range of 400 m to 500 m as the DVM depth, regardless of the fact that deeper migrant scattering layers had also been observed in the region (Ariza et al., unpub.). Therefore, our approach is considered conservative on this respect.

We also assumed in our calculations that the migrant biomass measured at night in the upper 150 m depth would reach mesopelagic waters during the day, thereby disregarding the predation factor in our calculations. Some studies suggest that mesopelagic fish remove about 1% to 4% of the zooplankton biomass in the upper 200 m depth , but it is unclear which part of this consumption would affect the zooplankton migrant fraction [Hopkins and Gartner, 1992, Watanabe et al., 2002, Hudson et al., 2014]. Other authors have also addressed the predation impact on vertically migrating micronekton; unfortunately, none of these studies were quantitative [Kozlov, 1995, Sutton and Hopkins, 1996, Choy et al., 2013]. Considering the poor knowledge on this respect, we decided no to apply correction factors. This might constitute therefore a possible source of overestimation.

Concerning zooplankton fluxes, they were calculated only in organisms larger than 1 mm in length, because the day-night biomass ratios only evidenced migrant activity within this fraction (Table 2.1). Using analogous sampling settings, Hernández-León et al. [2002] also observed increases in nocturnal biomass only in large zooplankton. We also proposed the equation (2.4) for estimating the mass-specific ETS activity due only to the migrant part of the sample, which was apparently primarily formed by juvenile euphausiids. This was motivated due to $ETS_{>1mm}$ activities being systematically higher during the night than during the day (Table 2.1), likely reflecting the fact that the migrant biota had higher metabolism rates than their non-migrant relatives, a fact also observed by Minutoli and Guglielmo [2009] in the Mediterranean Sea. In this sense, we believe that the increase in zooplankton active flux (139%) following the application of the equation (2.4) is justified, as it reflects the higher metabolism of the migrant fraction. Certainly, the equation considers the ETS contribution of migrant and non-migrant organisms based on their biomass ratio, but disregards the metabolic differences among species. However, most of the variance in respiration rates among zooplankton is due to body weight, habitat temperature, habitat depth and physiological activity, whereas taxonomy is of lesser importance [Bode et al., 2013, Ikeda, 2014]. These explanatory parameters are likely to be distinctive between migrant and non-migrant zooplankton groups, regardless of the species. Additionally, performing the ETS analyses at species level in zooplankton was not as approachable as in the case of micronekton, since the time required for isolating the specimens can considerably decrease enzymatic activity [Ahmed et al., 1976, Båmstedt, 1980]. We therefore considered that our approach was the most suitable, taking into account such difficulties.

Respiration rates can be derived from ETS activities using correlations, or by directly measuring the oxygen uptake of living animals. Although the predictive accuracy of the first approach has been questioned due to the intra- and interspecific variability of such correlations [Båmstedt, 1980, Hernández-León and Gómez, 1996, Bode et al., 2013], the *in vivo* experiments also involve important operational difficulties. Stress, starvation, crowding or bacterial growth can introduce substantial errors to the incubation-based measurements. In addition, certain animals such as mesopelagic fish, are extremely difficult to maintain alive for long enough periods to acquire reliable data [Torres et al., 1979, Donnelly and Torres, 1988]. The ETS approach was therefore adopted in the present study to circumvent these problems, but using a conservative R/ETS ratio of 0.5 for all taxa, according to averaged values ranging from 0.46 to 0.65 in mixed large zooplankton [Hernández-León and Gómez, 1996], euphausiids (Hernández-León et al., unpub.) and fish [Ikeda, 1989]. In fact, Figure 2.7 shows that the differences between our estimates and those based on *in vivo* experiments were not prominent [Donnelly and Torres, 1988].

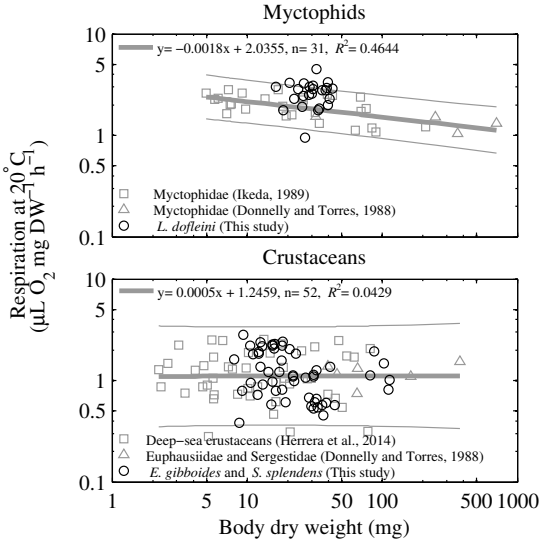

FIGURE 2.7: Mass-specific respiration of micronekton normalized to 20°C; includes own data (dark color) and estimates from existing literature (gray color). Values from Donnelly and Torres [1988] refers to oxygen consumption *in vivo* measurements, while those from Ikeda [1989] and Herrera et al. [2014] are respiration rates derived from ETS activities. Regression lines with 95% confidence intervals for literature data were also plotted (thick and thin lines, respectively). See methods section for further information about how the data from other sources were obtained.

Particularities of zooplankton and micronekton active flux

In terms of respiration, zooplankton and micronekton export similar amounts of carbon out of the euphotic zone, with the former's flux (3.4±1.9 mg C m^{-2} d^{-1}) slightly higher than that of the latter (2.9±1.0 mg C m^{-2} d^{-1}). This resulted because both zooplankton and micronekton also provided similar biomass and respiratory rates. However, there are other mechanisms of carbon export that are expected to differ markedly where zooplankton and micronetkon are concerned. Gut flux refers to the downward transport of non-assimilated food in the gut of animals and later released by defecation. Unlike respiration, which produces dissolved inorganic carbon (DIC), the gut flux contributes to the particulate organic carbon (POC) pool. This flux is expected to work more efficiently in micronekton, because of their slower gut clearance rates compared to that of zooplankton, which means a higher proportion of fecal matter actively exported below the seasonal pycnocline. In fact, gut clearance only takes a few minutes in copepods [Dam and Peterson, 1988] and about 30 min to 90 min in euphausiids [Gurney et al., 2002, Pakhomov et al., 2004], while in fish, estimates range from 12 h to days [Baird et al., 1975, Clarke, 1982]. If we assume a nocturnal distribution at roughly a 50 m depth and a mean downwards migration velocity of 5 cm s^{-1} [Davison et al., 2013], organisms trespassing the base of the mixed layer (∼150 m depth) will take about 30 min. This infers that no fecal matter will be actively exported by copepods, euphausiid gut flux

will be partial, while most non-assimilated food in the fish guts will be released into the mesopelagic zone.

Gut flux was not measured for the present study, however, using energy budgets, defecation can be roughly estimated from respiration. According to energy budgets listed by Brett and Groves [1979], carnivorous fish defecate approximately an amount equivalent to 40% of the respired carbon. As only half of the daily respiration occurs in the mesopelagic zone, but most fecal matter is actively transported there, the gut flux of fishes will as a result represent about 80% of their respiratory carbon flux, which in the present study corresponds to 2.1±0.7 mg C m^{-2} d^{-1}. Together with the respiratory flux mediated by both zooplankton and micronekton, this will account for 8.5±3.6 mg C m^{-2} d^{-1}, meaning about 70% of the gravitational flux measured at 150 m depth. Below this depth and after defecation, the fast sinking fecal pellets would reinforce the already weakened gravitational flux coming from surface, bypassing carbon from active to passive flux at mesopelagic depths [see Alonso-González et al., 2013]. At this point, there are also important differences between zooplankton and micronekton since larger animals produce larger fecal pellets, which are expected to sink faster and to reach greater depths before decomposition [Small et al., 1979, Robison and Bailey, 1981, Røstad and Kaartvedt, 2013]. Other exporting mechanisms such as the carbon inputs via excretion [Steinberg et al., 2000] and mortality [Williams and Koslow, 1997] still remain to be considered.

Beyond discussions regarding the amount of exported carbon, the depth range of active flux is another important issue that should be considered when comparing zooplankton and micronekton. Sameoto et al. [1987] found that juvenile euphausiids performed shallower migrations (170 m) than adults (350 m). Fish migrate to even deeper waters (>500 m) as they increase in size [Moteki et al., 2009]. In fact, the largest myctophid species inhabit bathypelagic (>1000 m) waters during the day [Badcock and Merrett, 1976]. Therefore, as juvenile euphausiids were in this instance the primary contributing component to zooplankton flux, while adult euphausiids and other larger species contributed to micronekton flux, we suggest that zooplankton flux may operate at a lower depth range than that of micronekton. This might be irrelevant in migratory flux calculations across the base of the euphotic zone (∼150 m depth), but nonetheless suggests that at deeper waters, micronekton might be the main carbon-exporting component. In addition, the active to passive flux ratio must be considerably higher at these depths since the gravitational flux decays exponentially with depth [Suess, 1980, Antia et al., 2001].

Taxa	Terms	Migrant biomass (mg C m^{-2})	Migratory flux (mg C m^{-2} d^{-1})	Gravitational flux (mg C m^{-2} d^{-1})	Migratory/Gravitational (%)	Location	Source
Zooplankton	*R*	*107-412 (266±126.6)*	*1.13-4.45 (3.44±1.94)*	*6.31-26.70 (11.89±5.84)*	*10-37 (29)*	*Canary Islands*	*This study*
	R,E,M	126	3.2-13.6	18.0	11-44	Hawaii	Steinberg et al. [2008]
	R,E,M	1280	31.1-91.6	23.1-61.8	26-200	N. W. Pacific	Steinberg et al. [2008]
	R	580 - 1280	1.85-8.28	15.8	11-52	Canary Islands	Yebra et al. [2005]
	R	261	1.92 - 4.29	9.5-12.0	16-45	Canary Islands	Hernández-León et al. [2001]
	R	145-448	7.3-19.05	54.8	13-35	W. Eq. Pacific	Hidaka et al. [2001]
	R,E,F,M	158	3.6	23.7	15	Hawaii	Al-Mutairi and Landry [2001]
	R,E	49-123	2.0-9.9	25.6	9-39	Bermuda	Steinberg et al. [2000]
	R	47	3.1	49.2	6	W. Eq. Pacific	Le Borgne and Rodier [1997]
	R	53	6.3-7.9	204.0	3-4	E. Eq. Pacific	Le Borgne and Rodier [1997]
	R,M	96-155	7.1-12.7	22.8-28.8	31-44	E. Eq. Pacific	Zhang and Dam [1997]
	R	82-536 (191±147)	6.2-40.6 (14.5±11.1)	25-58 (39±10)	18 - 70 (34±16)	Bermuda	Dam et al. [1995]
	R	-	2.8-8.8	64.0-86.0	4-14	Sargasso Sea	Longhurst et al. [1990]
Euphausiids	*R*	*6-19 (10±4)*	*0.06-0.19 (0.11±0.04)*	*6.31-26.70 (11.89±5.84)*	*0.5-1.6 (0.9)*	*Canary Islands*	*This study*[a‡]
	R	33-159	0.10-0.46	54.8	0.2-0.8	W. Eq. Pacific	Hidaka et al. [2001][b§]
	E, F, M	-	1-32	-	-	N. E. Atlantic	Angel and Pugh [2000][e‡]
Decapods	*R*	*15-28 (23±5)*	*0.09-0.17 (0.14±0.03)*	*6.31-26.70 (11.89±5.84)*	*0.4-1.4 (1.2)*	*Canary Islands*	*This study*[a‡]
	R	291	13	8.3	79	Northern Benguela	Schukat et al. [2013][d†]
	R	44-96	0.12-0.26	54.8	0.2-0.5	W. Eq. Pacific	Hidaka et al. [2001][b§]
	E, F, M	-	1-6	-	-	N. E. Atlantic	Angel and Pugh [2000][e‡]
Fishes	*R*	*88-242 (168±58)*	*1.41-3.86 (2.68±0.92)*	*6.31-26.70 (11.89±5.84)*	*12-32 (23)*	*Canary Islands*	*This study*[a‡]
	R	285	0.33-1.94 (0.92)	86.0-259.0	0.3-1.0	North Azores	Hudson et al. [2014][b‡]
	R, F, M	15-276 (92±72)*	8.0-30.8	45.5-166.0	18-19	N. E. Pacific	Davison et al. [2013][c‡]
	R	1778-3304	7.6-14.1	54.8	14-26	W. Eq. Pacific	Hidaka et al. [2001][b§]
	E, F, M	-	2-43	-	-	N. E. Atlantic	Angel and Pugh [2000][e‡]
	M	299	3.1-11.1	-	-	Tasmania	Williams and Koslow [1997][e§]
Micronekton	*R*	*115-264 (201±61)*	*1.61-4.02 (2.92±0.95)*	*6.31-26.70 (11.89±5.84)*	*14-34 (25)*	*Canary Islands*	*This study*[a‡]
	R	2137-3614	15.2-29.9	54.8	28-55	W. Eq. Pacific	Hidaka et al. [2001][b§]
Total	R	222-676 (467±187)	2.74- 8.47 (6.36±2.89)	*6.31-26.70 (11.88±5.84)*	23-71 (53)	*Canary Islands*	*This study*[a‡]
	R	2282-4062	22.5-49.0	54.8	41-89	W. Eq. Pacific	Hidaka et al. [2001][b§]

[a]14, 38 and 80% capture efficiency assumed for fishes, decapods and euphausiids.
[b]14% Capture efficiency assumed.
[c]Capture efficiency adjusted to concurrent acoustic biomass estimates. Migratory flux obtained from "fish-mediated export" by vertical migrating fishes.
[d]33% Capture efficiency assumed.
[e]Capture efficiency not corrected.
[†]Small frame trawl,[‡]big frame trawl,[§]commercial-sized midwater trawl
*Calculated from MOHT nocturnal shallow tows showed in supplementary Table A2 of Davison et al. (2013).

TABLE 2.3: Comparison of migrant biomass and migratory and gravitational fluxes from the literature. In the "Terms" column, "R" refers to respiratory flux, "E" to excretion, "F" to fecal, and "M" to mortality. Fluxes refers to carbon export beneath the epipelagic zone (150 m to 200 m depth, depending on the study). The type of trawl and capture efficiency corrections are indicated for micronekton data. Values are given as ranges, as well as means (in parentheses).

Migratory fluxes: comparisons among different studies

Zooplankton flux variability among different studies mainly relies on the terms used for calculations (respiration, defecation, excretion or mortality), as well as on the hydrographic characteristics of the region (Table 2.3). For example, our migrant biomass and ETS measurements for zooplankton were quite similar to those reported by Hernández-León et al. [2001] in waters around the Canary Islands and therefore, the respiratory fluxes were also similar. Zooplankton flux was also within the range of most estimates for similar oligotrophic regions, such as Hawaii and Bermuda. However, mesotrophic waters such as the subarctic North Pacific [Steinberg et al., 2008], or inside eddies with enhanced biological production [Yebra et al., 2005], yielded much greater biomass and fluxes.

Concerning micronekton, fluxes exhibited more variability than those of zooplankton (Table 2.3). In some cases, these differences were related to hydrographic conditions, such as the pronounced biomass of decapods in the highly productive Benguela upwelling system [Schukat et al., 2013]. However, in other cases, estimations conducted in similar oligotrophic regions also showed order-of-magnitude differences in biomass [e.g., Hidaka et al., 2001]. This variability was particularly pronounced among fish, and likely reflects the inherent sampling problem of micronekton: escapement and avoidance [Pakhomov et al., 2010, Kaartvedt et al., 2012b]. The different sampling gears used and the uncertainty concerning their capture efficiencies are most likely the major constraint to making valid comparisons across the globe.

To our knowledge, the first attempts to assess micronekton export flux were performed by Williams and Koslow [1997] and Angel and Pugh [2000]; however, these estimates are not comparable to the results in the present paper, as neither were based on respiration. As in the present study, Hidaka et al. [2001] estimated respiratory fluxes for dominant taxa belonging to micronekton in the western equatorial Pacific. These results are comparable to ours, as both were performed in low-productive and open-ocean areas, although Hidaka et al. [2001] used a commercial-sized midwater trawl. In this case, fluxes mediated by crustaceans were similar to ours, but that of fish was four- to five-fold higher, because their corrected biomass was also much higher. As a result of this difference among fish (the major component of DVM), and likely because Hidaka et al. [2001] also included a substantial flux that was mediated by squid (not found in the present paper); their estimate for the total respiratory flux of micronekton was roughly one order of magnitude higher compared to that in the present study (see values in Table 2.3).

Recently, Davison et al. [2013] estimated fish-mediated exports in both oceanic and productive coastal upwelling areas of the northeast Pacific. Using the same sampling gear as in the current study, their corrected biomass was similar to ours, while the estimated migratory flux in oceanic waters was 8 mg C m^{-2} d^{-1}, about three-fold higher than the carbon export by migrant fish here (Table 2.3). Our results and those of Davison et al. [2013] are not as different considering that they also included defecation, excretion and mortality in their flux calculations. According to fish energy budgets [Brett and Groves, 1979], the fish-mediated flux estimated here would be about two-fold higher if these exporting mechanisms were included. The most recent attempt to estimate carbon transport by fish was made by Hudson et al. [2014] along the Mid-Atlantic Ridge. Using a frame trawl with a 6x6 m mouth opening, this study reported a corrected migrant biomass close to our estimate, while based on the oxygen consumption rates reported by Donnelly and Torres [1988], a respiratory flux two- to five-fold lower than in the present study was calculated (Table 2.3).

It is therefore difficult to provide valid comparisons of migratory fluxes without evaluating the mechanisms involved (respiration, defecation, excretion, mortality), the components analyzed (copepods, euphausiids, decapods, fish, squid), the affecting hydrographic factors or the sampling gear used. Regardless of this variability, the fluxes estimated in the present study for micronekton, as well as those from previous studies (Table 2.3), all indicate values within the range of zooplankton fluxes. These results highlight the importance of including micronekton together with zooplankton when studying active carbon export.

Active and passive flux

Migratory fluxes vary regionally with changes in temperature and productivity [Davison et al., 2013], as does gravitational flux [Suess, 1980, Pace et al., 1987]; therefore, the former are often presented relative to the latter in order to clarify comparisons between different areas. Gravitational POC flux in this study was 11.9±5.8 mg C m^{-2} d^{-1}, which is similar to other estimates found around the Canary Islands [Neuer et al., 1997, Alonso-González et al., 2010]. Respiratory flux by zooplankton ranged from 10% to 37% (mean 29%) of gravitational flux measured at 150 m depth, which was found to be in reasonable agreement with values reported for the Canary Islands and to most other oligotrophic studies listed in Table 2.3. In summary, the respiratory flux of zooplankton and micronekton ranged from 23% to 71% (mean 53%) of the gravitational flux. This percentage was close to the range suggested by Hidaka et al. [2001] in the west equatorial Pacific (41% to 89%). On the other hand, our active flux estimates concurred with those of Hernández-León et al. [2010] found in Canary Islands waters. Based on the modeled

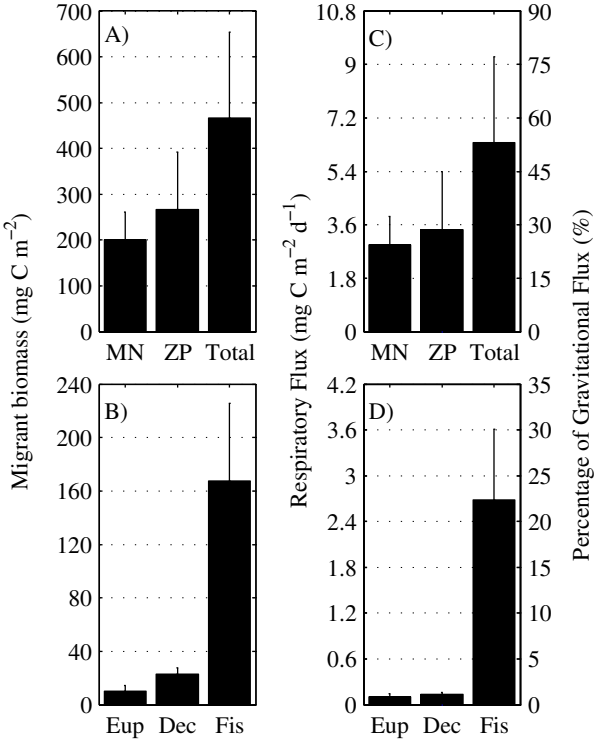

FIGURE 2.8: Migrant biomass (A, B) and respiratory flux (C, D) of euphausiids (Eup), decapods (Dec), fish (Fis), total micronecton (MN), migrant zooplankton (ZP) and micronekton plus migrant zooplankton (Total).

mortality rates of epipelagic zooplankton, the latter study predicted a carbon flux by zonal migrants with the same order of magnitude as the gravitational flux. A high ratio between the migratory and gravitational flux is expected in lowly productive zones such as the Canary Islands waters. These ecosystems are dominated by small organisms that produce slow-sinking fecal pellets. This implies that most of the pellets are remineralized in the euphotic zone, resulting in a lower sedimentation rate [Le Borgne and Rodier, 1997, Steinberg et al., 2008].

The gravitational flux from sediment-trap data [Martin et al., 1987, Karl et al., 1996, Neuer et al., 1997] are normally 30% to 50% lower than global estimates of export flux from ecosystem modeling [Schlitzer, 2002, Falkowski et al., 2003, Usbeck et al., 2003]. We suggest that the inclusion of zooplankton and micronekton as mechanisms of carbon export, together with the gravitational flux, are able to at least partly reconcile this imbalance. The migratory flux should also be considered in calculations of the e-ratio, that is, the relationship between the carbon export flux and primary production (PP) in the ocean. This ratio has been traditionally estimated by only considering the export flux according to sinking POC, such as in oceanic waters near the Canary Islands, where the e-ratio ranges between 1% and 5% of PP [Neuer et al., 2007]. In the present study, our POC flux was 3% of the PP throughout the sampling period (399.3±91.3 mg C m^{-2} d^{-1}), as

derived from satellite values (http://science.oregonstate.edu/ocean.productivity). However, the e-ratio will almost double, to 5%, by totaling the respiratory flux according to zooplankton and micronekton.

Conclusions

In summary, we observed similar migrant biomass in both zooplankton and micronekton. The primary component that contributed to DVM within zooplankton was juvenile euphausiids, whereas micronekton were mainly dominated by fish, followed by a small contribution of adult euphausiids and decapods. The mean respiratory flux by total migrants accounted for 53% (range 23% to 71%) of the gravitational flux measured at a 150 m depth, with no significant differences between the contribution of zooplankton (29%) and micronekton (25%). However, based on larger migratory ranges and gut clearance rates, micronekton are expected to be the dominant contributor to carbon export at deeper waters. Although micronekton amounts are variable due to regional differences and difficulties in calculating biomass, estimates in the present study and those from existing literature suggest that carbon fluxes driven by this community are important for future models of the biological carbon pump.

Acknowledgements: We are grateful to Lidia Nieves, Gara Franchy and Laia Armengol for hydrographic data collection and water samples analyses. We also thank Alfredo Jaramillo for his work with sediment traps and Loreto Torreblanca for zooplankton samples processing. Our special gratitude to all of them, as well as the rest of the participants (students, laboratory colleagues and the crew of the R/V *Atlantic Explorer*) for their kind support at sea. Thanks also to two anonymous reviewers for critical comments and suggestions that significantly improved the quality of this paper. This work was funded by the Spanish Government through the projects LUCIFER (CTM2008-03538) and MAFIA (CTM2012-39587). Alejandro Ariza was supported by a postgraduate grant from the Spanish Ministry of Science and Innovation (BES2009-028908).

Chapter 3

The submarine volcano eruption off El Hierro Island: Effects on the scattering migrant biota and the evolution of the pelagic communities.

Alejandro Ariza, Stein Kaartvedt, Anders Røstad, Juan Carlos Garijo, Javier Arístegui, Eugenio Fraile-Nuez, and Santiago Hernández-León (2014).

Published in *PLoS ONE* 9(7):e102354.

Abstract

The submarine volcano eruption off El Hierro Island (Canary Islands) on 10 October 2011 promoted dramatic perturbation of the water column leading to changes in the distribution of pelagic fauna. To study the response of the scattering biota, we combined acoustic data with hydrographic profiles and concurrent sea surface turbidity indexes from satellite imagery. We also monitored changes in the plankton and nekton communities through the eruptive and post-eruptive phases. Decrease of oxygen, acidification, rising temperature and deposition of chemicals in shallow waters resulted in a reduction of epipelagic stocks and a disruption of diel vertical migration (nocturnal ascent) of mesopelagic organisms. Furthermore, decreased light levels at depth caused by extinction in the volcanic plume resulted in a significant shallowing of the deep acoustic

scattering layer. Once the eruption ceased, the distribution and abundances of the pelagic biota returned to baseline levels. There was no evidence of a volcano-induced bloom in the plankton community.

Introduction

Submarine volcanoes are seabed fissures that spew mantle-derived materials and heat into the ocean. Erupted material mixes with the seawater and may thereby induce severe physical-chemical changes in the water column, in turn affecting the marine biota [Hall-Spencer et al., 2008, Mantas et al., 2011, Olgun et al., 2013, Hamme et al., 2010]. A submarine volcano eruption off El Hierro Island (Canary Islands) occurred from 10 October 2011 to 5 March 2012 at ∼200 m depth 2 km south of La Restinga headland [Rivera et al., 2013]. Fraile-Nuez et al. [2012] documented effects on the hydrography and the pelagic biota during the eruptive episode. They reported divergent responses among picophytoplankton groups and the first observation of changes in the vertical distribution of the biota forming acoustic scattering layers. Santana-Casiano et al. [2013] described the chemical changes in the water from the onset of the volcano to the post-eruptive phase. Their results showed strong deoxygenation and acidification across an extended region affected by the eruption, as well as increases in iron, nitrate, phosphate and silicate close to the volcano. Here, we focus on the effects of the volcano on the Deep and the Migrant Scattering Layers (DSL and MSL). We also report on changes in the plankton and nekton communities together with the volcano-induced abiotic perturbation. The study period spans from the most hostile scenario at the beginning of the eruption to the post-eruptive phase.

The DSL is acoustic backscatter from organisms inhabiting the mesopelagic zone [Dietz, 1948, Tucker, 1951], the oceanic region between the base of the euphotic or epipelagic zone (100-200 m depth) and the top of the bathypelagic zone (1000 m depth) [Robinson et al., 2010]. Part of this biota feeds during the night in the epipelagic zone, forming what we here refer to as the MSL. This so-called Diel Vertical Migration (DVM) occurs on a daily basis around the world's oceans by large zooplankton and micronekton [Barham, 1966, Roe, 1974, Pearre, 2003]. Abiotic factors including temperature [Watanabe et al., 1999], oxygen concentration [Ekau et al., 2010, Bianchi et al., 2013a] and light irradiance [Roe, 1983, Staby and Aksnes, 2011] play an important role in the distribution and behavior of these migrants, and they, in turn, have important implications for trophic connections and biogeochemical exchanges between the upper layers and the deep ocean [Angel and Pugh, 2000, Hidaka et al., 2001, Davison et al., 2013, Schukat et al., 2013, Irigoien et al., 2014].

Due to its offshore position far away from the NW African upwelling, El Hierro Island borders one of the most oligotrophic and transparent waters of the Canarian Archipelago [Barton et al., 1998, Davenport et al., 2002] and the epipelagic zone is characterized by low mesozooplankton densities and well-oxygenated waters [Arranz, 2007]. Despite its low productivity, fisheries resources are abundant since the volcano-affected zone is a marine protected area, where only artisan fishing is allowed [Tuya et al., 2006]. Furthermore, acoustic observations prior to the eruption [Arranz et al., 2011] showed a dielly migrating DSL typically distributed between 400 and 700 m depth during daytime and forming strong scattering layers in the epipelagic zone at night.

The eruption promoted changes in the vertical structure of these acoustic scattering layers as a result of dramatically altered physical and chemical parameters. The sea surface acidified and warmed up, the surface oxygen was almost depleted and the waters became extremely turbid [Fraile-Nuez et al., 2012]. The perturbation affected the pelagic biota, and we here address changes in DVM patterns and the vertical distribution of the DSL. The eventual cessation of the volcanic activity allowed us to study the restoration of the plankton and nekton communities as well as the effects of the nutrient enrichment caused by the volcano emissions [Santana-Casiano et al., 2013].

Here, we report on the relationship between acoustic scattering anomalies with concurrent sea surface turbidity data from satellite imagery and water perturbation as determined by oxygen profiles. We provide results from a six-month period, during and subsequent to the eruption episode, when levels of chlorophyll *a*, epipelagic mesozooplankton and vertical migrant micronekton were monitored.

Methods

Ethics statement

Field work was performed at the submarine volcano (27°37'07"N - 017°59'28"W) and around the volcano-affected coast off El Hierro Island (Canary Islands) under a permit issued by the Spanish Government to the Spanish Oceanographic Institute. Studies did not involve endangered or protected species.

Surveys

Six cruises were conducted over the course of the eruptive and post-eruptive episodes (Fig. 3.1). On 5 November 2011, three weeks after the onset of the eruption, the Spanish

Oceanographic Institute started operating the R/V *Ramón Margalef* southeast of El Hierro Island with the intention of monitoring the eruptive process. Five oceanographic surveys with hydrographic and biological samplings were performed until late February 2012 to study the effects of the volcano emissions on the pelagic biota. Epipelagic mesozooplankton and vertical migrant micronekton were assessed by plankton nets and acoustic sampling. Once the eruption stopped, a second oceanographic vessel, the R/V *Cornide de Saavedra*, performed the sixth and last survey in April 2012. This time, a pelagic trawl was included to collect larger organisms that had been detected by the echosounders throughout the previous cruises.

Hydrography

Vertical profiles of conductivity and temperature were collected using a SeaBird 9/11-plus CTD equipped with dual conductivity and temperature sensors. The CTD sensors were calibrated at the SeaBird laboratory prior to the cruises. Water samples were obtained using a rosette of 24 10-liter Niskin bottles. In addition, a dissolved oxygen sensor (SeaBird SBE-43) and a fluorometer for chlorophyll *a* estimation (WetLabs ECO-FL) were linked to the CTD unit. Seawater analysis of dissolved oxygen (Winkler titrations) and Chlorophyll *a* extractions were performed to calibrate the voltage readings of both sensors. Analyses were carried out in accordance with the JGOFS recommendations [UNESCO, 1994]. Temperature and oxygen profiles of each survey were averaged from available stations within the volcano-affected area.

Satellite Data

One kilometer spatial resolution data around El Hierro Island were used to monitor and visualize the evolution of the volcanic emissions. Data were obtained from the MODIS aqua sensor from the archive of the OceanColor Website (http://oceancolor.gsfc.nasa.gov). The standard product Sea Surface Reflectance (SSR, units: sr^{-1}) at 667 nm was selected as a tracer of the volcanic plume since this spectral band has been found to be very effective for detecting turbidity anomalies in oceanic waters [Doxaran et al., 2009, Nechad et al., 2010]. Remote sensing of chlorophyll *a* was used as a proxy for phytoplankton concentrations, but only during the post-eruptive phase as this algorithm is based in the blue/green band ratio, which is also sensitive to non-living particles including suspended volcanic material [Claustre et al., 2002, Lin et al., 2011]. Due to cloudy weather, there was some missing data (empty pixels) from the satellite images. To overcome this lack of data, the daily images were averaged with both the prior and next day images. After

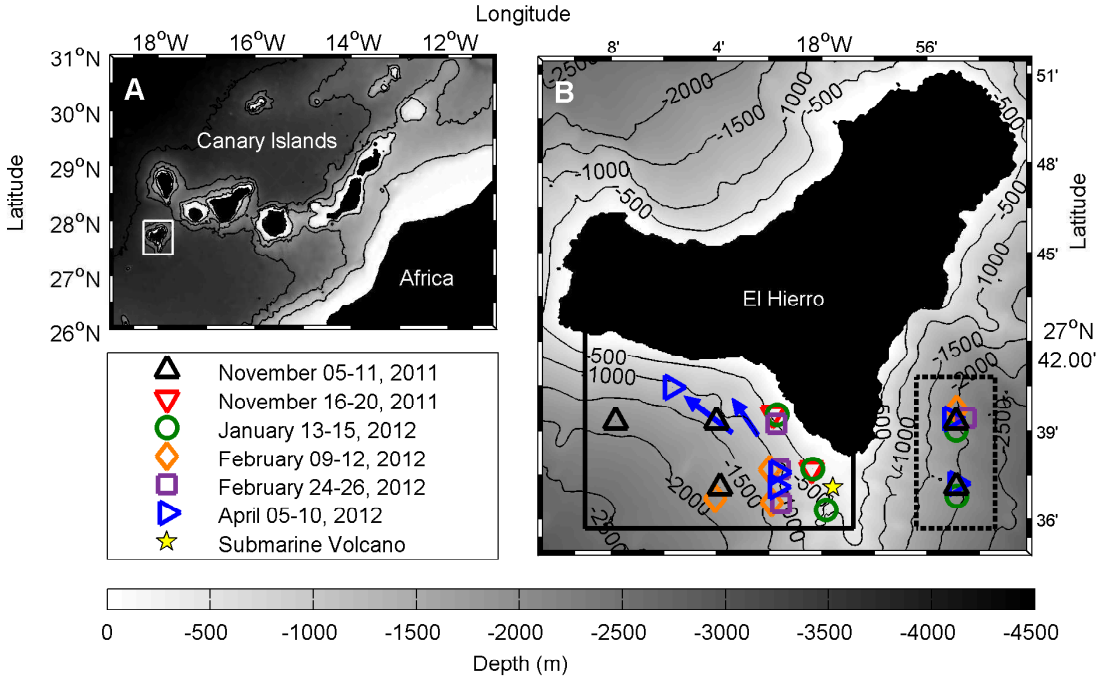

FIGURE 3.1: Position of El Hierro Island (A) and sampling points (B). The yellow star marks the position of the volcano. Symbols and arrows indicate oceanographic stations and locations of trawl tows, respectively. Colors refer to different surveys performed during the sampling period. Solid and dashed frames delimit experimental (volcano affected) and control (non-affected) zones, where satellite and acoustic data were collected along time-series.

that, remaining missing data were calculated by linear interpolation of the bordering pixels. Processing of satellite imagery was performed with SeaDAS software.

Acoustic sampling

Hull-mounted SIMRAD EK60 echosounders (7° beam width) operating at 38 and 200 kHz were used for recording acoustic data (detection ranges of about 200 and 1000 m depth, respectively). The configuration was set at a 1024 μs pulse duration and a 1 s^{-1} ping rate. Acoustic data were not available for the upper 15 m due to the depth of the transducers (8 m on the R/V *Ramón Margalef* and 5 m on R/V *Cornide de Saavedra*) and because data down to 7 m below the transducers were excluded due to vessel-caused bubbles and near-field effects [MacLennan and Simmonds, 1992]. Since the volcano eruption was an unforeseen event, the R/V *Ramón Margalef* performed its first mission at sea without prior *in situ* acoustic calibration. For that reason, the acoustic data collected with this vessel were calibrated using correction factors obtained by standard calibration techniques [Foote et al., 1987] after the surveys. Echo sounders

on the R/V *Cornide de Saavedra* were calibrated prior to the cruise, also using standard procedures.

Net sampling

Epipelagic mesozooplankton was sampled from 200 m depth to the surface using a WP-2 plankton net equipped with 100 μm mesh. Samples were immediately fixed in 4% buffered formalin. In the laboratory, samples were digitalized using a scanner at a resolution of 1200 dpi and the organisms were automatically counted, measured and classified using ZooImage software according to the procedures described by Grosjean and Denis [2007]. Taxonomic groups were established by a manually entered training set, achieving a global error rate of only 4.7% in the classification. The area of the organisms was then converted into biomass using the equations given by Lehette and Hernández-León [2009].

Vertical migrant micronekton was captured using a midwater trawl with a 300 m^2 mouth area and ∼45 m length. The mesh size was 80 cm near the opening, decreasing to 1 cm in the cod end. In the last survey, two tows were performed obliquely in the MSL. The trawl was monitored by a Scanmar depth sensor and was guided into the MSL by information provided by the echosounders. The trawling speed varied between 2 and 3 knots and the effective fishing time was one hour. Samples were fixed in 4% buffered formalin for later identification and enumeration.

Acoustic analysis

Anomalies in the distribution of acoustic targets were observed with the 38 kHz frequency related to the increment of surface turbidity and the oxygen depletion. For that reason, acoustic transects were made throughout the emission plumes, and their time-based echograms were displayed at this frequency together with corresponding latitude-longitude SSR from satellite imagery and spatially coincident profiles of dissolved oxygen. The acoustic measuring unit was the Volume Backscattering Strength (S_v, units: dB re 1 m^{-1}) and the minimum detection threshold was set at -80 dB. Acoustic, satellite and hydrographic data were integrated and plotted using MATLAB software. In Fig. 3.2, two acoustic transects are shown: one between the main plume surrounding the volcano and an anticyclonic eddy, which was advecting emissions toward the open ocean (Fig. 3.3), and the other crossing a secondary plume, which drifted to the north side of the island (Fig. 3.4).

The upper depth of the DSL (i.e., the part of the deep scattering apparently not involved with DVM) was mapped together with the contour of the plume to depict their geographical coupling. Since the upper part of the DSL appeared to be shallow beneath the plume (see Results), we manually traced the top boundary along the 38 kHz echogram using LSSS software. The averaged upper depth every 0.2 nm was afterwards map-projected and interpolated using the DIVA algorithm [Troupin et al., 2012]. Day and nighttime DSL depths were interpolated together as we did not observe significant differences between the two. Nevertheless, original data points are shown in the map in black (night) and white (day) to distinguish them (Fig. 3.5a). The outer limit of the plume was set in the SSR isoline of 0.2 10^{-3} sr^{-1} because this was the averaged sea surface reflectance found in clean waters near the plume. In addition, the relationship between the DSL depth and the geographically coincident SSR was plotted and linear regressions were run for both day and nighttime values (Fig. 3.5b).

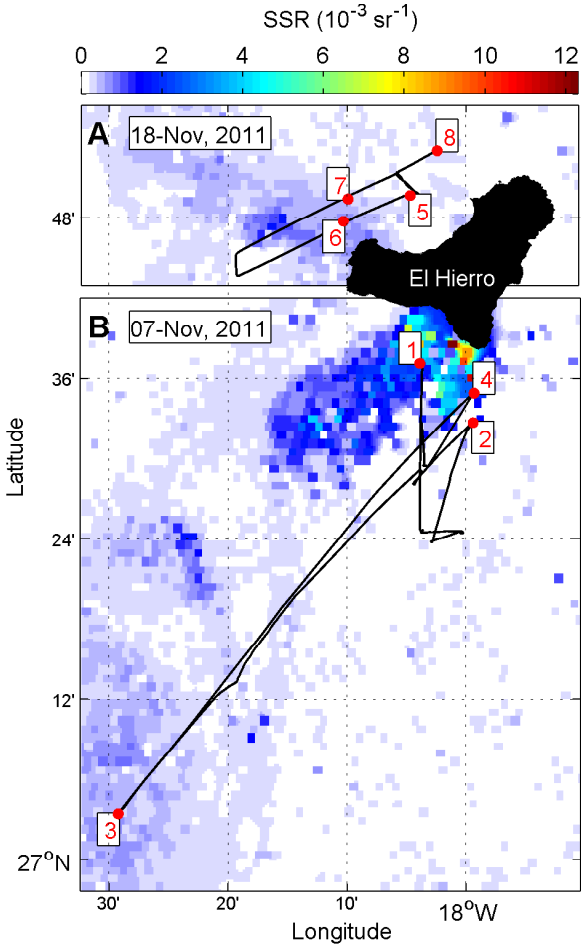

FIGURE 3.2: Sea Surface Reflectance (SSR) from satellite imagery. SSR indicates the degree of water turbidity and reveals the distribution of volcanic emissions. Red dots are CTD stations and black lines depict acoustic transects performed between them. Echograms corresponding to the transect lines and oxygen profiles from each station are shown in Fig. 3.3 (7 Nov.) and 3.4 (18 Nov.).

In addition to the net sampling (see above), the presence of epipelagic mesozooplankton and vertical migrant micronekton was also assessed using acoustics. The acoustic density of the former was calculated using the 200 kHz frequency, as the average length of members of this community (0.2-2 cm) fit quite well with its lowest resolution limit (wavelength of 0.75 cm). Fluid-like elongated mesozooplankton was the most abundant group collected by net sampling (see results). The detection threshold was therefore lowered to -100 dB in order to cover the weak backscattering caused by this group [Stanton and Chu, 2000]. To exclude noise and echoes from mesopelagic migrants, only daytime acoustic data collected above 100 m depth were used and fish-like schools were removed before the echo integration. Vertical migrant micronekton (2-10 cm) was monitored by acoustic sampling, but during the last survey, the composition of this community was assessed by trawlings in the MSL. The MSL acoustic density was estimated with 38 kHz (wavelength of 3.9 cm) as that frequency has been shown to be optimal for fish detection [Love et al., 2004, Simmonds and MacLennan, 2005]. Fish was the main group forming the MSL in the Canary Islands according with our results and previous works [Bordes et al., 2009, Wienerroither et al., 2009]. Only nighttime data collected above 200 m depth was used and the minimum threshold for integration was set at -80 dB to exclude weaker echoes caused by smaller organisms. Acoustic processing (noise removal and animal group allocation) was achieved using LSSS software [Korneliussen, 2000, Korneliussen et al., 2009]. The averaged form of Sv, i.e., the mean volume backscattering strength (MVBS), was used as an indicator of animal density. We therefore refer to $MVBS_{200\ kHz}$ and $MVBS_{38\ kHz}$ as proxies for the density of epipelagic mesozooplankton and vertical migrant micronekton, respectively. Because full species discrimination was not possible using the acoustics, these allocations should be interpreted as approximations based on the dominant communities found in net samples rather than exclusive taxonomic groups (i.e., macrozooplankton and gelatinous taxa were also expected to be within the MSL, but micronekton was the dominant group, and they were likely the most visible targets of the 38 kHz frequency).

Monitoring of the pelagic biota

Temperature, oxygen, chlorophyll *a*, epipelagic mesozooplankton and vertical migrant micronekton were measured during six months covering the eruptive and post-eruptive phases. As an indicator of the degree of volcanic emissions, five-day averaged SSRs are also shown (Fig. 3.6 and 3.7). Two zones were set for collecting samples and data: the experimental zone, in the south bay of the island where the erupted material remained blocked most of the time, and the control zone outside the bay, to the east of La Restinga front (see Fig. 3.1). Although the magmatic eruptive phase officially stopped on 5 March

2012 [Rivera et al., 2013], waters along the south bay of the island were significantly cleaner around early February (according to SSR data). To study the effects on the surrounding pelagic biota, we designate the post-eruptive phase as starting in February 2012.

Chlorophyll *a* collected at 5 m depth and from remote sensing data was used as a proxy for the phytoplankton biomass. During the third and fifth cruises, *in situ* measurements of chlorophyll *a* were not available, so we derived the data from the fluometer sensor, which was calibrated using regression equations derived from chlorophyll *a* measurements performed during adjacent surveys. Epipelagic mesozooplankton and vertical migrant micronekton densities were assessed from both acoustic and net sampling approaches (see above). All those variables were replicated in the two zones. Data from water and net samplings were averaged from oceanographic stations that were selected within each zone. Satellite and acoustic data were also collected within those zones. The MVBS acoustic data were averaged from cells collected every 0.2 nm along the zones.

Results

Acoustic tracks and echograms

The 38 kHz echogram (Fig. 3.3) recorded during the acoustic transect on 7 November 2011 (Fig. 3.2b) was dominated by two scattering layers: the DSL at around 300-700 m depth during both day and night and the MSL above 200 m during nighttime. According to catches (Table 3.2) those scattering layers were composed of small fishes, cephalopods and shrimps, but they were largely dominated by myctophids. The echogram registered the upward and downward migrations of the MSL respectively coinciding with the sunset and sunrise. In addition to the typical DVM behavior, two anomalies were observed in the nocturnal echogram associated with the plume: a strong weakening of the MSL (73 ± 18 %) and an elevation of the upper limit of the DSL (∼100-150 m). During the first and fourth CTD cast (in the plume) both anomalies occurred, coinciding with an increase of the SSR (the surface was more turbid) and a dramatic decrease in the dissolved oxygen around 70-80 m depth (∼50%). The second and third casts were performed during daytime, when we observed a weaker scattering layer above 50 m depth produced by non-migrant biota. This scattering layer and the DSL did not display anomalies at the second station (outside the plume), nor did the oxygen profile or the SSR. Nevertheless, at the third station (the anticyclonic eddy), the DSL increased again and the S_v also decreased in shallow waters. That coincided with an increase of SSR but this time the oxygen profile remained unchanged.

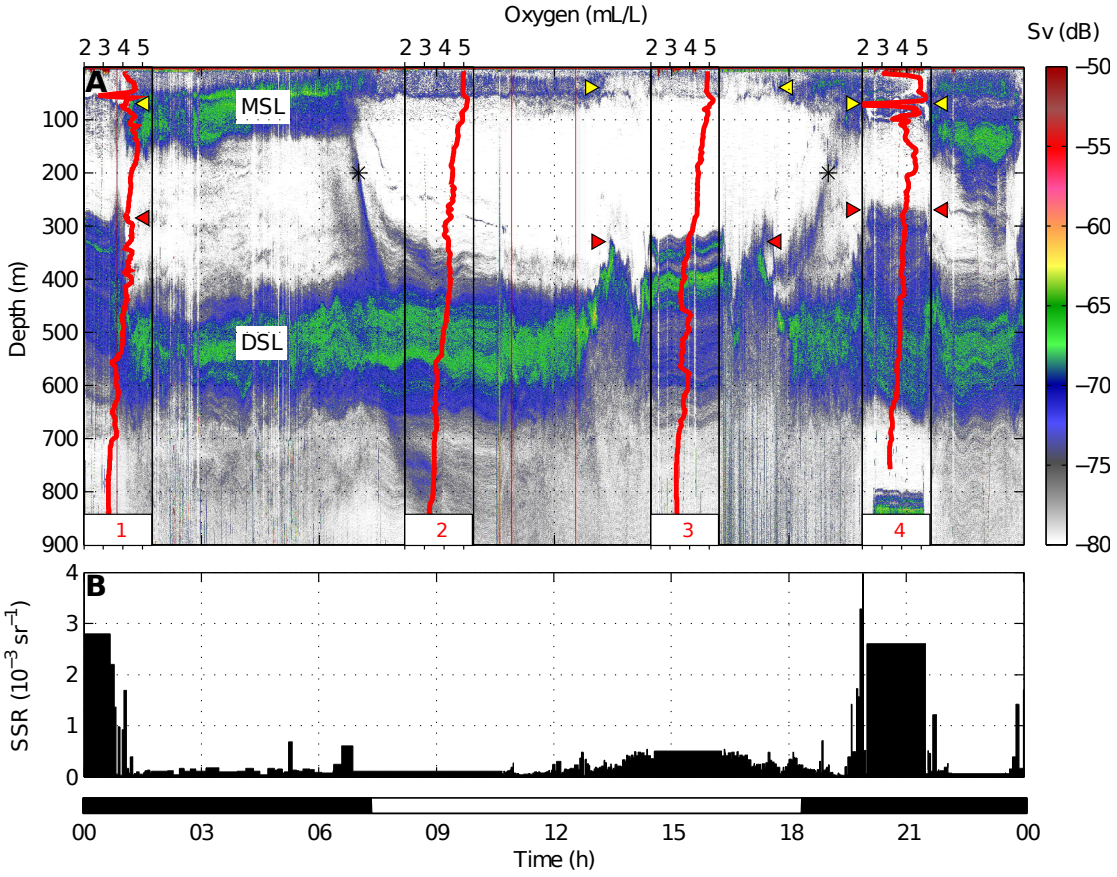

FIGURE 3.3: 38 kHz echogram (A) and Sea Surface Reflectance (B) on 7 November 2011 along the acoustic transects indicated in Fig. 3.2b. The color scale refers to backscattering strength (Sv). Migrant and Deep Scattering Layers (MSL and DSL) as well as both diel migrations (∗) are indicated. Acoustic anomalies are also indicated: the MSL weakening (yellow triangles) and the elevations of the DSL (red triangles). Red lines depict the dissolved oxygen profiles established during the acoustic track. The black color in the time scale refers to nighttime and white to daytime.

According to remote sensing data, the plume was less dense on the northern side of the island by 18 November 2011 (Fig. 3.2a). The 38 kHz echogram (Fig. 3.4) revealed the same scattering layers as in previous results and the acoustic anomalies also occurred with an increase in SSR accompanied by hypoxia (see station 6 and 7). No anomalies were detected in the scattering biota where the waters remained clean and normoxic (station 8). In the case of the station 5, the oxygen sensor registered a decrease while SSR was quite low (no water dimming). Here, the MSL was depleted but the upper limit of the DSL remained in its normal depth range.

DSL depth and SSR coupling

The upper limit of the DSL shown in Fig. 3.5a was markedly closer to the surface beneath the volcanic plume than in the surrounding non-affected waters. The upper

fringe of the DSL was well above 200 m in the plume, but around 400 m outside. This pattern occurred both day and night and did not differ in magnitude with the diel cycle. Furthermore, the relationship between the depth of the DSL and the SSR followed a positive logarithmic curve, becoming shallower both during the day and night (Fig. 3.5b). It is noteworthy that a small increase in the sea surface reflectance, by about 0.3 10^{-3} units above the turbidity level under normal conditions, was enough to raise the DSL up to 300 m below the surface.

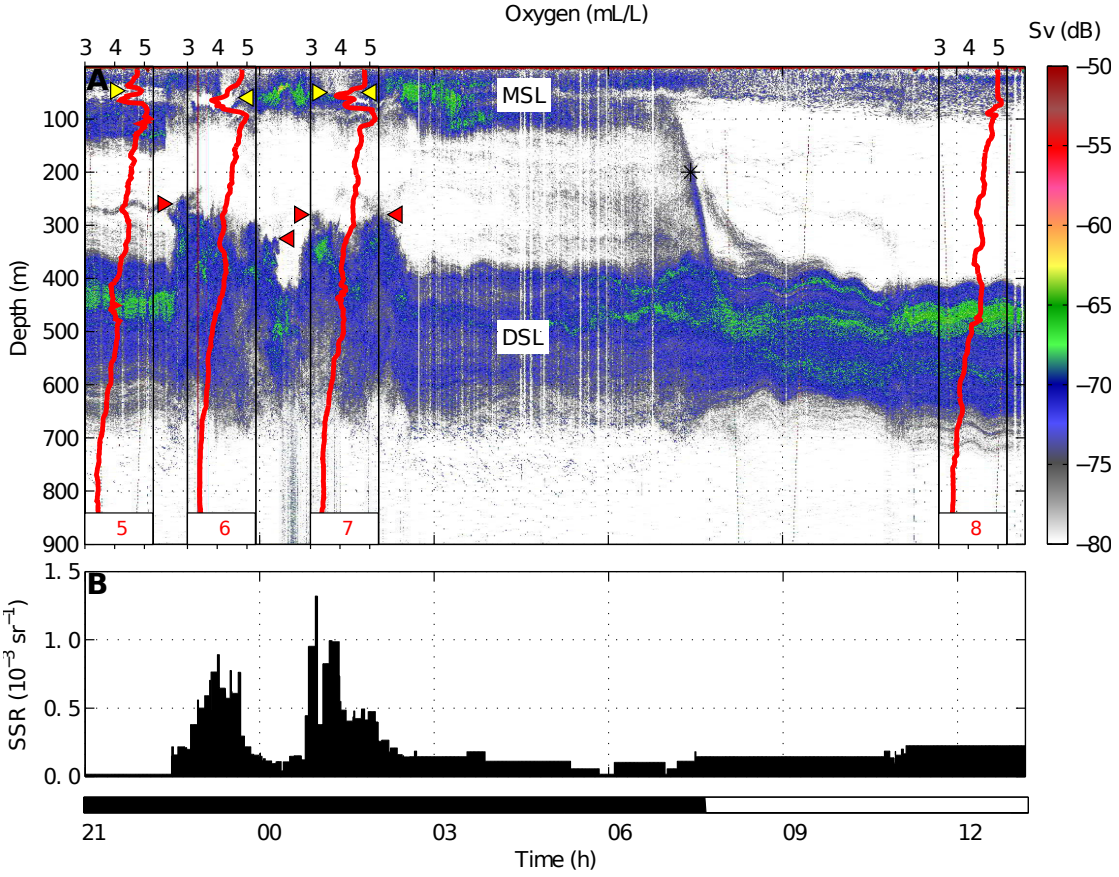

FIGURE 3.4: 38 kHz echogram (A) and Sea Surface Reflectance (B) on 18 November 2011 along the acoustic transects indicated in Fig. 3.2a. The color scale refers to backscattering strength (Sv). Migrant and Deep Scattering Layers (MSL and DSL) as well as the downward diel migration (∗) are indicated. Acoustic anomalies are also indicated: the MSL weakening (yellow triangles) and the elevations of the DSL (red triangles). Red lines depict the dissolved oxygen profiles established during the acoustic track. The black color in time scale refers to nighttime and white to daytime.

Temporal changes in the pelagic biota

During the eruptive phase, the water column was characterized by a strong thermocline at around 80-90 m depth and high deoxygenation from 80 to 170 m depth (Fig. 3.6). The first sign of the eruption on the sea surface appeared on 12 October 2011, when the SSR increased from 0.1 10^{-3} to 0.5 10^{-3} sr^{-1}, reaching the highest degree of water

dimming by the end of October (0.8 10^{-3} sr^{-1}). Around one week later, two consecutive biological samplings were performed (Fig. 3.7). Chlorophyll *a* was below 0.1 mg m^{-3} and mesozooplankton values ranged 700-950 ind m^{-3} and 3.0-4.2 mg m^{-3} (dry weight). The acoustic proxy for epipelagic mesozooplankton density ($MVBS_{200\ kHz}$) was below -67 dB while the vertical migrant micronekton ($MVBS_{38\ kHz}$) registered higher scattering levels, around -54 dB. Values for $MVBS_{200\ kHz}$ in the control zone (outside the plume) did not differ significantly from those collected in the plume, while $MVBS_{38\ kHz}$ was lower inside the plume than in the non-affected area. According to SSR, mantle-derived materials continued spilling over the sea surface, but with progressively decreasing intensity pulses until the eruption stopped in early February. During this time, small turbidity pulses were also registered within the control zone.

Shortly before the end of the eruption, the concentration of *in situ* chlorophyll *a* in the volcano-affected area started to increase moderately but was still somewhat lower than in the control zone (January). Afterwards, chlorophyll *a* measurements were slightly higher in the affected area, reaching an average maximum of 0.33 mg m^{-3} during late February, when the eruption stopped. Remote sensing chlorophyll *a* measurements during March in the affected area were similar to *in situ* adjacent measurements, but slightly increased to 0.40 mg m^{-3} in the control zone. $MVBS_{200\ kHz}$ also started to recover by January, registering a relative maximum backscattering (-63 dB) coinciding with the chlorophyll *a* peak. The same pattern was found in epipelagic mesozooplankton abundances and biomass, where average maxima were 2370 ind m^{-3} and 5.8 mg m^{-3}. $MVBS_{38\ kHz}$ also increased, but the maximum average backscattering (-48 dB) was reached one month after the eruption ceased (early April). During the post-eruptive phase, both acoustic proxies revealed considerably higher backscattering in the volcano-affected zone compared with those in the control zone. It should be noted that relative peaks of all biological parameters also coincided with the breakdown of the thermocline and with normoxic conditions in the water column (See Fig. 3.6 from February on).

Mesozooplankton and Micronekton composition

Concerning epipelagic mesozooplankton, no significant differences (Student's t-test) were found when comparing the relative abundances of each taxa among the sampling surveys, nor between the experimental and control areas. Their averaged relative abundances are given for the whole sampling period (Table 3.1). Copepods largely dominated the community (94%), followed by chaetognaths (3%) and other organisms with abundances well below 1%.

Group	Abundance (%)	
	Average	SD
Chaetognatha	3.01	1.22
Copepoda	94.23	1.50
Euphausiids like	0.29	0.22
Gelatinous	0.65	0.26
Others	1.98	0.69

TABLE 3.1: Averaged mesozooplankton abundance along the sampling period. Data are shown in percentage of total abundance.

The micronektonic composition (Table 3.2) corresponding to the MSL during the last survey was dominated by Lanternfishes of the family Myctophidae (70%). The family Enoploteuthidae was the most important within squids (11%), while shrimps from the family Oplophoridae were the most abundant group of decapods (8%). Other minor groups also appeared but in quite low abundances ($\lesssim$1%).

Group	Family	Abundance (%)	
		Average	SD
Fishes	Myctophidae	71.30	2.28
	Gonostomatidae	1.33	1.22
Decapods	Oplophoridae	8.19	4.33
	Sergestidae	1.02	0.64
Cephalopods	Enoploteuthidae	11.16	9.99
Others	-	7.07	1.52

TABLE 3.2: Averaged micronekton abundance within the MSL during the last survey. Data are shown in percentage of total abundance. Trawls are indicated as blue arrows in the map showed in Fig 3.1b.

Discussion

The weakening of the Migrant Scattering Layer

Based on the measured parameters, we related the weakening of the MSL to low oxygen concentrations in the upper layers. However, we consider the shallow hypoxia as a tracer of perturbations from the eruption rather than as a unique factor affecting the pelagic biota. Hypoxia was not the only perturbation observed in shallow waters during the submarine eruption. Fraile-Nuez et al. [2012] observed temperature anomalies in the vicinity of the volcano (+3°C at 75 m depth) and chemical compounds containing Fe, Cu, Cd, Pb and Al were observed at the sea surface. Santana-Casiano et al. [2013] also reported that emissions of reduced sulfur compounds promoted a decrease in both the redox potential and the concentration of dissolved oxygen. Moreover, changes in the

carbonate system contributed to the water acidification (-0.5 units at 75 m depth along the plume).

The depletion of the scattering biota was evidence of the harmful effects of the volcano. By comparing the acoustic densities of the volcano-affected MSL with the neighboring non-affected zones, we observed that the former had a $MVBS_{38\ kHz}$ that was $71 \pm 11\%$ lower than that of the latter. That was partially balanced in the mesopelagic zone since the $MVBS_{38\ kHz}$ of the DSL was $41 \pm 19\%$ higher in the affected areas than in the non-affected areas. It seems feasible that part of the normally migrant biota remained in the midwaters when the emissions covered the surface. Nevertheless, another part ($\sim$30%) just disappeared from the ensonified volume. This disappearance could be explained by (1) horizontal migrations to find surrounding clean waters, as well as by (2) mortality caused by extreme physical-chemical perturbations. Support for the latter possibility was the occurrence of many mesopelagic species (mainly myctophids, hatchetfishes and deep-sea squids) floating dead at the surface during the strongest episodes of volcanic unrest (Escánez, pers. comm.). This is not surprising, because it is probable that the magnitude of the eruption did not leave scope for adaptation although deep-sea animals have a high tolerance threshold for varying oxygen [Ekau et al., 2010] and temperature conditions [Watanabe et al., 1999]. Many mesopelagic organisms tolerate hypoxia by reducing their metabolism as the consequence of lower temperatures in the deep ocean [Ekau et al., 2010], but in warmer waters, the oxygen consumption increases dramatically [Torres et al., 1979, Donnelly and Torres, 1988]. Presumably, the oxygen demands of vertical migrants during feeding activity were therefore much higher than in existing reserves in shallow waters of El Hierro Island. Besides, it has recently been documented in myctophids (main group forming the MSL) that heat shock responses under warm conditions might be triggered by the oxidative stress that occurs in normoxic waters [Lopes et al., 2013]. It thus seems likely that the natural plasticity of the migrant biota no longer worked under the atypical scenario of low oxygen and high temperature. This, along with adverse effects of ocean acidification [Fabry et al., 2008, Hall-Spencer et al., 2008] and the presence of toxic chemical compounds, suggests that both vertical and horizontal evasion would be the only means to avoid death.

The elevation of the Deep Scattering Layer

The presence of unusual acoustic scattering layers up to 200 m above the normal upper limit of the DSL might be interpreted both as an elevation of the DSL or as a lowering of the MSL. Since that phenomenon also occurred during daytime, when there was no migration, we are inclined to favor the former hypothesis although we do not reject the idea that during nighttime backscattering was also induced by arrested migrants. Those

elevations were likely promoted by the light attenuation caused by the water turbidity at the surface. Chemical perturbations seemed to have a limited effect since the DSL was closer to the surface below turbid waters, even though no hypoxia was registered (St. 3 in Fig. 3.3). It remained, however, at normal depth coinciding with clean waters despite the oxygen and acoustic anomalies found at the surface (St. 5 in Fig. 3.4).

Light-induced vertical migrations of scattering layers are well documented although most of the information refers to time-based patterns [Clarke and Backus, 1953, Boden and Kampa, 1967, Roe, 1983] rather than to spatial variations. In discussions of temporal patterns, the difficulty of discerning to what extent behavior is controlled by an external stimulus (e.g., light irradiance) or by endogenous biological rhythms has been raised [Neilson and Perry, 1990]. The pattern reported here is not a diel migration since it occurred all day and varied with geographic location rather than with time. Apparently, these vertical relocations were triggered by light alone (or indirect knock-on effects) but not by time. Daytime elevations of acoustic scattering layers have also previously been reported in relation to varying light, including variable cloudiness [Baliño and Aksnes, 1993, Staby and Aksnes, 2011] or harmonic migrations caused by shading from turbid surface layers that varied in thickness due to internal waves [Kaartvedt et al., 2012a]. Corresponding to the present study, shading-induced migrations have also been documented in the spatial dimension. Sassa et al. [2010] observed patches with shallower distributions of the lanternfish *Benthosema pterotum* coinciding with turbid areas caused by suspended sediments, while Kaartvedt et al. [1996] reported shallow scattering layers below waters inside a front characterized by higher light extinction. These unpredictable shading effects over the deep scattering biota show that although internal clocks might also operate, the external stimulus is a main trigger for the migrant behavior within the mesopelagic zone.

It is generally assumed that migrant planktivores increase their food intake as they move to upper layers but also that the mortality risk increases since the higher illumination in the upper layers exposes them to larger predators. Dawn and dusk provide intermediate levels of light intensity in upper waters, where the ratio of mortality risk to feeding rate reaches a minimum. These brief antipredation windows of time in upper waters [Clark and Levy, 1988] occur twice per day during the DVM. We suggest that fortuitous shadings in the water column, like those produced by the volcano eruption, might be exploited by migrants to stretch out the antipredation window and, therefore, to increase their feeding rate. Exploitation of additional feeding windows has also previously been suggested when high algal densities in upper layers diminish the light penetration in the water column [Kaartvedt et al., 1996, 2012a].

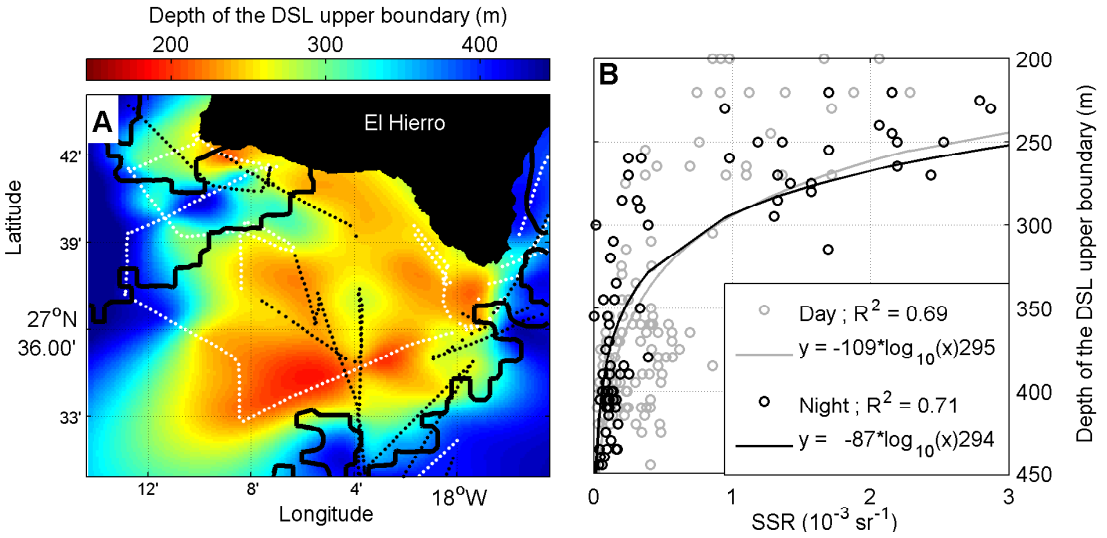

FIGURE 3.5: DSL depth throughout the volcanic plume. (A) Horizontal interpolation of the upper DSL depth. Dots indicate the positions of the original data points; the black ones refer to those collected during nighttime and the white ones during daytime. The solid black line depicts the outer contour of the volcanic plume. (B) Relationships between the upper DSL depth and the Sea Surface Reflectance (SSR, water turbidity proxy). Black and gray colors refer to data collected during night and daytime, respectively. Solid lines depict logarithmic regression curves fitted to data points. The vertical dashed line refers to the averaged SSR outside the volcanic plume.

The evolution of the pelagic biota along the volcanic unrest

Waters outside the main influence of the eruption, used here as control zones, were also somewhat affected since the satellite reflectances also registered some small turbidity pulses during the strongest eruptive episodes. This might explain the fact that phyto- and mesozooplankton indices were likewise low in the affected and the control zones, at least at the beginning of the monitoring. On the contrary, vertical migrant micronekton formed a stronger MSL in the control zone. A feasible explanation for the divergent responses observed between these communities outside the main plume could be that, in the case of phyto- and mesozooplankton, we were actually sampling organisms advected from the affected zone (the undermined stocks would reach the control zone in the same way as turbid waters did). In contrast, vertical migrant micronekton could avoid the water perturbations by remaining in deeper waters (see discussion about the weakening of the MSL). Once the adverse conditions were temporarily alleviated (between turbidity pulses), the migrants could again occupy the shallow waters while the epipelagic plankton community would be restoring its population.

According to the biological indices analyzed, it seems clear that plankton and nekton in shallow waters were negatively affected during the first and strongest episodes of the volcanic unrest. In situ chlorophyll *a* values were 0.04-0.05 mg m^{-3} while the values in the Canary Islands, during the same season (stratified water column and at the leeward

side of the island), ranged from 0.06 to 0.34 [Arístegui et al., 1997]. Our values were even lower than those collected by Davenport et al. [2002] during the same season in oligotrophic oceanic waters northward of the archipelago (0.09 mg m^{-3}). Epipelagic mesozooplankton densities were certainly low (2.8-4.4 mg DW m^{-3}) but not so different from those reported by Arranz [2007] around the volcano area before the eruption and during the same season (4.4-13.1 mg DW m^{-3}). The vertical migrant micronekton was also affected as suggested by the weak MSL in the zone influenced by the eruption compared to the control zone.

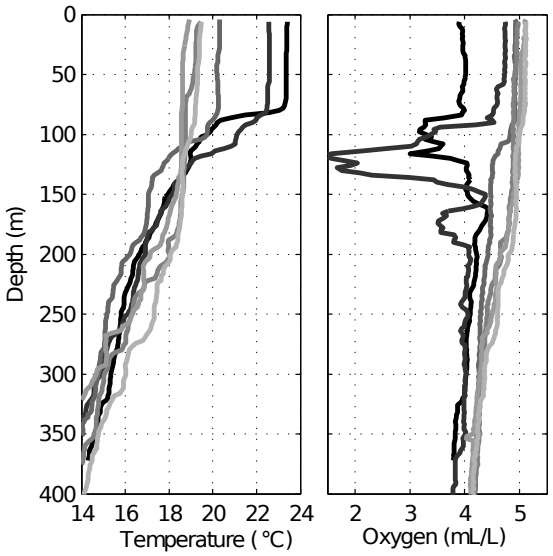

FIGURE 3.6: Temperature and dissolved oxygen profiles during the sampling period. The black lines indicate the first survey at the beginning of the eruption; the remaining surveys are indicated by progressively lighter gray lines (post-eruption) in chronologic order. Profiles were averaged from CTD casts performed within the affected zone.

All biological parameters increased slightly in magnitude immediately after the eruption stopped. Whether these enhancements were caused by a potential fertilization due to the volcano eruption [Santana-Casiano et al., 2013], or to natural inputs of nutrients due to winter mixing, is difficult to know unless we study changes in nutrients field over the course of the study across the whole region. Nevertheless, the cessation of the eruption coincided with the lowest temperatures in the water column (February), a period otherwise characterized by the so-called late winter bloom [Arístegui et al., 2001, Hernández-León et al., 2004]. This natural bloom is related to weakening of the thermocline as a result of surface cooling, allowing a small vertical flux of nutrients, and therefore, promoting biological production. Thus, the observed biological growth might be due to the late winter bloom as well as to fertilization by the volcano. After the eruption, *in situ* chlorophyll *a* in the affected area ranged from 0.17 to 0.35 mg m^{-3} (0.11-0.24 from remote sensing data) whereas Arístegui et al. [1997] obtained values between 0.16-0.77 during the late winter bloom, leeward of Gran Canaria Island. The

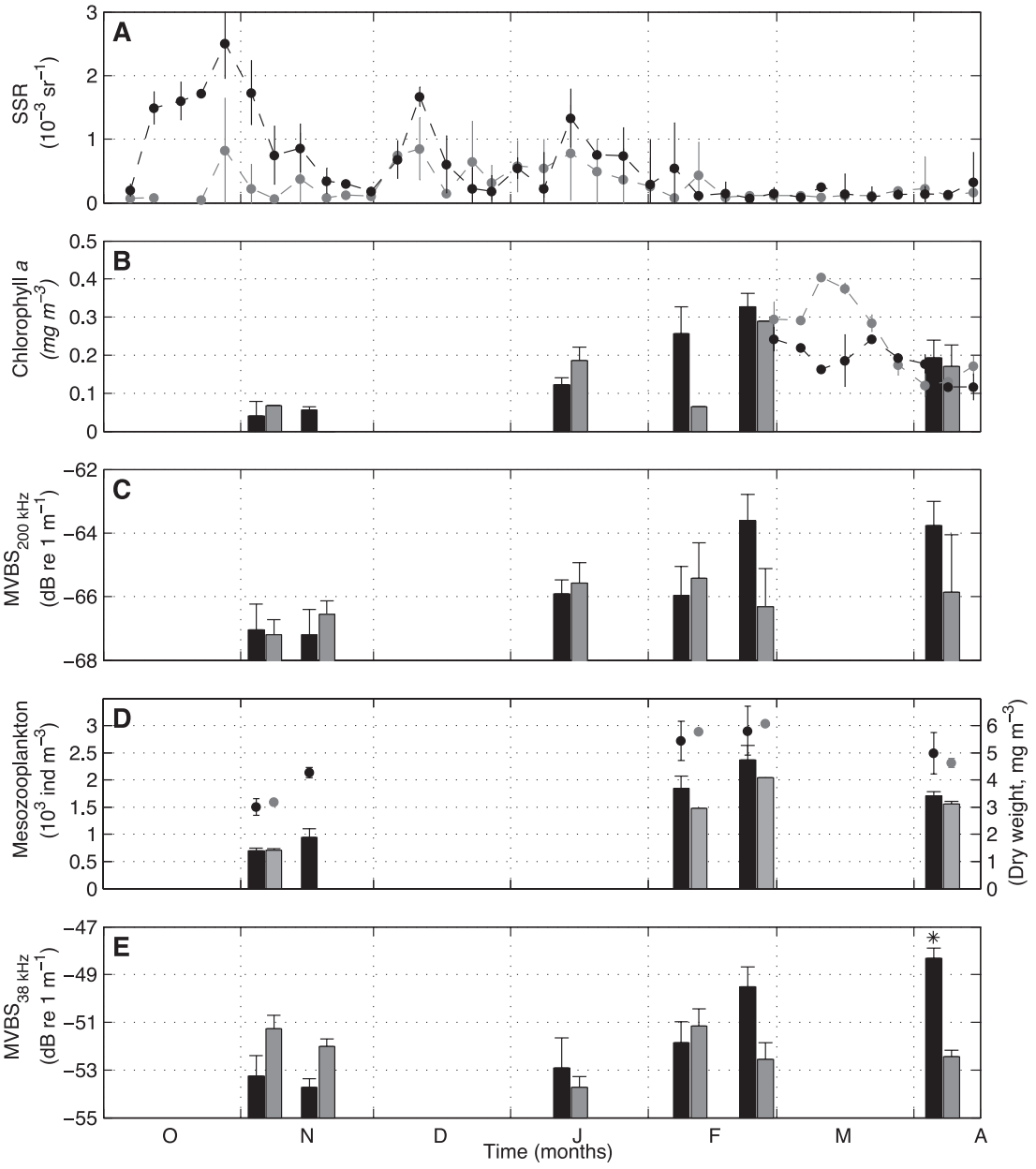

FIGURE 3.7: Time series with averaged parameters collected within the volcano-affected (black) and non-affected area (gray). (A) Evolution of the Sea Surface Reflectance (SSR) as an indicator of the degree of volcanic emissions over the sea surface. (B) *In situ* (bars) and remote sensing (dots) chlorophyll *a* concentration as a proxy of phytoplankton biomass. (C) Mean Volume Backscattering Strength at 200 kHz ($MVBS_{200\ kHz}$) as a proxy of mesozooplankton biomass. (D) Mesozooplankton abundance (bars) and dry weight (dots) from WP-2 net hauls. (E) $MVBS_{38\ kHz}$ representing the acoustic density of the MSL (proxy of migrant micronekton biomass). Asterisk indicates that in the last survey, the composition of the MSL was characterized with concurrent trawling data (See Table 3.2).

same author reported a maximum of ∼1.12 mg m^{-3} during a bloom in March in a time-series also performed in the Canary Islands [Arístegui et al., 2001]. In sum, we consider that the concentration of chlorophyll *a* during the post-eruptive phase was not above the normal range observed during this season in the Canary waters.

Concerning epipelagic mesozooplankton: in February, we obtained biomass values ranging from 4.1 to 6.8 mg DW m^{-3} whereas, in the same zone and before the volcano eruption, Arranz [2007] obtained higher values during a bloom in April-March (6.0-14.3 mg DW m^{-3}). Our values were also lower than those compiled by Hernández-León et al. [2007] for the bloom conditions in the Canary Islands (8.7-13.5). Thus, as in the case of chlorophyll *a*, the mesozooplankton biomass was higher after the volcano eruption, but within the normal range for this season. On the other hand, during the post-eruptive phase, all the biological parameters were somewhat higher in the volcano-affected area than in the control zone (except mesozooplankton in terms of biomass). We attribute this increment to an island-mass effect [Doty and Oguri, 1956] rather than to volcano fertilization. This phenomenon produces richer nutrient waters as a result of the current flow perturbations occurring in the downstream wakes of the islands. Island-mass effects have previously been documented in the Canary Islands and with stronger gradients of biological production by Hernández-León [1988] and Arístegui et al. [1997], who observed biomass increments (up to three-fold higher) in both chlorophyll *a* and mesozooplankton as they approached to the wake of Gran Canaria Island. According to our values and baseline levels around the coastal Canary waters, we found no evidence of a volcano-induced bloom during the post-eruptive phase. We posit that surface chlorophyll *a*, epipelagic mesozooplankton and vertical migrant micronekton simply restored to normal levels in the area.

In summary, biological monitoring that ran in parallel with a submarine volcanic episode provided valuable observations of both adverse effects and adaptive responses by pelagic biota. The environmental stressors accompanying the eruption promoted the depletion of epipelagic stocks, changed the vertical distribution of the deep scattering biota and interrupted the diel vertical migration. In contrast, the post-eruptive phase indicated the restoration capacity of pelagic ecosystems after volcanic perturbations. We underline the importance of studying these phenomena as they provide a valuable understanding of how the marine ecosystem responds to environmental stressors.

Acknowledgments

We are grateful to the crew of the R/V *Ramón Margalef* for their work and support at sea. We would like to thank Verónica Benítez-Barrios and Isis Comas for collecting

and processing hydrographic data. We also thank Minerva Espino and Laia Armengol for chlorophyll *a* analyses and their assistance on board, as well as Lidia Nieves for technical and logistical work. Special gratitude goes to Rupert Wienerroither, José María Landeira and Alejandro Escánez for micronekton identification and for sharing data, and to Natacha Aguilar de Soto and the crew of the R/V *Cornide de Saavedra* for making the last cruise and sampling possible. Finally, thanks are also due to Virginia Unkefer for editorial work on the manuscript and to two reviewers for providing insightful suggestions.

Chapter 4

Eddy-induced variability of the deep mesopelagic biota.

Alejandro Ariza, Javier Arístegui, Pablo Sangrà, Bàrbara Barceló-Llull and Santiago Hernández-León (2015).

In preparation.

Abstract

Eddies are common but hidden structures traveling through the oceans. These mesoscale features (100 km) are capable to force physical and biogeochemical gradients, providing singular ecosystems for pelagic organisms. The influence that eddies exerts over plankton and top predators is fairly well documented. However, there is a lack in knowledge at intermediate trophic levels such as micronekton, which mainly include small fish, decapods and squid. Studies with limited spatial resolution suggest that eddies may affect the abundance and the species composition of micronekton, but little is known about how these animals adjust their distribution with respect to the eddy structure. Here we combine hydrographic and acoustic *in-situ* measurements with satellite remote sensing to investigate, for the first time, the micronekton distribution along mesoscale features of the Canary Eddy Corridor. The three-dimensional structure of the scattering biota was analyzed by sectioning systematically an anticyclonic eddy from the surface to 1000 m depth with a 38 kHz echosounder. We observed horizontal differences in scattering layers between 700 a 900 m depth, with the most important gradients finely tuned to the eddy borders. Acoustic gradients outlined three different regions for micronekton, one inside and two outside the eddy. Assuming that these regions were composed by

the same species, the eddy structure and its surrounding waters may produce up to three-fold biomass differences in animals inhabiting between 700 and 900 m depth. Regardless of whether this variability reflected different biomass or different species, the pattern observed here suggests a high level of micronekton patchiness over the eddy field. Our results also highlight that eddies may shape the distribution of animals inhabiting down to 900 m depth, even though these structures hardly extend to 400 m depth. We hypothesized that the interaction between eddies and micronekton may occur near the surface at night, through the vertical migration that these animals conduct on a daily basis

Introduction

The Canarian Archipelago , acts as barrier to the southwestward flowing Canary Current. As a consequence, mesoscale eddies (10-100 km) are generated downstream the Islands, enhancing the hydrographic variability and the biological production of an otherwise oligotrophic region [Barton et al., 2004, Neuer et al., 2007]. Cyclonic and anticyclonic eddies, are recurrently spun off from the islands with a period ranging from days to weeks [Arístegui et al., 1997]. Most of the eddies drift westward forming part of an eddy corridor with life spans of at least several months [Sangrà et al., 2007]. This "Canary Eddy Corridor" is considered an stable oceanic system, responsible of about one fourth of the Canary Current mass transport, while accounting for a primary production similar to that of the NW Africa coastal upwelling at the same latitudinal range [Sangrà et al., 2009].

At earlier formation stages, cyclonic eddies pump cold nutrient-rich waters into their surface cores and thus enhancing the primary production. On the contrary, anticyclonic eddies accumulate surface warm waters in their centers, deepening the mixed layer, and reducing production [Arístegui and Montero, 2005]. However, during more mature stages wind-stress curl may cause downward and upward velocities inside cyclonic and anticyclonic eddies, respectively, reversing the effect of the role of cyclones/anticyclones in eddy productivity [McGillicuddy et al., 2007]. Anticyclonic eddies can also, entrain chlorophyll-rich waters from the islands' shelf, or from upwelling filaments, transporting them towards open-ocean [Arístegui et al., 1997]. This mechanism also concentrate and transport zooplankton, enhancing diel vertical migration (DVM), and consequently, the carbon export to deeper waters [Hernández-León et al., 2001, Yebra et al., 2005, Landeira et al., 2010]. On the other hand, tagging and sighting studies at other regions with high mesoscale activity have proved that top predators such as tuna, seabirds, seals

or whales seek these vortices for foraging purposes [Kai and Marsac, 2010, Woodworth et al., 2012, Bertrand et al., 2014, Cotté et al., 2015].

All these clues indicate that eddies may catalyze energy from primary producers to the top of the food chain. However, little is known about the role of intermediate trophic levels such as micronekton [Brodeur et al., 2005]. They are mainly small fish, decapods and squid belonging to third and fourth trophic positions [Burghart, 2006, Choy et al., 2012], and which are also considered as a key component in the redistribution of energy and organic matter through the deep ocean [Hidaka et al., 2001, Davison et al., 2013, Schukat et al., 2013, Irigoien et al., 2014, Ariza et al., 2015]. Few studies based in trawl sampling suggest that mesoscale eddies may affect the species composition of pelagic fish and decapods [Brandt, 1983, Griffiths and Wadley, 1986]. Unfortunately, little is known about the mechanisms governing this variability, or how animals adjust their distribution to the eddy shape. This requires different methodological approaches able to finely resolve mesoscale structures.

Low frequency echosounders proved very sensitive to micronekton layers dominating the epipelagic (0-200 m depth) and mesopelagic (200-1000 m depth) waters of the Canary Islands [Ariza et al., in prep.; Ariza et al., 2014] Mounted on moving vessels, they can successfully resolve hundred kilometers sections within hours, at vertical and horizontal resolutions of meters [Godø et al., 2014]. Therefore, they could be a powerful tool to assess biophysical interactions along eddies. Few studies have used this approach. In the Mozambique Channel (Indian Ocean), patchy fish aggregations and varying acoustic densities have been observed along eddies [Sabarros et al., 2009, Béhagle et al., 2014]. Also at mesopelagic waters in the North Atlantic, the scattering biota peaked near eddy regions [Conte et al., 1986, Fennell and Rose, 2015]. Unfortunately, the lack of accurately georeferenced outputs prevented to finely relate the micronekton distribution to mesoscale structures. Recently, Godø et al. [2012] shed some light on this respect working on anticyclonic eddies near Iceland and Norway. Coupling accurately acoustics to physical gradients, they reported shallow scattering layers intensifying along the inner periphery, and deep ones sinking below the cores. In conjunction, sound layers acquired a characteristic "bowl" or "wheel shape" with increased biomasses below the vortices. With just one observation so far, the question arising is whether this phenomenon is widespread, or variable along different mesoscale systems and pelagic communities.

Here we combine hydrographic and acoustic *in-situ* measurements with satellite remote sensing to investigate, for the first time, biophysical interactions between eddies and micronekton in the Canary Islands. The study focuses on an intrathermocline eddy (ITE), the typical anticyclonic structure for the Canary Eddy Corridor, characterized by dome-shaped isotherms above the thermocline and bowl-shaped below (Barceló-Llull

et al., in prep.). The three-dimensional structure of the scattering biota was analyzed by sectioning systematically the ITE from the surface to 1000 m depth with a 38 kHz echosounder. These recordings were afterwards translated to specific animal groups based on regional descriptions of acoustic layers, and also on previous reports about the vertical distribution of micronekton.

Methods

Remote sensing monitoring

Mesoscale activity around the Canary Eddy Corridor was routinely monitored five months prior to the survey. Sea level anomaly (SLA) imagery were downloaded and examined from the archiving, validation, and interpretation of satellite oceanographic remote sensing service (AVISO), in order to find potential eddies to be investigated. On 6 June 2014, an anticyclonic eddy (ITE) just generated at Tenerife Island was detected and selected as the subject of this study.

Hydrography

The hydrographic sampling was carried out on board the R/V *Hespérides* from the 1^{th} to the 20^{th} of September 2014, with the ITE being 3-months old (mature stage) and located approximately at 26°N and 20°W according to merged altimeters images (Fig. 4.1). The survey comprised five legs, which were used to study further physical and biogeochemical properties of the ITE (Arístegui et al., in prep.; Barceló-Llull et al., in prep.). In the present study we address the legs one and three.

Conductivity, temperature and depth fields were recorded using two CTDs (SeaBird 9/11-plus), one towed from the stern in a SeaSoar undulating system while the vessel was performing transects, and the other attached to a rosette of 24-10-liter Niskin bottles for vertical profiles at stations. Both CTDs were further equipped with fluorometers for chlorophyll *a* estimations (WetLabs ECO-FL). The SeaSoar was towed at 7-8 knots, and undulated from the surface to 400 m depth in cycles of approximately 12-15 min. This achieved an horizontal resolution of a about 3 km. The voltage readings of the CTD fluorometer were calibrated with chlorophyll *a* concentrations measured from extracted pigments. For this, 500 ml of seawater were filtered through 25 mm Whatman GF/F filters using low vacuum. The filters were frozen at -20°C before pigments were extracted in 90% acetone for 24 h in the dark at 4°C. Chlorophyll *a* concentrations (mg m^{-3})

were estimated by fluorometry in a Turner Designs fluorometer calibrated with pure chlorophyll *a* (Sigma Chemical).

During the leg one, the vessel conducted a transect starting and finishing at two cyclonic structures, and crossing in the middle the ITE that we were interested in. This was performed following the preliminary positions derived from SLA images (Fig. 4.1). In this phase, the ITE was for the first time *in-situ* located, as derived from temperature anomalies. The leg three consisted of nine parallel transects separated 10 nautical miles between them and disposed along the north-south axis of the eddy (Fig. 4.2). The first six transects were performed using the SeaSoar and hull-mounted sensors, but due to a malfunction of the former, the last three transects (B-D in Fig. 4.2) were completed with 400 m depth vertical casts separated 10 nautical miles one from the other.

Echosounder

A hull-mounted SIMRAD EK60 echosounder operating at 38 kHz was used for recording acoustic scattering layers occurring in epipelagic and mesopelagic waters. Data were stored at a 6-s ping interval with a pulse duration of 1024 μs. Considering that the vessel navigated from 7 to 8 knots during the hydrographic transects, the spatial resolution of the echosounder ranged between 22 and 25 meters. In order to present distance-based echograms, first, we removed those pings recorded during station time or at another circumstance where the vessel was not performing transects. Secondly, we calculated the distance increments between pings based on longitude and latitude coordinates. And finally, we allocated the closest pings in a monotonically increasing distance vector of 100 m resolution. No ping was included if the closest ping was at 100 m or more from a given distance point. Due to the draft of the transducer, and to prevent near-field effects [Simmonds and MacLennan, 2005], acoustic data for the first 6 meters depth were not included. In order to avoid range-increasing noise [Korneliussen, 2000], maximum depth of data used was 1000 m. Minimum detection threshold was set to -80 dB.

All echograms show an upper bar with white and black colors indicating respectively whether it was day or night, and also a symbol consisting in 3 consecutive angles where the vertexes point to the recording direction. The last indication was necessary because the echograms from westward transects were exceptionally displayed from right to left in order to facilitate the georeferencing of the acoustic data. Special care must be taken with these figures (vertexes pointing left) because, although the projection is correct in spatial terms, time is inverted. This means that upward migrations look like downward migrations and *vice versa*.

Echograms were projected using the logarithmic unit "Volume backscattering strength" (Sv, dB re 1 m^{-1}). However, acoustic density comparisons between zones were conducted using the linear unit "nautical area backscattering coefficient" (NASC, m^2 nmi^{-2}). Units nomenclature and conversions were applied according to Maclennan et al. [2002]. Since we detected mesoscale variability in a scattering layer between 700 and 900 m depth, we developed an acoustic anomaly index (AAI) to quantify the magnitude of changes along transects during the leg three. First, we calculated and integrated NASC from 700 to 900 m depth. AAI was afterwards calculated as the ratio of NASC to the total averaged NASC minus one, and expressed in terms of percentage (see equation 4.1).

$$\mathrm{AAI} = 100 \left(\frac{\mathrm{NASC_i}}{\frac{1}{\mathrm{n}} \left(\sum_{\mathrm{i=1}}^{\mathrm{n}} \mathrm{NASC_i} \right)} - 1 \right) \tag{4.1}$$

Prior to any echogram projection or analysis, interferences from other acoustic instruments, typically looking as vertical sticks of relative high backscattering, were removed using an algorithm which based its detection sensitivity on differences among consecutive pings and the vertical repetitions of these differences. Detection thresholds were adjusted by visualizing echograms and checking that only the interferences were removed while minimizing loss of data. Missing values were replaced by linear interpolation between side pings. Steaming noise episodes did not compromise any result since all occurred out of transect time. All acoustic data were processed using customized applications in Matlab software.

Results

Zonal section across the eddy field

First anomalies observed with the 38kHz echosounder occurred at the eddy reconnaissance transect during the leg one (Fig. 4.1). The westward recorded echogram took approximately one day and a half, covering two upward and one downward migration events. Three distinct scattering regions were identified (Fig. 4.1C), a shallow scattering layer above 150 m depth (SSL), and two deep scattering layers in the mesopelagic zone (DSL). The first DSL was approximately between 400 and 600 m depth, presenting a relative high acoustic density (-70 to -60 dB), while the second one lied from 700 to 900 m depth, exhibiting less sound reflection (-75 to -70 dB). Regardless of whether it was day or night, acoustic scattering at 700-900 m depth enhanced inside eddies, while

diminished between them. The enhancement of the deep layer was similar for both side cyclonic eddies and the ITE.

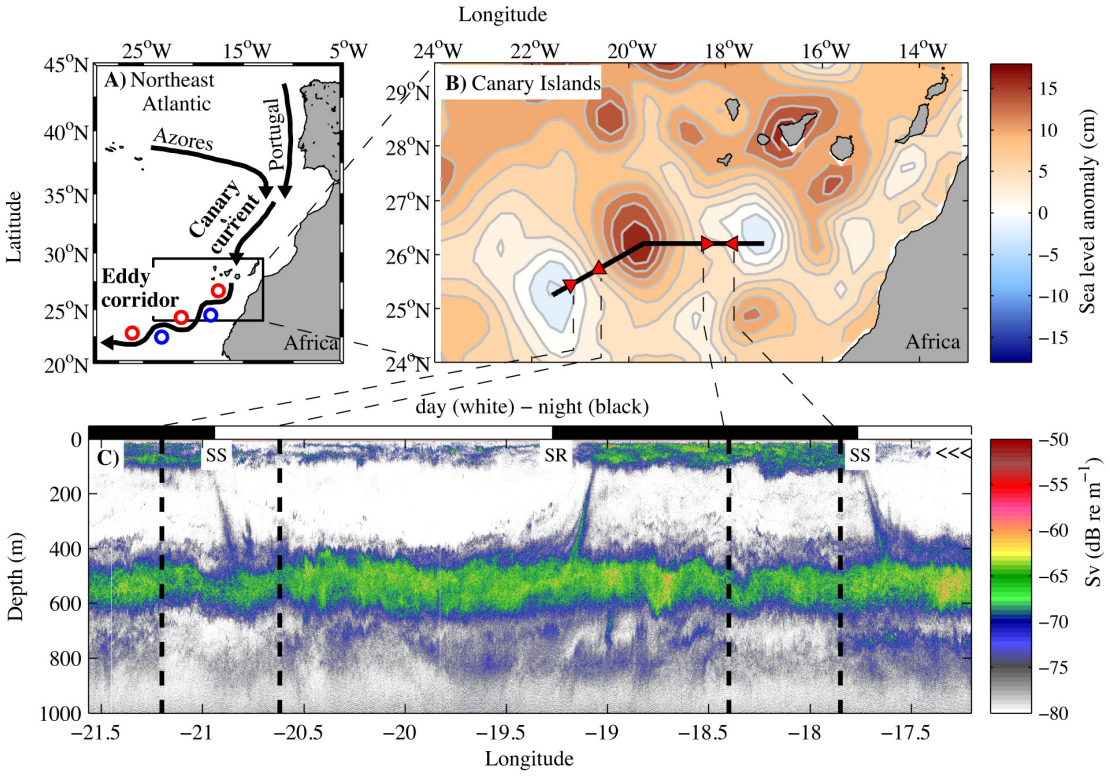

FIGURE 4.1: (A) Schematic of the Canary Islands location, the Canary Current, and the Canary Eddy Corridor. (B) Sea level anomaly showing the anticyclonic eddy selected for this study at 26°N-20°W, and two cyclonic eddies on both sides. The black line indicates an acoustic transect from east to west. (C) 38 kHz echogram showing anomalies in scattering layers between 700 and 900 m depth. The location of these anomalies are indicated with red triangles in the upper right panel. White and black at the top of the echogram depict day and night, respectively. SR and SS stand for sunrise and sunset. Angles in a row point to the recording direction of the echogram.

Systematical transects across the ITE

In the leg three, transects across the ITE showed the same layout of acoustic scattering layers than in the leg one. Anomalies also concentrated between 700 and 900 m depth. The most abrupt changes within this strata occurred systematically along the ITE periphery. The distribution of subsurface chlorophyll maxima also outlined the eddy borders (Fig. 4.2A). Positive acoustic anomalies surrounded the northeast frontier, indicating higher backscattering below 700 m depth in this area (see transects B to E in Fig. 4.2). However, negative anomalies disposed outlining the southwest boundary. They were characterized by a short weakening of the layer near the border and followed by a permanent attenuation of acoustic backscattering once outside the ITE (see transects F to J in Fig. 4.2). We did not registered important anomalies inside the

vortex, where the acoustic scattering always exhibited similar density and structure. All described anomalies occurred regardless of whether it was day or night.

Acoustic profiles among ITE regions

In general, the 38 kHz profiles among the different regions of the ITE were quite similar except between 700 and 900 m depth (Fig. 4.3). Within this interval, southwest profiles peaked slightly deeper (800-900 m) than those in the northeast or at the ITE core (700-800 m). The integrated acoustic backscattering between 700 and 900 m depth (NASC) doubled at the ITE core and tripled in the northeast periphery with respect to the southwest region. Differences described among profiles occurred both during day and night.

Discusion

Acoustics, what we see and what we do not see

The advantage of using acoustics to evaluate pelagic fauna is the high spatio-temporal resolution. This allows quasi-synoptic views of animal structures extending hundred kilometers at scales below one meter [Godø et al., 2014]. In return, difficulties arise when translating from decibels to organisms without net catches. Therefore, ground-truthing by trawling is a prerequisite to give biological significance to sound scattering in the ocean [Davison et al., 2015].

There is extensive literature relating low frequency scattering layers to micronekton throughout the oceans. In particular, the 38 kHz constitutes an standard for the detection of small pelagic fish [Kloser et al., 2002, Kaartvedt et al., 2009, Peña et al., 2014]. This frequency was recently associated to specific taxa in the Canary Islands by concurrent acoustic and net samplings (Ariza et al., in prep.). The strong deep scattering layer between 500 and 600 m depth was mainly attributed to *Cyclothone braueri*, a non-migrant small fish highly abundant in mesopelagic waters. The weak layer below, which exhibited variability along the eddy, was linked either to migrant fish or decapods, or maybe both. Probably from families Myctophidae and Sergestidae, according to conclusions in Ariza et al. (in prep.), and also to previous reports of micronekton vertical distribution in the region [Badcock, 1970, Foxton, 1970b].

It does not mean, however, that the investigated eddy exclusively affected fish or decapods inhabiting between 700 and 900 m depth. The whole mesopelagic zone is inhabited by many species not responding at the insonifying frequency [Korneliussen and

Ona, 2003, Benoit-Bird, 2009], while others are simply masked by stronger and more numerous scatterers such as *Cyclothone braueri*. On the contrary, the 38 kHz echogram must be regarded as a biased view, raising the question of whether other animals might be influenced by the physical gradients of eddies.

Eddy interaction with deep mesopelagic animals

Probably the main finding of this study is that anticyclonic eddies may shape the distribution of animals inhabiting the deep mesopelagic zone. Within the ITE, and between 700 and 900 m depth, the scattering biota exhibited distinctive features in comparison to those of surrounding waters (Fig. 4.1 and 4.2). This biota, was finely tuned to the eddy shape, with changes along the scattering layers occurring near submesoscale (<10 km). Only in the ITE and its surrounding waters, we identified three different regions, which suggest a high degree of micronekton patchiness along eddy field. After these observations, questions arise regarding the mechanisms behind this patchy distribution, or in what sense the mesopelagic communities are different across these structures.

Varying scattering levels in a given layer may result from different abundances of same organisms. However, this may also reflects distinct organisms, either a change in the species assemblage, or different age structures within the same population. For instance, juvenile fish bearing gas-filled swimbladders may produce much more sound reflection than adults with atrophied swimbladders, or decapods with sizes near the wavelength of the insonifying frequency may cause higher reflection than specimens shorter or larger [Kloser et al., 2002, Korneliussen and Ona, 2003, Simmonds and MacLennan, 2005]. Unfortunately, without net sampling, it is impossible to know whether this acoustic variability reflected different densities or different organisms.

If acoustic targets were the same along the surveyed area, it would imply that mesoscale structures may produce from two- to threefold higher micronekton biomass between 700 and 900 m depth (see Fig. 4.3). According to this assumption, it seems that the deep mesopelagic biota concentrated beneath eddies, no matter if cyclonic or anticyclonic. Or seem from a different viewpoint, animals may disperse across front regions. This is easily appreciated in the zonal section across the eddy field, as well as in the southermost transects along the ITE (Fig. 4.1 and 4.2F-J).

However, the enhanced acoustic densities in the outer northeast part contrasts to the observations at the southwest (Fig. 4.2B-E). This might be related with the asymmetric structure of the ITE. Notice that the eddy is elliptical with its major axis oriented in the NW-SE direction (Fig. 4.2A), and according to Barceló-Llull et al. (in prep.), velocity fields indicates that the circulation accelerates in the southwest part, while

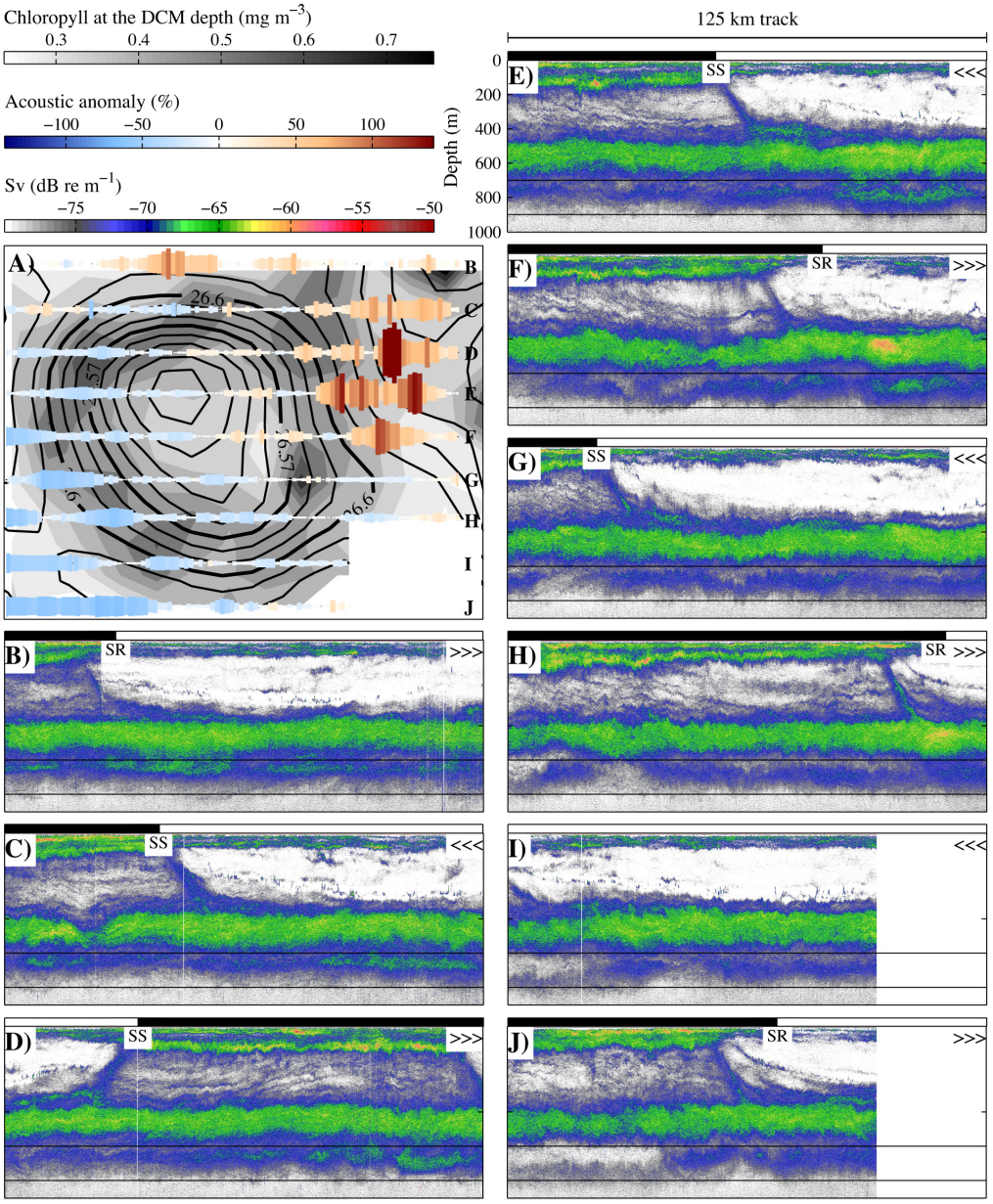

FIGURE 4.2: (A) ITE structure as derived from density anomalies at 200 m depth (contour lines). Grayscale background shows the distribution of subsurface chlorophyll, and blue-red colored bars represent acoustic anomalies at 700-900 m depth along nine transects conducted throughout the ITE. (B-J) 38 kHz echograms corresponding to these nine transects. Horizontal black lines delimit the range depth where the acoustic anomaly index in panel A was calculated. White and black at the top of the echograms depict day and night, respectively. SR and SS stand for sunrise and sunset. Angles in a row point to the recording direction of the echogram.

decelerates dramatically in the northeast part, being nearly stagnant. Therefore, planktonic organisms are expected to accumulate in the northeast slow part, while they will tend to disperse in the southwest. This could increased predator-prey encounters in the northeast periphery, leading to a higher trophic efficiency and attracting micronekton.

On the other hand, if we assume that changing acoustic features actually reflects different mesopelagic communities, we should take into account that a higher backscattering does not necessarily mean a higher biomass. Some studies suggest species differentiation among mesoscale structures based on the eddy history. This includes the chance of trapping certain larval species during the eddy formation near the islands, subsequent interactions with filaments, or the degree of isolation with the surrounding waters [Brandt, 1983, Griffiths and Wadley, 1986, Lobel and Robinson, 1988, Muhling et al., 2007].

In summary, it is difficult to know whether this patchiness is a consequence of a variable local production resulting in different micronekton biomasses, or it just reflects eddy-specific communities. What it seems clear is that the eddy-micronekton interaction occurs near surface at night, through the vertical migration that these animals perform on a daily basis (Ariza et al., in prep.). Otherwise it would be impossible considering that eddies hardly reach waters of 400 m depth [Arístegui et al., 1994, Sangrà et al., 2007, 2009], and that this ITE in particular disappeared at about 300 m depth (Barceló-Llull, in prep.). Physical gradients of eddies might directly shape the micronekton distribution while they are in shallow waters, or maybe the interaction occurs through trophic connections, *e.g.*, micronekton seeking prey patches shaped by eddies.

Study relevance and future research

Knowledge about biophysical interactions in the Canary eddy corridor was limited to planktonic organisms so far [Arístegui et al., 1997, Hernández-León et al., 2001, Yebra et al., 2005, Landeira et al., 2010]. Now, this study reveals that the influence of these mesoscale structures extends to higher trophic levels and down to 900 m depth. We should therefore reconsider the role of eddies in ecological and biogeochemical processes involving the micronekton community. For instance, since migrant micronekton behave as efficient vehicles moving and storing carbon into the deep ocean [Hidaka et al., 2001, Davison et al., 2013, Schukat et al., 2013, Irigoien et al., 2014, Ariza et al., 2015], the control that eddies might exert over the biological pump must be higher than previously assumed.

On the other hand, the way in which mesoscale systems introduce patchiness in micronekton must be variable and highly dependent on the eddy properties and the type of community. This can be seen in the work of Godø et al. [2012] in anticyclonic structures near Iceland and Norway. As in the present study, they observed singular scattering biota adjusted to the eddy shape, but the structure and behavior of layers were completely different. The eddy studied here has also shown very complex physical and

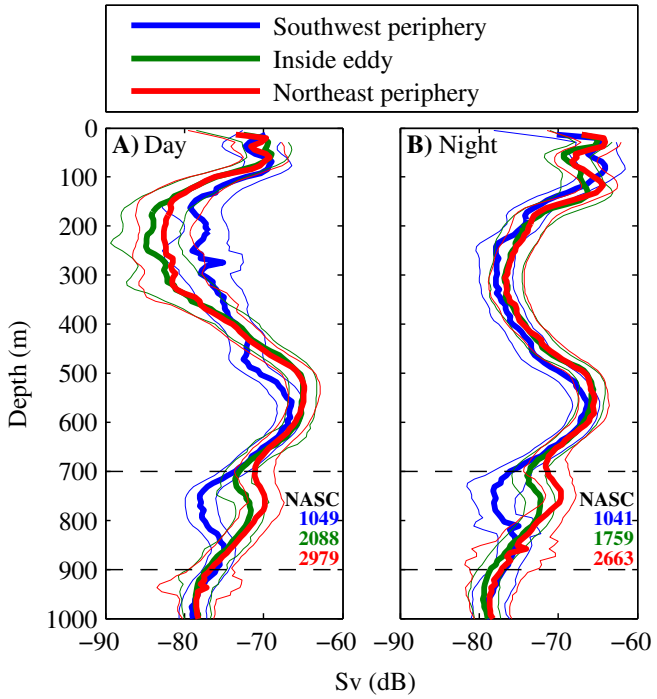

FIGURE 4.3: Daytime (A) and nighttime (B) 38 kHz profiles averaged from pings recorded at the southwest (blue) and northeast (red) peripheries, as well as inside the ITE (green). The ITE periphery was agreed as the area outside the isopycnal 26.60 kg m^{-3}. The ITE core was agreed as the area within the isopycnal 26.57 kg m^{-3} (see Fig. 4.2a). Thick and thin lines depict means and standard deviations, respectively. Nautical area backscattering coefficient (NASC) integrated from 700 to 900 m depth is also indicated for each profile.

biogeochemical features not previously seen in similar structures (Arístegui et al., in prep.; Barceló-Llull et al., in prep.). These signals suggest that eddies may behave as unique ecosystems with singular organisms, from primary producers to top predators.

The mechanisms through which eddies introduce variability in mesopelagic communities and the nature of these differences are still a matter of debate. In this respect, the present study raise more questions than answers. Addressing these questions in the future will require to study mesoscale eddies from their formation to the decay stage, while using acoustics in combination with net sampling.

Acknowledgements: We are grateful to the members of the UTM (Unidad de Tecnología Marina), as well as to the officers and the crew of the R/V *Hespérides* for their work and support at sea. We also express our gratitude to our colleagues who assisted in the field work during the survey. This work was funded by the Spanish Government project PUMP (CTM2012-33355). Alejandro Ariza was supported by a postgraduate grant from the Spanish Ministry of Science and Innovation (BES2009-028908).

Part III

Synthesis and further research

Overall discussion

Stratified vertical migration, stratified active flux

The active flux has been traditionally addressed as the amount of carbon exported below the base of the euphotic zone (<150 or 200 m depth), assuming a unique migratory pathway while playing down the magnitude and extent of any transport beyond this depth. Following this approach, the active carbon flux has been estimated here in chapter 2, and in many other studies [Longhurst et al., 1990, Steinberg et al., 2000, Hidaka et al., 2001, Davison et al., 2013, Schukat et al., 2013]. This procedure is useful to compare with sediment traps, which are normally deployed at these depths. In this way, the active and passive carbon inputs to the mesopelagic zone are estimated and compared. However, while the passive flux can be roughly estimated in deeper waters based on depth-attenuation algorithms [Suess, 1980, Betzer et al., 1984, Antia et al., 2001], the vertical distribution of the active flux is still barely predictable. This is because the active flux is driven by diel vertical migration, a complex process involving a large variety of species [Tucker, 1951, Barham, 1966, Roe, 1974, Angel and Pugh, 2000, Pearre, 2003], each following diverse migratory patterns (chapter 1), while contributing to vertical transport with different biomasses and metabolic rates (chapter 2). Hence, its assessment requires an approach that takes account of all migratory groups and their singularities. This will provide reliable vertical profiles that reflect the active carbon inputs over the water column.

The bulk of migratory fluxes are generally assumed to conclude approximately near the middle of the mesopelagic zone (400-700 m depth) since, according to observations made by conventional acoustic and net sampling methods, this is where most scattering layers are found (see general introduction). The 38 kHz echosounder, standard frequency for mesopelagic fish assessments, closely reflects this distribution in open ocean waters [Kloser et al., 2009, Irigoien et al., 2014]. However, as shown in chapter 1, echograms at 18 kHz and deep trawling also reveal scattering layers and migrations extending from 700 to 1000 m depth, including fish, decapods and cephalopods (see also Fig. S1a). In fact, studies considering the whole mesopelagic community highlight the fact that most of the mesopelagic zone is actually inhabited by migratory animals [Domanski, 1984], regardless of their visibility at certain acoustic frequencies.

Vertical migration ranges are of importance as, the deeper the carbon inputs, the less likely they are to be pumped back to the surface by physical processes. For instance, cyclonic eddies are known to upwell dissolved carbon from 400-700 m depth [Arístegui et al., 1994, González-Dávila et al., 2006, Sangrà et al., 2007]. Intermediate waters begin at approximately 600 m depth [Hernández Guerra et al., 2001, Machín and Pelegrí,

2009]; these waters have slower circulation rates and are therefore less often upwelled and ventilated than upper level waters. Accordingly, migrations below 600-700 m depth could be considered as a more effective carbon export process than shallower ones. Hence, the vertical extent of DVM and its magnitude over the water column should be matters of interest for the assessment of the biological pump.

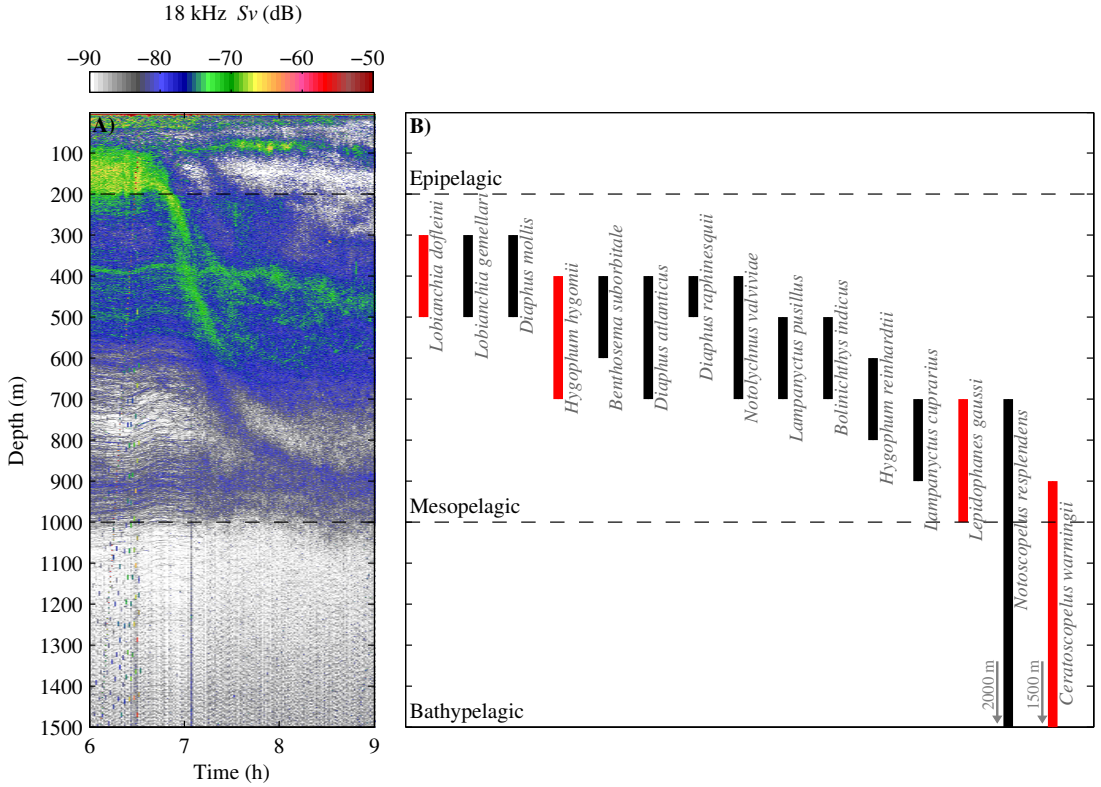

FIGURE S1: (A) Biota backscattering signal for a dawn descent measured with a 18 kHz echosounder. *Sv* is the volume backscattering strength in decibels. (B) Fish vertical distribution during daytime according to Badcock and Merrett [1976]. Species that contribute more to migrant biomass, according to chapter 1, are indicated in red

Active flux beyond 1000 m depth

In addition to the above, there are also some fingerprints indicating that the active flux might be operating in a substantial way even in the bathypelagic zone, where carbon could be sequestered for several hundred years [Lampitt and Antia, 1997, Koppelmann and Frost, 2008]. To our knowledge, Badcock and Merrett [1976] undertook the deepest and highest resolution vertical profile of fish in the Atlantic Ocean so far (Fig. S1b). In that study, they reported that *Ceratoscopelus warmingii* and *Notoscopelus resplendens* (large lanternfishes, *Myctophidae*) inhabited the bathypelagic zone during the day; the same species that we found absent in the mesopelagic at similar times (chapter 1). According to our calculations, only *C. warmingii* accounts for about 30% of the fish migrant

biomass in our region (see Table 1.1). Species biomass is not a common output in deep-sea studies, but other reports in the region also refer to *C. warmingii* as a dominant fish in the migratory layers at night according to abundance tables [Badcock, 1970, Bordes et al., 2009, Wienerroither et al., 2009]. Assuming our biomass calculations, the vertical migration of *C. warmingii* would imply a substantial amount of carbon exported to the ocean interior. Later, based on the same collections used by Badcock and Merrett [1976] and other samples collected aboard the RRS Discovery in the North Atlantic, Kinzer and Schulz [1985] documented other myctophid species undertaking extensive diel vertical migrations. According to their results, several *Lampanyctus* species also inhabited near or beyond 1000 m depth during daytime (in addition to *C. warmingii* and *N. resplendens*). Kinzer and Schulz [1985] also confirmed the extensive migrations of these large myctophids based on the finding of shallow-living prey in their stomach contents. All this suggests that the migrant biomass entering the bathypelagic domain could be much larger than previously assumed in the context of biogeochemical oceanography.

However, none of the echograms collected during the present thesis have indicated this important migration into the bathypelagic zone (see example in Fig. S1a). First, because range-increasing noise at 38 kHz makes it difficult to detect targets beyond 1000 m depth [Korneliussen, 2000] and, secondly, because although 18 kHz can see deeper, there are reasons to believe that the species involved in this migration might not be detectable at this frequency. The reasons for this, amongst other factors, could be the change of resonance with depth, atrophy of the swimbladder in large fishes, and the signal to sampling volume ratio, which at these depths could be below the detection threshold of the echosounder (see discussion in chapter 1).

There is however evidence indicating that the extensive migrations documented by Badcock and Merrett [1976] were not location specific. First, *Ceratoscopelus warmingii* and *Notoscopelus resplendens* extend at least along 40°N - 40°S, and there are also other large bathyal lanternfish that occupy similar ecological niches around the world's oceans [Froese and Pauly, 2014]. For instance, Burghart [2006] also found large lanternfish in the Gulf of Mexico at depths below 1000 m during daytime, together with many migrant decapods. Secondly, recordings from acoustic doppler current profilers (ADCP) at higher frequencies (67-75 kHz) have shown migratory patterns near 1200 m depth in the subtropical Pacific and Atlantic oceans [see Fig. S2; Plueddemann and Pinkel, 1989, Ochoa et al., 2013, van Haren, 2007, van Haren and Compton, 2013]. Unfortunately, without biological samples, understanding the nature of these scattering layers results almost impossible. In the case of Plueddemann and Pinkel [1989], they attributed this phenomenon to a large variety of species, from zooplankton to nekton, while other authors have assumed that the scattering was most likely caused by zooplankton. Species

allocation is not a trivial matter. If *C. warmingii* is involved, in addition to other organisms, it would mean that one of the species contributing more to migrant biomass in the subtropical northeast Atlantic would be performing one-step diel vertical migrations from the surface to the bathypelagic zone. Consequences for the active flux would be that a substantial input of carbon would be reaching bathyal waters without losses derived from trophically-interconnected migrations, such as the "Ladder of migrations" or the "Bucket brigade" models [Vinogradov, 1962, Ochoa et al., 2013].

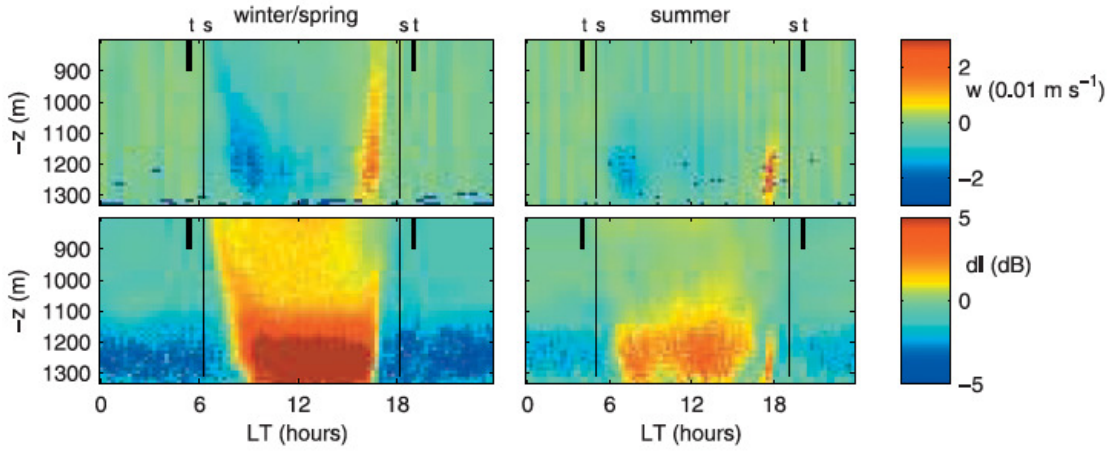

FIGURE S2: 24-h vertical velocities (w) and echo anomalies (dl) in bathypelagic waters of the Canary Basin. Winter/spring seasons on the left and summer on the right. "t" indicates nautical twilight, while "s" depicts sunrise and sunset. From van Haren [2007].

Another clue supporting the argument that the active flux might be important below 1000 m depth comes from the vertical profiles of particulate organic carbon (POC). During an oceanographic survey, Alonso-González et al. [2009] sampled these compounds moving laterally through discrete layers in mesopelagic and bathypelagic waters of the Canary Current. Each time they detected a POC peak at 500 and 700 m depth, near the deep scattering layer, a replicate also appeared at 1200 m depth (see Figs. 2 and 6 of their study). The last signal occurred within the depth range and in the same oceanographic region where both net sampling (Fig. S1b) and ADCP recordings (Fig. S2) show migratory activity. Alonso-González et al. [2009] proposed several sources of POC fueling these layers, either from continental margins, or from diverse mesoscale processes. Since it seems that there is also important migratory activity near 1200 m depth, we propose diel vertical migration as another mechanism for the transfer of carbon to bathyal waters. Organic matter bypassed by interzonal migrants has been proposed in the past to explain carbon peaks in mesopelagic waters [Steinberg et al., 2000, Alonso-González et al., 2013]. Here, the same mechanism is proposed, but we extend its influence beyond 1000 m depth. Accordingly, biogeochemical models for the deep ocean should be revised since the active flux has so far been only considered down to the mesopelagic zone [Koppelmann and Frost, 2008, Arístegui et al., 2009, Robinson

et al., 2010, Passow and Carlson, 2012]. Based on the above, the present thesis proposes a new biogeochemical model that includes the active flux, mediated by both zooplankton and nekton, within the mesopelagic realm and beyond 1000 m depth (see Fig. S3).

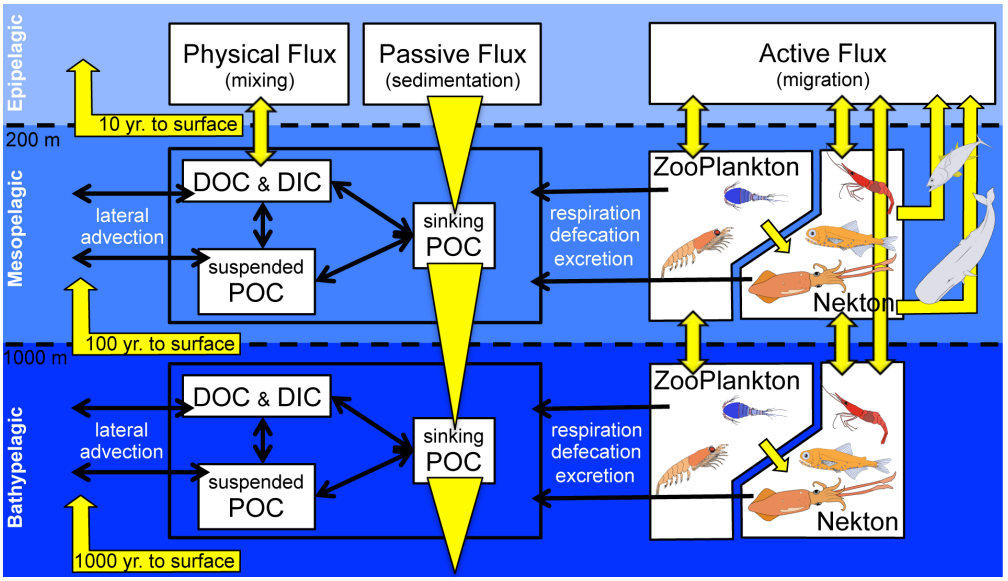

FIGURE S3: New schematic of the ocean carbon pump. Adapted from Arístegui et al. [2009] and Passow and Carlson [2012], with migratory fluxes established according to the present thesis proposals. Dissolved inorganic and organic carbon (DIC and DOC) at the surface is exported to deeper waters by physical processes (mixing), while particulate organic carbon (POC) is exported via passive fluxes (sedimentation). Once in deep waters, biological processes convert POC into suspended or dissolved carbon pools that are susceptible to lateral transport, in this way decreasing the sinking rates of particles. However, all these carbon pools are also fueled by the active flux of vertical migrants, reinforcing the passive flux with sinking fecal pellets (defecation), while releasing DIC (respiration) and DOC (excretion). Migrants are able to transport carbon into the mesopelagic and bathypelagic zones, but while the zooplankton flux into bathyal waters works through trophically-interconnected migrations, the nekton flux might also operate by direct migration. The top predators can also move carbon back to surface by feeding in the mesopelagic zone, and afterwards respiring, defecating and excreting in shallow waters. Flux out of the epipelagic zone is called the export flux (10 to 100 years for atmospheric ventilation), whereas the flux out of the mesopelagic is called the sequestration flux (100 to 1000 years).

Sinking POC, zooplankton and micronekton: Towards an holistic approach

The importance of micronekton in the active flux is not only a consequence of their extensive vertical migrations (section above), but also of their relative contribution to migrant biomass and particular ecophysiology. In Chapter 2 we highlighted how the migrant biomasses of zooplankton and micronekton were quite similar, while the gut flux of the latter might be more efficient due to their slower evacuation rates and fast-sinking fecal pellets. All these features provide evidence that the micronekton may

play an important role in the biological carbon pump; however, as summarized in Table 2.3 (references therein), most research involving the active flux has been exclusively dedicated to zooplankton.

The inclusion of micronekton in this work, as a contributory mechanism for the active flux, has filled gaps in our knowledge about carbon export in subtropical Atlantic waters and, it may reconcile, at least in part, current imbalances in the oceanic carbon budget. For instance, prior to the present thesis, Hernández-León et al. [2010] predicted a carbon export mediated by migrants on the order of the gravitational flux. The micronekton flux was estimated in this study based on the mortality rates of epipelagic zooplankton. Now we estimate that migrant zooplankton and micronekton export, via respiration, about 50% of the gravitational flux measured at 150 m depth (Chapter 2). DOC and POC peaks in mesopelagic and bathypelagic waters [Arístegui et al., 2003, Alonso-González et al., 2009] also suggest the intervention of migrants, among other mechanisms (see section above). On the other hand, global estimates of carbon export, based on ecosystem modeling, are approximately two times higher than those measured from sediment traps [Schlitzer, 2002, Falkowski et al., 2003, Usbeck et al., 2003]. Direct geochemical-based measurements are even higher [Maiti et al., 2009]. We believe that the inclusion of carbon export mediated by zooplankton and micronekton, together with the sinking POC, might reduce this imbalance.

Very recent studies are raising the role of micronektonic fishes [Davison et al., 2013, Hudson et al., 2014] and decapods [Podeswa, 2012, Schukat et al., 2013] in ocean carbon export, but to our knowledge, only the work of Hidaka et al. [2001] in the equatorial west Pacific and the present thesis in the subtropical northeast Atlantic have addressed the flux of micronekton together with that of zooplankton and sinking POC. Holistic approaches encompassing all passive and active mechanisms are needed because both fluxes are interconnected, and may feedback upon each other in many ways, such as the reprocessing or bypassing of POC by interzonal migrants [Steinberg et al., 2008, Robinson et al., 2010, Alonso-González et al., 2013]. We therefore advocate for integrative rather than comparative studies in order to better understand the functioning of the biological carbon pump.

Environmental factors affecting micronekton

During the course of the present thesis we have had the opportunity to test the behavior of scattering layers under the influence of distinct environmental factors. We studied the effects under the uncommon but natural event of a submarine volcano eruption that

occurred at the island of El Hierro, and also across common oceanic structures such as mesoscale eddies.

The abundance, vertical distribution and migratory behavior of the scattering biota were strongly affected by the volcanic plume (Chapter 3). Aspects that, as explained above, have important implications for the biogeochemical exchanges between the upper layers and the deep ocean. Temperature, dissolved oxygen, or light irradiance were some of the oceanographic properties altered during this event. All have been identified as being amenable to change under global warming conditions [Levitus et al., 2000, Keeling et al., 2010, Stramma et al., 2008], and also as important factors governing DVM [Dickson, 1972, Roe, 1983, Watanabe et al., 1999, Bianchi et al., 2013a]. Therefore, the acoustic anomalies observed during the volcanic unrest might be of value in predicting future changes in mesopelagic ecosystem functioning.

On the other hand, common and widespread oceanic structures such as eddies are proven to efficiently affect animals inhabiting waters down to 900 m depth. The variability found in this limited sampling space suggests a high degree of patchiness within this community across the eddy field (Chapter 4). Since micronekton are involved in the redistribution of organic matter and energy between shallow and deep waters [Hidaka et al., 2001, Davison et al., 2013, Schukat et al., 2013, Irigoien et al., 2014, Ariza et al., 2015], we should therefore reconsider the role of eddies in ecological and biogeochemical processes occurring in the ocean.

The factors that govern abundance, distribution and diel vertical migration at global scales are of importance due to the recent interest in developing oceanographic predictors for the functioning of the biological pump in future global warming scenarios [Bianchi et al., 2013a,b, Doney and Steinberg, 2013].

Conclusions

The main conclusions that arise from this thesis are:

1.- Three scattering zones have been identified associated with different mesopelagic fauna in the Canary Islands: (1) at 400-500 m depth, a resonant layer at 18 kHz mainly formed by gas-bearing migrant fishes such as *Vinciguerria* spp. and *Lobianchia dofleini*, (2) at 500-600 m depth, a dense layer at 38 kHz primarily resulting from resonance of the gas-bearing and non-migrant fish *Cyclothone braueri*, and (3) between 600-800 m depth, a weak signal at both 18 and 38 kHz ascribed either to migrant fish or decapods.

2.-Diverse active flux pathways have been observed connecting these mesopelagic zones with epipelagic waters. The shallower migrations, from 400-600 m depth, were moving at about 4 cm s^{-1}, while the deeper ones, from 600-800 m depth, were moving approximately at 12 cm s^{-1}.

3.- Zooplankton and micronekton contributions to migrant biomass are quite similar in the Canary waters. The main component that contributed to diel vertical migration within zooplankton were juvenile euphausiids, whereas micronekton were mainly dominated by fish, followed by a small contribution from adult euphausiids and decapods.

4.- Respiratory carbon fluxes from both zooplankton and micronekton accounted for 82% (range 47-166%) of the gravitational flux measured at 150 m depth in oligotrophic waters of the Canary basin, with zooplankton being the major contributor (58%) due to their higher respiration rates. However, the extensive diel vertical migrations undertaken by micronekton in comparison with those of zooplankton suggest that micronekton should be the dominant contributor to the active flux in deeper waters.

5.-Light attenuation in the water column due to varying turbidity at the sea surface strongly affects the vertical distribution of the mesopelagic biota. Extreme environmental factors in shallow waters, such as temperature, oxygen, or pH, also affect the normal functioning of diel vertical migration, shortening the nocturnal ascent while undermining organisms performing migration.

6.-Mesoscale eddies can shape the distribution of animals inhabiting depths down to 900m, even though these structures barely extend to 400 m depth. Interactions between

eddies and micronekton must therefore occur near the surface at night, through diel vertical migration.

7.-Mesoscale eddies introduce a high degree of patchiness to the deep mesopelagic fauna, with changes along acoustic scattering layers finely tuned to the eddy borders. This patchiness may increase the spatial variability of biogeochemical processes involving micronekton across mesoscale systems.

Future lines of research

According to the present findings and the literature revision conducted during the course of this thesis, three important subjects have been identified as major constraints on the assessment of diel vertical migration and its implications for ocean carbon export. These are: (1) biomass underestimation, (2) limited knowledge of ecophysiology and (3) scant monitoring of DVM patterns at long-term and global scales.

Biomass underestimation of fast-swimming organisms has traditionally been of major concern in fisheries management due to the requirement for accurate estimates in order to establish adequate fishing quotas. This issue is today also of interest for biological oceanographers, since recent studies are raising the important role that micronekton play in the ocean carbon budget [Hidaka et al., 2001, Bianchi et al., 2013a, Davison et al., 2013, Schukat et al., 2013, Irigoien et al., 2014, Ariza et al., 2015]. However, although both issues are of paramount importance for ocean ecosystems assessment, much uncertainty still remains about the accuracy of different sampling procedures currently available for biomass estimates.

Inter-calibration of micronekton sampling gears has been conducted only for small-sized frame trawls originally designed to sample macrozooplankton or juvenile fish, which besides biasing abundance estimates towards the smaller fraction of the micronekton, also shows order-of-magnitude differences in catch quantities [Wiebe et al., 2002, Pakhomov et al., 2010]. Large pelagic trawls are the only ones that efficiently capture the adult micronekton fraction, however there are no standard definitions regarding dimensions, mesh characteristics and sampling procedures. Standardization is not only important for comparisons between different studies, but also because existing correction factors for pelagic trawls [Koslow et al., 1997, Kloser et al., 2009, Kaartvedt et al., 2012b] are hardly applicable if sampling procedures can not be exactly reproduced.

In addition to this, acoustic-based correction factors also involve considerable uncertainty since the migrant community is composed of a large variety of species with different sizes and acoustic properties. This makes it highly difficult to accurately estimate biomass [see Davison et al., 2015]. Using multifrequency instruments together with a better understanding of the acoustic properties of animals may lead to improvements in discrimination between acoustic groups, thus gaining precision in biomass estimates. The problem is that high frequencies (>100 kHz) can barely cover the epipelagic zone when the instrument is mounted on the vessel.

Hence, in order to provide more reliable biomass estimates, two actions are specially recommended: First, to agree on the best performance pelagic trawl and trawling settings in order to establish a standard for micronekton sampling, similarly to what was

done in the late sixties for zooplankton sampling [UNESCO, 1968]. Secondly, major development of lowered multifrequency instruments, and implementation of backscattering models for the deep-sea fauna. This will allow a better discrimination of different acoustic groups and, therefore, more accurate biomass estimates.

Ecophysiology and metabolism in migrant micronekton is a profound lack in knowledge. This is particularly evident for mesopelagic fishes since it is extremely difficult to keep them alive in captivity for sufficient time to measure physiological rates [Robison, 1973, Torres et al., 1979]. Crustaceans, on the other hand, have been subject to further study as they exhibit greater resistance during *in-vivo* experiments. Nevertheless, most knowledge about the physiological energetics of crustaceans is biased towards zooplankton [Ikeda and Motoda, 1978, Omori and Ikeda, 1984, Ikeda and Kirkwood, 1989, Hernández-León and Ikeda, 2005] while metabolic budgets of deep-sea decapods are scarce [Ikeda, 2013]. As a result, it is common practice to use general fish energy budgets to calculate carbon export mediated by mesopelagic fishes [Davison et al., 2013] or adopting zooplankton metabolic rates for estimates with decapod [Schukat et al., 2013].

The most common input parameter used in metabolic budgets to calculate other physiological rates is respiration (R), a measurement which is hard to obtain on board due to the difficulties explained above. That is why the enzymatic activity of the Electron Transfer System (ETS) is widely used as a proxy for respiration [Packard, 1985, Gómez et al., 1996, Hernández-León and Gómez, 1996]. Unfortunately, few R/ETS ratios for migrant micronekton are available in the literature. To our knowledge, there is only one ratio reported for coral fishes that has been used for mesopelagic fishes [Ikeda, 1989], and one ratio for migrant decapods of the Benguela upwelling system [Schukat et al., 2013].

Although the use of these energy budgets and R/ETS ratios can be deemed appropriate under the current lack of better solutions, it is evident that more accurate models would considerably increase the reliability of active carbon flux estimates. Thus, research lines developing specific metabolic budgets and R/ETS ratios for vertical migrant micronekton are highly recommended. This is of particular importance for mesopelagic fishes as they are the main contributors to DVM and their metabolic rates are specially unknown.

Monitoring DVM patterns and migrant biomass of both zooplankton and micronekton is essential to address biogeochemical processes in the ocean. Several studies indicate that DVM is subject to change on monthly, seasonal and annual basis [van Haren, 2007, Staby et al., 2011, Wang et al., 2014], while spatial variations from regional to global scales have also been observed [Dickson, 1972, Kaartvedt et al., 1996, Bianchi et al., 2013a]. In addition to this, the vertical distributions of pelagic biota is

also likely to shift as a result of global climate change, although the nature of these changes is controversial [Robinson et al., 2010, Doney et al., 2012, Doney and Steinberg, 2013].

The assessment of DVM at such spatial and temporal scales requires systematic monitoring of the migrant biota that can not be approached through traditional oceanographic cruises. In this regard, it is necessary to develop predictive models of DVM depth and migrant biomass based on oceanographic parameters governing these organisms such as temperature, light irradiance, dissolved oxygen or primary production [Bianchi et al., 2013a]. These parameters can today be remotely sensed from satellites, or are available from ocean atlases. These predictive models would allow continuous monitoring of DVM at global and long-term scales.

There is also an urgent need for the inclusion of echosounders and optical instruments in permanent oceanographic stations. This will help to obtain *in-situ* zooplankton and micronekton metrics in conjunction with other parameters routinely collected through oceanic time-series operations [Karl and Lukas, 1996, Steinberg et al., 2001].

Parte IV

Resumen en español (Spanish summary)

Introducción

Migración Vertical Diaria: Historia y protagonistas

La migración vertical diaria es el movimiento sincronizado de animales más importante que ocurre en el océano, y muy probablemente, representa el mayor proceso de migración del planeta [Angel y Pugh, 2000, Hidaka et al., 2001, Hays, 2003]. Los primeros documentos que dieron constancia de este fenómeno provienen de las Expediciones del Challenger a mediados del siglo XIX [Murray y Hjort, 1912]. Sin embargo, no fue hasta el desarrollo de los sónares modernos cuando pudo verse por primera vez el alcance en profundidad y el patrón temporal que seguían estas migraciones [Dietz, 1948, Eyring et al., 1948]. Por aquel entonces, los registros acústicos que hoy en día llamamos ecogramas, mostraban capas de reflexión acústica concentradas fundamentalmente entre los 400 y 700 m de profundidad durante el día, y por encima de los 100 m durante la noche. Ambas capas conectadas mediante un ascenso al anochecer y un descenso al atardecer (Fig. I1). Este patrón día-noche muy pronto puso de manifiesto que el fenómeno debía ser causado por organismos que realizaban migraciones verticales, hipótesis que pudo posteriormente ser verificada gracias al muestreo directo de estas capas acústicas mediante pescas de profundidad [Tucker, 1951].

Hoy en día sabemos que aunque la mayor causa de resonancia acústica en el océano esta causada por los contenidos gaseosos de determinadas especies animales, como la vejiga natatoria de los peces o las vesículas de gas de los sifonóforos [Hersey y Backus, 1954, Barham, 1966], existe una gran variedad de organismos del plancton y del necton que también están involucrados en el proceso de migración vertical. Copépodos [Roe, 1984b], eufausiáceos [Roe et al., 1984b], decápodos [Roe, 1984a], peces [Roe y Badcock, 1984], y cefalópodos [Roper y Young, 1975] son los taxones más comunes que realizan migraciones interzonales, es decir, entre la zona epipelágica (0-200 de profundidad) y mesopelágica (200-1000 m de profundidad). De hecho, cuando se tiene en cuenta toda la comunidad de migradores, independientemente de si son visibles o no en los ecogramas, toda la zona mesopelágica parece estar efectivamente habitada por migradores, cada especie cubriendo diferentes intervalos de profundidad [Domanski, 1984].

No obstante, aunque la migración vertical diaria es realizada por una amplia gama de especies y rangos de talla, hay que subrayar que las migraciones más masivas y que cubren mayores rangos de profundidad son realizadas, por un lado, por la fracción más grande del zooplancton, y por otro, por el micronecton (Fig. I2). Esto básicamente incluye a peces, crustáceos y calamares desde 1 hasta 10 cm de longitud [Brodeur et al., 2005]. Mientras que el krill (familia Euphausiidae) es probablemente el grupo migrador más importante dentro del zooplancton, los peces linterna (familia Myctophidae) son

los que dominan dentro del micronecton. Se estima que los peces linterna, o mictófidos, constituyen casi el 80 % de la biomasa migrante en el océano [Koslow et al., 1997, Hidaka et al., 2003]. Dado que estos peces son muy numerosos y sus vejigas natatorias los convierte en objetos altamente resonantes [Butler y Pearcy, 1972, Yasuma et al., 2010], ellos son de hecho la mayor fuente de reflexión acústica en el mar, enmascarando frecuentemente las señales de otros grupos migradores en ecogramas de rutina [Godø et al., 2009, Kloser et al., 2009].

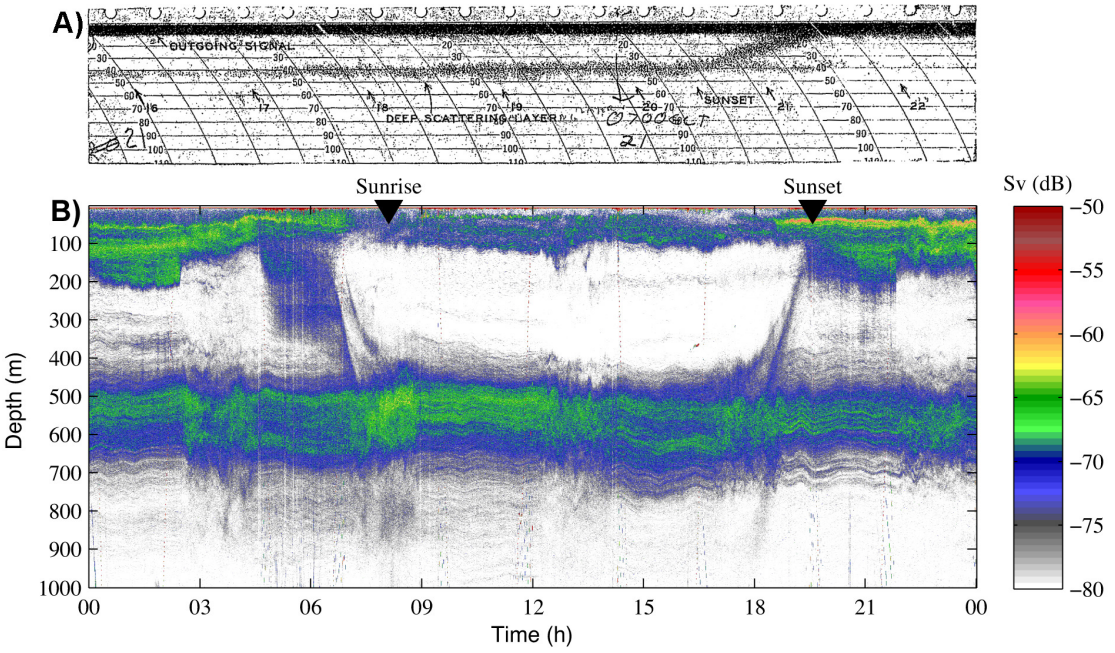

FIGURA I1: (A) Primer ecograma publicado mostrando la migración vertical diaria (ascenso nocturno) desde la zona mesopelágica hasta aguas someras en el Pacífico ecuatoria central [Dietz, 1948]. (B) Ecograma actual mostrando el descenso al amanecer y el ascenso al anochecer en aguas oceánicas de las Islas Canarias. *Sv* (volumen de eco reflejado) indica la densidad de eco de los animales.

Factores que gobiernan el proceso de migración vertical

Los mecanismos que desencadenaban la migración vertical y su significado adaptativo fue la segunda cuestión que surgió tras conocer la naturaleza de este fenómeno acústico. Desde los primeros estudios sobre migración vertical, la coincidencia de los desplazamientos con el amanecer y anochecer señalaron a la luz como el principal factor que gobernaba la migración [Johnson, 1948]. Las primeras hipótesis postulaban que la migración era el resultado de una selección vertical del hábitat con el fin de mantenerse dentro de un rango estrecho de luminosidad [Kampa y Boden, 1954, Boden y Kampa, 1967, Blaxter, 1974]. Sin embargo, estudios posteriores demostraron que la biota migrante realmente se localizaba dentro de márgenes de luminosidad relativamente amplios [Roe, 1983, Frank y Widder, 2002, Staby y Aknes, 2011]. La hipótesis isolumínica fue

por tanto abandonada, y hoy en día es ampliamente aceptado que las diferentes especies mesopelágicas se distribuyen dentro de rangos de intensidad lumínica preferidos [Badcock, 1970, Foxton, 1970b]. Por otra parte, también surgió la duda de si la migración vertical estaba controlada por relojes internos (ritmos circadianos) ajustados a las variaciones naturales de la luz, y no por la luz en sí misma [Neilson y Perry, 1990]. Sin embargo, es poco probable que esto fuera cierto ya que también se han observado capas de reflexión acústica reaccionando ante fluctuaciones de luz no predecibles, como ocurre con la nubosidad variable o los eclipses solares [Kampa, 1975, Baliño y Aknes, 1993].

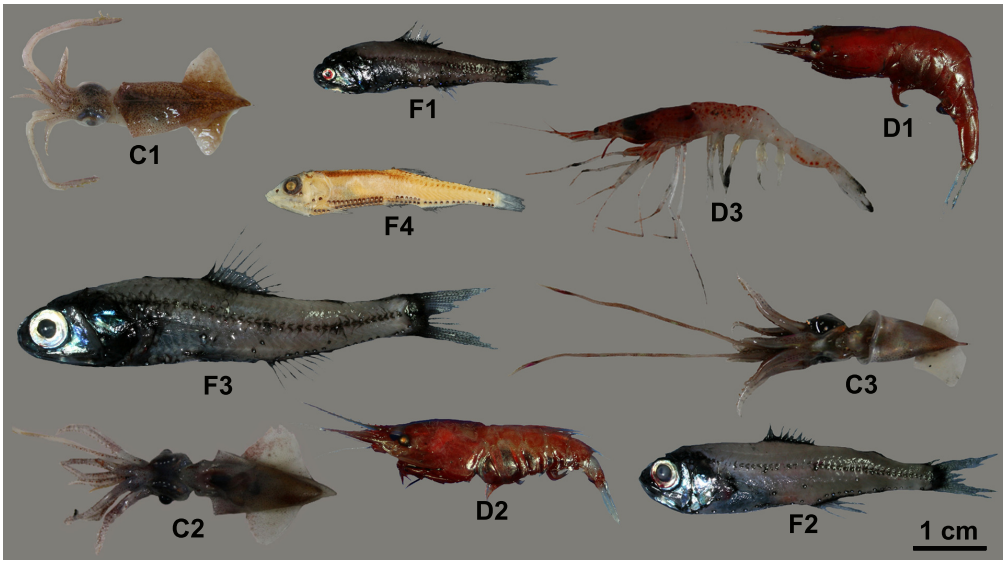

FIGURA I2: Peces, decápodos y cefalópodos dominantes que realizan migraciones verticales en el Atlántico nordeste subtropical: (F1) *Lobianchia dofleini*, (F2) *Hygophum hygomii*, (F3) *Ceratoscopelus warmingii*, (F4) *Vinciguerria attenuata*, (D1) *Systellaspis debilis*, (D2) *Oplophorus spinosus*, (D3) *Deosergestes corniculum*, (C1) *Onychoteuthis banksii*, (C2) *Abraliopsis morisii*, y (C3) *Pyroteuthis margaritifera*.

Por tanto, que la luz sea el principal factor que gobierna el proceso de migración vertical es una idea ampliamente aceptada. Existe sin embargo, mayor debate en relación al significado adaptativo de este comportamiento animal. La explicación más aceptada es que, dado que la luz es imprescindible para la búsqueda de alimento, pero también aumenta la posibilidad de ser visto por otros depredadores, la migración vertical sería un juego de selección de hábitat que consistiría en compensar la necesidad de comer con la evitación de ser predado [Clark y Levy, 1988, Hays, 2003]. En qué medida una determinada especie se expone a cierto nivel lumínico dependerá de su umbral de detección de presas y de su capacidad de camuflaje [Warrant y Locket, 2004], factores que juntos determinarán la profundidad y el ajuste horario de la migración [Aksnes y Giske, 1993, De Robertis, 2002, Busch y Mehner, 2011]. Por otra parte, la hipótesis de la eficiencia bioenergética "caza en caliente, descansa en frío" defiende que el ahorro energético que supone permanecer en aguas más frías es la primera razón para el descenso, en lugar de la evitación de depredadores [Brett, 1971, Sims et al., 2006]. El metabolismo reducido es

algo característico en animales que habitan en profundidad, ocurre como consecuencia de las bajas temperaturas y puede ser ventajoso para ahorrar enería [Childress, 1975, Torres et al., 1979, Childress y Seibel, 1998]. Sin embargo, esto no implica que la cuestión bionergética sea la principal razón para migrar diariamente. Debe tenerse en cuenta que ninguna de las propuestas es capaz por sí sola de explicar la migración en todos los casos, ya que existe un amplio espectro de especies y circunstancias. Parece por tanto, que los motivos de la migración vertical engloban tanto cuestiones de eficiencia energética, como incrementar las oportunidades de alimentación, o reducir el riesgo de ser depredado [Mehner, 2012].

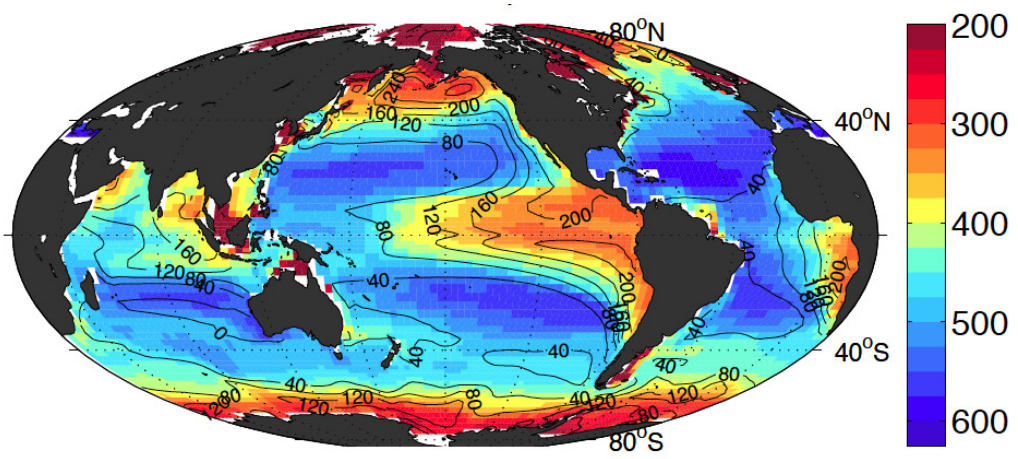

FIGURA I3: Profundidad de migración a escala global, en metros. Modelado a partir de variables oceanográficas como el oxígeno subsuperficial, el gradiente epipelágico de temperatura, la concentración de clorofila superficial o la profundidad de la capa de mezcla. Los contornos se refieren a la diferencia de oxígeno (mmol m^{-3}) existente entre la superficie (0-25 m) y la parte superior mesopelágica (150-500 m). Extraído de Bianchi et al. [2013a].

De hecho, como consecuencia de la variable distribución de presas y factores ambientales presentes en cada ecosistema marino, se pueden observar distintas estrategias de migración a lo largo de las regiones oceanográficas. El patrón normal de migración (NDVM) de "ascender al anochecer y descender al amanecer" es por tanto, una descripción generalizada y simplista mas que una explicación válida para todas las variantes de este fenómeno. Por ejemplo, estudios recientes han descrito patrones donde algunos individuos de especies migradoras no migran todos los días, quedando siempre parte de la población en profundidad [NoDVM, Dypvik et al., 2012]. En otros casos toda la población migra [TDVM, Dypvik y Kaartvedt, 2013]. Incluso se han registrado migraciones inversas, es decir, descender al anochecer y ascender al amanecer [IDVM, Dypvik et al., 2011], o hundimientos durante la medianoche [Prihartato et al., 2015]. Las distintas estrategias de migración se relacionan con la disposición variable de recursos y con las limitaciones fisiológicas frente a determinados factores ambientales, pudiendo cambiar estos a lo largo de las estaciones o entre ecosistemas.

Por otro lado, la luz no solo gobierna la migración a escala temporal, sino que su influencia es también evidente a escala espacial. La turbidez variable en la superficie del mar modula la radiación lumínica en la columna de agua, afectando a su vez a la distribución vertical de las capas de reflexión profunda. Esto ocurre tanto a pequeña [Kaartvedt et al., 1996] como a gran escala [Dickson, 1972] en el océano. Aparte de la luz, hay otros factores oceanográficos que también determinan la distribución de los migradores, como la temperatura, el oxígeno disuelto o las distintas masas de agua [Fasham y Foxton, 1979, Bianchi et al., 2013a, Wang et al., 2014, Cade y Benoit-Bird, 2015]. También se han documentado cambios en la distribución de capas acústicas al cruzar remolinos oceánicos [Godø et al., 2012, Béhagle et al., 2014]. Recientemente, Bianchi et al. [2013a] modelaron la profundidad de los migradores a escala global, basándose en parámetros oceanográficos. La mayoría de la variabilidad en el modelo se explicaba por la concentración de oxígeno, donde los valores mínimos limitaban la extensión en profundidad de los migradores (Fig. I3). Sin embargo, la luz presentaba una correlación muy baja de acuerdo con los autores de este estudio. La mayor limitación de este modelo es que se refiere a la profundidad de capas de reflexión detectadas con perfiladores acústicos de corriente (ADCP). Como hemos dicho anteriormente, otros migradores se encuentran también por encima y por debajo de estas capas a pesar de no ser detectados. Muchos de ellos están muy bien adaptados a las zonas mínimas de oxígeno [Childress y Seibel, 1998, Ekau et al., 2010], además de estar fuertemente influenciados por la luz [e.g., Roe, 1983, Frank y Widder, 2002, Staby y Aknes, 2011]. Por tanto, el modelo de Bianchi et al. [2013a] podría reproducir con fidelidad la profundidad de migración de un grupo acústico determinado, pero no sería representativo para el resto de la comunidad migrante. La conjunción de todos estos factores (luz, temperatura, oxígeno, masas de agua y remolinos) puede resultar, por tanto, en patrones de migración y distribuciones muy variadas.

En resumen, la migración vertical no es simplemente un movimiento vertical de peces resonantes en el océano. Ahora sabemos que se trata de un mecanismo mucho más complejo que implica a una enorme variedad de especies, cubriendo diferentes rutas migratorias en la columna de agua, y con variadas modalidades de migración a lo largo del océano.

Importancia de la migración vertical en las redes tróficas marinas

Mientras que el zooplancton migrador se alimenta fundamentalmente de fitoplancton y de microzooplancton, alternando entre el segundo y tercer nivel trófico [Vinogradov, 1962, Wilson et al., 2010], la mayoría del micronecton es zooplanctívoro, ocupando la tercera posición en las redes tróficas marinas [Kozlov, 1995, Burghart et al., 2010, Choy

et al., 2012]. De acuerdo con esto, los migradores interzonales pueden ser considerados como consumidores de primer y de segundo orden. Esto supone que la producción primaria en aguas someras es transformada en biomasa mesopelágica, como mucho, a través de dos niveles intermedios. Una vía trófica relativamente corta que se traduce en una eficiente tranferencia de energía desde la superficie hasta el océano profundo (Fig. I4). De hecho, estimaciones recientes de la biomasa de peces mesopelágicos han puesto de manifiesto que la eficiencia de transferencia entre los productores primarios en superficie y la fauna profunda es más alta de lo que se había asumido tradicionalmente en los ecosistemas oligotróficos [Davison et al., 2013, Irigoien et al., 2014].

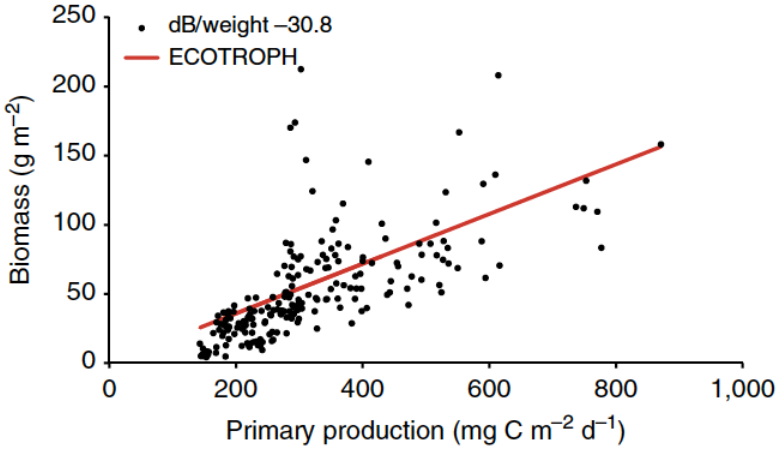

FIGURA I4: Biomasa de peces mesopelágicos en función de la producción primaria. Los puntos negros son estimaciones acústica de biomasa *in-situ*, mientras que la línea roja representa la biomasa modelada asumiendo una eficiencia de transferencia de 0.1 y considerando que el 90 % de la producción primaria se incorpora en las redes tróficas. Extraído de Irigoien et al. [2014].

Sin embargo, no toda la producción biológica dirigida por los migradores verticales acaba debajo de la zona eufótica. Aparte de los depredadores profundos como peces [Choy et al., 2013] y calamares [Passarella y Hopkins, 1991] mesopelágicos, los migradores también son predados por muchos animales que viven en la superficie del océano, los cuales o bien se sumergen en la zona mesopelágica para comer, o bien esperan el ascenso nocturno para alimentarse de ellos en superficie. Entre los depredadores de buceo profundo hay muchos mamíferos marinos [Santos et al., 2001] y varias especies de túnidos [Matsumoto et al., 2013], mientras que los depredadores superficiales más comunes son pequeños peces pelágicos [Cabral y Murta, 2002], delfines [Pusineri et al., 2007], peces espada y atunes [Potier et al., 2007]. De hecho, los migradores deben afrontar un riesgo de mortalidad relativamente alto en las aguas superficiales dado que es allí donde aumentan su movilidad durante el periodo alimenticio, siendo por tanto más fácilmente localizados por sus depredadores.

En resumen, los migradores interzonales juegan un papel fundamental en los ecosistemas pelágicos no solo porque ocupan una posición relevante en las redes tróficas, sino porque

su naturaleza migradora los convierte en un aporte alimenticio fundamental tanto para la zona epipelágica como para la mesopelágica. De hecho, las interacciones tróficas sugieren que los migradores son igualmente importantes para conducir la producción primaria al océano profundo [Irigoien et al., 2014], así como para sustentar la actividad pesquera a escala global [Pauly y Christensen, 1995, Lam y Pauly, 2005].

Relación con el ciclo del carbono en el océano y con el cambio climático

La bomba oceánica de carbono se refiere al conjunto de procesos fisiológicos, ecológicos y físicos mediante los cuales el dióxido de carbono atmosférico (CO_2) es secuestrado en el océano profundo (Fig. I5). El proceso de secuestro comienza en superficie con la fijación del carbono inorgánico mediante fotosíntesis (ver ecuación abajo) y su posterior transformación mediante procesos tróficos en diferentes formas de carbono orgánico. Bien formando parte de organismos vivos, o como materia orgánica inerte en la columna de agua. Mediante este proceso, los organismos fotosintéticos desplazan el equilibrio del sistema del carbonato en el mar, acelerando de este modo la difusión del CO_2 de la atmósfera al océano [Millero, 1995]. Llegados a este punto, el carbono orgánico puede ser remineralizado otra vez mediante la respiración de consumidores epipelágicos o por la actividad microbiana [del Giorgio y Duarte, 2002]. Sin embargo, también puede ser exportado hacia el interior del océano por tres mecanismos: (1) mediante la dinámica del océano, (2) por gravedad, o (3) intermediado por el proceso de migración vertical.

$$CO_2 + H_2O \underset{fotosíntesis}{\overset{respiración}{\leftrightarrows\leftrightarrows\leftrightarrows\leftrightarrows}} CH_2O + O_2$$

El primer mecanismo se refiere al carbono orgánico e inorgánico disuelto (DOC, DIC) que se exporta mediante procesos físicos, como la mezcla convectiva [Arístegui et al., 2003], el hundimiento de masas de agua [Sarmiento et al., 2004], o la difusión a través de isopicnas [Arcos-Pulido et al., 2014]. El segundo mecanismo, conocido como "flujo pasivo" o "gravitacional", ocurre con la formación de agregados de carbono orgánico particulado (POC) con tendencia a hundirse [Fowler y Knauer, 1986]. En el último mecanismo, conocido como "flujo activo" o "migratorio", el carbono orgánico viaja formando parte de los tejidos y del contenido digestivo de los migradores verticales, el cual es liberado posteriormente en aguas profundas mediante los procesos de respiración [Longhurst et al., 1990], defecación [Steinberg et al., 2000], excreción [Turner, 2002] y mortalidad [Zhang y Dam, 1997]. Cuando la exportación de carbono es exclusivamente dirigida mediante procesos físicos hablamos de la "bomba física", mientras que al flujo pasivo y activo se le conoce como la "bomba biológica".

Comprender los procesos que determinan el equilibrio del CO_2 entre la atmósfera y el océano no es un asunto trivial. Los océanos almacenan alrededor de 50 veces más carbono que la atmósfera, lo que implica que pequeños cambios en el ciclo oceánico del carbono pueden tener consecuencias atmosféricas de gran impacto. Esto adquiere aún más importancia si consideramos que el CO_2 es el principal gas responsable del actual escenario de calentamiento global, y que además se espera que su presión parcial en la atmósfera se duplique para finales del presente siglo [IPCC, 2014]. Además, la bomba oceánica de carbono no solo juega un papel clave en el cambio climático, sino que también es susceptible de verse alterada en futuros escenarios con altos niveles de CO_2 atmosférico, aunque la naturaleza de los cambios es aún un controvertido asunto de debate [Robinson et al., 2010, Doney et al., 2012].

Aproximadamente dos tercios del flujo vertical de carbono en el océano se debe a la bomba biológica, mientras que el resto es debido a la bomba física [Passow y Carlson, 1912]. En consecuencia, en las dos últimas décadas, los programas internacionales que investigaban el papel del océano en el cambio climático (JGOFS, GLOBEC, IMBER) se han centrado en el estudio de los procesos biológicos involucrados en el secuestro de carbono [Steinberg et al., 2001, Weingartner et al., 2002]. Sin embargo, mientras que el flujo pasivo ha sido objeto de mayor atención, el papel de los migradores ha sido pobremente considerado por aquellos que estudiaban los balances del carbono en el océano.

Las estimas actuales indican que el zooplancton migrador puede estar exportando hacia la zona mesopelágica aproximadamente entre el 10 y el 50 % del flujo pasivo en las aguas subtropicales [Steinberg et al., 2000, Hernández-León et al., 2001, Steinberg et al., 2008]. En consecuencia, los últimos estudios están comenzando a considerar este mecanismo de exportación en los modelos biogeoguímicos conceptuales [Arístegui et al., 2009, Robinson et al., 2010, Passow y Carlson, 2012]. Pese a ello, su contribución raramente es considerada en los cómputos globales. Si sumamos los flujos de carbono mediados por el zooplancton y los debidos al hundimiento de las partículas, el carbono exportado resultante continua siendo menor que las estimaciones globales que se han realizado mediante modelos ecológicos [Schlitzer, 2002, Falkowski et al., 2003, Usbeck et al., 2003]. Las discrepancias también son evidentes debajo del dominio mesopelágico, donde tanto los niveles de carbono orgánico, como la demanda microbiana de carbono no pueden sustentarse solo mediante el flujo gravitacional [Baltar et al., 2009]. Todos estos desequilibrios han sido justificados por errores en las medidas de flujo pasivo [Buesseler et al., 2007], por no considerar las entradas de carbono mediante transporte lateral [Alonso-González et al., 2009], y recientemente, por no incluir en los cálculos los aportes de

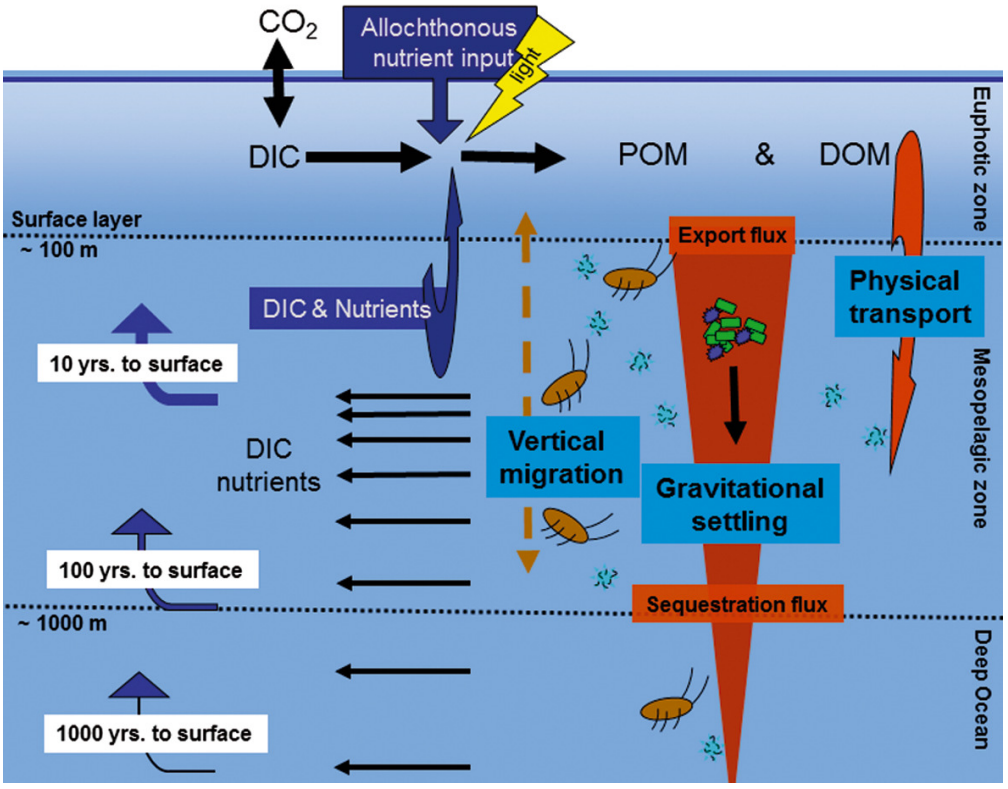

FIGURA I5: Esquema de la bomba biológica de carbono. Nótese que el flujo activo no es considerado por debajo de los 1000 m de profundidad, mientras que el micronecton tampoco es representado en el proceso de migración vertical, solamente el zooplancton. Extraído de Passow y Carlson [2012].

carbono transportados por el zooplancton migrador [Steinberg et al., 2008]. Sin embargo, el carbono exportado por el micronecton nunca ha sido considerado como una opción (Fig I5).

Se sabe que el micronecton realiza migraciones verticles, y por tanto, que está involucrado en el flujo activo, desde las primeras descripciones faunísticas de las capas migrantes de reflexión acústica en el océano [Tucker, 1951, Hersey y Backus, 1954, Barham, 1966]. No ha sido pues el desconocimiento lo que ha mantenido al micronecton fuera del punto de mira de la oceanografía biogeoquímica. Lo cierto es que las dificultades que conlleva su muestreo es probablemente la razón por la que el micronecton ha sido excluído de los cómputos de carbono en el océano. Esta comunidad posee mucha más capacidad natatoria que el zooplancton, por lo que se necesitan redes mayores y más caras que requieren mucho tiempo de maniobra para muestrear adecuadamente [Koslow et al., 1997, Pakhomov et al., 2010, Kaartvedt et al., 2012b]. Sin embargo, precisamente por su alta movilidad, el micronecton es capaz de realizar migraciones de gran magnitud, incluso más allá de los 1000 m de profundidad [Badcock y Merret, 1976, Kinzer y Schulz, 1985, Burghart, 2006]. Esto convierte potencialmente al micronecton migrador en un mecanismo altamente eficiente para el secuestro de carbono en el océano profundo.

Para nuestro conocimiento, el único trabajo que combina el flujo activo del zooplancton y del micronecton fue realizado por Hidaka et al. [2001] en el Pacífico oeste ecuatorial, sus estimaciones se duplicaron cuando incluyó a ambos componentes migratorios. En el Atlántico nordeste subtropical, Hernández-León et al. [2010] señaló al micronecton como un importante componente que faltaba en la bomba biológica, basándose en la tasas de mortalidad que esta comunidad causaba sobre el zooplancton. Recientemente se han publicado otros estudios sobre la contribución de los peces [Davison et al., 2013, Hudson et al., 2014] y los decápodos [Schukat et al., 2013] a la exportación de carbono, en el Pacífico nordeste, al norte de la Dorsal Atlántica, y en el afloramiento de Benguela. Desafortunadamente, las pocas estimas existentes difieren órdenes de magnitud entre ellas, dependiendo del grupo analizado, de la región oceanográfica y del dispositivo de muestreo usado. Lo último, siendo probablemente la mayor fuente de variabilidad debido a la incertidumbre que existe acerca de las eficiencias de captura de las redes [Pakhomov et al., 2010]. En este aspecto, las estimaciones de zooplancton están más consolidadas ya que existen muchos más estudios disponibles, y a que las medidas están basadas en procedimientos estándar más precisos [UNESCO, 1968]. Además, la mayoría de las estimaciones de flujo activo se refieren a la exportación de carbono por debajo de la zona eufótica (<150 o 200 m de profundidad), mientras que muy poco se sabe acerca de la magnitud y la extensión de este transporte por debajo de esa cota. Esto último sería de especial interés en el caso del micronecton ya que esta comunidad puede cubrir mayores rangos de migración en comparación con el zooplancton, incrementando de este modo la eficiencia de la bomba biológica.

Por tanto, la evaluación de la exportación del carbono en el océano requiere una mayor investigación del proceso de migración vertical, prestando especial atención a la contribución del micronecton a lo largo de la región mesopelágica y batipelágica. De no ser así, podríamos estar ignorando a uno de los mayores componentes de la bomba biológica de carbono.

Objetivos y planteamiento de la investigación

La evaluación eficiente del flujo activo de carbono implica conocer la composición de las capas migrantes de reflexión acústica en una región determinada, así como la extensión y la magnitud de la exportación de carbono que realiza cada componente migrador. Sin embargo, se sabe muy poco de la biota acústica mesopelágica en el Atlántico nordeste subtropical. Casi toda la investigación concerniente al flujo activo se ha centrado fundamentalmente en la exportación del zooplancton y por debajo de la capa fótica.

El objetivo de esta tesis es investigar el papel de la comunidad micronectónica en la migración vertical y en el flujo de carbono en el Atlántico nordeste subtropical, centrándonos en su composición, los factores ambientales que gobiernan su distribución, así como en la magnitud y la extensión de las migraciones a lo largo de las zonas mesopelágica y batipelágica. Conforme a esto, los objetivos específicos de este trabajo pretenden dar respuesta a las siguientes preguntas:

¿Cuál es la composición faunística de las capas de reflexión acústica que se observan en el Atlántico nordeste subtropical y que patrones de migración siguen? **Capítulo 1**

Para responder a esta pregunta describimos los fenómenos acústicos observados en aguas superficiales y mesopelágicas de las Islas Canarias mediante la combinación de registros acústicos con frecuencias de 18 y 38 kHz, y también con muestreo de redes en differentes profundidades a lo largo del día y la noche.

¿Cuál es la contribución del zooplancton y del micronecton a la biomasa migrante y a la exportación de carbono en el Atlántico nordeste subtropical? **Capítulo 2**

Para responder a esta cuestión medimos simultáneamente el flujo pasivo y activo a lo largo de varias campañas de muestreo en aguas oceánicas al norte de la isla de Gran Canaria. La biomasa migrante del zooplancton y del micronecton fue estimada mediante el uso de una nueva red rectangular de arrastre, mientras que la exportación de carbono fue estimada a partir de las tasas de respiración medidas en especies migradoras dominantes.

¿De qué modo las perturbaciones ambientales afectan al proceso de migración vertical y a la fauna mesopelágica? **Capítulo 3**

Esta cuestión fue abordada gracias a un estudio de oportunidad acontecido durante la presente tesis: La erupción volcánica submarina de la Isla de El Hierro provocó alteraciones en el régimen lumínico del mar, en la temperatura y en el oxígeno disuelto,

anomalías que produjeron cambios en el ecosistema pelágico. Las respuestas de la biota migrante fueron estudiadas mediante muestreo acústico y de redes.

¿Qué efecto causan los remolinos oceánicos sobre la fauna mesopelágica? **Capítulo 4**

Combinando medidas hidrográficas y acústicas *in-situ* con parámetros de satélite se ha podido investigar, por primera vez, las interacciones entre los remolinos y el micronecton en las Islas Canarias. Se analizó la estructura tridimensional de la fauna mesopelágica seccionando sistemáticamente un remolino anticiclónico, desde superficie hasta 1000 m de profundidad, con una ecosonda de 38 kHz.

¿Cuál es el rol del micronecton en la exportación de carbono a lo largo de la zona mesopelágica y más allá de los 1000 m de profundidad? **Discusión general**

Basándonos en los resultados de la presente tesis, así como revisando las distribuciones verticales del micronecton en la región, discutimos acerca de la contribución relativa del micronecton a la exportación de carbono a lo largo de la zona mesopelágica y más allá de los 1000 m de profundidad.

Metodología

Con el fin de lograr los objetivos planteados, durante la presente tesis se recurrieron a diversos procedimientos metodológicos. A continuación describimos en términos generales las técnicas usadas:

Muestreo acústico

El uso de ecosondas científicas para la observación de las capas de reflexión acústica en el océano ha sido una de las técnicas clave para el estudio de la distribución, densidad y comportamiento de la biota pelágica.

Durante esta tesis se han usado ecosondas EK60 SIMRAD de haz dividido en dos configuraciones según la campaña oceanográfica: con los transductores (encargados de la transmisión y recepción de la señal acústica) instalados en el casco de los buques de investigación, o con transductores sumergidos en el agua colgando de un cabo, en el caso de embarcaciones menores no provistas de instalación acústica.

Se han usado frecuencias de 18, 38, 120 y 200 kHz en los diferentes estudios. El uso de la multifrecuencia persigue la discriminación de los diferentes objetivos acústicos según su tamaño. Esto se basa en la longitud de onda (λ) de cada frecuencia, que determina el tamaño mínimo que el objetivo acústico debe tener para poder ser detectado. Las frecuencias bajas poseen mayor longitud de onda que las altas (e.g., $\lambda_{18\text{ kHz}} \sim 80$ mm; $\lambda_{200\text{ kHz}} \sim 8$ mm), de modo que las primeras se usan para estudiar organismos mayores normalmente pertenecientes al necton, y las segundas para los organismos menores del plancton. También se han usado otras propiedades acústicas para diferenciar organismos, como puede ser la resonancia de estructuras gaseosas como la vejiga natatoria de los peces, que son capaces de producir ecos muy intensos. Además, la forma de los registros acústicos (formando bancos o capas), la intensidad del eco recibido en cada frecuencia, o la distribución vertical también se han usado como indicativos para la identificación de los grupos animales. Ver Simmonds y MacLennan [2005] para más información acerca de las técnicas de idetificación en acústica. Por último, la composición de las capas de reflexión acústica era comprobada mediante muestreo directo con redes de plancton y de necton (ver siguiente sección).

Una vez interpretados los distintos grupos acústicos se procedía a estudiar las abundancias de cada grupo animal, su distribución y comportamiento migratorio. Para las abundancias usamos el volumen de eco reflejado (Sv) como indicador de la densidad relativa de animales. La distribución de la biota acústica en función de parámetros oceanográficos como la turbidez en superficie o perfiles verticales de temperatura, oxígeno

y clorofila, se realizaba mediante la combinación de los datos acústicos con mediciones realizadas por satélite o por diferentes instrumentos hidrográficos presentes en los buques de investigación. El comportamiento migratorio diario se estudiaba mediante la proyección de ecogramas en escala temporal de 24 horas, calculando así la velocidad de migración y observando la sincronización de los moviemientos verticales en función del amanecer y anochecer.

El proceso de filtrado e interpretación de datos, así como el cálculo de densidades de los diferentes grupos acústicos se realizó usando el programa comercial LSSS. La proyección de ecogramas, así como la combinación de los datos acústicos con datos satelitales e hidrográficos, o el cálculo de velocidades de migración se ha realizado con diversas aplicaciones desarrolladas para estos fines en lenguaje de programación MATLAB.

Muestreo biológico

El muestreo biológico se refiere a los procedimientos de captura, conservación, procesado e identificación de las muestras de zooplancton y de micronecton durante la presente tesis.

Las muestras de zooplancton eran obtenidas mediante pescas verticales desde 200 m de profundidad hasta la superficie, ascendiendo a una velocidad de 50 m por minuto. El modelo de red usada fue la WP-2 [UNESCO, 1968], con una luz de malla de 100 μm, y que está indicada para el muestreo de mesozooplancton. Con el fin de obtener datos de abundancia estandarizados por metro cúbico, el volumen de agua filtrado por la red era calculado mediante un medidor de flujo entrante TSK instalado en la boca de la red. Las muestras obtenidas eran fijadas inmediatamente en formaldehído tamponado al 4 % en agua de mar y eran almacenadas en oscuridad hasta su posterior procesamiento.

Una vez en el laboratorio, las muestras eran digitalizadas mediante escáner a una resolución de 1200 puntos por pulgada y los organismos eran identificados, contados y medidos usando el programa de procesamiento de imágenes Zooimage [Grosjean y Denis, 2007]. Los grupos taxonómicos eran identificados gracias a una sesión manual de aprendizaje del programa en la que se ingresaban imágenes ya identificadas de organismos típicos de la región, logrando un margen de error de identificación menor al 5 %. El área de cada individuo era posteriormente transformada a peso seco mediante las ecuaciones dadas por Hernández-León y Montero [2006], así como por Lehette y Hernández-León [2009].

Las muestras de micronecton fueron colectadas mediante arrastres oblicuos por popa con dos tipos de redes según el estudio: (1) una red de marco modelo MOHT [Oozeki

et al., 2004] de 5 m^2 de boca, usada en embarcaciones menores, y (2) una red de pesca comercial de 300 m^2 usada en buques de investigación adaptados para maniobras de arrastre por popa. La red MOHT utilizaba una red de malla de 0.4 cm y podía ser arrastrada a 4 o 5 nudos, mientras que la red comercial usaba mallas decrecientes desde 80 cm al comienzo hasta 1 cm en el copo, desarrollando velocidades de arrastre entre 2 y 3 nudos. Los tiempos efectivos de pesca para ambas redes eran de una hora. Las principales diferencias entre las redes era que la MOHT muestreaba eficientemente la fracción más pequeña del micronecton pero submuestreaba las tallas grandes, mientras que la red comercial de arrastre hacía lo contrario.

Las muestras de micronecton eran fijadas inmediatamente en formaldehído tamponado al 4 % en agua de mar y dos semanas después de su colección eran lavadas en agua y transvasadas a etanol al 70 % para su conservación a largo plazo. Posteriormente los peces, crustáceos y cefalópodos eran identificados hasta nivel de especie cuando era posible, y todos los individuos eran medidos y pesados.

Actividad del sistema de transporte de electrones

El sistema de transporte de electrones es una serie de complejos enzimáticos, que en el caso de los animales, está presente en las mitocondrias celulares. Se encarga de la producción de energía mediante la oxidación de los alimentos. En este proceso se consume oxígeno, por ello nos referimos a él como la respiración celular. La medición de la actividad enzimática de este sistema puede ser por tanto un indicador de la tasa de respiración de los organismos, pudiendo usarse también para inferir la cantidad de dióxido de carbono producido por unidad de tiempo. Por ello, esta técnica es usada comúnmente para conocer el nivel metabólico y para estimar los flujos respiratorios de carbono de los organismos marinos [Hernández-León et al., 2001, Packard y Gómez, 2013].

En la presente tesis, la actividad del sistema de transporte de electrones fue analizada en el zooplancton y el micronecton con el fin de estimar sus flujos respiratorios de carbono. En el caso del zooplancton, los ensayos fueron dirigidos sobre muestras fraccionadas por tallas entre 0.1-0.2, 0.2-0.5, 0.5-1.0 y >1.0 mm, y en el caso del micronecton, los análisis se realizaron sobre individuos de especies dominantes que conforman esta comunidad: *Lobianchia dofleini* (Myctophidae), *Sergia splendens* (Sergestidae) y *Euphausia gibboides* (Euphausiidae). Todas las muestras eran conservadas en nitrógeno líquido (-196°C) inmediatamente después de su muestreo.

Una vez en laboratorio, las fracciones de zooplancton y los especímenes de micronecton eran homogeneizados mecánicamente con la ayuda de una disolución tampón fosfato

(0.05M PO_4). Los análisis de la actividad enzimática del sistema de transporte de electrones eran seguidamente realizados de acuerdo con los métodos descritos por Packard [1971] y posteriormente modificados por Gómez et al. [1996]. Las mediciones obtenidas fueron corregidas para la temperatura *in-situ* correspondiente a la profundidad donde fueron obtenidas las muestras, esto se hizo mediante la ecuación de Arrhenius usando una energía de activación de 15 kcal mol^{-1} [Packard et al., 1975].

Determinación del flujo activo de carbono

La exportación de carbono inorgánico debido a la respiración del zooplancton y del micronecton fue calculada a partir de la actividad del sistema de transporte de electrones (sección anterior). Para ello se usó una relación conservadora de respiración/ETS = 0.5, de acuerdo con las relaciones existentes para los diferentes grupos animales [Ikeda, 1989, Hernández-León y Gómez, 1996, Schukat et al., 2013]. La tasas de oxígeno consumido fueron transformadas en producción de dióxido de carbono mediante cálculo estequiométrico (22.4 L O_2 = 12 g CO_2). Seguidamente se aplicaba un cociente respiratorio de 0.9, un valor también conservativo de acuerdo con aquellos obtenidos para zooplancton y micronecton en la literatura científica [Brett y Groves, 1979, Omori e Ikeda, 1984, Pakhomov et al., 1999].

En el caso del zooplancton, el flujo respiratorio fue calculado solo en la fracción de talla >1 mm debido a que es en esta fracción donde se encontraban los migradores, principalmente eufausiáceos. En el caso del micronecton, la tasas respiratorias de *Lobianchia dofleini* (Myctophidae), *Sergia splendens* (Sergestidae) y *Euphausia gibboides* (Euphausiidae), fueron usadas para calcular respectivamente los flujos respiratorios de peces, crustáceos y eufausiáceos, respectivamente.

La exportación diaria de carbono fuera de la zona eufótica, se calculó asumiendo que los migradores respiran en la zona mesopelágica aproximadamente durante 12 horas al día. El ETS usado para estos cálculos fue corregido por la temperatura *in-situ* que hay a 500 m de profundidad, coincidiendo con las capas profundas de reflexión acústica en la región [Bordes et al., 2009].

Resultados

El siguiente texto es un resumen en español de los los capítulos 1, 2, 3 y 4. Las figuras más importantes se han incorporado en este resumen, aunque también se hace referencia a otras figuras que pueden consultarse en los capítulos originales en versión inglesa.

Capítulo 1: Distribución vertical, composición y patrones migratorios de las capas de reflexión acústica en las Islas Canarias.

Alejandro Ariza, José María Landeira, Alejandro Escánez, Rupert Wienerroither, Natacha Aguilar, Anders Røstad, Stein Kaartvedt, y Santiago Hernández-León.

Enviado a *Journal of Marine Systems*.

El proceso de migración vertical diaria promueve las interacciones tróficas y los intercambios biogeoquímicos entre las aguas someras y el océano profundo [Ducklow et al., 2001, Hidaka et al., 2001, Robinson et al., 2010, Davison et al., 2013], por lo que su estudio es de gran importancia para comprender el funcionamiento de los sistemas pelágicos. Una manera fácil de estudiar la distribución y la actividad migratoria de estos animales es mediante el uso de ecosondas científicas [Kloser et al., 2002, Kaartvedt et al., 2009, Cade y Benoit-Bird, 2015]. Por ello, la vigilancia acústica podría ser una herramienta muy eficiente para la evaluación de la bomba biológica en el océano.

En las Islas Canarias, la distribución vertical de los migradores que habitan la zona mesopelágica fue meticulosamente estudiada durante las campañas oceanográficas SOND a mediados de los años sesenta [Foxton, 1969]. Sin embargo, debido a la limitada tecnología acústica existente en aquella época, no se pudo conocer a los organismos responsables de las distintas capas acústicas que observamos hoy con facilidad gracias a las modernas ecosondas científicas.

Por tanto, el objetivo de este capítulo fue describir las especies que conforman estas capas, así como sus patrones migratorios, con el fin de mejorar las interpretaciones derivadas de observaciones acústicas en esta región del océano. Para ello usamos las frecuencias estándar de 18 y 38 kHz, e hicimos pescas de arrastre a través de las distintas capas acústicas que se observaban en aguas epipelágicas y mesopelágicas del suroeste de La Palma y Tenerife (Fig. 1.1, 1.2, y 1.3).

Encontramos una gran diversidad de especies, como era de esperar en aguas mesopelágicas del Atlántico nordeste subtropical (152 species indentificadas, ver tabla 1.1 y anexo V). Esto introdujo una larga lista de animales que podían provocar eco, cada especie con propiedades acústicas muy diferentes. Sin embargo, nos centramos en las especies

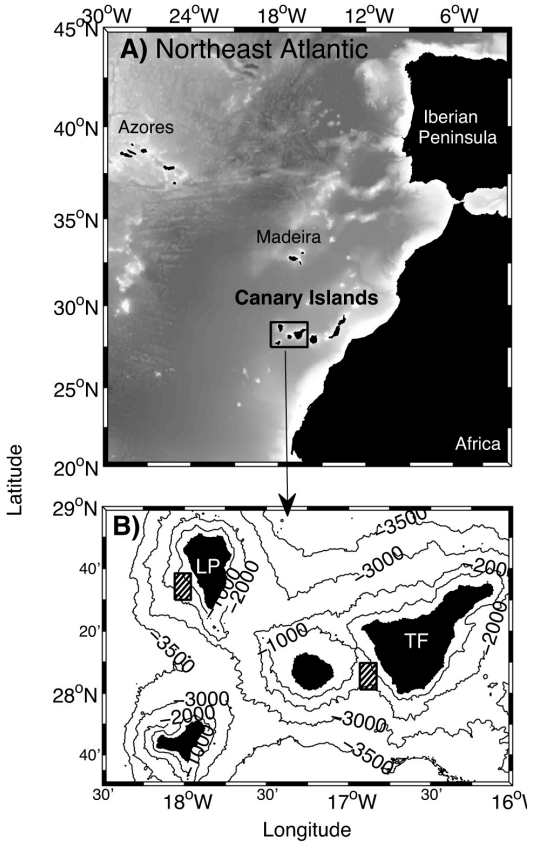

FIGURA 1.1: (A) Mapa mostrando la localización de las Islas Canarias al oeste de África. (B) Área de estudio al suroeste de las islas de La Palma y Tenerife, donde se realizaron los registros acústicos y los lances de pesca.

que dominaban en cada estrato, ya que se presume que las más escasas deben contribuir muy poco al volumen total de eco. No obstante, es importante recordar, que las zonas acústicas estarían habitadas por muchas otras especies, independientemente de si eran visibles o no en nuestros ecogramas.

La distribución de las capas acústicas fue muy similar tanto en aguas de La Palma como de Tenerife (Fig. 1.3). Se observaba sistemáticamente dos capas muy densas, una a 18 kHz entre 400 y 500 m de profundidad, y otra a 38 kHz entre 500 y 600 m. La más superficial (DSL1) parece un fenómeno de resonancia por los altos niveles de eco. De acuerdo al modelo de Kloser et al. [2002], a esta profundidad y frecuencia son susceptibles de producir resonancia animales con vesículas de gas de un radio esférico equivalente (ESR) entre 1.2 y 1.4 mm (Fig. 1.6a). De acuerdo a nuestras capturas, la DSL1 estaba fundamentalmente habitada por *Vinciguerria* spp., peces que portan una vejiga natatoria llena de gas con un ESR de aproximadamente 1.2 mm, por lo que esta sería la especie que con más probabilidad estaría produciendo el fenómeno de resonancia en la DSL1 (Tabla 1.2). El cambio de eco durante la migración vertical sería otro indicativo de que estamos ante un fenómeno de resonancia, pues pequeños cambios en profundidad

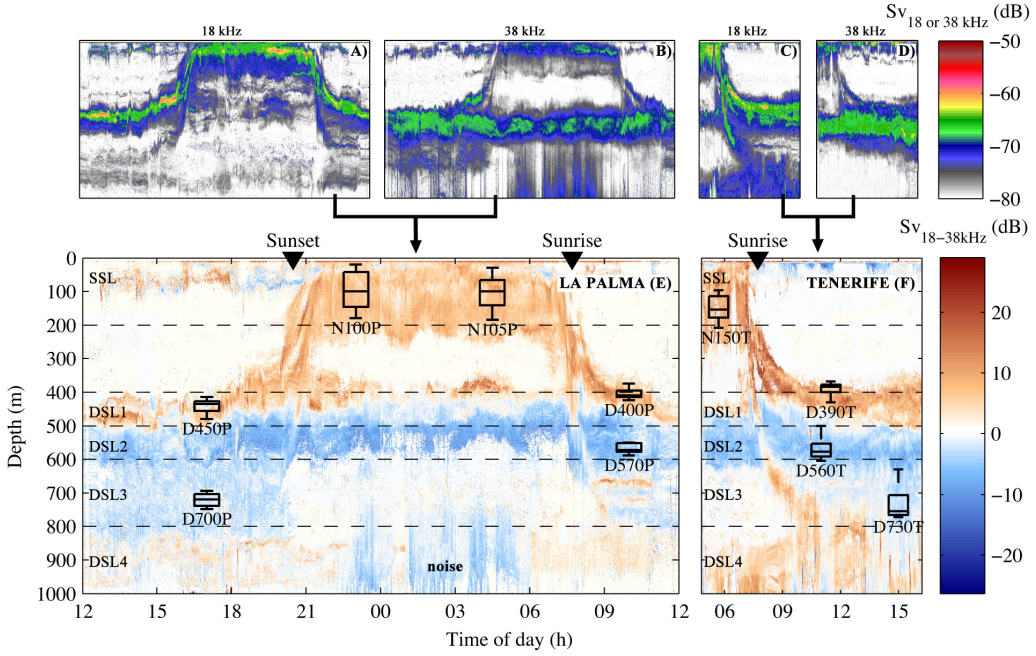

FIGURA 1.3: Ecogramas a 18 y 38 kHz en aguas cercanas a las islas de La Palma (A y B) y Tenerife (C y D), así como ecogramas diferenciales (18 menos 38 kHz) para las mismas localidades (E y F). Las capas acústicas se diferencian de acuerdo a su profundidad y respuesta a cada frecuencia: una capa de reflexión superficial en la zona epipelágica (SSL), y cuatro capas de reflexión profunda en la zona mesopelágica (DSL1, DSL2, DSL3 y DSL4). El tiempo y la profundidad de cada lance de pesca está representado por cajas, donde las líneas centrales representan la profundidad promedio, los límites de las cajas son los percentiles 25 y 75, y las líneas verticales indican las profundidades más alejadas del promedio, pero no consideradas valores anómalos.

producirían grandes cambios en las dimensiones de la vejiga natatoria, afectando esto a su comportamiento acústico [Andreeva, 1964, Godø et al., 2009].

En cuanto a la DSL2, la única especie dominante susceptible de llevar vejiga natatoria funcional sería *Cyclothone braueri*, el resto serían animales con menos capacidad para producir eco (Tabla 1.2). Esta especie podría producir resonancia a 38 kHz y en torno a 500-600 m de profundidad (Fig. 1.6b), de acuerdo con el modelo de Kloser et al. [2002]. *C. braueri* no fue la especie más abundante en nuestras capturas. Creemos que debido a su pequeño tamaño, escapaba fácilmente por la luz de malla de nuestra red. Sin embargo, estudios con mallas de red más apropiadas confirman que *C. braueri* se concentra entre 500 y 600 m de profundidad, y además en abundancias muy elevadas [Badcock, 1970, Badcock y Merret, 1976, Roe y Badcock, 1984]. En nuestro caso y aunque en bajas abundancias, la prevalencia de *C. braueri* en este estrato y la ausencia en el resto, también confirma que se concentraba dentro de la DSL2. Por tanto, considerando su elevado número y su capacidad de reflejar sonido (vejiga con gas), consideramos que *C. braueri* sería el mayor responsable del eco en la DSL2. *C. braueri* es una especie no migradora [Goodyear et al., 1972, Badcock y Merret, 1976], y esto se refleja en que

la DSL2 permanece siempre a la misma profundidad. No obstante, el hecho de que durante la noche descienda ligeramente el nivel de eco (Fig. 1.3b, 1.4a y 1.4b) pone de manifiesto que aparte de *C. braueri*, hay otros organismos migradores responsables del eco de la DSL2, como pueden ser el mictófido *Hygophum hygomii* o el decápodo *Oplophorus spinosus* (Fig. 1.5d).

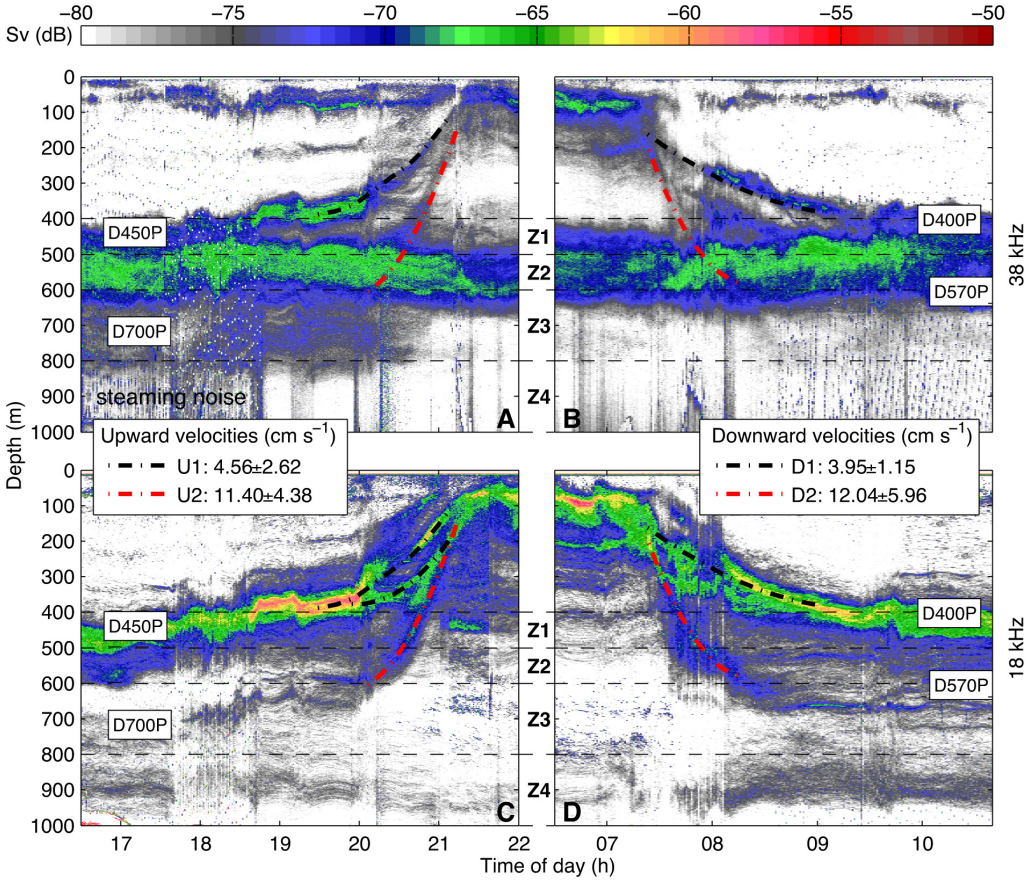

FIGURA 1.4: Mismos ecogramas vistos a 38 (A y B) y a 18 kHz (B y C) mostrando varias rutas de migración vertical. Los distintos ascensos (U1, U2) y descensos (D1, D2) se indican con líneas discontinuas y sus velocidades de migración promedio están señaladas en las legendas. Las diferentes zonas de reflexión acústica (DSL1, DSL2, DSL3 y DSL4) también están indicadas, conforme a la división propuesta en la Figura 1.3. Los letreros sobre los ecogramas indican la hora y profundidad de los lances de pesca.

La reflexión acústica fue considerablemente más baja a partir de los 600 m de profundidad, donde la respuesta a ambas frecuencias también indicaba que había dos estratos distintos (Fig. 1.3). La capa de 600 a 800 m (DSL3) debería estar causada principalmente por migradores, como evidencia los movimientos verticales diarios, tanto a 18 como a 38 kHz (Fig. 1.4). En la DSL3 las capturas estaban dominadas por *Cyclothone microdon* (Fig. 1.5), un pez que podría ser el causante de la reflexión acústica sino fuera por el hecho de que no realiza migraciones verticales. Además de que *C. microdon*, y otras especies del mismo género que habitan debajo de los 600 m, ya no serían buenos reflectores de sonido. Esto se debe a que atrofian su vejiga natatoria cuando alcanzan un

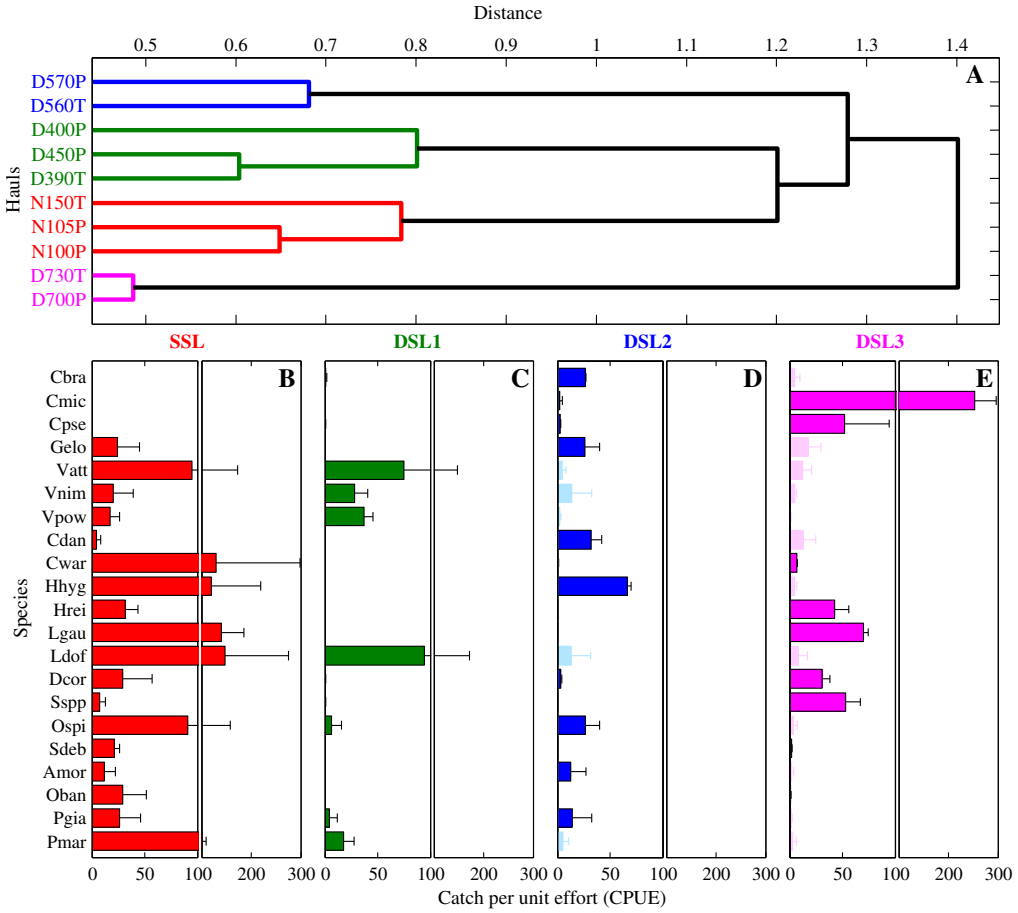

FIGURA 1.5: (A) Dendrograma mostrando la clasificación de los lances de pesca de acuerdo a las distancias de disimilaridad de Bray-Curtis. El tiempo y profundidad de cada lance puede comprobarse en la Figura 1.3. (B-E) Capturas por unidad de esfuerzo (CPUE) de las especies más importantes que contribuyen a las diferencias entre lances de pesca. Las barras con colores tenues indican que son animales que pueden provenir de contaminaciones de estratos más someros (ver discusión en capítulo 1). Abreviaciones de nombres de especie: *Cbra= Cyclothone braueri*; *Cmic= Cyclothone microdon*; *Cpse= Cyclothone pseudopallida*; *Gelo= Gonostoma elongatum*; *Vatt= Vinciguerria attenuata*; *Vnim= Vinciguerria nimbaria*; *Vpow= Vinciguerria poweriae*; *Cdan= Chauliodus danae*; *Cwar= Ceratoscopelus warmingii*; *Hhyg= Hygophum hygomii*; *Hrei= Hygophum reinhardtii*; *Lgau= Lepidophanes gaussi*; *Ldof= Lobianchia dofleini*; *Dcor= Deosergestes corniculum*; *Sspp= Sergestes* spp.; *Ospi= Oplophorus spinosus*; *Sdeb= Systellaspis debilis*; *Amor= Abraliopsis moriisi*; *Oban= Onychoteuthis banksii*; *Pgia=Pterygioteuthis giardi*; *Pmar= Pyroteuthis margaritifera*.

determinado tamaño y profundidad [Badcock y Merret, 1976, 1977]. Por tanto, deben ser los migradores más abundantes de la DSL3 lo causantes del eco. Entre otros, los peces *Lepidophanes gaussi* e *Hygophum reinhardtii*, así como varias especies de sergéstidos (Fig. 1.5e). De acuerdo con la literatura, tanto *L. gaussi* como *H. reinhardtii* portan vejiga natatoria, que en el caso de estar funcional, produciría resonancia a 18 kHz. A pesar de que carecemos de esta información (Tabla 1.2), los niveles de eco por debajo de 600 m de profundidad no son indicativos de resonancia. Esto es además coherente con el hecho de que las vejigas natatorias de los mictófidos están normalmente atrofiadas en los

ejemplares grandes que alcanzan estas profundidades (ver siguiente párrafo). Por tanto, es probable que tanto peces como decápodos migradores se comporten como reflectores poco eficientes, pero que sus altas abundancias causen la DSL3.

La atrofia de la vejiga natatoria es un rasgo común en las especies de mictófidos de tamaño medio y grande. Esto es lo mismo que decir, que la funcionalidad de la vejiga natatoria desaparece al aumentar la profundidad de migración [Marshall, 1960, Butler y Pearcy, 1972, Davison, 2011a]. Esto puede verse en nuestra área de estudio, donde el mictófido más pequeño, *Lobianchia dofleini*, está en los estratos más someros, mientras que las especies más grandes, como *Ceratoscopelus warmingii* y *Notoscopelus resplendens*, alcanzan aguas batipelágicas [Badcock y Merret, 1976]. Puesto que las vejigas atrofiadas se llenan casi en su totalidad de un "tejido algodonoso", estas dejarían de ser un reflector eficiente de sonido [Capen, 1967, Klecner y Gibbs, 1972]. Así, basándonos en catálogos de vejigas natatorias, los peces que portaban gas en nuestra región de estudio se situaban por encima de los 600 m de profundidad, mientras que los peces con vejigas no funcionales se posicionaban debajo de esta cota (ver Tabla 1.2). En términos acústicos, esto significa que la zona mesopelágica profunda está habitada por organismos que no reflejan bien el sonido, y donde no podemos hacer uso de los modelos de resonancia (Fig. 1.6). Esto además explicaría porqué las abundancias relativamente altas de nuestros lances profundos no se ven reflejadas en los ecogramas.

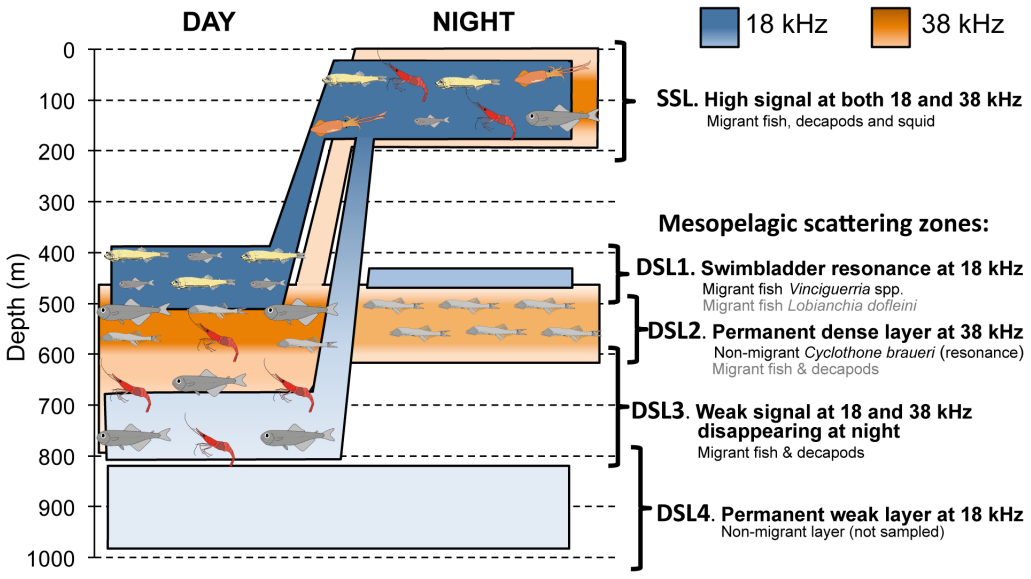

FIGURA 1.7: Distribución de capas de reflexión acústica someras y profundas (SSL y DSLs), basado en observaciones realizadas a 18 y 38 kHz en aguas de Canarias (límites de detección entre -80 y -50 dB). Se indican solo las especies dominantes que probablemente estén reflejando más sonido (los organismos principales en negro, y los secundarios en gris). El azul y el naranja indican las frecuencias de 18 y 38 kHz, respectivamente, siendo los colores oscuros los ecos más fuertes, y lo colores claros los más débiles. Consultar el texto para más detalles.

En general, la asociación de capas acústicas y animales que proponemos aquí (Fig. 1.7) es coherente con los esquemas de distribución vertical previamente observados durante la expedición SOND en las Islas Canarias, y también por otros estudios en aguas oceánicas cercanas [Foxton, 1969, Badcock y Merret, 1976, Roe et al., 1984a]. En particular, Badcock [1970] así como Badcock y Merret [1976] apuntaban a que la mayor diversidad de mictófidos poblaban aguas entre 400 y 600 m de profundidad, mientras que unas pocas especies de tamaño más grande aparecían por debajo de los 700 m. Sus tablas de abundancias también dejan patente que *Vinciguerria* spp. y *Lobianchia dofleini* eran las especies más someras, mientras que *Cyclothone braueri* mostraba sus máximas abundancias entre 500 y 600 m de profundidad. Estos dos aspectos coinciden con nuestras descripciones de la DSL1 y DSL2. Por otro lado, Foxton [1970b] documentaba abundancias máximas de decápodos por debajo de los 650 m de profundidad. A este respecto, tanto los estudios de Badcock como los de Foxton, proponían una distinción de "faunas mesopelágicas someras y profundas", y que ellos atribuían a adaptaciones a diferentes tipos de luz. De acuerdo a esto, la interfase acústica que hemos observado entre resonancia y ecos débiles, podría estar poniendo de manifiesto este cambio faunístico o "bioclina"[Lezama-ochoa et al., 2014], con animales pequeños portadores de gas arriba, y otros más grandes y sin estructuras reflectantes abajo. De hecho, la mayor velocidad de migración de la biota profunda también apoyaría esta idea (Fig. 1.4). Estos animales se podrían desplazar más rápido no solo por su mayor tamaño, sino porque no precisarían reajustar el volumen de gas durante los ascensos y descensos [Marshall, 1960, Butler y Pearcy, 1972, Kleckner y Gibbs, 1972].

En conclusión, este estudio ha revelado que existe una gran diversidad dentro de la comunidad de micronecton mesopelágica (152 especies identificadas), aunque con pocas especies dominantes que probablemente son las responsables de los fenómenos acústicos en la región. Proponemos que la DSL1 (400-500 m) esta producida principalmente por resonancia acústica del pez *Vinciguerria* spp., migrador vertical y con vejiga natatoria llena de gas. La DSL2 (500-600 m) estaría fundamentalmente producida por la resonancia de *Cyclothone braueri*, un pez no migrador y también portador de gas. La DSL3 (600-800 m) se debe a peces y decápodos migradores que no producen resonancia, pero al igual que otras capas más profundas, se desconocen los especies concretas. Todas las capas migradoras alcanzaban la zona epipelágica al anochecer. Las migraciones que partían entre 400 y 600 m de profundidad se desplazaban a 4 cm s^{-1} y las que lo hacían entre 600 y 800 m se movían a 12 cm s^{-1}. El presente trabajo reduce las incertidumbres en la interpretación de las capas acústicas. Futuras descripciones más precisas requerirán muestreos con redes a más profundidad, con mayor resolución vertical, así como el empleo de ecosondas con más frecuencias.

Capítulo 2: Biomasa migrante y flujo respiratorio de carbono del zooplancton y el micronecton en el Atlántico nordeste subtropical (Islas Canarias).

Alejandro Ariza, Juan Carlos Garijo, José María Landeira, Fernando Bordes, y Santiago Hernández-León (2015).

Publicado en *Progress in Oceanography* 134:330-342.

Mediante el proceso de migración vertical, tanto el zooplancton como el micronecton contribuyen a la exportación de carbono hacia el océano profundo en magnitudes que aún son muy poco conocidas. Tradicionalmente se ha dedicado mayor esfuerzo a evaluar la exportación de carbono debido al flujo gravitacional, y en menor medida, a la migración del zooplancton. Sin embargo, el flujo activo del micronecton ha sido prácticamente ignorado debido a que muestrear estos organismos requiere maniobras muy costosas y difíciles de llevar a cabo en el mar. En este capítulo, evaluamos el flujo gravitacional, así como el flujo activo mediado por la respiración del zooplancton y el micronecton migrador en un muestreo semanal de dos meses en el Atlántico nordeste subtropical (Fig. 2.1, 2.2, y 2.3). Para ello, calculamos la biomasa migrante y la tasa respiratoria mediante mediciones de la actividad del sistema de transporte de electrones en ambos componentes migratorios.

Nuestros resultados señalan que el principal componente migrador del zooplancton son los organismos mayores de 1 mm, de acuerdo con las diferencias halladas entre el día y la noche. Los juveniles de eufausiáceos son los más abundantes en esta fracción de talla y los que más biomasa migrante aportan (Fig. 2.4, Tabla 2.1). Dentro del micronecton, los migradores más abundantes fueron los eufausiáceos adultos, seguidos de peces y decápodos. No obstante, en términos de biomasa, lo peces constituyeron la mayor parte de la biomasa migrante del micronecton, siendo los mictófidos la familia dominante (Fig. 2.5, Tabla 2.2).

Hemos advertido sin embargo, que la red usada para muestrear el micronecton captura eficientemente a los eufausiáceos pero no a la fracción adulta de peces (Fig. 2.6), probablemente debido a la alta capacidad que estos animales tienen para evitar la red. Usamos por tanto unos factores de corrección para este modelo de red obtenidos por Davison [2011b] en el Pacífico nordeste. Con ello, obtuvimos una biomasa migrante para el zooplancton y el micronecton de 266±127 y 201±61 mg C m^{-2}, respectivamente (Tabla 2.3). En el caso del micronecton, solo los peces suponían el 83 % de la biomasa. Nuestras estimaciones para el zooplancton son cercanas a las de otras regiones oceánicas con similares características. Sin embargo, nuestros valores de micronecton y los de la literatura muestran una gran variabilidad. Estas diferencias en el micronecton probablemente se

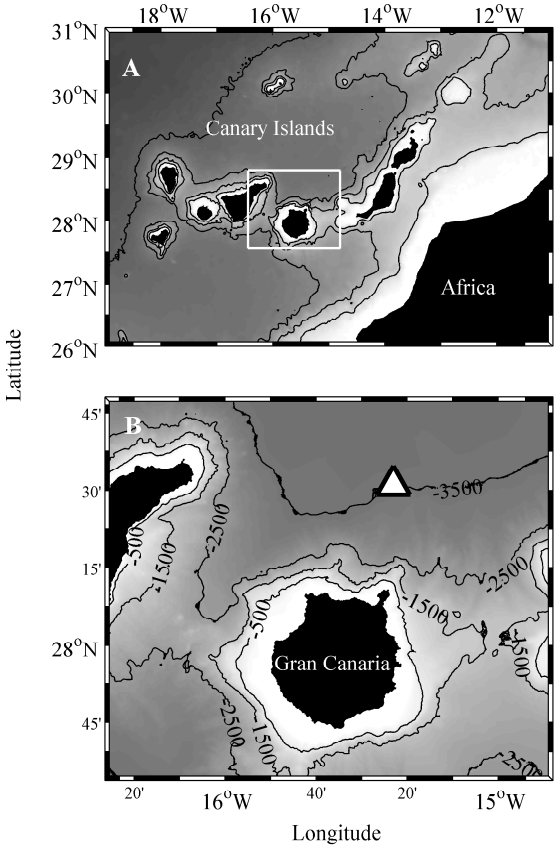

FIGURA 2.1: (A) Situación de las Islas Canarias al oeste de África, y la isla de Gran Canaria señalada con un recuadro blaco. (B) Estación oceanográfica donde se realizó la serie temporal, en aguas oceánicas al norte de Gran Canaria.

deben a las estimas de biomasa migrante y no a las medidas de respiración, que son cercanas a otros estudios (Fig. 2.7). La incertidumbre que existe acerca de la eficiencia de captura de las distintas redes usadas para muestrear a estos esquivos animales debe ser la principal fuente de variabilidad [Pakhomov et al., 2010].

En términos de respiración, ambos grupos migradores exportan cantidades similares de carbono fuera de la zona epipelágica, 3.4±1.9 mg C m^{-2} d^{-1} el zooplancton, y 2.9±1.0 mg C m^{-2} d^{-1} el micronecton. Esto se debe a que, de acuerdo con nuestras estimaciones, ambos poseen una biomasa migrante y un metabolismo respiratorio parecido (Tabla 2.3). Sin embargo, existen otros mecanismos de exportación en los que se estima que habría grandes diferencias entre el zooplancton y el micronecton. El flujo del tracto digestivo se refiere al transporte de carbono en forma de alimentos no asimilados, que son vertidos vía defecación en aguas más profundas tras la migración. Se espera que este flujo sea más eficiente en el micronecton porque sus tasas de evacuación del tracto digestivo son mucho más lentas que las del zooplancton, lo que significaría que una mayor parte del alimento no asimilado sería vertido fuera de la zona epipelágica. De hecho, se estima que los copépodos requieren pocos minutos para vaciar el tracto digestivo [Dam y Peterson,

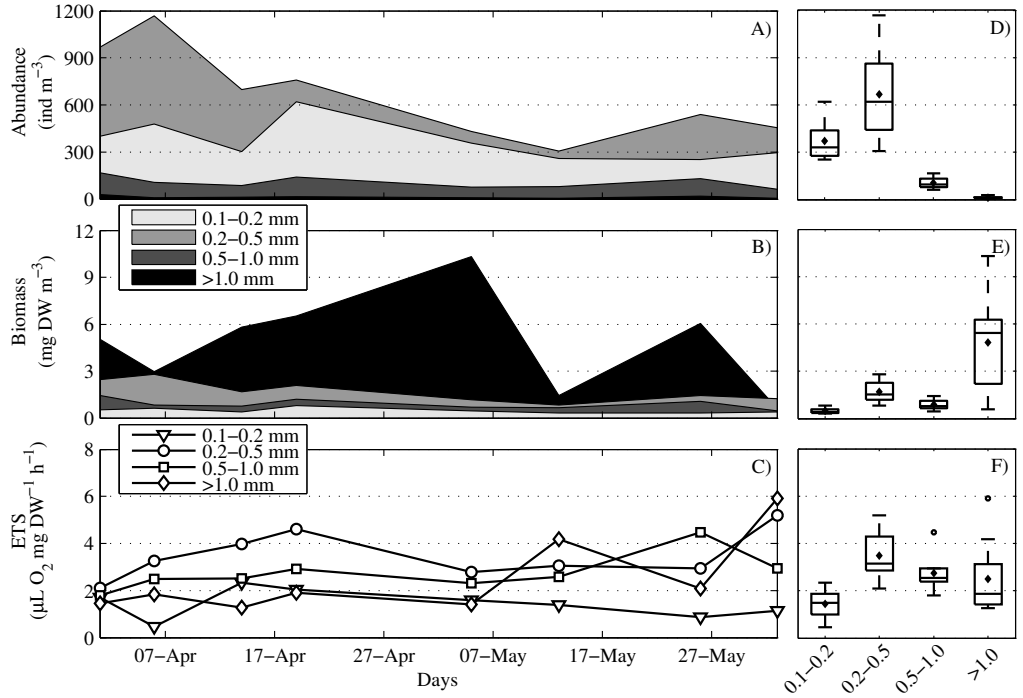

FIGURA 2.4: A la izquierda: serie temporal semanal mostrando (A) abundancia, (B) biomasa y (C) la actividad del sistema de transporte de electrones en diferentes fracciones de tallas de zooplancton capturado durante la noche. A la derecha: los mismos parámetros pero promediados en un gráfico de cajas. En cada caja, los diamantes centrales representan la media, las líneas centrales son las medianas, los límites de la caja son los percentiles 25 y 75, las líneas verticales se extienden hacía los datos más extremos no considerados valores anómalos. Los puntos representan los valores anómalos.

1988], los eufasiáceos entre 30 y 90 minutos [Gurney et al., 2002, Pakhomov et al., 2004], y los peces necesitan entre 12 horas y varios días [Baird et al., 1975, Clarke, 1982]. Si asumimos que los migradores se distribuyen en torno a los 50 m de profundidad al anochecer, y que descienden a 5 cm s^{-1} [Davison et al., 2013], esto implica que entrarían en la capa mesopelágica (<150 o 200 m) al cabo de 30 minutos. De acuerdo a esto, podríamos deducir que los copépodos no exportarían materia orgánica, los eufausiáceos lo harían parcialmente, mientras que prácticamente toda el alimento no asimilado por los peces se exportaría a la zona mesopelágica.

Cuando comparamos los valores de flujo respiratorio con la literatura vemos que nuestros valores del zooplancton son coherentes con otros estudios. Sin embargo, como consecuencia de los problemas en la estimación de biomasa, el flujo respiratorio del micronecton obtenido en este y en otros estudios es muy variable. A diferencia del zooplancton, apenas existen mediciones de la exportación de carbono mediada por el micronecton [Hidaka et al., 2001, Davison et al., 2013, Schukat et al., 2013, Hudson et al., 2014]. A pesar del evidente problema que existe con el micronecton para dar valores de exportación precisos, tanto nuestros resultados como los de otros trabajos, ponen de manifiesto que la cifras del micronecton están dentro del orden de magnitud del zooplancton (ver

Taxa	Terms	Migrant biomass (mg C m^{-2})	Migratory flux (mg C m^{-2} d^{-1})	Gravitational flux (mg C m^{-2} d^{-1})	Migratory/Gravitational (%)	Location	Source
Zooplankton	*R*	*107-412 (266±126.6)*	*1.13-4.45 (3.44±1.94)*	*6.31-26.70 (11.89±5.84)*	*10-37 (29)*	*Canary Islands*	*This study*
	R,E,M	126	3.2-13.6	18.0	11-44	Hawaii	Steinberg et al. [2008]
	R,E,M	1280	31.1-91.6	23.1-61.8	26-200	N. W. Pacific	Steinberg et al. [2008]
	R	580 - 1280	1.85-8.28	15.8	11-52	Canary Islands	Yebra et al. [2005]
	R	261	1.92 - 4.29	9.5-12.0	16-45	Canary Islands	Hernández-León et al. [2001]
	R	145-448	7.3-19.05	54.8	13-35	W. Eq. Pacific	Hidaka et al. [2001]
	R,E,F,M	158	3.6	23.7	15	Hawaii	Al-Mutairi and Landry [2001]
	R,E	49-123	2.0-9.9	25.6	9-39	Bermuda	Steinberg et al. [2000]
	R	47	3.1	49.2	6	W. Eq. Pacific	Le Borgne and Rodier [1997]
	R	53	6.3-7.9	204.0	3-4	E. Eq. Pacific	Le Borgne and Rodier [1997]
	R,M	96-155	7.1-12.7	22.8-28.8	31-44	E. Eq. Pacific	Zhang and Dam [1997]
	R	82-536 (191±147)	6.2-40.6 (14.5±11.1)	25-58 (39±10)	18 - 70 (34±16)	Bermuda	Dam et al. [1995]
	R	-	2.8-8.8	64.0-86.0	4-14	Sargasso Sea	Longhurst et al. [1990]
Euphausiids	*R*	*6-19 (10±4)*	*0.06-0.19 (0.11±0.04)*	*6.31-26.70 (11.89±5.84)*	*0.5-1.6 (0.9)*	*Canary Islands*	*This study*[a‡]
	R	33-159	0.10-0.46	54.8	0.2-0.8	W. Eq. Pacific	Hidaka et al. [2001][b§]
	E, F, M	-	1-32	-	-	N. E. Atlantic	Angel and Pugh [2000][e‡]
Decapods	*R*	*15-28 (23±5)*	*0.09-0.17 (0.14±0.03)*	*6.31-26.70 (11.89±5.84)*	*0.4-1.4 (1.2)*	*Canary Islands*	*This study*[a‡]
	R	291	13	8.3	79	Northern Benguela	Schukat et al. [2013][d†]
	R	44-96	0.12-0.26	54.8	0.2-0.5	W. Eq. Pacific	Hidaka et al. [2001][b§]
	E, F, M	-	1-6	-	-	N. E. Atlantic	Angel and Pugh [2000][e‡]
Fishes	*R*	*88-242 (168±58)*	*1.41-3.86 (2.68±0.92)*	*6.31-26.70 (11.89±5.84)*	*12-32 (23)*	*Canary Islands*	*This study*[a‡]
	R	285	0.33-1.94 (0.92)	86.0-259.0	0.3-1.0	North Azores	Hudson et al. [2014][b‡]
	R, F, M	15-276 (92±72)*	8.0-30.8	45.5-166.0	18-19	N. E. Pacific	Davison et al. [2013][c‡]
	R	1778-3304	7.6-14.1	54.8	14-26	W. Eq. Pacific	Hidaka et al. [2001][b§]
	E, F, M	-	2-43	-	-	N. E. Atlantic	Angel and Pugh [2000][e‡]
	M	299	3.1-11.1	-	-	Tasmania	Williams and Koslow [1997][e§]
Micronekton	*R*	*115-264 (201±61)*	*1.61-4.02 (2.92±0.95)*	*6.31-26.70 (11.89±5.84)*	*14-34 (25)*	*Canary Islands*	*This study*[a‡]
	R	2137-3614	15.2-29.9	54.8	28-55	W. Eq. Pacific	Hidaka et al. [2001][b§]
Total	R	222-676 (467±187)	2.74- 8.47 (6.36±2.89)	*6.31-26.70 (11.88±5.84)*	23-71 (53)	*Canary Islands*	*This study*[a‡]
	R	2282-4062	22.5-49.0	54.8	41-89	W. Eq. Pacific	Hidaka et al. [2001][b§]

[a]14, 38 and 80 % capture efficiency assumed for fishes, decapods and euphausiids.
[b]14 % Capture efficiency assumed.
[c]Capture efficiency adjusted to concurrent acoustic biomass estimates. Migratory flux obtained from "fish-mediated export"by vertical migrating fishes.
[d]33 % Capture efficiency assumed.
[e]Capture efficiency not corrected.
[†]Small frame trawl,[‡]big frame trawl,[§]commercial-sized midwater trawl
*Calculated from MOHT nocturnal shallow tows showed in supplementary Table A2 of Davison et al. (2013).

Tabla 2.3: Comparación de la biomasa migrante, el flujo gravitacional y migratorio, de acuerdo con la literatura. En la columna de términos, "R" se refiere a respiración, "E" a excreción, "F" a defecación, y "M" a mortalidad. Los flujos mostrados se refieren al carbono exportado debajo de la zona epipelágica (150-200 m dependiendo del estudio). Cuando ha sido necesario, los valores de la literatura han sido recalculados con el fin de estandarizar unidades, mediante el uso de conversores de masa explicados en la metodología. El tipo de red y las correcciones a la eficiencia de captura están también indicados. Los valores se muestran como rangos o promedios (en paréntesis) según la fuente.

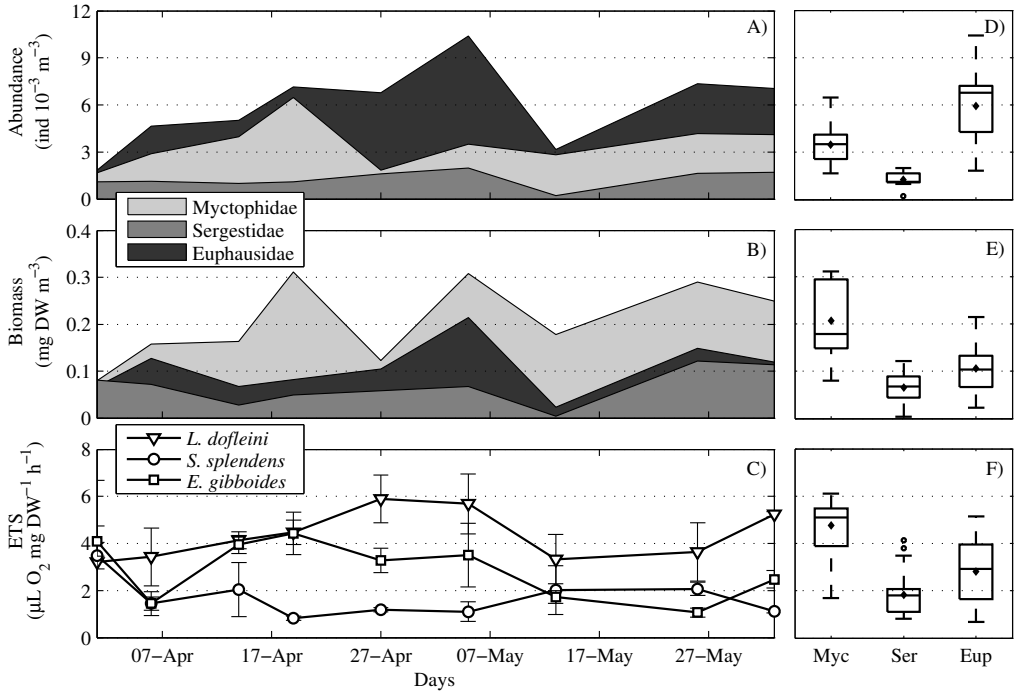

FIGURA 2.5: A la izquierda: serie temporal semanal mostrando (A) abundancia, (B) biomasa y (C) la actividad del sistema de transporte de electrones en tres especies dominantes de migradores verticales del micronecton. A la derecha: los mismos parámetros pero promediados en un gráfico de cajas. En cada caja, los diamantes centrales representan la media, las líneas centrales son las medianas, los límites de la caja son los percentiles 25 y 75, las líneas verticales se extienden hacía los datos más extremos no considerados valores anómalos. Los puntos representan los valores anómalos.

Tabla 2.3 y Figura 2.8). Esto deja patente que no hay razones para seguir excluyendo al micronecton de los cómputos globales de carbono en el océano. Ambos componentes migratorios, zooplancton y micronecton, deben ser rutinariamente muestreados cuando se evalua el flujo activo.

Las trampas de sedimento estimaron un flujo gravitacional de 11.9±5.8 mg C m^{-2} d^{-1} a 150 m de profundidad, estos valores son cercanos a otras estimas realizadas cerca de las Islas Canarias [Neuer et al., 1997, Alonso-González et al., 2010]. Si comparamos con el flujo activo, el zooplancton supuso un promedio del 29 % del flujo gravitacional, que asciende a un 53 % cuando incluimos al micronecton. Nuestras cifras están dentro del rango de valores de Hidaka et al. [2001], que obtuvieron un flujo migratorio total entre el 41 y el 89 % del flujo gravitacional en el Pacífico ecuatorial. También son coherentes con los resultados de Hernández-León et al. [2010], que basándose en mediciones directas sobre el zooplancton y en predicciones de consumo del micronecton en base a las tasas de mortalidad del zooplancton, estimaron un flujo migratorio del mismo orden de magnitud que el gravitacional.

Actualmente la exportación del carbono en el océano, según las mediciones con trampas

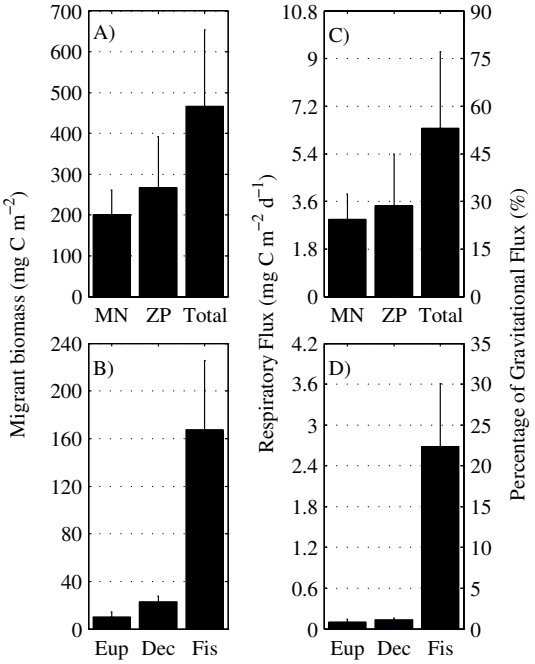

FIGURA 2.8: Izquierda: biomasa migrante (A, B). Derecha: flujo respiratorio. Se muestran mediciones para eufausiáceos (Eup), decápodos (Dec), peces (Fis), micronecton (MN), zooplancton migrador (ZP), y para la suma del micronecton y zooplancton migrador (Total).

de sedimento [Martin et al., 1987, Karl et al., 1996, Neuer et al., 1997], son entre un 30 y 50 % más bajas que lo que se calcula mediante modelos ecosistémicos [Schlitzer, 2002, Falkowski et al., 2003, Usbeck et al., 2003]. De acuerdo con este y otros trabajos que han medido el flujo activo, creemos que la inclusión del zooplancton y el micronecton junto con el flujo gravitacional como mecanismos de exportación de carbono podría mitigar estos desajustes entre las mediciones de campo y los modelos teóricos. En nuestro estudio, la exportación total debido a la sedimentación y a la migración supuso un 5 % de la producción primaria en aguas oceánicas del Atlántico nordeste subtropical.

Capítulo 3: El volcán submarino de la isla de El Hierro, efectos sobre la biota migrante y evolución de las comunidades pelágicas.

Alejandro Ariza, Stein Kaartvedt, Anders Røstad, Juan Carlos Garijo, Javier Arístegui, Eugenio Fraile-Nuez, y Santiago Hernández-León (2014).

Publicado en *PLoS ONE* 9(7):e102354.

Entre el 10 de octubre de 2011 y el 5 de Marzo de 2012 una erupción submarina tuvo lugar 2 km al sur de la isla de El Hierro, a 200 m de profundidad. La pluma volcánica que se extendió en superficie, tuvo consecuencias sobre el proceso de migración vertical, en la distribución de las capas de reflexión profunda, y afectó notablemente a las poblaciones

de plancton y necton alrededor de la isla. En este capítulo, estudiamos los efectos sobre la biota migrante al comienzo de la erupción submarina e hicimos un seguimiento de la evolución del plancton y del necton durante las etapas eruptiva y post eruptiva. Todo ello a partir de observaciones acústicas, muestreo con redes y seguimiento del proceso eruptivo mediante imágenes de satélite (Fig. 3.1 y 3.2).

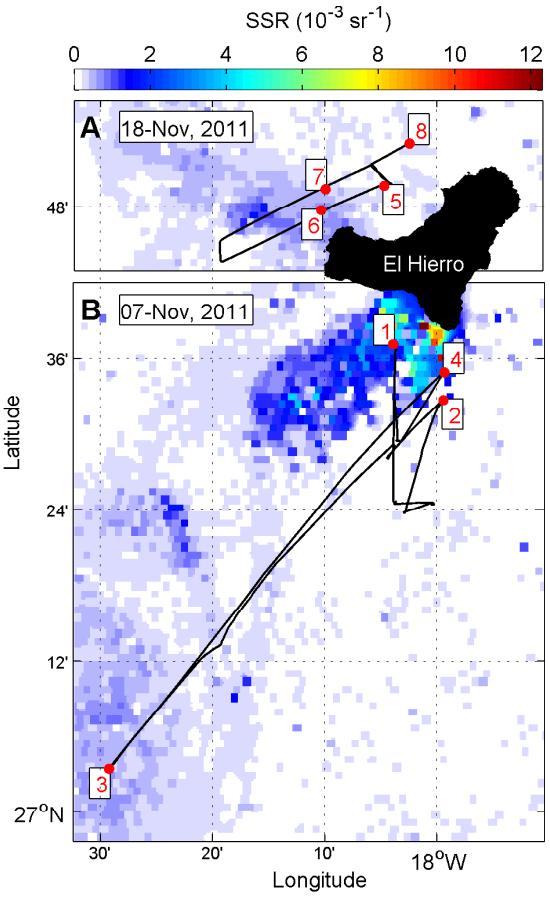

FIGURA 3.2: Reflectancia de la superficie oceánica según datos de satélite, representa el grado de turbidez del agua a consecuencia de la erupción volcánica. Los puntos rojos son estaciones oceanográficas, y las líneas negras ilustran los transectos acústicos que se realizaron entre ellas. Los ecogramas correspondientes a estos transectos y los perfiles de oxígeno de cada estación pueden verse en las Figuras 3.3 y 3.4.

Se observaron dos anomalías acústicas en las zonas donde se extendía la pluma volcánica. Por un lado, la capa migrante en superficie durante la noche se encontraba muy debilitada, y por otro, la capa de reflexión profunda estaba elevada con respecto a su distribución normal en la zona (Fig. 3.3 y 3.4). En algunos lugares donde se extendía la pluma volcánica, estas capas profundas estaban a 200 m de profundidad, mientras que fuera de la zona de afección se situaban a 400 m de profundidad. Esto ocurría tanto de día, como de noche. Cuanto más turbia estaba la superficie como consecuencia del material eruptivo, más se elevaban estas capas de reflexión en la zona mesopelágica (Fig. 3.5).

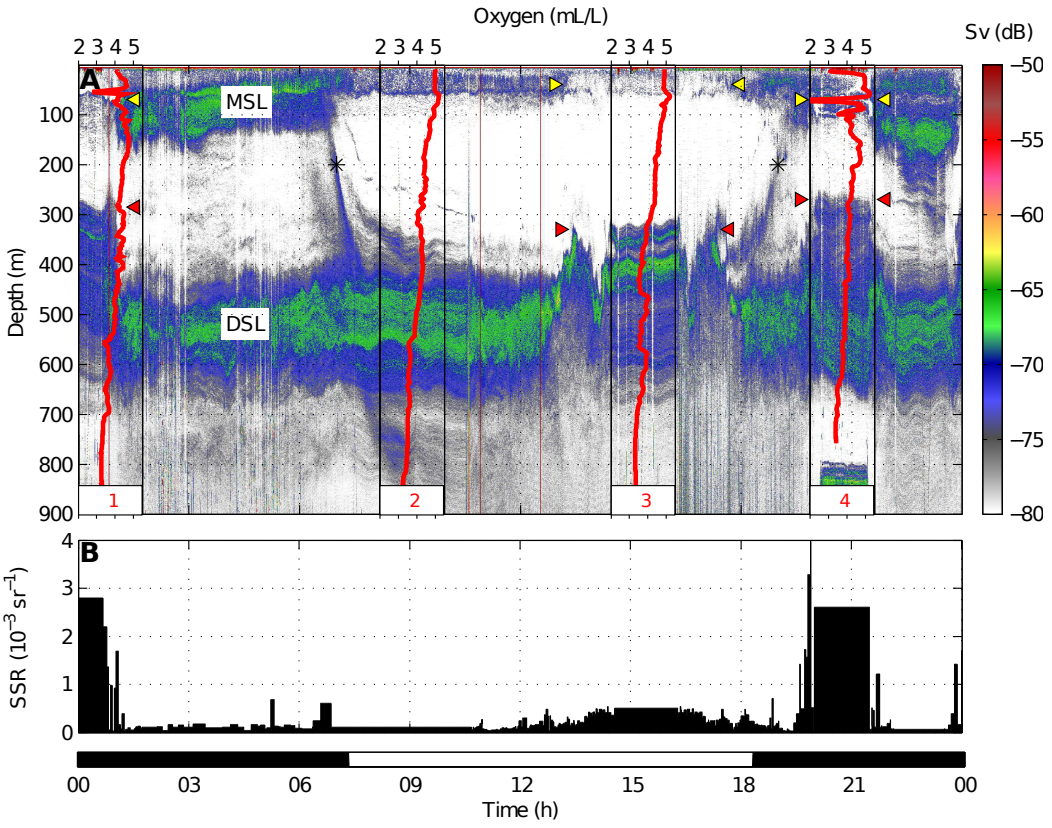

FIGURA 3.3: (A) Ecograma a 38 kHz y (B) Reflectancia de la superficie oceánica. Datos correspondientes al transecto acústico mostrado en la Figura 3.2b. La escala de colores indica el volumen de eco reflejado en decibelios (Sv). Las migraciones entre la capa de reflexión profunda (DSL) y la migrante (MSL) están indicadas con asteriscos. Los indicadores amarillos señalan el debilitamiento de la capa migrante, y los rojos, la elevación de la capa de reflexión profunda. Las líneas rojas muestran los perfiles de oxígeno disuelto en cada estación. Los colores blanco y negro en la escala de 24 h de la parte inferior indican las horas diurnas y nocturnas, respectivamente.

Ambas anomalías acústicas estaban relacionadas con la desoxigenación y el enturbiamiento de las aguas superficiales. Creemos que la interrupción parcial del proceso de migración se debía fundamentalmente a las condiciones de hipoxia y no a la turbidez, dado que existen observaciones donde encontramos solo la primera perturbación, pero la capa migrante también se encontraba muy debilitada. Debido a que la densidad acústica de los migradores en aguas someras menguó aproximadamente un 70 %, y que por el contrario, aumentó un 40 % en la zona mesopelágica, creemos que parte de los migradores permanecían en aguas profundas durante la noche para salvaguardarse de las perturbaciones causadas en superficie por la erupción. El 30 % restante probablemente murieran por los efectos del volcán, así lo indicaban también las numerosas especies mesopelágicas que se encontraron muertas en superficie durante el proceso eruptivo.

El efecto de elevación de la capa de reflexión profunda parece que tuvo que ver con el enturbiamiento del agua más que con las condiciones de hipoxia, ya que encontramos

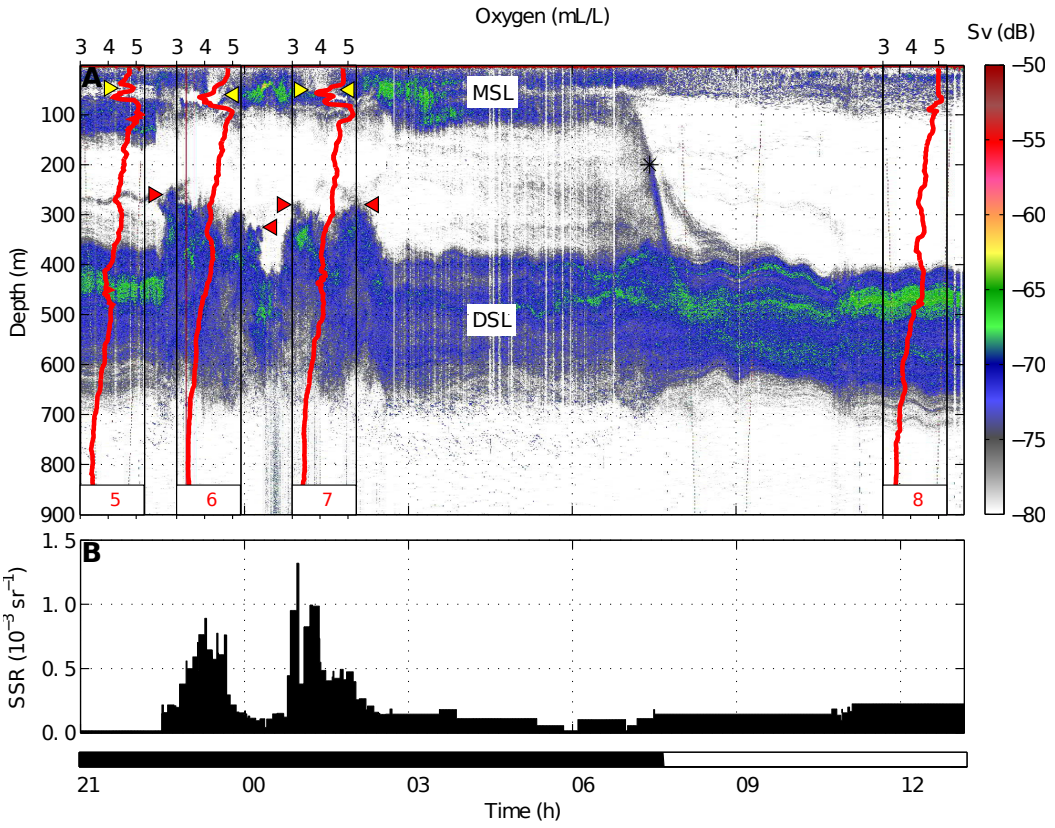

FIGURA 3.4: (A) Ecograma a 38 kHz y (B) Reflectancia de la superficie oceánica. Datos correspondientes al transecto acústico mostrado en la Figura 3.2a. La escala de colores indica el volumen de eco reflejado en decibelios (Sv). Las migraciones entre la capa de reflexión profunda (DSL) y la migrante (MSL) están indicadas con asteriscos. Los indicadores amarillos señalan el debilitamiento de la capa migrante, y los rojos, la elevación de la capa de reflexión profunda. Las líneas rojas muestran los perfiles de oxígeno disuelto en cada estación. Los colores blanco y negro en la escala de 24 h de la parte inferior indican las horas diurnas y nocturnas, respectivamente.

zonas donde esto ocurría en situaciones con concentraciones normales de oxígeno, pero con la superficie notablemente turbia. Esto no es de extrañar, pues las partículas en suspensión en el agua tienen un marcado efecto en la atenuación lumínica en la columna de agua, y esto último, sabemos que afecta a la distribución vertical de la biota mesopelágica [Dickson, 1972, Roe, 1983]. Por ejemplo, Kaartvedt et al. [1996] encontró que las capas mesopelágicas de reflexión acústica se encontraban por encima de su distribución normal en zonas con mayor producción, algo que atenuaba la luz entrante en la columna de agua. De un modo similar, Sassa et al. [2010] observó que en zonas con sedimentos suspendidos, había especies de mictófidos que habitaban en agua más superficiales.

El proceso de migración se ha relacionado normalmente con variaciones lumínicas que ocurren de manera programada a lo largo del día (e.g., anochecer y amanecer), por lo que siempre ha sido difícil diferenciar entre si el proceso esta gobernado por ritmos endógenos ajustados a los cambios diarios de luz, o si esta controlado por la luz per se [Neilson y

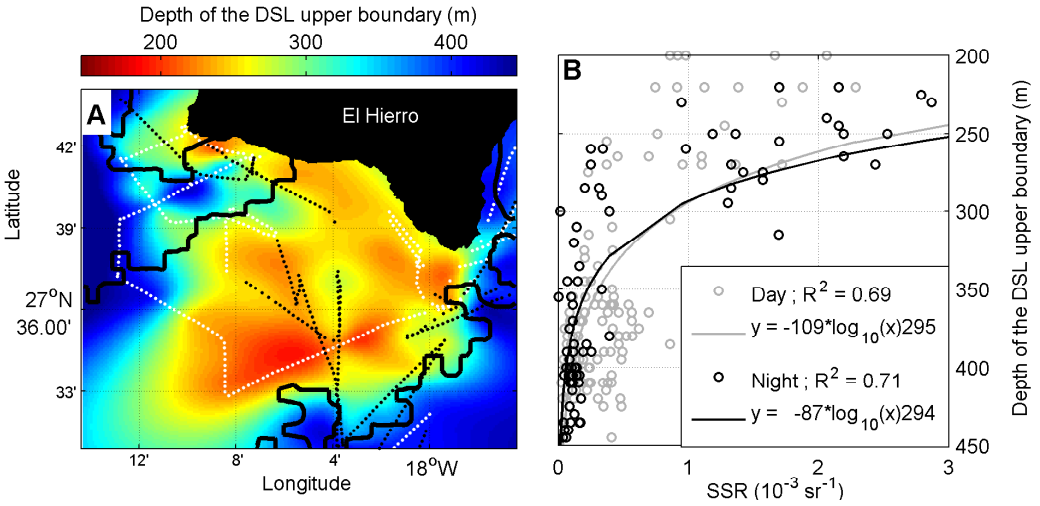

FIGURA 3.5: (A) Profundidad de la capa de reflexión profunda en las inmediaciones de la erupción volcánica. Los puntos indican la posición de los datos reales (blancos = diurnos; negros = nocturnos), mientras que la escala de color muestra los valores interpolados. La línea negra representa el contorno externo de la zona de extensión de la pluma volcánica. (B) Relación entre la profundidad de la capa de reflexión profunda y la reflectancia de la superficie oceánica. Los círculos grises y negros son datos colectados durante el día y la noche, respectivamente. La líneas sólidas representan curvas logarítmicas ajustadas a los datos.

Perry, 1990]. El valor de las observaciones del presente estudio reside en que el efecto de sombra de la pluma volcánica ocurría de un modo impredecible, no programado en el tiempo. Sin embargo la biota mesopelágica reaccionaba igualmente. Esto sugiere que la luz en sí es el principal estímulo que desata la migración y no los ritmos endógenos.

En cuanto al significado de estas elevaciones no programadas, creemos que se trata de un comportamiento oportunista. Se conoce que los animales planctívoros incrementan sus posibilidades de alimentación conforme se acercan a superficie, pues las densidades de zooplancton son mucho mayores allí. Sin embargo, el riesgo de ser predado también es mayor cerca de superficie que en aguas profundas. En este sentido, se ha hipotetizado que el anochecer y el atardecer ofrece unos niveles intermedios de luminosidad, donde el riesgo de mortalidad respecto al éxito de alimentación alcanza valores mínimos. Esto es lo que se conoce como "ventanas antipredatorias", ocurriendo dos veces al día en condiciones normales, una al anochecer y otra al amanecer [Clark y Levy, 1988]. Creemos que el enturbiamiento fortuito de la superficie del agua ofrecía un tiempo extra de ventana antipredatoria y que este era aprovechado por los migradores. Este tipo de comportamiento también ha sido sugerido en casos en los que el florecimiento de algas en superficie producían ensombrecimientos fortuitos en el mar [Kaartvedt et al., 1996, 2012a]. Así, de ser cierta esta hipótesis, este efecto del volcán constituiría más una oportunidad que un perjuicio.

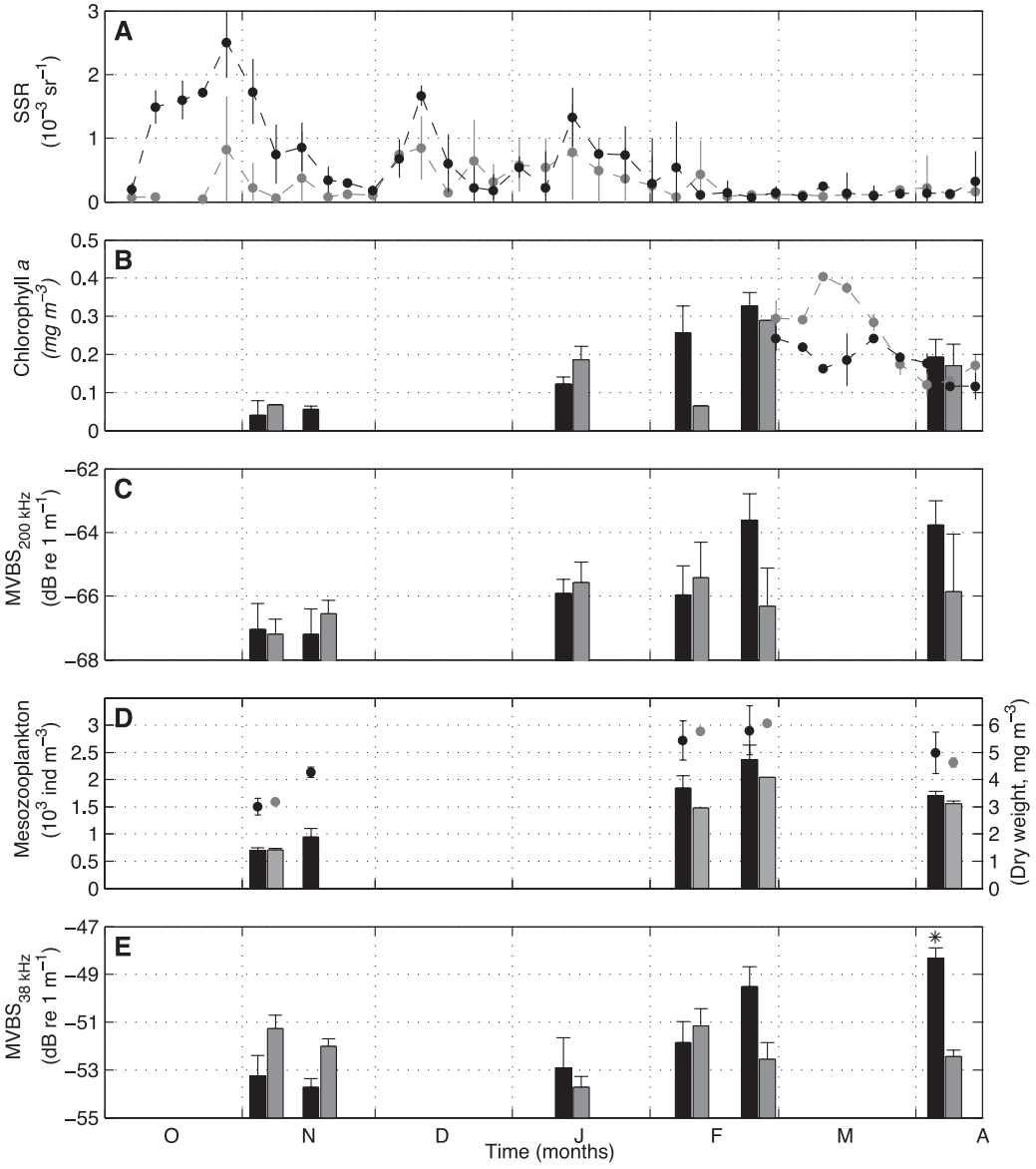

FIGURA 3.7: Serie temporal con parámetros promediados dentro (negro) y fuera (gris) de la zona de afección volcánica. (A) Evolución de la reflectancia de la superficie oceánica, como indicador de turbidez en el agua. (B) Concentración de clorofila *a* obtenida *in situ* (barras) o por satélite (puntos), como indicador de la densidad de fitoplancton. (C) Densidad acústica a 200 kHz, como indicador de la biomasa de mesozooplancton. (D) Abundancia (barras) y peso seco (puntos) de mesozooplancton. (E) Densidad acústica a 38 kHz, como indicador de biomasa de micronecton migrador.

Los indicadores acústicos, satelitales, las muestras de agua y las pescas con redes, mostraron que las comunidades planctónicas y el micronecton migrador estaban notablemente mermados durante la fase más agresiva del volcán, que aconteció entre octubre y noviembre. Una vez finalizado el proceso eruptivo en Febrero, todas estas poblaciones se recuperaron muy rápidamente, aunque con densidades dentro del rango normal que existe en esta época del año al sur de las Islas Canarias (Fig. 3.6 y 3.7). Por ello se considera

que tras la erupción el ecosistema se restauró, no existiendo sin embargo ninguna evidencia de que los nutrientes vertidos por el volcán tuvieran un efecto fertilizante que indujeran a una sobreproducción planctónica.

Capítulo 4: Variabilidad de la fauna mesopelágica profunda inducida por remolinos.

Alejandro Ariza, Javier Arístegui, Pablo Sangrà, Bàrbara Barceló-Llull, y Santiago Hernández-León.

En preparación.

El Archipiélago Canario actúa como una barrera frente a la corriente de Canarias que fluye hacia el suroeste. En consecuencia, se generan remolinos a nivel de mesoescala (∼100 km) al sur de las islas que incrementan la variabilidad hidrográfica y producción biológica de una zona en principio considerada como oligotrófica [Barton et al., 2004, Neuer et al., 2007]. En los estadíos más tempranos, los remolinos ciclónicos bombean aguas profundas y ricas en nutrientes aumentando la productividad en superficie. Los remolinos anticiclónicos, sin embargo, acumulan aguas superficiales en el centro sin incrementar la producción primaria [Arístegui y Montero, 2005]. En estadíos más maduros, el estrés por viento también puede causar hundimientos o afloramientos en ciclones y anticiclones, respectivamente, invirtiendo el papel de estas estructuras en cuanto a la productividad [McGillicuddy et al., 2007]. Los anticiclónicos a su paso por las islas, o al contactar con filamentos que provienen del afloramiento africano, son capaces de retener aguas ricas en fitoplancton y zooplancton [Arístegui et al., 1997, Hernández-León et al., 2001, Yebra et al., 2005, Landeira et al., 2010]. Por otra parte, estudios de avistamientos y marcado también muestran que los remolinos son zonas de alimentación para depredadores de alto nivel, como aves marinas, atunes, focas y ballenas [Kai y Marsac, 2010, Woodworth et al., 2012, Bertrand et al., 2014, Cotté et al., 2015].

Todo esto indica que los remolinos son capaces de catalizar la energía desde los productores primarios, hasta el final de la cadena alimenticia. Sin embargo, se sabe muy poco sobre el papel que juegan los niveles tróficos intermedios como el micronecton. Existen estudios con redes, y de limitada resolución espacial, que indican que los remolinos afectan a la composición de peces y decápodos [Brandt, 1983, Griffiths y Wadley, 1986]. Pero no se sabe cómo estos animales ajustan su distribución a la forma del remolino. Esto requeriría otro tipo de muestreo capaz de resolver eficientemente las estructuras de mesoescala. Por ejemplo, las ecosondas de baja frecuencia montadas en barcos son capaces resolver estructuras de animales de cientos de kilómetros en unas pocas horas, con resoluciones horizontales y verticales de metros [Godø et al., 2014].

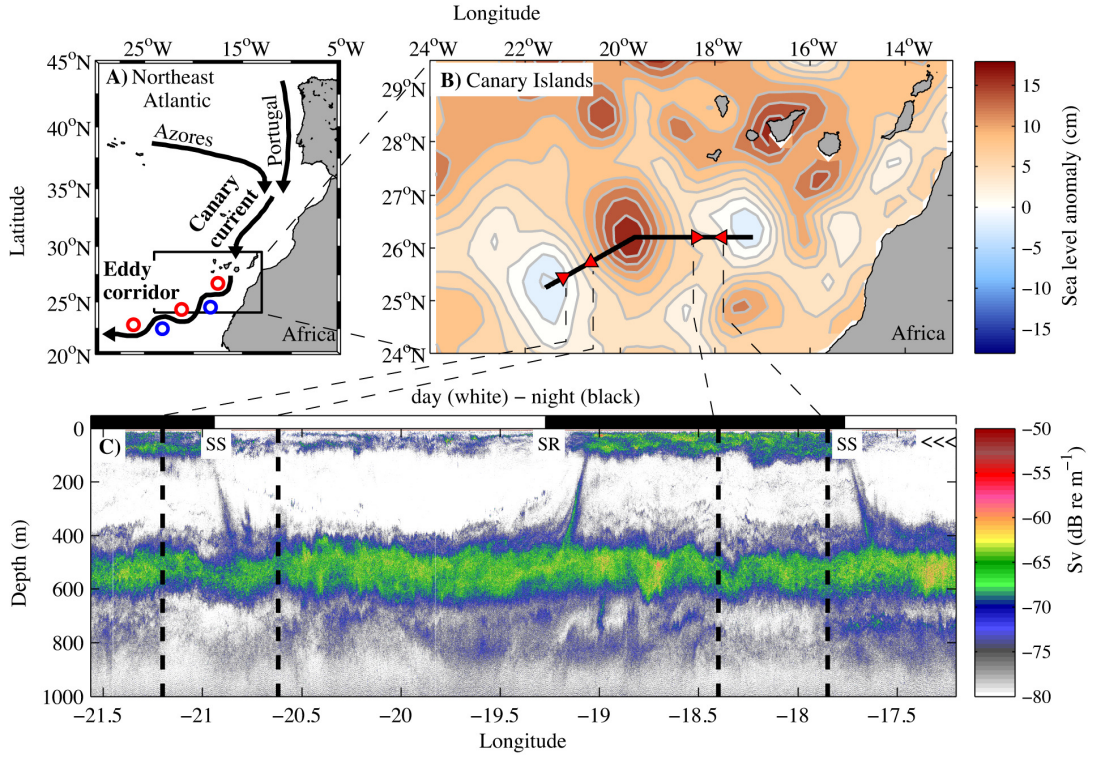

FIGURA 4.1: (A) Esquema de la corriente y el corredor de remolinos de Canarias. (B) Anomalía del nivel del mar mostrando el remolino anticiclónico objeto de estudio (26°N-20°O) y dos remolinos ciclónicos a ambos lados. La línea negra indica el transecto acústico, realizado de este a oeste. (C) Ecograma a 38 kHz mostrando anomalías en la capa situada entre 700 y 900 m de profundidad. La localización de estas anomalías se indican con triángulos rojos en el panel superior derecho. El blanco y negro encima del ecograma indica el día y la noche, respectivamente. SR y SS significan amanecer y anochecer, respectivamente. Los ángulos en fila indican la dirección de grabado.

En este trabajo, se combinan medidas hidrográficas y acústicas *in-situ* con imágenes satélite para investigar, por primera vez, las interacciones entre el micronecton y los remolinos en las Islas Canarias. La estructura tridimensional de las capas acústicas ha sido estudiada seccionando sistemáticamente un remolino anticiclónico desde superficie hasta 1000 m de profundidad con una ecosonda de 38 kHz. Los registros acústicos son posteriormente traducidos a grupos animales específicos en base a descripciones previas de las capas acústicas en la región.

Nuestros resultados muestran anomalías acústicas en capas animales que se extienden entre los 700 y 900 m de profundidad, y que acontecen sistemáticamente en torno a los bordes de los remolinos (Fig. 4.1 y 4.2). Estas anomalías definen tres regiones diferentes en torno al remolino anticiclónico objeto de estudio, una dentro del remolino, y dos en los alrededores, al suroeste y al nordeste. Estas regiones muestran perfiles acústicos singulares que indican diferentes comunidades animales (Fig. 4.3).

Las mayor conclusión derivada de nuestros resultados es que los remolinos tienen la capacidad de afectar a animales que habitan hasta 900 m de profundidad, introduciendo un alto grado de parcheamiento de estas comunidades en zonas con gran actividad de mesoescala. Sin embargo, es díficil comprender en qué sentido varían las capas mesopelágicas al cruzar los remolinos.

La variación en los niveles de eco de una determinada capa puede resultar de diferentes abundancias de los mismos organismos, o también puede significar un cambio en la comunidad. Por ejemplo, hay peces de pequeño tamaño que portan vejigas cargadas de gas que producen mucho más eco, en comparación con peces más grandes carentes de gas. También si un decápodo tiene un tamaño cercano a la longitud de onda de una frecuencia determinada, éste reflejará más eficientemente el sonido que sus semejantes más pequeños o más grandes [Kloser et al., 2002, Korneliussen y Ona, 2003, Simmonds y MacLennan, 2005]. De ahí que nuestros resultados no nos permitan saber si la variabilidad acústica inducida por el remolino es causada por diferentes densidades o por diferentes organismos. En este sentido, el muestreo con redes hubiera sido indispensable para resolver esta cuestión.

Si asumimos que la comunidad entre 700 y 900 m era la misma, de nuestros resultados se extrae que la actividad de mesoescala del corredor canario de remolinos es capaz de doblar o triplicar la abundancia de animales a estas profundidades (ver Fig. 4.3). De acuerdo a esta asunción, parece que el micronecton se concentra bajos los remolinos, no importa si ciclónicos o anticiclónicos. O visto de otro modo, que el micronecton se dispersa en los frentes. Esto se ve claramente en la primera sección zonal, o en los transectos sistemáticos al sur del remolino anticiclónico (Fig. 4.1 y 4.2F-J).

Es cierto que el incremento de densidad acústica en la periferia nordeste del remolino anticiclónico contrasta con el resto de observaciones (Fig. 4.2B-E). Creemos que esto debe estar relacionado con la estructura asímetrica del remolino. De acuerdo a Barceló-Llull et al. (in prep.), los campos de velocidad indican que la circulación se acelera en la parte suroeste, y decelera drásticamente al nordeste, estando casi estancada. Por tanto, es de esperar que los organismos planctónicos se dispersen en el suroeste y se acumulen al nordeste. Esto debería incrementar los encuentros entre predadores y presas, aumentando la eficiencia trófica y atrayendo al micronecton.

En cambio, si asumimos que la variabilidad acústica indica la presencia de organismos distintos, hay que tener en cuenta que un mayor nivel de eco no implica necesariamente mayores abundancias. Algunos estudios han propuesto la diferenciación de comunidades entre estructuras de mesoscala basándose en la historia del remolino. Es decir, la oportunidad de atrapar determinadas larvas durante su formación, la interacción posterior con filamentos, o el grado de aislamiento, serían acontecimientos que definirían el tipo

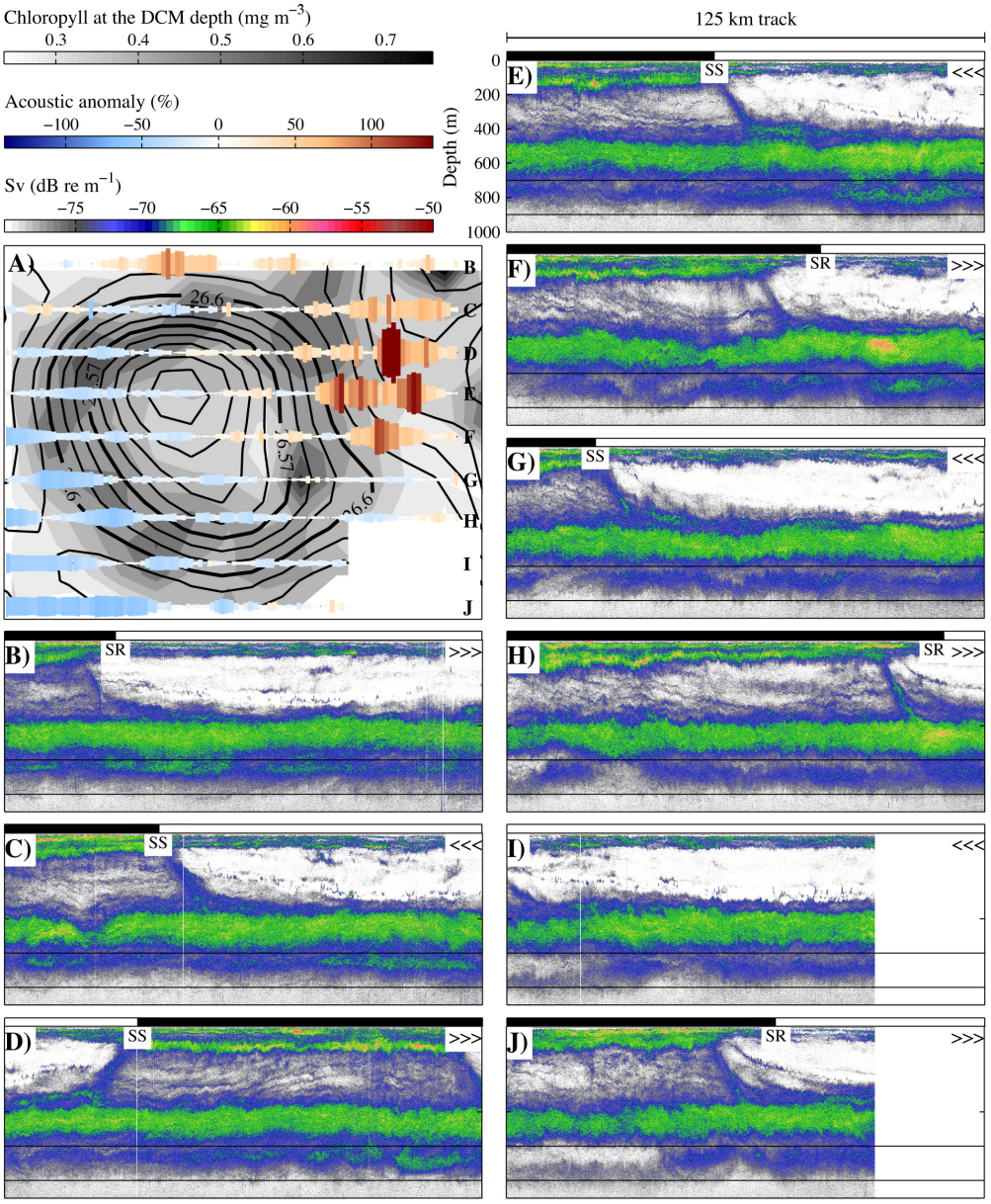

FIGURA 4.2: (A) Estructura del remolino a partir de las anomalías de densidad a 200 m de profundidad (contornos en negro). El fondo en escala de grises muestra la distribución de la clorofila subsuperficial. Las barras en rojo y azul representan anomalías acústicas a 700-900 m, extraídas de 9 transectos acústicos realizados a lo largo del remolino. (B-J) Ecogramas a 38 kHz correspondientes a los 9 transectos acústicos. Las líneas negras horizontales delimitan el rango de profundidad donde se calcularon las anomalías acústicas del panel A. El blanco y negro encima del ecograma indica el día y la noche, respectivamente. SR y SS significan amanecer y anochecer, respectivamente. Los ángulos en fila indican la dirección de grabado.

de comunidad que porta cada remolino [Brandt, 1983, Griffiths y Wadley, 1986, Lobel y Robinson, 1988, Muhling et al., 2007].

Nuestros resultados impiden saber si el parcheamiento observado corresponde a una productividad variable que afecta a la biomasa del micronecton, o simplemente refleja comunidades específicas de los remolinos. Lo que parece claro es que esta interacción

entre el micronecton y los remolinos debe ocurrir cerca de superficie durante la noche, mediante la migración vertical que estos animales realizan diariamente (Ariza et al., in prep.). Sería imposible de otro modo teniendo en cuenta que los remolinos difícilmente alcanzan los 400 m de profundidad [Arístegui et al., 1994, Sangrà et al., 2009], y que este en particular apenas llegaba a los 300 m (Barceló-Llull et al., in prep.). Los gradientes físicos de los remolinos deben directamente moldear la distribución del micronecton mientras están cerca de superficie, o tal vez la interacción ocurre por vía trófica, *e.g.*, el micronecton siguiendo parches de presas que se distribuyen de acuerdo la estructura de los remolinos.

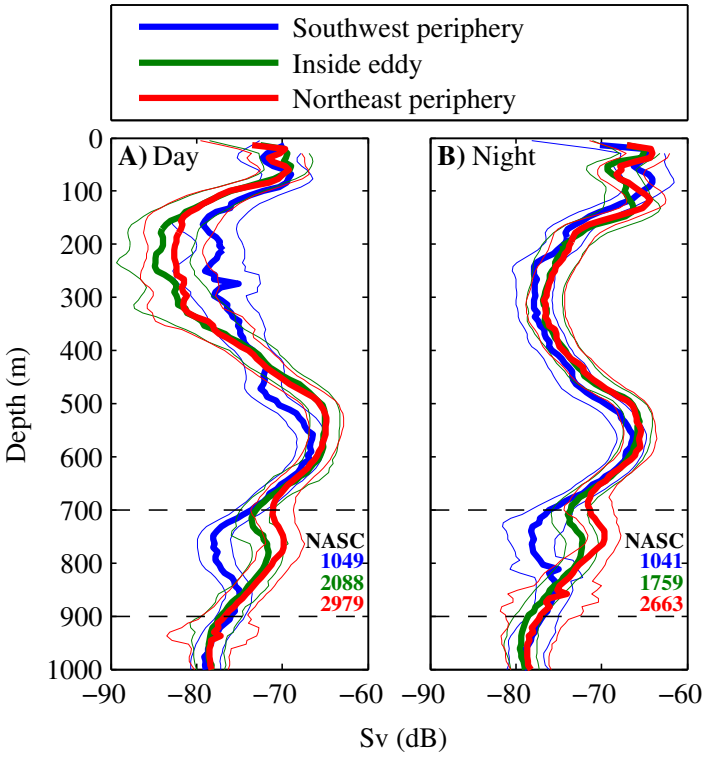

FIGURA 4.3: Perfiles acústicos diurnos (A) y nocturnos (B) a 38 kHz, promediados en la zonas suroeste (azul), noreste (rojo) y dentro del remolino (verde). Se consideraron zonas externas del remolino aquellas fuera de la isopicna 26.60 kg m^{-3}. El interior del remolino fue acordado como la región dentro de la isopicna 26.57 kg m^{-3} (ver Fig. 4.2a). Las líneas gruesas y finas representan el promedio y la desviación estándar, respectivamente. También se indica para cada perfil el área total de sonido integrada desde 700 a 900 m de profundidad (NASC).

Nuestras observaciones tienen poco que ver con el único estudio similar hecho hasta la fecha en aguas oceánicas entre Islandia y Noruega [Godø et al., 2012]. En este trabajo, las capas acústicas también se ajustaban con precisión a la forma de remolinos anticiclónicos, pero la estructura era muy distinta. Además, el remolino estudiado en el presente trabajo ha mostrado complejas características físicas y biogeoquímicas que no se habían descrito anteriormente (Arístegui et al., in prep.; Barceló-Llull et al., in prep.). Todo ello sugiere que los remolinos deben comportarse como ecosistemas únicos

con comunidades singulares, desde los productores primarios hasta los depredadores de alto nivel.

No obstante, los mecanismos mediante los cuales los remolinos afectan a las comunidades animales profundas siguen siendo materia de debate. Abordar estas cuestiones en el futuro requerirá estudiar los remolinos desde su nacimiento hasta la decadencia, usando paralelamente medios acústicos y muestreos con redes.

Síntesis y discusión

Migración vertical estratificada, flujo activo estratificado

La cuestión del flujo activo se ha abordado tradicionalmente como la cantidad de carbono exportado por debajo de la capa fótica, asumiendo una única vía migratoria y desatendiendo la magnitud y la extensión de este transporte más allá de esta profundidad. Esta aproximación fue la que seguimos para estimar el flujo activo de carbono en el capítulo 2, al igual que en otros muchos estudios [Longhurst et al., 1990, Steinberg et al., 2000, Hidaka et al., 2001, Davison et al., 2013, Schukat et al., 2013]. Este procedimiento es de utilidad cuando comparamos con las trampas de sedimento, que habitualmente también se sitúan en estas cotas. De este modo, se estima y se compara los aportes de carbono hacia la zona mesopelágica, mediante flujo activo y pasivo. Sin embargo, mientras el flujo pasivo puede estimarse a mayores profundidades, basándose en modelos de atenuación [Suess, 1980, Betzer et al., 1984, Antia et al., 2001], la distribución vertical del flujo activo es, por el momento, difícilmente predecible. Esto se debe a que el flujo activo está gobernado por la migración vertical, un proceso complejo que involucra a una gran variedad de especies, cada una siguiendo diversos patrones migratorios y contribuyendo con diferente biomasa y metabolismo a la exportación de carbono (Capítulo 2). En consecuencia, su evaluación requiere una aproximación que tenga en cuenta a todos los grupos migratorios y sus particularidades. Esto hará posible obtener perfiles verticales fiables que reflejen las entradas de carbono a lo largo de la columna de agua.

A pesar de esto, es ampliamente aceptado que la mayoría de los flujos migratorios concluyen aproximadamente en medio de la zona mesopelágica (400-700 m) ya que, de acuerdo con las observaciones realizadas con técnicas acústicas convencionales, allí es donde aparecen la mayoría de las capas de reflexión acústica (ver introducción general). Las ecosondas a 38 kHz, frecuencia estándar para la evaluación de peces mesopelágicos, refleja fielmente esta distribución en aguas oceánicas [Kloser et al., 2009, Irigoien et al., 2014]. Sin embargo, como se muestra en el capítulo 1, los ecogramas a 18 kHz y los arrastres profundos también revelan capas y migraciones más allá de los 700 m de profundidad, incluyendo peces, decápodos y cefalópodos (ver tambiíen Fig. S1a). De hecho, los estudios que han considerado a toda la comunidad mesopelágica subrayan que prácticamente toda la columna de agua está habitada por animales migradores [Domanski, 1984], independientemente de si son visibles o no a determinadas frecuencias acústicas.

La amplitud de las migraciones son importantes ya que cuanto más profundo se exporta el carbono, más difícil es que vuelva a superficie por procesos puramente físicos. Por ejemplo, se sabe que los remolinos ciclónicos pueden aflorar aguas de hasta 400 o 700 m de profundidad [Arístegui et al., 1994, González-Dávila et al., 2006, Sangrà et al., 2007].

Además, aproximadamente a partir de los 600 m es donde empiezan las aguas intermedias [Hernández Guerra et al., 2001, Machín y Pelegrí, 2009], que tienen una circulación más lenta y, por tanto, afloran y se ventilan con la atmósfera con menor frecuencia. De acuerdo a esto, las migraciones por debajo de los 600-700 m de profundidad deberían ser consideradas como un proceso de secuestro de carbono mucho más efectivo que las que son más someras. Por esta razón, la amplitud y la magnitud de las migraciones deberían ser un asunto de primer orden en la evaluación de la bomba biológica.

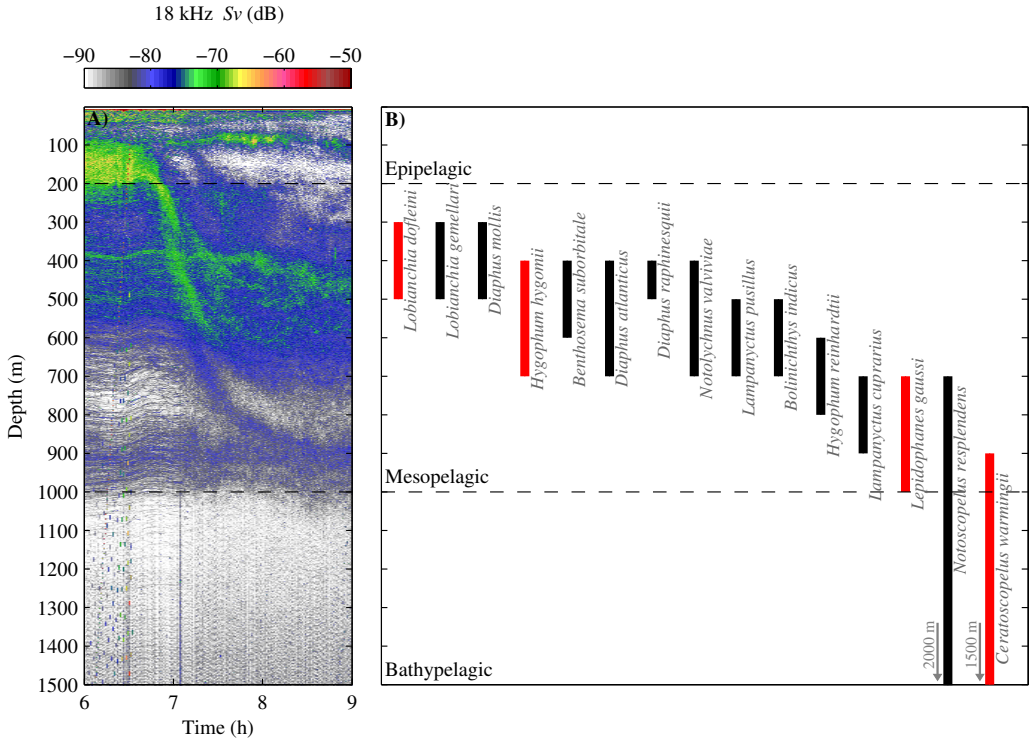

FIGURA S1: (A) Descenso al amanecer de la capa de reflexión acústica a 18 kHz. *Sv* es el volumen de eco reflejado en decibelios. (B) Distribución vertical de peces durante el día de acuerdo con Badcock y Merret [1976]. Las especies que más contribuyen a la biomasa migrante están señaladas en rojo, de acuerdo a los resultados en el capítulo 1.

Flujo activo más allá de los 1000 m de profundidad

Además de lo comentado en la sección anterior, existen indicios que indican que el flujo activo podría estar operando de un modo substancial incluso dentro de la zona batipelágica, donde el carbono queda secuestrado por cientos de años [Lampitt y Antia, 1997, Koppelmann y Frost, 2008]. Badcock y Merret [1976] realizaron el perfil de peces de más alta resolución vertical y más profundo que se conoce hasta la fecha (Fig. S1b). En este estudio documentaron que *Ceratoscopelus warmingii* y *Notoscopelus resplendens* (peces linterna de gran tamaño, Myctophidae) habitaban aguas batipelágicas durante el día. Estas son las mismas especies que se encontraban ausentes a horas similares en los

lances mesopelágicas del capítulo 1. De acuerdo con nuestros cálculos, solo *C. warmingii* supone un 30 % de la biomasa migrante de peces en nuestra zona de estudio (ver Tabla 1.1). La biomasa por especies no es un dato que abunde en estudios de aguas profundas, pero otros trabajos en la región también destacan a *C. warmingii* como un pez dominante en las capas nocturnas de migración, de acuerdo a sus resultados de abundancias [Badcock, 1970, Bordes et al., 2009, Wienerroither et al., 2009]. Si asumimos nuestros cálculos de biomasa, la migración vertical de *C. warmingii* implicaría que una cantidad considerable de carbono se estaría incorporando diariamente en aguas batipelágicas. Posteriormente, Kinzer y Schulz [1985] mostraron que otras especies de mictófidos también realizaban grandes migraciones. Se basaban en las mismas colecciones usadas por Badcock y Merret [1976], y otras muestras obtenidas en el *RSS Discovery* a lo largo del Atlántico Norte. De acuerdo con sus resultados, varias especies de *Lampanyctus* también habitaban cerca o más allá de los 1000 m de profundidad durante el día (además de *C. warmingii* y *N. resplendens*). Kinzer y Schulz [1985] también confirmaron las grandes migraciones de estos peces gracias al hallazgo de presas que habitan en superficie dentro de sus contenidos estomacales. Todo esto sugiere que la biomasa migrante que entra dentro de la zona batipelágica podría ser mayor de lo que se contemplaba hasta ahora en la oceanografía biogeoquímica.

Sin embargo, ninguno de los ecogramas registrados en esta tesis ha podido detectar estas migraciones profundas (véase el ejemplo en la Fig. S1a). Esto se debe, primero, a que el ruído de fondo a 38 kHz impide detectar organismos más allá de los 1000 metros de profundidad [Korneliussen, 2000], y segundo, porque aunque a 18 kHz se alcanza mayor profundidad, hay razones para creer que las especies implicadas en esta migración no serían sensibles a esta frecuencia. Entre otras, el cambio de resonancia en profundidad, el atrofiamiento de la vejiga natatoria en peces grandes, y también la relación entre la señal acústica y volumen de agua muestreado, que a estas profundidades estaría por debajo del límite de detección de las ecosondas (ver discusión en el capítulo 1).

Hay sin embargo evidencias de que las migraciones de más de 1000 m documentadas por Badcock y Merret [1976] no son un hecho aislado. En primer lugar, *Ceratoscopelus warmingii* y *Notoscopelus resplendens* se extienden más allá de los 40°N y los 40°S [Froese y Pauly, 2014]. También existen otros mictófidos batiales que ocupan nichos ecológicos similares en todos los océanos del mundo. Por ejemplo, Burghart [2006] encontró que las especies grandes de mictófidos del Golfo de Méjico también habitan más allá de los 1000 m de profundidad, junto con decápodos migradores. En segundo lugar, hay registros acústicos de perfiladores de corrientes (ADCP, de 67-75 kHz) que también detectan movimientos migratorios cerca de los 1200 m de profundidad, tanto en el Atlántico como en el Pacífico [ver Fig. S2; Plueddemann y Pinkel, 1989, Ochoa et al., 2013, van Haren, 2007, van Haren y Compton, 2013]. Por desgracia, sin muestras biológicas es

imposible asegurar la naturaleza de estas migraciones. En el caso de Plueddemann y Pinkel [1989], atribuyeron este fenómeno a una gran variedad de especies, incluyendo zooplancton y necton. Otros autores asumían que la señal migratoria estaba causada por zooplancton. La asignación de qué especies son las responsables no es un asunto trivial. Por ejemplo, si aparte de otros organismos, *C. warmingii* está involucrada, esto supondría que la especie que más contribuye a la biomasa migrante estaría realizando migraciones verticales directas, desde superficie hasta la zona batipelágica. Las consecuencias para el flujo activo serían que una cantidad considerable de carbono estaría alcanzando aguas batiales sin que existieran pérdidas derivadas de migraciones conectadas tróficamente, como el modelo de "Escalera de migraciones" o la "Brigada de cubos" [Vinogradov, 1962, Ochoa et al., 2013].

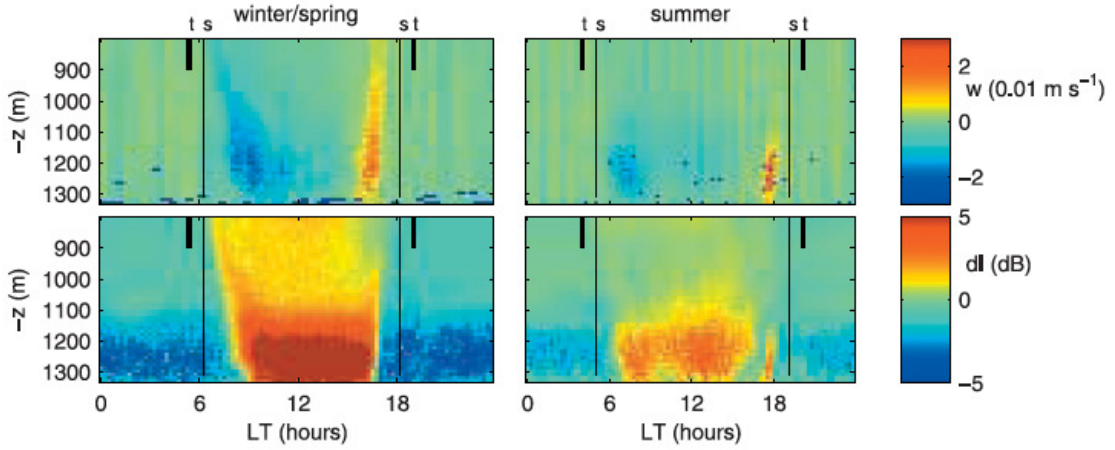

FIGURA S2: Velocidades verticales (w) y anomalías de eco (dl) en aguas batipelágicas de la Cuenca de Canarias. Invierno-primavera a la izquierda y verano a la derecha. "t" indica las horas del crepúsculo, y "s" se refiere al amanecer y atardecer. Extraído de van Haren [2007].

Otro indicio que apoya que el flujo activo podría operar substancialmente más allá de los 1000 m puede extraerse de los perfiles de carbono orgánico particulado (POC). Durante una campaña oceanográfica, Alonso-González et al. [2009] encontró estos compuestos desplazándose lateralmente en capas repartidas entra las zonas mesopelágicas y batipelágicas de la corriente de Canarias. Cada vez que se detectaba un pulso de carbono orgánico entre 500 y 700 m de profundidad, cerca de la capa de reflexión profunda, aparecía una réplica en torno a los 1200 m de profundidad (ver figuras 2 y 6 de ese estudio). Esta última señal aparecía en el rango de profundidad y en la misma región oceanográfica donde tanto los muestreos con redes como los registros de ADCP muestran actividad migratoria. Alonso-González et al. [2009] propusieron diferentes fuentes de carbono que alimentara estas capas, bien que provinieran de los márgenes continentales, o mediante diversos procesos de mesoescala. Puesto que existe también una importante actividad migratoria cerca de los 1200 m de profundidad, es plausible que la migración fuera otro

mecanismo que introdujera carbono en aguas batiales. El "puenteo" del flujo de partículas mediante migradores interzonales es una idea que ya se ha propuesto en el pasado para explicar los picos de carbono orgánico en aguas mesopelágicas [Steinberg et al., 2000, Alonso-González et al., 2013]. Aquí se propone el mismo mecanismo, pero más allá de los 1000 m de profundidad. De acuerdo a este nuevo planteamiento, los modelos biogeoquímicos para el océano profundo deberían ser revisados, ya que hasta la fecha, el flujo activo no se ha considerado más allá del dominio mesopelágico [Koppelmann y Frost, 2008, Arístegui et al., 2009, Robinson et al., 2010, Passow y Carlson, 2012]. En base a esto, la presente tesis propone un nuevo modelo biogeoquímico que incluye al zooplancton y al necton, en el dominio mesopelágico y más allá (see Fig. S3).

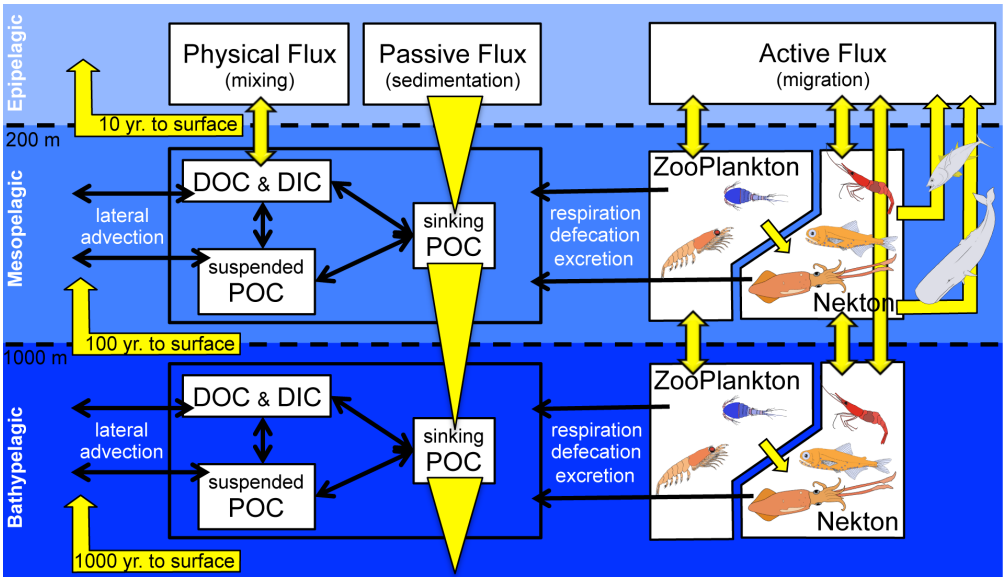

FIGURA S3: Nuevo esquema de la bomba oceánica de carbono. Adaptado de Arístegui et al. [2009] y de Passow y Carlson [2012], con flujos migratorios establecidos de acuerdo a las propuestas de la presente tesis. El carbono orgánico e inorgánico disuelto (DOC y DIC) en superficie se exporta a aguas profundas mediante procesos físicos (mezcla), mientras que el carbono orgánico particulado (POC) se exporta vía flujo pasivo (sedimentación). Una vez en aguas profundas, los procesos biológicos convierten las partículas que se hunden en compuestos de carbono suspendidos o disueltos que son susceptibles de transportarse lateralmente. De este modo se disminuye la tasa de hundimiento de las partículas. Sin embargo, estas reservas de carbono también se incrementan mediante el flujo activo de los migradores verticales. Este mecanismo refuerza el flujo pasivo por el aporte de heces en profundidad (defecación), pero también libera carbono disuelto inorgánico (respiración) y orgánico (excreción). Los migradores son capaces de transportar carbono en zonas mesopelágicas y batipelágicas, pero mientras el flujo mediado por el zooplancton en aguas batiales operaría mediante migraciones tróficamente conectadas, el flujo del necton también podría hacerlo mediante migraciones directas. Los depredadores de alto nivel pueden también delvolver carbono a la superficie cuando se alimentan en la zona mesopelágica y después respiran, defecan y excretan en aguas superficiales. Al flujo fuera de la zona epipelágica se le denomina "flujo exportado" (de 10 a 100 años para que se ventile en la atmósfera), mientras que al flujo más allá de la capa mesopelágica se conoce como "flujo secuestrado" (de 100 a 1000 años antes de aflorar a superficie).

Flujo pasivo, zooplancton y micronecton: hacia un enfoque holístico

La importancia del micronecton no solo se basa en la magnitud de sus migraciones (ver sección anterior), sino también en su contribución a la biomasa migrante y su particular fisiología. En el capítulo 2 subrayábamos que la biomasa migrante del zooplancton y el micronecton eran bastante similares, pero que el flujo del tracto digestivo del micronecton podría ser más efectivo debido a que sus tasas de evacuación son más lentas y a que sus heces se hunden más rápido. Todos estos aspectos indican que el micronecton debe jugar un papel de gran importancia en la bomba biológica de carbono, sin embargo, como resumíamos en la Tabla 2.3 (referencias dentro), la mayoría de la investigación sobre el flujo activo se ha dedicado al zooplancton.

La inclusión del micronecton en este trabajo, como mecanismo de flujo activo, ha contribuido al conocimiento de la exportación de carbono en aguas subtropicales del Atlántico, y además reconcilia algunos desequilibrios en los modelos del carbono en el océano. Por ejemplo, previamente a esta tesis, Hernández-León et al. [2010] estimaban que el carbono exportado vía migración estaba dentro del orden de magnitud del flujo gravitacional. Ahora hemos estimado que el zooplancton y el micronecton son capaces de exportar, vía respiración, aproximadamente un 50 % del flujo gravitacional medido a 150 m de profundidad (Capítulo 2). Los máximos de carbono orgánico disuelto y particulado en aguas mesopelágicas y batipelágicas [Arístegui et al., 2003, Alonso-González et al., 2009] también sugieren la intervención de los migradores (ver sección anterior). Por otro lado, las estimaciones globales de carbono exportado, en base a modelos ecosistémicos, son aproximadamente dos veces mayores que lo que miden las trampas de sedimento [Schlitzer, 2002, Falkowski et al., 2003, Usbeck et al., 2003]. Creemos que la inclusión del carbono exportado por parte del zooplancton y el micronecton, además del aportado por el fujo gravitatorio, podría reducir estos desajustes.

Estudios muy recientes están destacando el papel de los peces [Davison et al., 2013, Hudson et al., 2014] y decápodos [Podeswa, 2012, Schukat et al., 2013] en la exportación de carbono, pero hasta la fecha, solo el trabajo de Hidaka et al. [2001] en el Pacífico ecuatorial y la presente tesis en el Atlántico nordeste subtropical han evaluado el flujo del micronecton junto con el zooplancton y las partículas. Es necesario que halla estudios holísticos que abarquen todos los mecanismos, tanto pasivos como activos, ya que ambos flujos están interconectados y se retroalimentan entre sí de muchos modos, como cuando los migradores reprocesan o "puentean" el flujo de partículas [Steinberg et al., 2008, Robinson et al., 2010, Alonso-González et al., 2013]. Por tanto, esta tesis aboga por estudios integrativos más que comparativos con el fin de mejorar nuestra compresión de la bomba biológica.

Factores ambientales que afectan al micronecton

Durante el curso de la presente tesis, se tuvo la oportunidad de estudiar reacción de las capas de reflexión acústica ante distintos factores ambientales. Se investigó su comportamiento ante un episodio de erupción submarina, y también a largo de estructuras de mesoscala como los remolinos.

Las densidad, la distribución vertical y el comportamiento migratorio de las capas acústicas alrededor de la Isla de El Hierro se vieron fuertemente afectados por la erupción submarina ocurrida en octubre de 2011 (Capítulo 3). Aspectos que, como explicábamos anteriormente, tienen importantes implicaciones en los intercambios biogeoquímicos entre las capas superficiales y el océano profundo. Temperatura, oxígeno disuelto e irradiación lumínica fueron las principales propiedades oceanográficas que se vieron alteradas durante este evento. Todas ellas identificadas como susceptibles de cambiar en condiciones de calentamiento global [Levitus et al., 2000, Keeling et al., 2010, Stramma et al., 2008], y también como factores importantes que gobierna la migración vertical [Dickson, 1972, Roe, 1983, Watanabe et al., 1999, Bianchi et al., 2013a]. Por tanto, las anomalías observadas durante este episodio volcánico podrían ser de gran valor para predecir cambios futuros en el funcionamiento de los ecosistemas de profundidad.

Por otra parte, otras estructuras más frecuentes en el océano como los remolinos evidenciaron que eran capaces de modelar la distribución del micronecton hasta los 900 m de profundidad. La variabilidad que encontramos en un espacio de estudio tan reducido sugiere que hay un alto grado de "parcheamiento" animal en estos sistemas de mesoscala (Capítulo 4). Así, se debería reconsiderar el papel que los remolinos juegan en los procesos ecológicos y biogeoquímicos del océano, ya que el micronecton esta muy involucrado en la distribución de la materia orgánica y la energía entre aguas superficiales y profundas [Hidaka et al., 2001, Davison et al., 2013, Schukat et al., 2013, Irigoien et al., 2014, Ariza et al., 2015].

Qué factores gobiernan la abundancia, distribución y la migración vertical a escala global es una cuestión de primer orden, debido al creciente interés en desarrollar predictores oceanográficos para el funcionamiento de la bomba biológica en futuros escenarios de cambio climático [Bianchi et al., 2013a,b, Doney y Steinberg, 2013].

Conclusiones

Las principales conclusiones extraídas de la presente tesis son:

1.- Se han identificado cuatro capas acústicas asociadas a diferentes faunas mesopelágicas en las Islas Canarias: (1) a 400-500 m de profundidad, una capa resonante a 18 kHz, principalmente formada por peces migradores que portan gas en la vejiga, como *Viciguerria* spp. y *Lobianchia dofleini*, (2) a 500-600 m, una capa densa a 38 kHz que resulta principalmente de la resonancia de *Cyclothone braueri*, un pez no migrador y portador de gas, y (3) a 600-800 m, una señal débil tanto a 18 como a 38 kHz, atribuida a peces y decápodos migradores.

2.-Se han observado varias vías de migración que conectan las zonas epipelágica y mesopelágica. Las más someras parten entre 400 y 600 m de profundidad y se desplazaban aproximadamente a 4 cm s^{-1}, mientras que las más profundas parten entre 600 y 800 m y se movían a 12 cm s^{-1}.

3.-La contribución del zooplancton y micronecton a la biomasa migrante es muy similar en las Islas Canarias. El principal grupo que contribuye a la migración dentro del zooplancton son estadíos juveniles de eufausiáceos, mientras que el micronecton está principalmente dominado por peces, seguido de eufausiáceos adultos y decápodos.

4.- El flujo respiratorio tanto del zooplancton como del micronecton supone un 82 % (rango 47-166 %) del flujo gravitacional medido a 150 m de profundidad en aguas oligotróficas de la Cuenca de Canarias, siendo el zooplancton el que más aporta (58 %) debido a que tiene una mayor tasa respiratoria. Sin embargo, las migraciones de larga distancia que realiza el micronecton con respecto al zooplancton sugiere que el micronecton debe ser el principal contribuidor al flujo activo en aguas más profundas.

5.-La atenuación lumínica en la columna de agua , debido a turbidez variable en la superficie del mar, afecta considerablemente a la distribución vertical de la fauna mesopelágica. Otras variaciones en superficie, como la temperatura, oxígeno o el pH, también interfieren en el normal funcionamiento de la migración vertical, acortando el ascenso nocturno, y menguando las abundancias de los migradores.

6.-Los remolinos de mesoescala pueden moldear la distribución de animales que habitan hasta los 900 m de profundidad, pese a que estas estructuras difícilmente se extienden más allá de los 400 m. Esto quiere decir que las interacciones entre los remolinos y el micronecton deben ocurrir cerca de la superficie y por la noche, mediante el proceso de migración vertical.

7.-Los remolinos de mesoescala son capaces de introducir un alto grado de parcheamiento en la fauna mesopelágica profunda, con cambios en las capas acústicas que se ajustan con precisión a los márgenes del remolino. Este parcheamiento debe incrementar la variabilidad espacial de los procesos biogeoquímicos en los que está involucrado el micronecton.

Futuras líneas de investigación

De acuerdo a los hallazgos y la revisión de literatura científica durante el curso de la presente tesis, se han identificado las principales restricciones para el avance en materia de migración vertical y flujos de carbono. Estas han sido divididas en tres bloques: (1) subestimación de la biomasa, (2) limitado conocimiento en ecofisiología y (3) escaso monitoreo de los patrones migratorios tanto a largo plazo como a escala global.

La subestimación de la biomasa de animales de natación rápida ha sido siempre motivo de preocupación en la gestión pesquera debido a que en este ámbito se requieren estimaciones muy precisas para el establecimiento de cuotas de pesca adecuadas. Esto es ahora también un asunto de interés en la oceanografía biológica, ya que estudios recientes están poniendo de manifiesto el importante papel que juega el micronecton en las cómputos globales de carbono [Hidaka et al., 2001, Bianchi et al., 2013a, Davison et al., 2013, Schukat et al., 2013, Irigoien et al., 2014, Ariza et al., 2015]. Sin embargo, aunque ambas cuestiones son de vital importancia para la gestión de los océanos, todavía persisten grandes incertidumbres acerca de la precisión de los diferentes equipos de muestreo que se usan para estimar biomasas.

Se han realizado intercalibraciones para muestreadores de micronecton, pero solo en redes rectangulares pequeñas, originalmente diseñadas para muestrear macrozooplancton y estadíos juveniles de peces. Estas redes, además de sesgar las abundancias hacia la fracción más pequeña del micronecton, también pueden mostrar diferencias en las capturas de varios órdenes de magnitud entre sí [Wiebe et al., 2002, Pakhomov et al., 2010]. Las grandes redes de arrastre pelágico son las únicas capaces de muestrear eficientemente a la fracción adulta del micronecton, sin embargo, no existen estándares acerca de las dimensiones, características de las mallas, o procedimientos de muestreo. La estandarización no es solo importante para la comparación entre diferentes estudios, también porque los pocos factores de corrección que existen para redes de arrastre pelágico [Koslow et al., 1997, Kloser et al., 2009, Kaartvedt et al., 2012b] son difícilmente aplicables si las condiciones de muestreo no se pueden reproducir con exactitud.

Por otra parte, los factores de corrección basados en estimaciones acústicas de biomasa también conllevan mucha incertidumbre, debido a que la comunidad migratoria está compuesta por una gran variedad de especies, de diferentes tallas y propiedades acústicas. Esto hace extremadamente difícil estimar con precisión la biomasa [ver Davison et al., 2015]. El uso de instrumentos en multifrecuencia, y un mayor entendimiento de las propiedades acústicas de los animales podrían mejorar nuestra capacidad para discriminar grupos acústicos, y por tanto, calcular mejor la biomasa. El problema es que las altas

frecuencias (>100 kHz) difícilmente cubren más allá de la zona epipelágica cuando están instaladas en el barco.

Por tanto, se requieren dos acciones para realizar estimaciones de biomasa más fiables: Primero, fijar el modelo de red de arrastre y los procedimientos con mayor rendimiento con el fin de establecer un estándar para el muestreo del micronecton, similar a lo que ya se hizo con el zooplancton en los años sesenta [UNESCO, 1968]. Segundo, un mayor desarrollo de instrumentos en multifrecuencia que puedan ser bajados a gran profundidad, junto con una mejora de los modelos de eco que existen para la fauna migradora. Esto permitirá una mayor discriminación de los diferentes grupos acústicos, y estimaciones de biomasa más precisas.

La ecofisiología y el metabolismo del micronecton migrador son unos grandes desconocidos. Esto es particularmente notorio en los peces mesopelágicos ya que es extremadamente difícil mantenerlos con vida en cautividad durante periodos de tiempo suficientemente largos para poder medir sus tasas fisiológicas [Robison, 1973, Torres et al., 1979]. Los crustáceos, por otra parte, han sido objeto de mayor investigación ya que muestran más resistencia a los experimentos *in-vivo*. Aún así la mayoría del conocimiento sobre fisiología y bioenergética de crustáceos está sesgado hacia el zooplancton [Ikeda y Motoda, 1978, Omori e Ikeda, 1984, Ikeda y Kirkwood, 1989, Hernández-León e Ikeda, 2005], siendo muy escasos los modelos metabólicos en decápodos de profundidad [Ikeda, 2013]. Como resultado, es una práctica común usar modelos energéticos generales de peces para calcular carbono exportado por peces mesopelágicos [Davison et al., 2013], o adoptar las tasas metabólicas del zooplancton para estimaciones en decápodos [Schukat et al., 2013].

Además, el parámetro de entrada más usado en modelos bioenergéticos para calcular el resto de tasas fisiológicas es la respiración (R), una medida que es muy difícil de obtener a bordo por la problemática explicada anteriormente. Por esta razón la actividad enzimática del Sistema de Transporte de Electrones (ETS) es un indicador ampliamente usado para la respiración [Packard, 1985, Gómez et al., 1996, Hernández-León y Gómez, 1996]. Desafortunadamente, hay muy pocas relaciones R/ETS para el micronecton migrador en la literatura. Tan solo existe una relación obtenida con peces de coral que se usa para peces mesopelágicos [Ikeda, 1989], y una relación para decápodos migradores del afloramiento de Benguela [Schukat et al., 2013].

Pese a que el uso de estos modelos energéticos y relaciones R/ETS es conveniente ante la falta de mejores soluciones, es evidente que modelos más precisos incrementarían considerablemente la fiabilidad de nuestras estimaciones en los flujos de carbono. Por tanto, se recomiendan especialmente las líneas de investigación que desarrollen modelos metabólicos y relaciones R/ETS específicas para el micronecton migrador. Esto es de

especial importancia en los peces mesopelágicos, ya que ellos son los que más contribuyen a la migración y sus tasas metabólicas son especialmente desconocidas.

El monitoreo de los patrones de migración y la biomasa migrante, tanto del zooplancton como del micronecton son esenciales para comprender los procesos biogeoquímicos en el océano. Varios estudios indican que la migración vertical es susceptible de cambiar con ritmos mensuales, estacionales y anuales [van Haren, 2007, Staby et al., 2011, Wang et al., 2014]. También se han observado variaciones espaciales, de escalas regionales hasta globales [Dickson, 1972, Kaartvedt et al., 1996, Bianchi et al., 2013a]. Además, el proceso de migración es también susceptible de variaciones debido al cambio climático, aunque la naturaleza de estas anomalías es todavía muy discutida [Robinson et al., 2010, Doney et al., 2012, Doney y Steinberg, 2013].

Sin embargo, la evaluación de la migración vertical a estas escalas temporales y espaciales requieren un monitoreo sistemático que no puede ser abordado con los tradicionales buques de investigación. En este sentido, se precisa desarrollar modelos predictivos de migración vertical y biomasa migrante basados en los parámetros oceanográficos que gobiernan a estos organismos, como la temperatura, la luz, el oxígeno o la producción primaria [Bianchi et al., 2013a]. Estas medidas son facilmente accesibles gracias a los satélites que vigilan a diario la superficie del mar y a los atlas oceánicos disponibles en la red. Estos modelos predictivos podrían permitir un seguimiento a largo plazo y a escala global de la migración vertical.

También existe la necesidad urgente de incluir ecosondas e instrumentos ópticos en estaciones oceanográficas permanentes. Esto ayudará a obtener medidas *in-situ* de zooplancton y micronecton, junto con otros parámetros de rutina que se miden normalmente en las grandes series temporales del océano [Karl y Lukas, 1996, Steinberg et al., 2001].

Part V

Appendices

Species abundance raw data from Chapter 1

Species are sorted by fishes (fish), crustaceans (crus) and cephalopods (ceph).

Group	Family	Species	N100p	N105p	N150t	D390t	D400p	D450p	D570t	D600p	D700p	D730t
Fish	Nemichthyidae	*Avocettina infans*										3
		Nemichthys curvirostris			1					1	1	4
		Nemichthys scolopaceus	1	1	2	1						
	Serrivomeridae	*Serrivomer* spp.		2				1	1	7	19	24
	Bathylagidae	*Bathylagichthys greyae*			2							
		Dolicholagus longirostris	4	1	1							15
		Melanolagus bericoides		2								
	Opisthoproctidae	*Opisthoproctus soleatus*										
	Alepocephalidae	*Xenodermichthys copei*										1
	Gonostomatidae	*Bonapartia pedaliota*				2	4	12	4		1	
		Cyclothone braueri						2	26	27	8	
		Cyclothone microdon								4	284	223
		Cyclothone pseudopallida						1	2	3	82	22
		Cyclothone spp.						2				
		Diplophos taenia							1			
		Gonostoma denudatum	17	11						1		
		Gonostoma elongatum	3	44	26				16	36	26	9
		Margrethia obtusirostra	3	5	1	7	2					
	Sternoptychidae	*Argyropelecus aculeatus*	28	37	4	21	9	29	7		1	3
		Argyropelecus gigas									1	1
		Argyropelecus hemigymnus				8	3	3	8	5	2	4
		Sternoptyx diaphana				2				4	26	28
		Valenciennellus tripunctulatus				5	3	12		2	1	
	Phosichthyidae	*Ichthyococcus ovatus*				3	4	1		2		1
		Polymetme corythaeola					3					
		Vinciguerria attenuata	64	184	37	158	23	43	2	7	18	6
		Vinciguerria nimbaria	16	41	4	25	42	17		27	6	3
		Vinciguerria poweriae	19	25	8	33	47	31	1	3		1
	Chauliodontinae	*Chauliodus danae*	8	4					25	39	4	21
		Chauliodus sloani	3	6				7	3	5		5
		Chauliodus spp.								37		
	Stomiinae	*Stomias boa*	6								2	
		Stomias brevibarbatus									1	
		Stomias sp.						1				
	Astronesthinae	*Astronesthes gemmifer*	1								3	1
		Astronesthes indicus	2								1	
		Astronesthes leucopogon										1
		Astronesthes macropogon	2	2	4							
		Astronesthes micropogon	2							4	1	
		Astronesthes neopogon									1	
		Astronesthes niger		1							2	
		Borostomias mononema										
	Melanostomiinae	*Bathophilus brevis*						1				
		Bathophilus nigerrimus		1								
		Bathophilus vaillanti	6		1			4	1	2		
		Chirostomias pliopterus										1
		Eustomias braueri										2
		Eustomias filifer	1	2	1							
		Eustomias obscurus			3						3	1
		Eustomias schmidti		1							1	
		Eustomias spp.		1						1		1
		Eustomias tetranema		1								
		Flagellostomias boureei									1	1
		Melanostomias spp.			1							
		Photonectes dinema	3	2							1	
		Photonectes spp.								2		
	Malacosteinae	*Malacosteus niger*										2
	Malacosteinae	*Photostomias guernei*	11	12	6						16	9
		Photostomias spp.	12							4	2	9
	Idiacanthinae	*Idiacanthus fasciola*	5	6						2	14	3
	Scopelarchidae	*Scopelarchus analis*						3		1	1	
		Scopelarchus michaelsarsi	1									
	Notosudidae	*Ahliesaurus berryi*									5	
		Scopelosaurus spp.	1	2							8	
	Paralepididae	*Lestidiops* spp.		2								
		Paralepis brevirostris								1		
		Sudis hyalina	1	3	1		1					

Continued on next page

Table 4 – *Continued from previous page*

Group	Family	**Species**	**N100p**	**N105p**	**N150t**	**D390t**	**D400p**	**D450p**	**D570t**	**D600p**	**D700p**	**D730t**
	Evermannellidae	*Evermannella melanoderma*									1	2
	Myctophidae	*Benthosema suborbitale*			17				15			
		Bolinichthys indicus	8	25	33				4	3	13	5
		Bolinichthys supralateralis									3	1
		Ceratoscopelus maderensis					1					
		Ceratoscopelus warmingii	324	28	39				1		6	7
		Diaphus brachycephalus	1	2								
		Diaphus dumerilii	1	1	5	3					2	2
		Diaphus effulgens	3							1		
		Diaphus mollis	9	4	1		9	5	4	1	4	
		Diaphus perspicillatus	2		3	5	8	2	4		5	
		Diaphus rafinesquii	6	3	41	36	23	4		2		9
		Diaphus spp.							2			
		Diaphus taaningi					2					
		Diaphus termophilus							4			4
		Diogenichthys atlanticus										
		Gonichthys cocco									1	
		Hygophum hygomii	222	116	25				69	64	2	6
		Hygophum reinhardtii	28	22	45						52	33
		Hygophum taaningi	83	41	4						15	26
		Lampadena chavesi	5	14							1	1
		Lampadena urophaos									2	2
		Lampanyctus alatus	5	6	9						7	51
		Lampanyctus crocodilus	4	1								
		Lampanyctus photonotus	2		8							3
		Lampanyctus pusillus			4				13			1
		Lampanyctus spp.	7	9	11						1	
		Lepidophanes gaussi	111	116	193						73	67
		Lobianchia dofleini	272	153	18	93	17	173		26	2	14
		Lobianchia gemellarii	43	6	7	9	11	2	3	1	1	
		Lobianchia spp.	117	14	31		2	6				
		Loweina rara			1							
		Myctophum nitidulum							1	2	11	5
		Myctophum selenops	15	12	11	5	6	12		1	2	
		Nannobrachium atrum	9	1	3						17	17
		Nannobrachium cuprarium	5	7	1						16	24
		Nannobrachium lineatum	7	7							2	4
		Nannobrachium spp.		12	16						3	
		Notolychnus valdiviae			1							
		Notoscopelus caudispinosus	1									3
		Notoscopelus resplendens	22	18	3							3
		Notoscopelus spp.									2	
		Symbolophorus veranyi										1
		Taaningichthys minimus								1		
		Taaningichthys spp.										2
	Melamphaidae	*Melamphaes* spp.										1
		Poromitra spp.	1		1							2
	Diretmidae	*Diretmichthys parini*		2		3		3		2		
		Diretmus argenteus									1	
	Centriscidae	*Macroramphosus scolopax*		1	2							
	Howellidae	*Howella brodiei*		1	3							
	Carangidae	*Trachurus picturatus*		2	1							2
	Caristiidae	*Platyberyx opalescens*	1	1								
	Centracanthidae	*Centracanthus cirrus*		3								
	Gempylidae	*Diplospinus multistriatus*	16	17	7				8	2	3	
		Nealotus tripes								1		
	Trichiuridae	*Aphanopus* spp.	2	29	7	1	7	3	1	1	3	
	Nomeidae	*Cubiceps gracilis*		1				1		2		
	Caproidae	*Capros aper*						1		1		
Crus	Benthesicymidae	*Gennadas tinayrei*	3	4	5						3	9
		Gennadas valens								1	2	
	Penaeidae	*Funchalia villosa*	1	9	5	4	2	4	4	13	5	
	Sergestidae	*Allosergestes pectinatus*	5		24	3	1					3
		Allosergestes sargassi		4						1		
		Deosergestes corniculum	59	3	25			1	4	2	36	25
		Deosergestes henseni		4							4	
		Eusergestes arcticus										8
		Neosergestes edwardsii										
		Parasergestes armatus			11		1	2	19	14	1	
		Parasergestes diapontius	1	5	5							
		Sergestes atlanticus	2		8						2	1
		Sergestes spp.	2	13	6			1			63	43

Continued on next page

Table 4 – *Continued from previous page*

Group	Family	**Species**	**N100p**	**N105p**	**N150t**	**D390t**	**D400p**	**D450p**	**D570t**	**D600p**	**D700p**	**D730t**
		Sergia extenauta		1								11
		Sergia grandis	1							4	3	6
		Sergia robusta										8
		Sergia splendens	14	1	9							
		Sergia wolffi	1									7
		Sergia spp.	1	2								
	Pasiphaeidae	*Eupasiphae gilesii*										
		Pasiphaea hoplocerca										1
	Acanthephyridae	*Acanthephyra purpurea*		1	2							29
		Ephyrina ombango										1
		Meningodora mollis										1
	Oplophoridae	*Oplophorus spinosus*	15	141	117	1	17	1	36	17	6	
		Systellaspis debilis	26	16	21						2	1
	Pandalidae	*Plesionika* spp. (larvae)	5	8	1	1	8	1	1			2
		Stylopandalus richardi	1		1							
	Scyllaridae	*Scyllaridae* spp. (larvae)	2	3	4	5		2				
	Homolidae	*Homola barbata* (larvae)	3		8	5	3	2	4	4	2	
Ceph	Sepiolidae	*Heteroteuthis dispar*	6	5	1	1	2		1			1
	Chtenopterygidae	*Chtenopteryx* sp.	1									
		Chtenopteryx canariensis			1							1
		Chtenopteryx sicula		1								2
	Lycoteuthidae	*Lampadioteuthis megaleia*										
	Eneploteuthidae	*Abraliopsis moriisi*	23	9	3				2	23		3
		Abralia veranyi				1						
		Enoploteuthis anapsis			1							
		Enoploteuthis sp.								1		
	Onychoteuthidae	*Onychoteuthis banksii*	41	43	3							1
	Pyroteuthidae	*Pterygioteuthis giardi*	11	49	18		13		1	27		2
		Pyroteuthis margaritifera	95	99	111	7	27	19	9	1		5
	Histioteuthidae	*Histioteuthis corona*	1							6		1
		Histioteuthis meleagroteuthis	1	2								
		Histioteuthis spp.		1					2	2		
		Stigmatoteuthis arcturi							1			
	Brachioteuthidae	*Brachioteuthis riisei*	3									
		Brachioteuthis sp.										1
	Chiroteuthidae	*Chiroteuthis* sp.	1									
		Chiroteuthis verany verany		1								
	Mastigoteuthidae	*Mastigoteuthis hjorti*		2								4
		Mastigoteuthis spp.	1	2	1							
	Cranchiidae	*Cranchia scabra*	1	1			1					1
		Leachia atlantica		1			1		1	1		
		Megalocranchia oceanica	9		3							1
		Taonius pavo										
		Bathothauma lyromna							1	1		
		Helicocranchia pfefferi										
	Argonautidae	*Argonauta argo*	1									
	Bolitaeninae	*Japetella diaphana*										1
	Octopoteuthidae	*Octopoteurhis* sp.										1
	Ommastrephidae	*Todarodes sagittatus*	1	9	1			1				1
		Ommastrephes spp.		3								

Bibliography

Aguilar Soto, N., Johnson, M. P., Madsen, P. T., Díaz, F., Domínguez, I., Brito, A., and Tyack, P. (2008). Cheetahs of the deep sea: deep foraging sprints in short-finned pilot whales off Tenerife (Canary Islands). *Journal of Animal Ecology*, 77(5):936–947.

Ahmed, S. I., Kenner, R. A., and King, F. D. (1976). Preservation of enzymic activity in marine plankton by low-temperature freezing. *Marine Chemistry*, 4(2):133–139.

Aksnes, D. L. and Giske, J. (1993). A theoretical model of aquatic visual feeding. *Ecological Modelling*, 67(2):233–250.

Al-Mutairi, H. and Landry, M. R. (2001). Active export of carbon and nitrogen at Station ALOHA by diel migrant zooplankton. *Deep Sea Research Part II: Topical Studies in Oceanography*, 48(8–9):2083–2103.

Alonso-González, I. J., Arístegui, J., Lee, C., and Calafat, A. (2010). Regional and temporal variability of sinking organic matter in the subtropical northeast Atlantic Ocean: a biomarker diagnosis. *Biogeosciences*, 7(7):2101–2115.

Alonso-González, I. J., Arístegui, J., Lee, C., Sánchez-Vidal, A., Calafat, A., Fabrés, J., Sangrá, P., and Mason, E. (2013). Carbon dynamics within cyclonic eddies: insights from a biomarker study. *PloS one*, 8(12):e82447.

Alonso-González, I. J., Arístegui, J., Vilas, J. C., and Hernández-Guerra, A. (2009). Lateral POC transport and consumption in surface and deep waters of the Canary Current region: A box model study. *Global Biogeochemical Cycles*, 23(2):1–12.

Andreeva, I. B. (1964). Scattering of sound by air bladders of fish in deep sound-scattering ocean layers. *Soviet Physics-Acoustics*, 10(1):17–20.

Angel, M. V. and Pugh, P. R. (2000). Quantification of diel vertical migration by micronektonic taxa in the northeast Atlantic. *Hydrobiologia*, 440(1):161–179.

Antia, A. N., Koeve, W., Fischer, G., Blanz, T., Schulz-Bull, D., Schölten, J., Neuer, S., Kremling, K., Kuss, J., Peinert, R., Hebbeln, D., Bathmann, U., Conte, M., Fehner, U., and Zeitzschel, B. (2001). Basin-wide particulate carbon flux in the Atlantic

Ocean: Regional export patterns and potential for atmospheric CO_2 sequestration. *Global Biogeochemical Cycles*, 15(4):845–862.

Arcos-Pulido, M., Rodríguez-Santana, A., Emelianov, M., Paka, V., Arístegui, J., Benavides, M., Sangrà, P., Machín, F., García-Weil, L., and Estrada-Allis, S. (2014). Diapycnal nutrient fluxes on the northern boundary of Cape Ghir upwelling region. *Deep Sea Research Part I: Oceanographic Research Papers*, 84:100–109.

Arístegui, J., Barton, E., Montero, M., García-Muñoz, M., and Escánez, J. (2003). Organic carbon distribution and water column respiration in the NW Africa-Canaries Coastal Transition Zone. *Aquatic Microbial Ecology*, 33:289–301.

Arístegui, J., Gasol, J. M., Duarte, C. M., and Herndl, G. J. (2009). Microbial oceanography of the dark ocean's pelagic realm. *Limnol. Oceanogr*, 54(5):1501–1529.

Arístegui, J., Hernández-León, S., Montero, M. F., and Gómez, M. (2001). The seasonal planktonic cycle in coastal waters of the Canary Islands. *Scientia Marina*, 65:51–58.

Arístegui, J. and Montero, M. F. (2005). Temporal and spatial changes in plankton respiration and biomass in the Canary Islands region : the effect of mesoscale variability. *Journal of Marine Systems*, 54:65–82.

Arístegui, J., Sangrà, P., Hernández-León, S., Cantón, M., Hernández-Guerra, A., and Kerling, J. L. (1994). Island-induced eddies in the Canary Islands. *Deep Sea Research Part I: Oceanographic Research Papers*, 41(10):1509–1525.

Arístegui, J., Tett, P., Hernández-Guerra, A., Basterretxea, G., Montero, M. F., Wild, K., Sangrá, P., Cantón, M., García-Braun, J. A., Pacheco, M., and Barton, E. D. (1997). The influence of island-generated eddies on chlorophyll distribution : a study of mesoscale variation around Gran Canaria. *Deep Sea Research Part I*, 44(1):71–96.

Ariza, A., Garijo, J. C., Landeira, J. M., Bordes, F., and Hernández-León, S. (2015). Migrant biomass and respiratory carbon flux by zooplankton and micronekton in the subtropical northeast Atlantic Ocean (Canary Islands). *Progress in Oceanography*, 134:330–342.

Ariza, A., Kaartvedt, S., Røstad, A., Garijo, J. C., Arístegui, J., Fraile-Nuez, E., and Hernández-León, S. (2014). The Submarine Volcano Eruption off El Hierro Island: Effects on the Scattering Migrant Biota and the Evolution of the Pelagic Communities. *PLoS ONE*, 9(7):e102354.

Arranz, P. (2007). Composición y distribución del ictioplancton de la reserva marina de El Hierro, Islas Canarias. *MS Thesis, Universidad de Las Palmas de Gran Canaria.*

Arranz, P., Aguilar de Soto, N., Madsen, P. T., Brito, A., Bordes, F., and Johnson, M. P. (2011). Following a foraging fish-finder: diel habitat use of Blainville's beaked whales revealed by echolocation. *PloS one*, 6(12):e28353.

Backus, R. H. and Craddock, J. E. (1977). Pelagic faunal provinces and sound-scattering levels in the Atlantic Ocean. In Andersen, N. R. and Zahuranec, B. J., editors, *Oceanic sound-scattering prediction*, pages 529–549. Plenum Press, New York.

Badcock, J. (1970). The Vertical Distribution of Mesopelagic Fishes Collected on the SOND Cruise. *Journal of the Marine Biological Association of the United Kingdom*, 50:1001–1044.

Badcock, J. and Merrett, N. R. (1976). Midwater fishes in the eastern North Atlantic–I. Vertical distribution and associated biology in 30°N, 23°W, with developmental notes on certain myctophids. *Progress in Oceanography*, 7(1):3–58.

Badcock, J. and Merrett, N. R. (1977). On the distribution of midwater fishes in the eastern North Atlantic. In Andersen, N. R. and Zahuranec, B. J., editors, *Oceanic sound-scattering prediction*, pages 248–282. Plenum Press, New York.

Baird, R. C., Hopkins, T. L., and Wilson, D. F. (1975). Diet and Feeding Chronology of *Diaphus taaningi* (Myctophidae) in the Cariaco Trench. *Copeia*, 2:356–365.

Baker, A. D. C. (1970). The Vertical Distribution of Euphausiids Near Fuerteventura, Canary Islands ("Discovery" SOND Cruise, 1965). *Journal of the Marine Biological Association of the United Kingdom*, 50(02):301–342.

Baliño, B. M. and Aksnes, D. (1993). Winter distribution and migration of the sound scattering layers, zooplankton and micronekton in Masfjoerden, western Norway. *Marine Ecology Progress Series*, 102:35–50.

Baltar, F., Arístegi, J., Gasol, J. M., Sintes, E., and Herndl, G. J. (2009). Evidence of prokaryotic metabolism on suspended particulate organic matter in the dark waters of the subtropical North Atlantic. *Limnology and Oceanography*, 54(1):182–193.

Båmstedt, U. (1980). ETS activity as an estimator of respiratory rate of zooplankton populations. The significance of variations in environmental factors. *Journal of Experimental Marine Biology and Ecology*, 42(3):267–283.

Barham, E. G. (1966). Deep scattering layer migration and composition: Observations from a diving saucer. *Science*, 151(3716):1399–1403.

Barton, E. D., Arístegui, J., Tett, P., Cantón, M., García-Braun, J., Hernández-León, S., Nykjaer, L., Almeida, C., Almunia, J., Ballesteros, S., Basterretxea, G., Escánez,

J., García-Weil, L., Hernández-Guerra, A., López Laatzen, F., Molina, R., Montero, M. F., Navarro-Pérez, E., Rodríguez, J. M., van Lenning, K., Vélez, H., and Wild, K. (1998). The transition zone of the Canary Current upwelling region. *Progress in Oceanography*, 41(4):455–504.

Barton, E. D., Arístegui, J., Tett, P., and Navarro Pérez, E. (2004). Variability in the Canary Islands area of filament-eddy exchanges. *Progress in Oceanography*, 62:71–94.

Béhagle, N., du Buisson, L., Josse, E., Lebourges-Dhaussy, A., Roudaut, G., and Ménard, F. (2014). Mesoscale features and micronekton in the Mozambique Channel: An acoustic approach. *Deep Sea Research Part II: Topical Studies in Oceanography*, 100:164–173.

Benoit-Bird, K. J. (2009). The effects of scattering-layer composition, animal size, and numerical density on the frequency response of volume backscatter. *ICES Journal of Marine Science*, 66(3):582–593.

Bertrand, A., Grados, D., Colas, F., Bertrand, S., Capet, X., Chaigneau, A., Vargas, G., Mousseigne, A., and Fablet, R. (2014). Broad impacts of fine-scale dynamics on seascape structure from zooplankton to seabirds. *Nature Communications*, 5(May):5239.

Betzer, P. R., Showers, W. J., Laws, E. A., Winn, C. D., DiTullio, G. R., and Kroopnick, P. M. (1984). Primary productivity and particle fluxes on a transect of the equator at 153°W in the Pacific Ocean. *Deep Sea Research Part A. Oceanographic Research Papers*, 31(1):1–11.

Bianchi, D., Galbraith, E. D., Carozza, D. A., Mislan, K. A. S., and Stock, C. A. (2013a). Intensification of open-ocean oxygen depletion by vertically migrating animals. *Nature Geoscience*, 6(7):545–548.

Bianchi, D., Stock, C., Galbraith, E. D., and Sarmiento, J. L. (2013b). Diel vertical migration: Ecological controls and impacts on the biological pump in a one-dimensional ocean model. *Global Biogeochemical Cycles*, 27(2):478–491.

Blaxter, J. H. S. (1974). The role of light in the vertical migration of fish—a review. In *Light as an ecological factor: II The 16th symposium of the British Ecological Society. Blackwell, Oxford*, pages 189–210.

Bode, M., Schukat, A., Hagen, W., and Auel, H. (2013). Predicting metabolic rates of calanoid copepods. *Journal of Experimental Marine Biology and Ecology*, 444:1–7.

Boden, B. P. and Kampa, E. M. (1967). The influence of natural light on the vertical migrations of an animal community in the sea. *Symp Zool Soc Lond*, 19.

Bordes, F., Wienerroither, R., Uiblein, F., Moreno, T., Bordes, I., and Hernández, V. (2009). Catálogo de especies meso y batipelágicas. Peces, moluscos y crustáceos. Colectadas con arrastre en las Islas Canarias durante las campañas realizadas a bordo del B/E "La Bocaina". *Informes del Instituto Canario de Ciencias Marinas*.

Brandt, S. B. (1983). Temporal and spatial patterns of lanternfish (family Myctophidae) communities associated with a warm-core eddy. *Marine Biology*, 74(3):231–244.

Bray, J. R. and Curtis, J. T. (1957). An ordination of the upland forest communities of southern Wisconsin. *Ecological monographs*, 27(4):325–349.

Brett, J. and Groves, T. (1979). Physiological energetics. In Hoar, W. S. and Randall, D. J., editors, *Bioenergetics and Growth, vol. 8*, pages 279–351. Academic Press, New York.

Brett, J. R. (1971). Energetic responses of salmon to temperature. A study of some thermal relations in the physiology and freshwater ecology of sockeye salmon (Oncorhynchus nerkd). *American zoologist*, 11(1):99–113.

Brinton, E. (1967). Vertical migration and avoidance capability of euphausiids in the California Current. *Limnology and Oceanography*, 12(3):451–483.

Brodeur, R. D., Seki, M. P., Pakhomov, E. A., and Suntsov, A. V. (2005). Micronekton - What are they and why are they important? *North Pacific Marine Science Organization. Pices Press*, 13:7–11.

Brooks, A. L. (1977). A study of the swimbladders of selected mesopelagic fish species. In Zuharanec, B. J. and Andersen, N. R., editors, *Oceanic sound-scattering prediction*, pages 565–590. Plenum Press, New York.

Buesseler, K. O., Antia, A. N., Chen, M., Fowler, S. W., Gardner, W. D., Gustafsson, O., Harada, K., Michaels, A. F., van der Loeff, M. R., Sarin, M., Steinberg, D. K., and Trull, T. (2007). An assessment of the use of sediment traps for estimating upper ocean particle fuxes. *Journal of Marine Research*, 65:345–416.

Burghart, S. E. (2006). Micronektonic community composition and trophic structure within the bathypelagic zone in the eastern Gulf of Mexico. *PhD Thesis, University of South Florida, Florida USA*.

Burghart, S. E., Hopkins, T. L., and Torres, J. J. (2010). Partitioning of food resources in bathypelagic micronekton in the eastern Gulf of Mexico. *Marine Ecology-Progress Series*, 399:131.

Busch, S. and Mehner, T. (2011). Size-dependent patterns of diel vertical migration: smaller fish may benefit from faster ascent. *Behavioral Ecology*, page arr177.

Butler, J. L. and Pearcy, W. G. (1972). Swimbladder morphology and specific gravity of myctophids off Oregon. *Journal of the Fisheries Board of Canada*, 29(8):1145–1150.

Cabral, H. N. and Murta, A. G. (2002). The diet of blue whiting, hake, horse mackerel and mackerel off Portugal. *Journal of Applied Ichthyology*, 18(1):14–23.

Cade, D. E. and Benoit-Bird, K. J. (2015). Depths, migration rates and environmental associations of acoustic scattering layers in the gulf of california. *Deep Sea Research Part I: Oceanographic Research Papers*, 102:78–89.

Capen, R. L. (1967). Swimbladder morphology of some mesopelagic fishes in relation to sound scattering. *Technical report. U. S. Navy Electronics Laboratory.*

Childress, J. J. (1975). The respiratory rates of midwater crustaceans as a function of depth of occurrence and relation to the oxygen minimum layer off Southern California. *Comparative Biochemistry and Physiology Part A: Physiology*, 50(4):787–799.

Childress, J. J. and Nygaard, M. (1974). Chemical composition and buoyancy of midwater crustaceans as function of depth of occurrence off Southern California. *Marine Biology*, 27:225–238.

Childress, J. J. and Nygaard, M. H. (1973). The chemical composition of midwater fishes as a function of depth of occurrence off southern California. *Deep Sea Research*, 20:1093–1109.

Childress, J. J. and Seibel, B. A. (1998). Life at stable low oxygen levels: adaptations of animals to oceanic oxygen minimum layers. *Journal of Experimental Biology*, 201(8):1223–1232.

Choy, C. A., Davison, P. C., Drazen, J. C., Flynn, A., Gier, E. J., Hoffman, J. C., McClain-Counts, J. P., Miller, T. W., Popp, B. N., Ross, S. W., and Sutton, T. T. (2012). Global trophic position comparison of two dominant mesopelagic fish families (Myctophidae, Stomiidae) using amino acid nitrogen isotopic analyses. *PloS one*, 7(11):e50133.

Choy, C. A., Portner, E., Iwane, M., and Drazen, J. C. (2013). Diets of five important predatory mesopelagic fishes of the central North Pacific. *Marine Ecology Progress Series*, 492:169–184.

Clark, C. W. and Levy, D. A. (1988). Diel vertical migrations by juvenile sockeye salmon and the antipredation window. *The American Naturalist*, 131(2):271–290.

Clarke, G. L. and Backus, R. H. (1953). Measurements of light penetration in relation to vertical migration and records of luminescence of deep-sea animals. *Deep Sea Research*, 4:1–14.

Clarke, K. R., Somerfield, P. J., and Gorley, R. N. (2008). Testing of null hypotheses in exploratory community analyses: similarity profiles and biota-environment linkage. *Journal of Experimental Marine Biology and Ecology*, 366(1):56–69.

Clarke, M. R. (1969). Cephalopoda collected on the SOND cruise. *Journal of the Marine Biological Association of the United Kingdom*, 49(04):961–976.

Clarke, T. M. (1982). Feeding habits of stomiatoid fishes from Hawaiian waters. *Fishery bulletin-United States, National Marine Fisheries Service (USA)*, 80:287–304.

Claustre, H., Morel, A., Hooker, S. B., Babin, M., Antoine, D., Oubelkheir, K., Bricaud, A., Leblanc, K., Quéguiner, B., and Maritorena, S. (2002). Is desert dust making oligotrophic waters greener? *Geophysical Research Letters*, 29(10).

Conte, M. H., Bishop, J. B., and Backus, R. H. (1986). Nonmigratory, 12-kHz, deep scattering layers of Sargasso Sea origin in warm-core rings. *Deep Sea Research Part A. Oceanographic Research Papers*, 33(11):1869–1884.

Cotté, C., D'Ovidio, F., Dragon, A. C., Guinet, C., and Lévy, M. (2015). Flexible preference of southern elephant seals for distinct mesoscale features within the Antarctic Circumpolar Current. *Progress in Oceanography*, 131:46–58.

Dam, H. G. and Peterson, W. T. (1988). The effect of temperature on the gut clearance rate constant of planktonic copepods. *Journal of Experimental Marine Biology and Ecology*, 123(1):1–14.

Dam, H. G., Roman, M. R., and Youngbluth, M. J. (1995). Downward export of respiratory carbon and dissolved inorganic nitrogen by diel-migrant mesozooplankton at the JGOFS Bermuda time-series station. *Deep Sea Research Part I: Oceanographic Research Papers*, 42(7):1187–1197.

Davenport, R., Neuer, S., Helmke, P., Perez-Marrero, J., and Llinas, O. (2002). Primary productivity in the northern Canary Islands region as inferred from SeaWiFS imagery. *Deep Sea Research Part II: Topical Studies in Oceanography*, 49(17):3481–3496.

Davison, P. (2011a). The specific gravity of mesopelagic fish from the northeastern Pacific Ocean and its implications for acoustic backscatter. *ICES Journal of Marine Science: Journal du Conseil*, 68(10):2064–2074.

Davison, P., Koslow, J. A., and Kloser, R. J. (2015). Acoustic biomass estimation of mesopelagic fish: backscattering from individuals, populations and communities. *ICES Journal of Marine Science*, page fsv023.

Davison, P. C. (2011b). The Export of Carbon Mediated by Mesopelagic Fishes in the Northeast Pacific Ocean. *PhD Thesis, University of California, San Diego USA*.

Davison, P. C., Checkley, D. M., Koslow, J. A., and Barlow, J. (2013). Carbon export mediated by mesopelagic fishes in the northeast Pacific Ocean. *Progress in Oceanography*, 116:14–30.

De Robertis, A. (2002). Size-dependent visual predation risk and the timing of vertical migration: An optimization model. *Limnology and Oceanography*, 47(4):925–933.

del Giorgio, P. A. and Duarte, C. M. (2002). Respiration in the open ocean. *Nature*, 420(6914):379–384.

Denman, K. L., Brasseur, G., Chidthaisong, A., Ciais, P., Cox, P. M., Dickinson, R. E., Hauglustaine, D., Heinze, C., Holland, E., Jacob, D., Lohman, U., Ramachadram, S., da Silva Dias, P. L., Wofsy, S. C., and Zhang, X. (2007). Couplings between changes in the climate system and biogeochemistry. In Solomon, S., Qin, D., Manning, M., Chen, Z., Marquis, M., Averyt, K. B., Tignor, M., and Miller, H. L., editors, *Climate Change 2007: The Physical Science Basis*, pages 499–587. Cambridge University Press, New York.

Dickson, R. R. (1972). On the relationship between ocean transparency and the depth of sonic scattering layers in the North Atlantic. *Journal du Conseil*, 34(3):416–422.

Dietz, R. S. (1948). Deep scattering layer in the Pacific and Antarctic Oceans. *Journal of marine research*, 7:430–442.

Domanski, P. (1984). The diel migrations and distributions within a mesopelagic community in the North East Atlantic. 8. A multivariate analysis of community structure. *Progress in oceanography*, 13(3):491–511.

Doney, S. C., Ruckelshaus, M., Duffy, J. E., Barry, J. P., Chan, F., English, C. A., Galindo, H. M., Grebmeier, J. M., Hollowed, A. B., Knowlton, N., and Others (2012). Climate change impacts on marine ecosystems. *Marine Science*, 4.

Doney, S. C. and Steinberg, D. K. (2013). The ups and downs of ocean oxygen. *Nature Geoscience*, 6(7):515–516.

Donnelly, J. and Torres, J. J. (1988). Oxygen consumption of midwater fishes and crustaceans from the eastern Gulf of Mexico. *Marine Biology*, 97(4):483–494.

Doty, M. S. and Oguri, M. (1956). The Island Mass Effect. *Journal du Conseil*, 22(1):33–37.

Doxaran, D., Froidefond, J.-M., Castaing, P., and Babin, M. (2009). Dynamics of the turbidity maximum zone in a macrotidal estuary (the Gironde, France): Observations from field and MODIS satellite data. *Estuarine, Coastal and Shelf Science*, 81(3):321–332.

Ducklow, H. W., Steinberg, D. K., and Buesseler, K. O. (2001). Upper ocean carbon export and the biological pump. *Ocenography - Washington DC - Oceanography Society*, 14(4):50–58.

Dypvik, E. and Kaartvedt, S. (2013). Vertical migration and diel feeding periodicity of the skinnycheek lanternfish (*Benthosema pterotum*) in the Red Sea. *Deep Sea Research Part I: Oceanographic Research Papers*, 72:9–16.

Dypvik, E., Klevjer, T. a., and Kaartvedt, S. (2011). Inverse vertical migration and feeding in glacier lanternfish (*Benthosema glaciale*). *Marine Biology*, 159(2):443–453.

Dypvik, E., Røstad, A., and Kaartvedt, S. (2012). Seasonal variations in vertical migration of glacier lanternfish, *Benthosema glaciale*. *Marine Biology*, 159(8):1673–1683.

Ekau, W., Auel, H., Pörtner, H.-O., and Gilbert, D. (2010). Impacts of hypoxia on the structure and processes in pelagic communities (zooplankton, macro-invertebrates and fish). *Biogeosciences*, 7:1669–1699.

Eyring, C. F., Christensen, R. J., and Raitt, R. W. (1948). Reverberation in the Sea. *The Journal of the Acoustical Society of America*, 20(4):462–475.

Fabry, V. J., Seibel, B. A., Feely, R. A., and Orr, J. C. (2008). Impacts of ocean acidification on marine fauna and ecosystem processes. *ICES Journal of Marine Science: Journal du Conseil*, 65(3):414–432.

Falkowski, P. G., Laws, E. A., Barber, R. T., and Murray, J. W. (2003). Phytoplankton and Their Role in Primary , New , and Export Production. In Fasham, M. J. R., editor, *Ocean Biogeochemistry*, pages 99–121. Springer-Verlag.

Fasham, M. J. R. (2003). *Ocean Biogeochemistry: The Role of the Ocean Carbon Cycle in the Global Change*. Springer.

Fasham, M. J. R. and Foxton, P. (1979). Zonal distribution of pelagic Decapoda (Crustacea) in the eastern North Atlantic and its relation to the physical oceanography. *Journal of experimental marine Biology and Ecology*, 37(3):225–253.

Fennell, S. and Rose, G. (2015). Oceanographic influences on deep Scattering Layers across the north Atlantic. *Deep Sea Research Part I: Oceanographic Research Papers*.

Foote, K., Knudsen, H., Vestnes, G., MacLennan, D., and Simmonds, E. (1987). Calibration of acoustic instruments for fish density estimation: a practical guide. *ICES Cooperative Research Report*, 144.

Fowler, S. W. and Knauer, G. A. (1986). Role of large particles in the transport of elements and organic compounds through the oceanic water column. *Progress in Oceanography*, 16(3):147–194.

Foxton, P. (1969). SOND Cruise 1965 Biological sampling methods and procedures. *Journal of the Marine Biological Association of the United Kingdom*, 49(03):603–620.

Foxton, P. (1970a). The Vertical Distribution of Pelagic Decapods [Crustacea: Natantia] Collected on the Sond Cruise 1965 I. The Caridea. *Journal of the Marine Biological Association of the United Kingdom*, 50(04):939–960.

Foxton, P. (1970b). The Vertical Distribution of Pelagic Decapods [Crustacea: Natantia] Collected on the Sond Cruise 1965 II. The Penaidea and General Discussion. *Journal of the Marine Biological Association of the United Kingdom*, 50(04):939–960.

Fraile-Nuez, E., González-Dávila, M., Santana-Casiano, J. M., Arístegui, J., Alonso-González, I. J., Hernández-León, S., Blanco, M. J., Rodríguez-Santana, A., Hernández-Guerra, A., Gelado-Caballero, M. D., Eugenio, F., Marcello, J., de Armas, D., Domínguez-Yanes, J. F., Montero, M. F., Laetsch, D. R., Vélez-Belchí, P., Ramos, A., Ariza, A. V., Comas-Rodríguez, I., and Benítez-Barrios, V. M. (2012). The submarine volcano eruption at the island of El Hierro: physical-chemical perturbation and biological response. *Scientific Reports*, 2(486).

Frank, T. and Widder, E. (2002). Effects of a decrease in downwelling irradiance on the daytime vertical distribution patterns of zooplankton and micronekton. *Marine Biology*, 140(6):1181–1193.

Froese, R. and Pauly, D. (2014). FishBase - World Wide Web electronic publication. Available from http://www.fisbase.org.

Gartner, J. V., Conley, W. J., and Hopkins, T. L. (1989). Escapement by fishes from midwater trawls: A case study using lanternfishes (Pisces: Myctophidae). *Fishery Bulletin*, 87(1):213–222.

Godø, O. R., Handegard, N. O., Browman, H. I., Macaulay, G. J., Kaartvedt, S., Giske, J., Ona, E., Huse, G., and Johnsen, E. (2014). Marine ecosystem acoustics (MEA): quantifying processes in the sea at the spatio-temporal scales on which they occur. *ICES Journal of Marine Science: Journal du Conseil*, page fsu116.

Godø, O. R., Patel, R., and Pedersen, G. (2009). Diel migration and swimbladder resonance of small fish: some implications for analyses of multifrequency echo data. *ICES Journal of Marine Science: Journal du Conseil*, 66(6):1143–1148.

Godø, O. R., Samuelsen, A., Macaulay, G. J., Patel, R., Hjøllo, S. S., Horne, J., Kaartvedt, S., and Johannessen, J. a. (2012). Mesoscale eddies are oases for higher trophic marine life. *PloS one*, 7(1):e30161.

Gómez, M., Torres, S., and Hernández-León, S. (1996). Modification of the electron transport system (ETS) method for routine measurements of respiratory rates of zooplankton. *South African Journal of Marine Science*, 17:15–20.

González-Dávila, M., Santana-Casiano, J. M., de Armas, D., Escánez, J., and Suarez-Tangil, M. (2006). The influence of island generated eddies on the carbon dioxide system, south of the Canary Islands. *Marine Chemistry*, 99(1-4):177–190.

Goodyear, R. H., Zahuranec, B. J., Pugh, W. L., and Gibbs, R. H. (1972). Ecology and vertical distribution of Mediterranean midwater fishes. *Mediterranean biological studies*, pages 91–229.

Griffiths, F. B. and Wadley, V. A. (1986). A synoptic comparison of fishes and crustaceans from a warm-core eddy, the East Australian Current, the Coral Sea and the Tasman Sea. *Deep Sea Research Part A. Oceanographic Research Papers*, 33(11):1907–1922.

Grosjean, P. and Denis, K. (2007). Zoo/PhytoImage version 1.2-0. User's Manual.

Gurney, L. J., Froneman, P. W., Pakhomov, E. A., and McQuaid, C. D. (2002). Diel feeding patterns and daily ration estimates of three subantarctic euphausiids in the vicinity of the Prince Edward Islands (Southern Ocean). *Deep Sea Research Part II: Topical Studies in Oceanography*, 49(16):3207–3227.

Hall-Spencer, J. M., Rodolfo-Metalpa, R., Martin, S., Ransome, E., Fine, M., Turner, S. M., Rowley, S. J., Tedesco, D., and Buia, M.-C. (2008). Volcanic carbon dioxide vents show ecosystem effects of ocean acidification. *Nature*, 454:1–4.

Hamme, R. C., Webley, P. W., Crawford, W. R., Whitney, F. a., DeGrandpre, M. D., Emerson, S. R., Eriksen, C. C., Giesbrecht, K. E., Gower, J. F. R., Kavanaugh, M. T., Peña, M. A., Sabine, C. L., Batten, S. D., Coogan, L. a., Grundle, D. S., and Lockwood, D. (2010). Volcanic ash fuels anomalous plankton bloom in subarctic northeast Pacific. *Geophysical Research Letters*, 37(L19604).

Hays, G. C. (2003). A review of the adaptive significance and ecosystem consequences of zooplankton diel vertical migrations. In *Migrations and Dispersal of Marine Organisms*, pages 163–170. Springer.

Hernández Guerra, A., López Laatzen, F., Machín, F., de Armas, D., and Pelegrí, J. L. (2001). Water masses, circulation and transport in the eastern boundary current of the North Atlantic subtropical gyre. *Sci. Mar*, 65(1):177–186.

Hernández-León, S. (1988). Gradient of mesozooplankton biomass and ETS activity in the wind-shear area as evidence of an island mass effect in the Canary Island waters. *Journal of Plankton Research*, 10(6):1141–1154.

Hernández-León, S., Almeida, C., Bécognée, P., Yebra, L., and Arístegui, J. (2004). Zooplankton biomass and indices of grazing and metabolism during a late winter bloom in subtropical waters. *Marine Biology*, 145:1191–1200.

Hernández-León, S., Almeida, C., Portillo-Hahnefeld, A., Gómez, M., Rodríguez, J. M., and Arístegui, J. (2002). Zooplankton biomass and indices of feeding and metabolism in relation to an upwelling filament off northwest Africa. *Journal of Marine Research*, 60(2):327–346.

Hernández-León, S., Franchy, G., Moyano, M., Menéndez, I., Schmoker, C., and Putzeys, S. (2010). Carbon sequestration and zooplankton lunar cycles: Could we be missing a major component of the biological pump? *Limnology and Oceanography*, 55(6):2503–2512.

Hernández-León, S. and Gómez, M. (1996). Factors affecting the respiration/ETS ratio in marine zooplankton. *Journal of Plankton Research*, 18(2):239–255.

Hernández-León, S., Gómez, M., and Arístegui, J. (2007). Mesozooplankton in the Canary Current System: The coastal – ocean transition zone. *Progress in Oceanography*, 74:397–421.

Hernández-León, S., Gómez, M., Pagazaurtundua, M., Portillo-Hahnefeld, A., Montero, I., and Almeida, C. (2001). Vertical distribution of zooplankton in Canary Island waters: implications for export flux. *Deep Sea Research Part I: Oceanographic Research Papers*, 48(4):1071–1092.

Hernández-León, S. and Ikeda, T. (2005). A global assessment of mesozooplankton respiration in the ocean. *Journal of Plankton Research*, 27(2):153–158.

Hernández-León, S. and Montero, I. (2006). Zooplankton biomass estimated from digitalized images in Antarctic waters: A calibration exercise. *Journal of Geophysical Research: Oceans (1978–2012)*, 111(C5).

Herrera, A., Gómez, M., Packard, T. T., Reglero, P., Blanco, E., and Barberá-Cebrián, C. (2014). Potential respiration estimated by electron transport system activity in deep-sea suprabenthic crustaceans off Balearic Islands (Western Mediterranean). *Journal of Marine Systems*, 138:104–111.

Hersey, J. B. and Backus, R. H. (1954). New evidence that migrating gas bubbles, probably the swimbladders of fish, are largely responsible for scattering layers on the continental rise south of New England. *Deep Sea Research*, 1(3):190–191.

Hidaka, K., Kawaguchi, K., Murakami, M., and Takahashi, M. (2001). Downward transport of organic carbon by diel migratory micronekton in the western equatorial pacific:

Its quantitative and qualitative importance. *Deep-Sea Research Part I: Oceanographic Research Papers*, 48(8):1923–1939.

Hidaka, K., Kawaguchi, K., Tanabe, T., Takahashi, M., and Kubodera, T. (2003). Biomass and taxonomic composition of micronekton in the western tropical–subtropical Pacific. *Fisheries Oceanography*, 12(2):112–125.

Hopkins, T. L. and Gartner, J. V. (1992). Resource-partitioning and predation impact of a low-latitude myctophid community. *Marine Biology*, 114(2):185–197.

Hudson, J. M., Steinberg, D. K., Sutton, T. T., Graves, J. E., and Latour, R. J. (2014). Myctophid feeding ecology and carbon transport along the northern Mid-Atlantic Ridge. *Deep Sea Research Part I: Oceanographic Research Papers*, 93:104–116.

Ikeda, T. (1989). Estimated respiration rate of myctophid fish from the enzyme activity of the electron-transport-system. *Journal of Oceanography*, 45(3):167–173.

Ikeda, T. (2013). Metabolism and chemical composition of pelagic decapod shrimps: synthesis toward a global bathymetric model. *Journal of Oceanography*, 69(6):671–686.

Ikeda, T. (2014). Respiration and ammonia excretion by marine metazooplankton taxa: synthesis toward a global-bathymetric model. *Marine Biology*, 161(12):2753–2766.

Ikeda, T. and Kirkwood, R. (1989). Metabolism and body composition of two euphausiids (*Euphausia superba* and *E. crystallorophias*) collected from under the pack-ice off Enderby Land, Antarctica. *Marine Biology*, 100(3):301–308.

Ikeda, T. and Motoda, S. (1978). Estimated zooplankton production and their ammonia excretion in the Kuroshio and adjacent seas. *Fishery Bulletin*, 76(2):357–367.

IPCC (2014). Climate Change 2014: Synthesis Report. Contribution of Working Groups I, II and III. *Fifth Assessment Report of the Intergovernmental Panel on Climate Change*.

Irigoien, X., Klevjer, T. A., Røstad, A., Martínez, U., Boyra, G., Acuña, J. L., Bode, A., Echevarría, F., González-Gordillo, J. I., Hernández-León, S., Agustí, S., Aksnes, D. L., Duarte, C. M., and Kaartvedt, S. (2014). Large mesopelagic fishes biomass and trophic efficiency in the open ocean. *Nature Communications*, 5:3271.

Johnson, M. W. (1948). Sound as a tool in marine ecology, from data on biological noises and the deep scattering layer. *Journal of marine research*, 7:443–458.

Jones, D. L. (2014). The Fathom Toolbox for Matlab: multivariate ecological and oceanographic data analysis. College of Marine Science, University of South Florida, St. Petersburg, Florida, USA. Available from: http://www.marine.usf.edu/user/djones/.

Kaartvedt, S., Klevjer, T. A., and Aksnes, D. L. (2012a). Internal wave-mediated shading causes frequent vertical migrations in fishes. *Marine Ecology Progress Series*, 452:1–10.

Kaartvedt, S., Melle, W., Knutsen, T., and Skjoldal, H. R. (1996). Vertical distribution of fish and krill beneath water of varying optical properties. *Marine Ecology Progress Series*, 136:51–58.

Kaartvedt, S., Røstad, A., Klevjer, T. A., and Staby, A. (2009). Use of bottom-mounted echo sounders in exploring behavior of mesopelagic fishes. *Marine Ecology Progress Series*, 395:109–118.

Kaartvedt, S., Staby, A., and Aksnes, D. (2012b). Efficient trawl avoidance by mesopelagic fishes causes large underestimation of their biomass. *Marine Ecology Progress Series*, 456:1–6.

Kaartvedt, S., Torgersen, T., Røstad, A., and Devine, J. A. (2008). Behavior of individual mesopelagic fish in acoustic scattering layers of Norwegian fjords. *Marine Ecology Progress Series*, 360:201–209.

Kai, E. T. and Marsac, F. (2010). Influence of mesoscale eddies on spatial structuring of top predators' communities in the Mozambique Channel. *Progress in Oceanography*, 86(1):214–223.

Kampa, E. M. (1975). Observations of a sonic-scattering layer during the total solar eclipse 30 June, 1973. *Deep Sea Research and Oceanographic Abstracts*, 22(6):417–423.

Kampa, E. M. and Boden, B. P. (1954). Submarine Illumination and the Twilight Movements of a Sonic Scattering Layer. *Nature*, 174(4436):869–871.

Karl, D. M., Christian, J. R., Dore, J. E., Hebel, D. V., Letelier, R. M., Tupas, L. M., and Winn, C. D. (1996). Seasonal and interannual variability in primary production and particle flux at Station ALOHA. *Deep Sea Research Part II: Topical Studies in Oceanography*, 43(2–3):539–568.

Karl, D. M. and Lukas, R. (1996). The Hawaii Ocean Time-series (HOT) program: Background, rationale and field implementation. *Deep Sea Research Part II: Topical Studies in Oceanography*, 43(2):129–156.

Keeling, R. F., Körtzinger, A., and Gruber, N. (2010). Ocean Deoxygenation in a Warming World. *Annual Review of Marine Science*, 2:199–229.

Kinzer, J. and Schulz, K. (1985). Vertical distribution and feeding patterns of midwater fish in the central equatorial Atlantic. *Marine biology*, 85(3):313–322.

Kiørboe, T. (2013). Zooplankton body composition. *Limnology and Oceanography*, 58(5):1843–1850.

Kleckner, R. C. and Gibbs, R. H. (1972). Swimbladder structure of mediterranean midwater fishes and a method of comparing swimbladder data with acoustic profiles. *Mediterranean biological studies*, pages 230–281.

Kloser, R. J., Ryan, T., Sakov, P., Williams, A., and Koslow, J. A. (2002). Species identification in deep water using multiple acoustic frequencies. *Canadian Journal of Fisheries and Aquatic Sciences*, 59:1065–1077.

Kloser, R. J., Ryan, T. E., Young, J. W., and Lewis, M. E. (2009). Acoustic observations of micronekton fish on the scale of an ocean basin: potential and challenges. *ICES Journal of Marine Science: Journal du Conseil*, page fsp077.

Koppelmann, R. and Frost, J. (2008). The ecological role of zooplankton in the twilight and dark zones of the ocean. *Biological Oceanography Research Trends.. Nova Science Publishers, Inc., New York*, pages 67–130.

Korneliussen, R. (2000). Measurement and removal of echo integration noise. *ICES Journal of Marine Science*, 57(4):1204–1217.

Korneliussen, R. J., Heggelund, Y., Eliassen, I. K., and Johansen, G. O. (2009). Acoustic species identification of schooling fish. *ICES Journal of Marine Science*, 66(6):1111–1118.

Korneliussen, R. J. and Ona, E. (2003). Synthetic echograms generated from the relative frequency response. *ICES Journal of Marine Science: Journal du Conseil*, 60(3):636–640.

Koslow, J. A., Kloser, R. J., and Williams, A. (1997). Pelagic biomass and community structure over the mid-continental slope off southeastern Australia based upon acoustic and midwater trawl sampling. *Marine Ecology Progress Series*, 146:21–35.

Kozlov, A. N. (1995). A review of the trophic role of mesopelagic fish of the family myctophidae in the Southern Ocean ecosystem. *CCAMLR Science*, 2:71–77.

Lam, V. and Pauly, D. (2005). Mapping the global biomass of mesopelagic fishes. *Sea around US Project Newsletter*, July/Augus(30):4.

Lampitt, R. S. and Antia, A. N. (1997). Particle flux in deep seas: regional characteristics and temporal variability. *Deep Sea Research Part I: Oceanographic Research Papers*, 44(8):1377–1403.

Landeira, J. M. and Fransen, C. H. J. M. (2012). New data on the mesopelagic shrimp community of the Canary Islands region. *Crustaceana*, 85(4):385–414.

Landeira, J. M., Lozano-Soldevilla, F., Hernández-León, S., and Barton, E. D. (2010). Spatial variability of planktonic invertebrate larvae in the Canary Islands area. *Journal of the marine biological association of the United Kingdom*, 90(06):1217–1225.

Lavery, A. C., Stanton, T. K., McGehee, D. E., and Chu, D. (2002). Three-dimensional modeling of acoustic backscattering from fluid-like zooplankton. *The Journal of the Acoustical Society of America*, 111(3):1197.

Le Borgne, R. and Rodier, M. (1997). Net zooplankton and the biological pump: a comparison between the oligotrophic and mesotrophic equatorial Pacific. *Deep Sea Research Part II: Topical Studies in Oceanography*, 44(9–10):2003–2023.

Lehette, P. and Hernández-León, S. (2009). Zooplankton biomass estimation from digitized images : a comparison between subtropical and Antarctic organisms. *Limnology and Oceanography: Methods*, 7:304–308.

Levitus, S., Antonov, J. I., Boyer, T. P., and Stephens, C. (2000). Warming of the World Ocean. *Science*, 287:2225–2229.

Lezama-ochoa, A., Irigoien, X., Chaigneau, A., Quiroz, Z., Lebourges-Dhaussy, A., and Bertrand, A. (2014). Acoustics Reveals the Presence of a Macrozooplankton Biocline in the Bay of Biscay in Response to Hydrological Conditions and Predator-Prey Relationships. *PloS one*, 9(2):e88054.

Lin, I. L., Hu, C., Li, Y. H., Ho, T. Y., Fischer, T. P., Wong, G. T. F., Wu, J., Huang, C. W., Chu, D. A., Ko, D. S., and Chen, J. P. (2011). Fertilization potential of volcanic dust in the low-nutrient low-chlorophyll western North Pacific subtropical gyre: Satellite evidence and laboratory study. *Global Biogeochemical Cycles*, 25:1–12.

Lobel, P. S. and Robinson, A. R. (1988). Larval fishes and zooplankton in a cyclonic eddy in Hawaiian waters. *Journal of Plankton Research*, 10(6):1209–1223.

Longhurst, A. R., Bedo, A. W., Harrison, W. G., Head, E. J. H., and Sameoto, D. D. (1990). Vertical flux of respiratory carbon by oceanic diel migrant biota. *Deep Sea Research Part A, Oceanographic Research Papers*, 37(4):685–694.

Lopes, A. R., Trübenbach, K., Teixeira, T., Lopes, V. M., Pires, V., Baptista, M., Repolho, T., Calado, R., Diniz, M., and Rosa, R. (2013). Oxidative stress in deep scattering layers: heat shock response and antioxidant enzymes activities of myctophid fishes thriving in oxygen minimum zones. *Deep Sea Research Part I: Oceanographic Research Papers*.

Love, R. H., Fisher, R. a., Wilson, M. a., and Nero, R. W. (2004). Unusual swimbladder behavior of fish in the Cariaco Trench. *Deep Sea Research Part I: Oceanographic Research Papers*, 51(1):1–16.

Lovegrove, T. (1966). The determination of the dry weight of plankton and the effect of various factors on the values obtained.

Lowry, O. H., Rosebrough, N. J., Farr, A. L., Randall, R. J., and Others (1951). Protein measurement with the Folin phenol reagent. *The Journal of Biological Chemistry*, 193(1):265–275.

Machín, F. and Pelegrí, J. L. (2009). Northward penetration of Antarctic intermediate water off Northwest Africa. *Journal of Physical Oceanography*, 39(3):512–535.

Maclennan, D. N., Fernandes, P. G., and J, D. (2002). A consistent approach to definitions and symbols in fisheries acoustics. *ICES Journal of Marine Science*, 59:365–369.

MacLennan, D. N. and Simmonds, E. J. (1992). *Fisheries Acoustics: Theory and Practice*. Chapman & Hall, London.

Maiti, K., Benitez-Nelson, C. R., Lomas, M. W., and Krause, J. W. (2009). Biogeochemical responses to late-winter storms in the Sargasso Sea, III—Estimates of export production using 234 Th: 238 U disequilibria and sediment traps. *Deep Sea Research Part I: Oceanographic Research Papers*, 56(6):875–891.

Mantas, V. M., Pereira, A., and Morais, P. V. (2011). Plumes of discolored water of volcanic origin and possible implications for algal communities. The case of the Home Reef eruption of 2006 (Tonga, Southwest Pacific Ocean). *Remote Sensing of Environment*, 115:1341–1352.

Marshall, N. B. (1960). Swimbladder structure of deep-sea fishes in relation to their systematics and biology. In *Discovery Reports*, volume 31, pages 1–122. Cambridge University Press.

Martin, J. H., Knauer, G. A., Karl, D. M., and Broenkow, W. W. (1987). VERTEX: carbon cycling in the northeast Pacific. *Deep Sea Research Part A. Oceanographic Research Papers*, 34(2):267–285.

Mathew, K. J. (1988). Net avoidance behaviour among larval, juvenile and adult euphausiids. *J. mar. biol. India*, 30(1-2):93–98.

Matsumoto, T., Kitagawa, T., and Kimura, S. (2013). Considerations on diving patterns of bigeye tuna Thunnus obesus based on archival tag data. *Fisheries science*, 79(1):39–46.

McGillicuddy, D. J., Anderson, L. A., Bates, N. R., Bibby, T., Buesseler, K. O., Carlson, C. A., Davis, C. S., Ewart, C., Falkowski, P. G., Goldthwait, S. A., and Others (2007). Eddy/wind interactions stimulate extraordinary mid-ocean plankton blooms. *Science*, 316(5827):1021–1026.

Mehner, T. (2012). Diel vertical migration of freshwater fishes - proximate triggers, ultimate causes and research perspectives. *Freshwater Biology*, 57(7):1342–1359.

Millero, F. J. (1995). Thermodynamics of the carbon dioxide system in the oceans. *Geochimica et Cosmochimica Acta*, 59(4):661–677.

Minutoli, R. and Guglielmo, L. (2009). Zooplankton respiratory Electron Transport System (ETS) activity in the Mediterranean Sea: spatial and diel variability. *Marine Ecology Progress Series*, 381:199–211.

Moteki, M., Horimoto, N., Nagaiwa, R., Amakasu, K., Ishimaru, T., and Yamaguchi, Y. (2009). Pelagic fish distribution and ontogenetic vertical migration in common mesopelagic species off Lützow-Holm Bay (Indian Ocean sector, Southern Ocean) during austral summer. *Polar biology*, 32(10):1461–1472.

Muhling, B. A., Beckley, L. E., and Olivar, M. P. (2007). Ichthyoplankton assemblage structure in two meso-scale Leeuwin Current eddies, eastern Indian Ocean. *Deep Sea Research Part II: Topical Studies in Oceanography*, 54(8):1113–1128.

Murray, J. and Hjort, J. (1912). *The depths of the ocean*. Macmillan, London.

Nechad, B., Ruddick, K., and Park, Y. (2010). Calibration and validation of a generic multisensor algorithm for mapping of total suspended matter in turbid waters. *Remote Sensing of Environment*, 114(4):854–866.

Neilson, J. D. and Perry, R. I. (1990). Diel Vertical Migrations of Marine Fishes: an Obligate or Facultative Process? *Advances in Marine Biology*, 26:115–168.

Neuer, S., Cianca, A., Helmke, P., Freudenthal, T., Davenport, R., Meggers, H., Knoll, M., Santana-Casiano, J. M., González-Davila, M., Rueda, M. J., and Llinás, O. (2007). Biogeochemistry and hydrography in the eastern subtropical North Atlantic gyre. Results from the European time-series station ESTOC. *Progress in Oceanography*, 71(1):1–29.

Neuer, S., Ratmeyer, V., Davenport, R., Fischer, G., and Wefer, G. (1997). Deep water particle flux in the Canary Island region: seasonal trends in relation to long-term satellite derived pigment data and lateral sources. *Deep Sea Research Part I: Oceanographic Research Papers*, 44(8):1451–1466.

Ochoa, J., Maske, H., Sheinbaum, J., and Candela, J. (2013). Diel and lunar cycles of vertical migration extending to below 1000 m in the ocean and the vertical connectivity of depth-tiered populations. *Limnology and Oceanography*, 58(4):1207–1214.

Olgun, N., Duggen, S., Langmann, B., Hort, M., Waythomas, C., Hoffmann, L., and Croot, P. (2013). Geochemical evidence of oceanic iron fertilization by the Kasatochi volcanic eruption in 2008 and the potential impacts on Pacific sockeye salmon. *Marine Ecology Progress Series*, 488:81–88.

Olivar, M., Bernal, A., Molí, B., Peña, M., Balbín, R., Castellón, A., Miquel, J., and Massutí, E. (2012). Vertical distribution, diversity and assemblages of mesopelagic fishes in the western Mediterranean. *Deep Sea Research Part I: Oceanographic Research Papers*, 62:53–69.

Omori, M. and Ikeda, T. (1984). Respiration and excretion: Conversion of respiration rate to carbon and calorific units. *Methods in Marine Zooplankton Ecology.*, pages 191–193.

Oozeki, Y., Hu, F., Kubota, H., Sugisaki, H., and Kimura, R. (2004). Newly designed quantitative frame trawl for sampling larval and juvenile pelagic fish. *Fisheries Science*, 70:223–232.

Pace, M. L., Knauer, G. A., Karl, D. M., and Martin, J. H. (1987). Primary production, new production and vertical flux in the eastern Pacific Ocean. *Nature*, 325(6107):803–804.

Packard, T. (1971). The measurement of respiratory electron-transport in marine phytoplankton. *Journal of marine research*, 29(3):235–244.

Packard, T. T. (1985). Oxygen Consumption in the Ocean: Measuring and Mapping with Enzyme Analysis. In *Mapping Strategies in Chemical Oceanography*, pages 177–209. American Chemical Society, Washington, D.C.

Packard, T. T., Devol, A. H., and King, F. D. (1975). The effect of temperature on the respiratory electron transport system in marine plankton. *Deep Sea Research*, 22(4):237–249.

Packard, T. T. and Gómez, M. (2013). Modeling vertical carbon flux from zooplankton respiration. *Progress in Oceanography*, 110:59–68.

Pakhomov, E. A., Atkinson, A., Meyer, B., Oettl, B., and Bathmann, U. (2004). Daily rations and growth of larval krill *Euphausia superba* in the Eastern Bellingshausen Sea during austral autumn. *Deep Sea Research Part II: Topical Studies in Oceanography*, 51:2185–2198.

Pakhomov, E. a., Froneman, P. W., Kuun, P. J., and Balarin, M. (1999). Feeding dynamics and respiration of the bottom-dwelling caridean shrimp *Nauticaris marionis* Bate, 1888 (Crustacea: Decapoda) in the vicinity of Marion Island (Southern Ocean). *Polar Biology*, 21(2):112–121.

Pakhomov, E. A., Yamamura, O., Brodeur, R. D., Domokos, R., Owen, K. R., Pakhomova, L. G., Polovina, J., Seki, M., and Suntsov, A. V. (2010). Report of the Advisory Panel on Micronekton Sampling Inter-calibration Experiment. *PICES Scientific Report*, 38:108.

Passarella, K. C. and Hopkins, T. L. (1991). Species composition and food habits of the micronektonic cephalopod assemblage in the eastern Gulf of Mexico. *Bulletin of Marine Science*, 49(1-2):638–659.

Passow, U. and Carlson, C. (2012). The biological pump in a high CO_2 world. *Marine Ecology Progress Series*, 470(2):249–271.

Pauly, D. and Christensen, V. (1995). Primary production required to sustain global fisheries. *Nature*, 374(6519):255–257.

Pearre, S. (2003). Eat and run? The hunger/satiation hypothesis in vertical migration: History, evidence and consequences. *Biological Reviews of the Cambridge Philosophical Society*, 78(1):1–79.

Peña, M., Olivar, M. P., Balbín, R., López-Jurado, J. L., Iglesias, M., Miquel, J., and Jech, J. M. (2014). Acoustic detection of mesopelagic fishes in scattering layers of the Balearic Sea (western Mediterranean). *Canadian Journal of Fisheries and Aquatic Sciences*, 71(999):1–12.

Plueddemann, A. J. and Pinkel, R. (1989). Characterization of the patterns of diel migration using a Doppler sonar. *Deep Sea Research Part A. Oceanographic Research Papers*, 36(4):509–530.

Podeswa, Y. (2012). Active carbon transport and feeding ecology of pelagic decapods in the North Pacific subtropical gyre. *MS Thesis, University of British Columbia, Vancouver*.

Potier, M., Marsac, F., Cherel, Y., Lucas, V., Sabatié, R., Maury, O., and Ménard, F. (2007). Forage fauna in the diet of three large pelagic fishes (lancetfish, swordfish and yellowfin tuna) in the western equatorial Indian Ocean. *Fisheries Research*, 83(1):60–72.

Prihartato, P. K., Aksnes, D. L., and Kaartvedt, S. (2015). Seasonal patterns in the nocturnal distribution and behavior of the mesopelagic fish *Maurolicus muelleri* at high latitudes. *Marine Ecology Progress Series*, 521:189–200.

Pusineri, C., Magnin, V., Meynier, L., Spitz, J., Hassani, S., and Ridoux, V. (2007). Food and feeding ecology of the common dolphin (*Delphinus delphis*) in the oceanic Northeast Atlantic and comparison with its diet in neritic areas. *Marine Mammal Science*, 23(1):30–47.

Rivera, J., Lastras, G., Canals, M., Acosta, J., Arrese, B., Hermida, N., Micallef, A., Tello, O., and Amblas, D. (2013). Construction of an oceanic island: Insights from the El Hierro (Canary Islands) 2011–2012 submarine volcanic eruption. *Geology*, 41(3):355–358.

Robinson, C., Steinberg, D. K., Anderson, T. R., Arístegui, J., Carlson, C. A., Frost, J. R., Ghiglione, J.-F., Hernández-León, S., Jackson, G. A., Koppelmann, R., and Others (2010). Mesopelagic zone ecology and biogeochemistry–a synthesis. *Deep Sea Research Part II: Topical Studies in Oceanography*, 57(16):1504–1518.

Robison, B. H. (1973). A system for maintaining midwater fishes in captivity. *Journal of the Fisheries Board of Canada*, 30(1):126–128.

Robison, B. H. and Bailey, T. G. (1981). Sinking rates and dissolution of midwater fish fecal matter. *Marine Biology*, 65(2):135–142.

Roe, H. S. J. (1974). Observations on the diurnal vertical migrations of an oceanic animal community. *Marine Biology*, 28(2):99–113.

Roe, H. S. J. (1983). Vertical distributions of euphausiids and fish in relation to light intensity in the Northeastern Atlantic. *Marine Biology*, 77:287–298.

Roe, H. S. J. (1984a). The diel migrations and distributions within a mesopelagic community in the north east Atlantic. 2. Vertical migrations and feeding of mysids and decapod crustacea. *Progress in Oceanography*, 13(3):269–318.

Roe, H. S. J. (1984b). The diel migrations and distributions within a mesopelagic community in the North East Atlantic. 4. The copepods. *Progress in Oceanography*, 13(3):353–388.

Roe, H. S. J., Angel, M. V., Badcock, J., Domanski, P., James, P. T., Pugh, P. R., and Thurston, M. H. (1984a). The diel migrations and distributions within a mesopelagic community in the north east Atlantic. 1. Introduction and sampling procedures. *Progress in Oceanography*, 13(3):245–268.

Roe, H. S. J. and Badcock, J. (1984). The diel migrations and distributions within a mesopelagic community in the North East Atlantic. 5. Vertical migrations and feeding of fish. *Progress in Oceanography*, 13(3-4):389–424.

Roe, H. S. J., James, P. T., and Thurston, M. H. (1984b). The diel migrations and distributions within a mesopelagic community in the north east Atlantic. 6. Medusae, ctenophores, amphipods and euphausiids. *Progress in oceanography*, 13(3):425–460.

Roper, C. F. E. and Young, R. E. (1975). *Vertical distribution of pelagic cephalopods*. Smithsonian Institution Press Washington, DC.

Røstad, A. and Kaartvedt, S. (2013). Seasonal and diel patterns in sedimentary flux of krill fecal pellets recorded by an echo sounder. *Limnology and Oceanography*, 58(6):1985–1997.

Sabarros, P. S., Ménard, F., Lévénez, J.-J., Tew-Kai, E., and Ternon, J.-F. (2009). Mesoscale eddies influence distribution and aggregation patterns of micronekton in the Mozambique Channel. *Mar. Ecol. Prog. Ser*, 395:101–107.

Sabine, C. L., Feely, R. A., Gruber, N., Key, R. M., Lee, K., Bullister, J. L., Wanninkhof, R., Wong, C. S., Wallace, D. W. R., Tilbrook, B., Millero, F. J., Peng, T.-H., Kozyr, A., Ono, T., and Rios, A. F. (2004). The Oceanic Sink for Anthropogenic CO_2. *Science*, 305(5682):367–371.

Saenger, R. A. (1989). Bivariate normal swimbladder size allometry models and allometric exponents for 38 mesopelagic swimbladdered fish species commonly found in the North Sargasso Sea. *Canadian Journal of Fisheries and Aquatic Sciences*, 46(11):1986–2002.

Sameoto, D., Guglielmo, L., and Lewis, M. K. (1987). Day/night vertical distribution of euphausiids in the eastern tropical Pacific. *Marine Biology*, 96(2):235–245.

Sangrà, P., Auladell, M., Marrero-Díaz, A., Pelegrí, J. L., Fraile-Nuez, E., Rodríguez-Santana, A., Martín, J. M., Mason, E., and Hernández-Guerra, A. (2007). On the nature of oceanic eddies shed by the Island of Gran Canaria. *Deep Sea Research Part I: Oceanographic Research Papers*, 54(5):687–709.

Sangrà, P., Pascual, A., Rodríguez-Santana, Á., Machín, F., Mason, E., McWilliams, J. C., Pelegrí, J. L., Dong, C., Rubio, A., Arístegui, J., Marrero-Díaz, A., Hernández-Guerra, A., Martínez-Marrero, A., and Auladell, M. (2009). The Canary Eddy Corridor: A major pathway for long-lived eddies in the subtropical North Atlantic. *Deep Sea Research Part I: Oceanographic Research Papers*, 56(12):2100–2114.

Santana-Casiano, J. M., González-Dávila, M., Fraile-Nuez, E., de Armas, D., González, A. G., Domínguez-Yanes, J. F., and Escánez, J. (2013). The natural ocean acidification and fertilization event caused by the submarine eruption of El Hierro. *Scientific reports*, 3(1140).

Santos, M. B., Clarke, M. R., and Pierce, G. J. (2001). Assessing the importance of cephalopods in the diets of marine mammals and other top predators: problems and solutions. *Fisheries Research*, 52(1-2):121–139.

Sarmiento, J. L. (1993). Ocean carbon cycle. *Chemical and Engineering News*, 71(22).

Sarmiento, J. L., Gruber, N., Brzezinski, M. A., and Dunne, J. P. (2004). High-latitude controls of thermocline nutrients and low latitude biological productivity. *Nature*, 427(6969):56–60.

Sassa, C., Tsukamoto, Y., Yamamoto, K., and Tokimura, M. (2010). Spatio-temporal distribution and biomass of *Benthosema pterotum* (Pisces: Myctophidae) in the shelf region of the East China Sea. *Marine Ecology Progress Series*, 407:227–241.

Schlitzer, R. (2002). Carbon export fluxes in the Southern Ocean: results from inverse modeling and comparison with satellite-based estimates. *Deep Sea Research Part II: Topical Studies in Oceanography*, 49(9–10):1623–1644.

Schukat, A., Bode, M., Auel, H., Carballo, R., Martin, B., Koppelmann, R., and Hagen, W. (2013). Pelagic decapods in the northern Benguela upwelling system: Distribution, ecophysiology and contribution to active carbon flux. *Deep Sea Research Part I: Oceanographic Research Papers*, 75:146–156.

Simmonds, E. and MacLennan, D. (2005). *Fisheries Acoustics: Theory and Practice*. Blackwell Science Ltd, London.

Sims, D. W., Wearmouth, V. J., Southall, E. J., Hill, J. M., Moore, P., Rawlinson, K., Hutchinson, N., Budd, G. C., Righton, D., Metcalfe, J. D., Nash, J. P., and Morritt, D. (2006). Hunt warm, rest cool: bioenergetic strategy underlying diel vertical migration of a benthic shark. *Journal of Animal Ecology*, 75(1):176–190.

Small, L. F., Fowler, S. W., and Ünlü, M. Y. (1979). Sinking rates of natural copepod fecal pellets. *Marine Biology*, 51(3):233–241.

Staby, A. and Aksnes, D. (2011). Follow the light-diurnal and seasonal variations in vertical distribution of the mesopelagic fish Maurolicus muelleri. *Marine Ecology Progress Series*, 422:265–273.

Staby, A., Røstad, A., and Kaartvedt, S. (2011). Long-term acoustical observations of the mesopelagic fish Maurolicus muelleri reveal novel and varied vertical migration patterns. *Marine Ecology Progress Series*, 441:241–255.

Stanton, T. K. and Chu, D. (2000). Review and recommendations for the modelling of acoustic scattering by fluid-like elongated zooplankton : euphausiids and copepods. *ICES Journal of Marine Science*, 57:793–807.

Steinberg, D. K., Carlson, C. A., Bates, N. R., Goldthwait, S. A., Madin, L. P., and Michaels, A. F. (2000). Zooplankton vertical migration and the active transport of dissolved organic and inorganic carbon in the Sargasso Sea. *Deep Sea Research Part I: Oceanographic Research Papers*, 47(1):137–158.

Steinberg, D. K., Carlson, C. A., Bates, N. R., Johnson, R. J., Michaels, A. F., and Knap, A. H. (2001). Overview of the US JGOFS Bermuda Atlantic Time-series Study (BATS): a decade-scale look at ocean biology and biogeochemistry. *Deep Sea Research Part II: Topical Studies in Oceanography*, 48(8):1405–1447.

Steinberg, D. K., Cope, J. S., Wilson, S. E., and Kobari, T. (2008). A comparison of mesopelagic mesozooplankton community structure in the subtropical and subarctic North Pacific Ocean. *Deep Sea Research Part II: Topical Studies in Oceanography*, 55(14–15):1615–1635.

Stramma, L., Johnson, G. C., Sprintall, J., and Mohrholz, V. (2008). Expanding oxygen-minimum zones in the tropical oceans. *Science*, 320(5876):655–658.

Suess, E. (1980). Particulate organic carbon flux in the oceans—surface. *Nature*, 288:261.

Sutton, T. T. and Hopkins, T. L. (1996). Trophic ecology of the stomiid (Pisces: Stomiidae) fish assemblage of the eastern Gulf of Mexico : Strategies, selectivity and impact of a top mesopelagic predator group. *Marine biology*, 127(2):179–192.

Torres, J. J., Belman, B. W., and Childress, J. J. (1979). Oxygen consumption rates of midwater fishes as a function of depth of occureence. *Deep Sea Research Part A. Oceanographic Research Papers*, 26(2):185–197.

Troupin, C., Barth, A., Sirjacobs, D., Ouberdous, M., Brankart, J.-M., Brasseur, P., Rixen, M., Alvera-Azcárate, A., Belounis, M., Capet, A., Lenartz, F., Toussaint, M.-E., and Beckers, J.-M. (2012). Generation of analysis and consistent error fields using the Data Interpolating Variational Analysis (DIVA). *Ocean Modelling*, 52-53:90–101.

Tucker, G. H. (1951). Relation of fishes and other organisms to the scattering of underwater sound. *Journal of marine research*, 10:215–238.

Turner, J. T. (2002). Zooplankton fecal pellets, marine snow and sinking phytoplankton blooms. *Aquatic Microbial Ecology*, 27(1):57–102.

Tuya, F., García-Díez, C., Espino, F., and Haroun, R. J. (2006). Assessment of the effectiveness of two marine reserves in the Canary Islands (eastern Atlantic). *Ciencias Marinas*, 32(3).

UNESCO (1968). *Zooplankton sampling - Part II, Monograph of Oceanographic Methodology*. UNESCO, Paris.

UNESCO (1994). Protocols for the Joint Global Ocean Flux Study (JGOFS) Core Measurements. Technical report, Intergovernmental Oceanographic Commission, UNESCO, Paris.

Usbeck, R., Schlitzer, R., Fischer, G., and Wefer, G. (2003). Particle fluxes in the ocean: comparison of sediment trap data with results from inverse modeling. *Journal of Marine Systems*, 39(3–4):167–183.

van Haren, H. (2007). Monthly periodicity in acoustic reflections and vertical motions in the deep ocean. *Geophysical research letters*, 34(12).

van Haren, H. and Compton, T. J. (2013). Diel vertical migration in deep sea plankton is finely tuned to latitudinal and seasonal day length. *PloS one*, 8(5):1–8.

Vinogradov, M. E. (1962). Feeding of the deep-sea zooplankton. *Journal du conseil pour l'Exploration de la Mer*, 153:114– 119.

Wang, Z., DiMarco, S. F., Ingle, S., Belabbassi, L., and Al-Kharusi, L. H. (2014). Seasonal and annual variability of vertically migrating scattering layers in the northern Arabian Sea. *Deep Sea Research Part I: Oceanographic Research Papers*.

Warrant, E. J. and Locket, N. A. (2004). Vision in the deep sea. *Biological Reviews*, 79(3):671–712.

Watanabe, H., Kawaguchi, K., and Hayashi, A. (2002). Feeding habits of juvenile surface-migratory myctophid fishes (family Myctophidae) in the Kuroshio region of the western North Pacific. *Marine Ecology Progress Series*, 236:263–272.

Watanabe, H., Moku, M., Kawaguchi, K., Ishimaru, K., and Ohno, A. (1999). Diel vertical migration of myctophid fishes (Family Myctophidae) in the transitional waters of the western North Pacific. *Fisheries Oceanography*, 8(2):115–127.

Weingartner, T. J., Coyle, K., Finney, B., Hopcroft, R., Whitledge, T., Brodeur, R., Dagg, M., Farley, E., Haidvogel, D., Haldorson, L., and Others (2002). The Northeast Pacific GLOBEC Program. *Oceanography*, 15(2):48.

Weston, D. E. (1967). Sound propagation in the presence of bladder fish. In Albers, V. A., editor, *Underwater acoustics*, volume 2 (5), pages 55–88. Plenum Press, New York.

Wiebe, P. H., Groman, R. C., and Allison, M. D. (2002). ICES/GLOBEC sea-going workshop for intercalibration of plankton samplers. *ICES Cooperative Research Report*, 250:25.

Wienerroither, R., Uiblein, F., Bordes, F., and Moreno, T. (2009). Composition, distribution, and diversity of pelagic fishes around the Canary Islands, Eastern Central Atlantic. *Marine Biology Research*, 5(4):328–344.

Williams, A. and Koslow, J. A. (1997). Species composition, biomass and vertical distribution of micronekton over the mid-slope region off southern Tasmania, Australia. *Marine Biology*, 130(2):259–276.

Wilson, S. E., Steinberg, D. K., Chu, F. L. E., and Bishop, J. K. B. (2010). Feeding ecology of mesopelagic zooplankton of the subtropical and subarctic North Pacific Ocean determined with fatty acid biomarkers. *Deep-Sea Research Part I: Oceanographic Research Papers*, 57(10):1278–1294.

Woodworth, P. A., Schorr, G. S., Baird, R. W., Webster, D. L., McSweeney, D. J., Hanson, M. B., Andrews, R. D., and Polovina, J. J. (2012). Eddies as offshore foraging grounds for melon-headed whales (*Peponocephala electra*). *Marine Mammal Science*, 28(3):638–647.

Yamamura, O., Suntsov, A. V., and Yasuma, H. (2010). Third Micronekton Intercalibration Experiment, MIE-3. In Pakhomov, E. and Yamamura, O., editors, *Report of the Advisory Panel on Micronekton Sampling Inter-calibration Experiment*, pages 59–65. PICES.

Yasuma, H., Sawada, K., Takao, Y., Miyashita, K., and Aoki, I. (2010). Swimbladder condition and target strength of myctophid fish in the temperate zone of the Northwest Pacific. *ICES Journal of Marine Science*, 67:135–144.

Yasuma, H. and Yamamura, O. (2010). Second Micronekton Inter-calibration Experiment, MIE-2. Comparison between Acoustic Estimates. In Pakhomov, E. and Yamamura, O., editors, *Report of the Advisory Panel on Micronekton Sampling Intercalibration Experiment*, pages 51–56. PICES.

Yebra, L., Almeida, C., and Hernández-León, S. (2005). Vertical distribution of zooplankton and active flux across an anticyclonic eddy in the Canary Island waters. *Deep Sea Research Part I: Oceanographic Research Papers*, 52(1):69–83.

Zhang, X. and Dam, H. G. (1997). Downward export of carbon by diel migrant mesozooplankton in the central equatorial Pacific. *Deep Sea Research Part II: Topical Studies in Oceanography*, 44(9-10):2191–2202.